Sorption of Selected Pesticides on Mineral Surfaces: Factors and Mechanisms

Dissertation

der Mathematisch-Naturwissenschaftlichen Fakultät

der Eberhard Karls Universität Tübingen

zur Erlangung des Grades eines

Doktors der Naturwissenschaften

(Dr. rer. nat.)

vorgelegt von

Leyla Gulu Zada

aus Baku/Aserbaidschan

Tübingen

2018

Gedruckt mit Genehmigung der Mathematisch-Naturwissenschaftlichen Fakultät der Eberhard Karls Universität Tübingen.

Tag der mündlichen Qualifikation:	05.02.2019
Dekan:	Prof. Dr. Wolfgang Rosenstiel
1. Berichterstatter:	Prof. Dr. Stefan B. Haderlein
2. Berichterstatter:	Prof. Dr. Carolin Huhn

To my parents

Acknowledgements

The present dissertation is a significant chapter of life. The scientific work described here took five years. I would like to express my gratitude to the following people, who helped me to make this work.

Stefan Haderlein for offering me a PhD position in 2013, for his wise supervision during these years.

The funding of the work by EXPAND graduate project (Excellence Initiative of Eberhard-Karls University of Tübingen).

I would like to thank the mineralogy and environmental chemistry working group for their readiness to help, especially to Monika, Edison, Xue, Silvia and Tu Trinh.

Hwa Yun Lee, Sang Hyun Ahn, and Suk Bong Hong for providing beta26 zeolites and discussions concerning zeolites' properties.

Polina Abdrakhimova and Igor Pavlowskiy for their proofreading and suggestions.

Emilio Sanchez for his help with Python code.

My sincere acknowledgemnets are for all the members of EXPAND project and personally to Carla Lorenz, Jorina Wicht, Elisabeth Früh, Leilei Luo, Reiner Anwander, Carolin Huhn, Heinz Köhler, Sandra Dietz for the valuable input and discussions.

Yucang Liang for the synthesis of the particles for the sorption experiments.

Martin Pattky and Benedikt Wimmer for the glyphosate analysis.

Sylvain Merel and Sascha Lege for LC-MS analysis of azole fungicides concentrations.

Boris Bugsel and Klaus Röhler for their help in the laboratory during my parental leave.

Annette Flicker for her assistance in ATR-FTIR analysis.

My dearest mother – thank you for understanding and support.

My parents in law for their readiness to help.

My husband and daughter, for all the love and patience.

Table of Contents

List of Figures

List of Tables

Abbreviations

AMPA - Aminomethyl phosphonic acid

ATMP – Amino Trimethylene Phosphonic Acid

ATR-FTIR – Attenuated total reflectance- Fourier transform infrared spectroscopy

BEA – beta type zeolite

BET – Brunauer-Emmett-Teller theory

Beta26 – BEA zeolite with Si/Al ratio 26

Beta360 – BEA zeolite with Si/Al ratio 360

BG electrolyte – background electrolyte

CE – Capillary electrophoresis

Csorb_max – maximum sorbed concentration

CTAB – cetyltrimethylammonium bromide

DTPMP – Diethylenetriaminopenta(methylenephosphonic Acid)

EDA interactions – electron-donor-acceptor interactions

EDTMP – Ethylenediaminetetramethylenephosphonic Acid

EOF – electroosmotic flow

ESI – Electrospray ionization

EXAFS – extended X-ray absorption fine structure

FAU – faujasite (or Y) type zeolite

Gla – glufosinate ammonium

Glu - glufosinate

Gly – Glyphosate

HA – humic acid

Hex – hexaconazole

HPLC – high performance liquid chromatography

I – ionic strength

IC – Imidacloprid

K_L – Langmuir equation coefficient

K_{ML} – complex formation constant of glyphosate with divalent cations

LA-ICP-MS – Laser Ablation – Inductively Coupled Plasma – Mass Spectrometry

LC – liquid chromatography

MCM-48 – mesoporous silica MCM-48

MS – mass spectrometry

NOM – natural organic matter

OM – organic matter

PBU – Primary building units

PMO-silica – periodic mesoporous organosilica

Prop – Propiconazole

PVA – Polyvinyl Acetate

PZC – point of zero charge

SBU – secondary building units

TC – Thiacloprid

Y12 – FAU zeolite with SiO_2/Al_2O_3 ratio 12

Y30 – FAU zeolite with SiO_2/Al_2O_3 ratio 30

Y65 – FAU zeolite with SiO_2/Al_2O_3 ratio 65

Y7,5 – FAU zeolite with SiO_2/Al_2O_3 ratio 7,5

Y80 – FAU zeolite with SiO_2/Al_2O_3 ratio 80

The decimal point in the present work is comma (DIN 1333 and DIN 5008)

Point was used for the thousand's separator

Abstract

Pesticides compose one of the biggest groups of the organic pollutants. Among the possible interactions, sorption is the one, that may have the most significant effect on the reactivity and bioavailability, as well as toxicity of the pesticides in the natural aqueous systems. However, many previous studies of the toxicity of the pesticides are mainly focused on the freely-dissolved compounds, neglecting the effect of sorption [Smit et al., 2015; Perez et al., 2011].

Present research is a part of an interdisciplinary study (EXPAND project). The main motivation of the EXPAND project was to investigate the toxic effects of particle-associated compounds on target and non-target organisms on an environmental level. This dissertation is aimed at investigating sorbent-sorbate interactions between pesticides and particles. The impact of environmental factors (pH, ionic strength, the presence of ions, competitive sorption) on these interactions was investigated in the batch experiments. The sorption experiments were performed on different sorbents and various insecticides (imidacloprid and thiacloprid), herbicides (glyphosate (with its metabolite AMPA) and glufosinate ammonium) and fungicides (hexaconazole and propiconazole).

The sorbents used in the experiment are zeolites (from FAU and BEA groups), amorphous alumina, periodic mesoporous organosilica (PMO-silica) and mesoporous silica MCM-48. The choice of the particles was done based on their environmental abundance, properties as potentially effective sorbents (specific surface area, chemical structure, and porosity) and applicability to the toxicological experiments (small size, facilitating an uptake by studied organisms).

The concentrations of the pesticides were determined with the following techniques: HPLC-UV, LC-MS, CE. ATR-FTIR technique was applied to explain the sorption mechanisms of pesticides on chosen sorbents.

The Langmuir model was fitted to the experimentally obtained data. An effect of environmental factor on the sorption of charged and non-charged pesticides varied significantly and was explained by different effects.

In general, the sorbents with high sorption capacity were found for each investigated pesticide. These results were used for the sorption mechanism interpretation and later on, for the toxicological studies [Lorenz et al., 2017 a, b], [Früh, in preparation].

The following mechanism of the interactions between thiacloprid and imidacloprid and the zeolites was proposed: a) coordination of C=N group with exchangeable cations of zeolites; b) π-anion EDA interactions between negatively charged zeolite surface and N atoms of pyridine ring of IC and TC molecules; c) hydrogen bond formation between Cl- of neonicotinoid molecule and hydrogens on

the zeolite surface. Moreover, it was suggested, that sorption of imidacloprid and thiacloprid on zeolites is limited by pore-filling process.

The proposed sorption mechanism of azole fungicides on PMO-silica involved hydrogen-N(triazole) and anion-N(triazole) bond formation. Additionally, aryl-ring was suggested for anion-π EDA interactions.

ATR-FTIR results imply inner-sphere coordination between posphonate functional group of glyphosate molecule and alumina surface, forming a nonprotonated monodentate complex or a nonprotonated bidentate binuclear complex. Moreover, outer-sphere coordination was proposed between carboxyl functional group and aluminium oxide.

Zusammenfassung

Heutzutage gehören Pestizide zu einer der größten Gruppen von organischen Kontaminanten. Die Mehrzahl der Arbeiten über die Toxizität von Pestiziden beschreiben lediglich den Effekt von freigelösten Stoffen ohne Berücksichtigung der Interaktionen mit Feststoffen [Smit et al., 2015; Perez et al., 2011]. Die Sorbant-Sorbens Interaktionen zwischen Pestiziden und Festpartikeln spielen in der Umwelt eine bedeutende Rolle. Die Sorption verändert Konzentrationen von freigelösten Pestiziden und in weiterer Folge deren Reaktivität, Toxizität sowie deren Bioverfügbarkeit.

Die vorliegende Dissertation ist Teil eines interdisziplinären Projektes namens EXPAND. Die Hauptmotivation des EXPAND Projektes war es die toxikologischen Effekte von Partikel-gebundenen Pestiziden auf Ziel- und Nichtzielorganismen zu untersuchen. Das Ziel der vorliegenden Arbeit war es die Sorbant-Sorbens Wechselwirkungen zwischen Pestiziden und Partikeln sowie den Einfluss von unterschiedlichen Umweltfaktoren (Ionische Stärke, pH, mono- und divalenten Kationen, Kompetitive Sorption, Phosphat) zu untersuchen. Mittels Batch Experimente wurde die Sorption von den jeweiligen Gruppen: Insektizide (Imidacloprid und Thiacloprid); Fungizide (Propiconazol und Hexaconazole); Herbizide (Glyphosat (mit seinem Metabolit AMPA), und Glufosinat) mit unterschiedlichen Partikeln als Sorbentien gemessen.

Folgende Sorbentien wurden verwendet: Zeolithe (FAU und BEA), amorphe Aluminiumoxid, periodische mesoporöse organische Siliziumoxid (PMO-silica) und mesoporöse Siliziumoxid (MCM-48). Die Partikeln wurden gewählt anhand deren Verbreitung, Kosten, und deren chemische Eigenschaften (spezifische Oberfläche, Porosität, chemische Struktur) sowie die Anwendbarkeit an toxikologischen Experimenten (kleine Partikelngröße, die von Organismen aufgenommen werden könnten).

Die Konzentrationen von Pestiziden wurden anhand der HPLC-UV, LC-MS, CE Methoden bestimmt. ATR-FTIR Methode wurde verwendet, um Sorptionsmechanismen zu bestimmen.

Die Sorptionsisothermen wurden nach Langmuir model gefittet und dargestellt.

Die Variationen von Umweltfaktoren hatten unterschiedliche Effekte auf ungeladene und geladene Pestizidmoleküle.

Für jedes ausgewählte Pestizid wurde ein Sorbent mit der höchsten Sorption ausgewählt. Diese Sorbant-Sorbens Paare wurden für Mechanismus Interpretation verwendet und weiter für toxikologische Experimente eingesetzt [Lorenz et al., 2017 a, b] und Früh [Dissertation, in Vorbeireitung].

Die folgenden Mechanismen wurden vorgeschlagen für Thiacloprid und Imidacloprid Interaktionen mit Zeolithe: a) Koordination zwischen C=N mit Austausch Kationen auf Zeolithen Oberfläche; b)

π-anion EDA Interaktionen zwischen negativ geladenen Zeolithen Öberflächen und Pyridin Ringe von Imidacloprid unf Thiacloprid Moleküle; c) Wasserstoff-Brücken mit Zeolithen Oberfläche.

Sorption von Pestiziden auf PMO-Silica Oberfläche hatte hydrophobischen Charakter und erhöhte sich in der Reihenfolge Imidacloprid < Thiacloprid < Propiconazol < Hexaconazol. Die Bindungsbildung zwischen Azol Fungizide und PMO-Silica Oberfläche involvierte Stickstoff-N(Triazol) oder Anion-N(triazol) und Anion-π EDA Interaktionen (mit Aryl Ring).

Aufgrund der ATR-FTIR Ergebnisse konnte festgestellt werden, dass der Sorptionsmechanismus von Glyphosat auf Aluminiumoxid durch die Phosphonat - Gruppe eine nichtprotonierte Monodentat- oder eine nichtprotonierte Bedentat-Binuclear-Komplexbildung zur Folge hatte. Die Interaktionen zwischen Carboxyl Gruppe und Aluminiumoxid Oberfläche resultierte in Außen-Komplexbindung.

Chapter 1 Introduction and objectives

Many anthropogenic activities cause various organic chemicals from different sources to be introduced into the environment and persist there [Dachs and Mejanelle, 2010; Gioia et al., 2011]. Some of the organic pollutants remain unchanged in the environment for long periods of time. Pesticides are one of the largest groups of organic pollutants. According to the U.S. Environmental Protection Agency, approximately 3 billion kilograms of pesticides were applied annually in the world between 2011 and 2012 [Atwood, 2017].

Pesticides are the organic compounds that are used all over the world at an industrial scale, as well as by individuals. The first generation of the pesticides had a non-target mode of action, therefore after application, they were harmful not only for the pests but also for non-target organisms including humans. In the last fifty years a lot of research was done on the synthesis of specific pesticides that would affect target groups and be harmless for the mammals and other non-target species [Jeschke et al., 2008; Venkateswarlu et al., 1997; McLean et al., 2002; Lepesheva et al., 2003; Steinrücken and Amrhein, 1980]. However, even selective pesticides are stable organic compounds, that accumulate in the environment. After the surface application, organic pollutants are transported to the subsurface and groundwater. There are various mechanisms of interaction between organic pollutants and subsurface particles, including sorption, advection and diffusion [Schwarzenbach et al., 2005].

Sorption may not only change pesticide availability but also alter its toxic properties. There are multiple studies, that focus on the sorption of pesticides in soils [Chaplain et al., 2011; Fernandez-Bayo et al., 2007; Liu et al., 2002; Chauhan et al., 2013]. Sorption was correlated with an organic carbon content in soils. Gonzales-Pradas et al., 1999 investigated sorption of imidacloprid, isoproturon, and atrazine on magnesium silicate clays and attenuation of the pesticides from water. Multiple studies investigated sorption on mesoporous silica [Popat et al., 2011] and montmorillonites [Morillo et al., 1997]. However, above-mentioned works described sorption as an attenuation method of pesticides but did not investigate the toxicological effect of the sorption. The toxicological properties of the pesticides for various target and non-target organisms in the aqueous environment were determined and documented in the literature [Perez et al., 2011; Rzymsky et al., 2013; Smit et al., 2015; Sumon et al., 2018]. However, the authors discussed the toxicity of the pesticides mainly as the freely-dissolved compounds, neglecting the interactions between the sediments and the organic molecules, which could alter the availability of the pesticides for the studied organisms, and therefore, result in different toxicity.

In the present work, the toxicity of the pesticides is investigated, considering the sorption of the pesticide, and the availability of freely-dissolved compounds in the aqueous system.

In order to provide an explanation of the sorbent-sorbate interactions on different pesticides, several pesticides from three classes were selected: insecticides (imidacloprid and thiacloprid), herbicides (glyphosate (with its metabolite AMPA) and glufosinate ammonium) and fungicides (hexaconazole and propiconazole).

Zeolites, aluminium oxide, mesoporous organosilica and periodic mesoporous organosilica were used as the possible adsorbents for the pesticides. The choice of the pesticides was based on different factors, such as inexpensiveness, wide distribution, small particle size, high specific surface area, the pore size. De Smedt et al., 2015; Rongchapo, 2015 used zeolites as the adsorbents for several pesticides, including neonicotinoids and determined very high sorption on these materials. Multiple studies reported high sorption of pesticides on mesoporous silica particles [Brankovich et al., 2017; Ng et al., 2017; Benhamou et al., 2009]. The PMO-silica was used in sorption experiments by Ganiyu et al., 2014 and Huq et al., 2001.

In the present research, the results of sorption of pesticides on the particles are used in the toxicological studies, which prompted the choice of a particle size to be sufficiently small to be consumed by the studied organisms (larvae *Chironomus riparius* [Lorenz et al., 2017 a, b] and ectomycorrhizal fungi *Laccaria bicolor, Amanita muscaria, Cenococcum geophilum* [Früh, in preparation]). To fulfil this requirement, the particles with average size <700 nm are selected. The chosen particles (except aluminium oxide) possess high porosity, which provides high surface area and the high number of the sorption sites. The use of alumina as a sorbent for thiacloprid is reasoned by the interest of the alumina for the toxicological experiments. Oberholster et al., 2011 reported the toxicological effects of aluminium oxide nanoparticles to the studied organisms [*Chironomus tentans* larvae]. Thus, the toxicological study of Lorenz et al., 2017 (a, b) is focused on the toxicology of thiacloprid, alumina and thiacloprid with alumina on the mortality of *Chironomus riparius* larvae [Lorenz et al., 2017 a, b].

The sorption mechanisms of the pesticides on different substrates were discussed by Goulson and Kleijn, 2013; Xiao and Pignatello, 2015 and Inyang and Dickenson, 2015. The sorption mechanism of glyphosate on metal oxide surfaces was reported by Sheals et al., 2002; Damonte et al., 2007. Damonte et al., 2007 proposed the formation of the complexes between phosphonate and carboxylic group of glyphosate molecule with the mineral surface. According to the published data, glyphosate has a similar to phosphate sorption mechanism, involving the phosphonate group of glyphosate [Gimsing et al., 2004; Gimsing and Borggaard, 2001; Gimsing et al., 2007]. The phosphate sorption mechanism was studied by Zheng et al., 2012 at pH 4 and pH 9.

Liu et al., 2002 investigated the sorption of imidacloprid on clay-containing soils and proposed the sorption mechanism involving C=N group of the pyridine group. Investigating the sorption of propiconazole, Li and Flood, 2008 suggested π-π EDA interaction. Various sorption experiments with triazoles implied hydrogen-N; anion-N and cation-N interactions [Crowley et al., 2010; Li et al., 2007; Camponovo et al., 2009]. However, there is insufficient research done on the sorption mechanisms of thiacloprid on zeolites and azole fungicides on mesoporous silica.

ATR-FTIR is an effective method to interpret the sorption mechanisms of different compounds, allowing to conduct the experiments "in-situ". Multiple studies were conducted to analyse glyphosate and its sorption with ATR-FTIR [Barja and dos Santos Afonso, 1998; Piccolo and Celano, 1993]. There is significantly less literature on the IC and Prop ATR-FTIR analysis, than on ATR-FTIR of glyphosate [Quintas et al., 2004; Aregahegn, 2017; Aziz et al., 2014; Best et al., 2014]. The ATR-FTIR data for TC and Hex is very scarce. To fulfill this knowledge gap, the sorption of imidacloprid and thiacloprid on zeolites and azole compounds on mesoporous silica were investigated using the ATR-FTIR technique.

The main objectives of the present work are:

i. Explain on the example of chosen compounds, how various classes of pesticides interact with the environmentally abundant particles in aqueous systems;
ii. Propose mechanism of sorption, using ATR-FTIR method;
iii. Evaluate the significance of the sorption for the target organisms, determining how the bioavailability and toxicology of the pesticides change after binding to the particle surface.

Chapter 2 Materials and Methods

2.1. Sorbents

The choice of sorbents was based on the following criteria: developed surface area, high porosity and chemical composition. The potentially effective sorbents of the model pesticides were chosen. The particle size of the sorbent was another determining criterion – the particles should be small enough to be consumed by the organisms.

All the minerals chosen for the present research are abundant in nature, inexpensive, and suitable for sorption tests and consequent toxicity tests. Table 2.1 summarizes the physical properties of the materials, which were used as sorbents for the chosen pesticides.

Table 2.1 Physical characteristics of the particles (from the specification sheet and experimentally determined)

Sorbent material	**Particle size [nm]**	**Corrections to the particle size**	**BET spec. surface area [m²/g]**	**pH_{pzc}**	**Pore diameter [nm]**	**For zeolites: Si/Al ratio**
Zeolite Y12	667	8,906 µm – original size before treatment**	730	<3	0,74	12
Zeolite Y15	200	200 nm – size after milling on Emax mill. Original particle size: 3-15 µm	618-700	<3	0,74	15
Zeolite Y30	712	5,838 µm – original size before treatment**	780	<3	0,74	30

Zeolite Y130	200	200 nm – size after milling on Emax mill. Original particle size: 3-15 µm	618	<3	0,74	130
Zeolite Y80	642	10,415 µm – original size before treatment**	780	<3	0,74	80
Beta 26	20860	30-40 nm – single crystal size	685	<3	0,5-0,6	26
Beta 360	639		620	<3	0,6	360
SiO_2	360-550		1523	<3	2,1	n/a
MCM-48	260		1150	>11	2,2	n/a
PMO(LL-17)	360		1050	<3	1,9	n/a
Al_2O_3	410		9	9,07	nonporous	n/a

Particle size of zeolites was measured on the Mastersizer Hydro 2000. Provided values are d(90). Original particle size is presented in corrections to the particle size column. Particle size of SiO_2, MCM-48, PMO(LL-17), Al_2O_3 was determined by TEM*

**d(90) – 90% of all the particles have size lower or equal to the provided value*

***Treatment of the zeolites: original particles were washed with MeOH and H_2O, dried in a fume hood, milled in rotary mill [Planetenmühle Fritsch laborette], centrifuged [Herolab HiCen21] and then dried [Table I, Appendix].*

2.1.1. Zeolites

Zeolites are naturally abundant materials (during last two centuries approximately 40 natural zeolites were discovered and identified) as well as there are more than 150 synthesized zeolites [Virta, 2001]. Being highly-abundant, zeolites are important materials in various branches as adsorbents, ion-exchangers, molecular sieves, catalysts and much more.

General formula of zeolite can be presented as $M_{x/n}[(AlO_2)_x(SiO_2)_y] \cdot z\ H_2O$ (M – alkali and alkaline-earth metals, n = charge of M) [Baerlocher et al., 2007]. In zeolites aluminum and silicon-atoms of AlO_4^-– and SiO_4–tetrahedra are interconnected through oxygen-bridges [Masters and Maschmeyer, 2011]. Si/Al

ratio (or SiO_2/Al_2O_3) determines most chemical and physical properties of the zeolite, as well as its stability [Masters and Maschmeyer, 2011]. According to the stability rule of Löwenstein, 1954 two AlO_4^- – tetrahedra cannot be next to each-other, therefore Si/Al ratio is always ≥1. Several classifications of zeolites exist. Union Carbide proposed using Latin Alphabet (zeolite A, X, Y, L) [Pariente and Sanchez-Sanchez, 2018].

The Atlas of Zeolite Structure types provides one of the fullest zeolite banks, which is regularly updated [Baerlocher et al., 2007]. The Atlas of Zeolite Structure types uses three-letter code for a framework topology. Thus, FAU stands for whole faujasite type zeolites (zeolite X, Y, being low and high silica-zeolites respectively). According to Si/Al ratio zeolites can be classified into the following groups [Ribeiro et al., 1984]:

a) "Low silica" zeolites: Si/Al ≈ 1 (Type A and X)
b) "Intermediate silica" zeolites: Si/Al ratio >2 (zeolite Y, mordenite, zeolite L)
c) "High silica" zeolites: Si/Al ratio >10

An affinity to nonpolar organic molecules increases with Si/Al ratio.

Structure of zeolite is determined by the dimension, the shape of a channel, as well as the arrangement of the channels to each other. The Atlas of Zeolite Framework Types classifies zeolites by their channel size [Baerlocher et al., 2007]: small (3,5-4,5 Å) with 8-ring pores [A zeolite], medium (4,5-6,0 Å) with 10-ring pores [ZSM-5], large (6,0-8,0 Å) port zeolites with 12-ring pores [Zeolite X, Y] and extra-large pore zeolites with 14-ring pores [UTD-1].

Advantages of synthesized zeolites are their uniform properties, such as particle size, pore size, surface area etc, which are much easier to be controlled and modified for specific goals, than of natural zeolites. For the current research, it was more representative to use synthetic zeolites.

Two large pore zeolites, faujasite (FAU, Y type zeolite) and beta zeolite (BEA), were chosen for the experiment. The choice was determined by the high surface area, large pore size and high silica content (Si/Al>10) of the selected zeolites. The high Si/Al defines zeolite's hydrophobicity and promotes sorption of organic molecules from the aqueous solutions.

Faujasite or Y type zeolite consists of 12-ring pore channels with the pore diameter d=7,4 Å [Baerlocher et al., 2007].

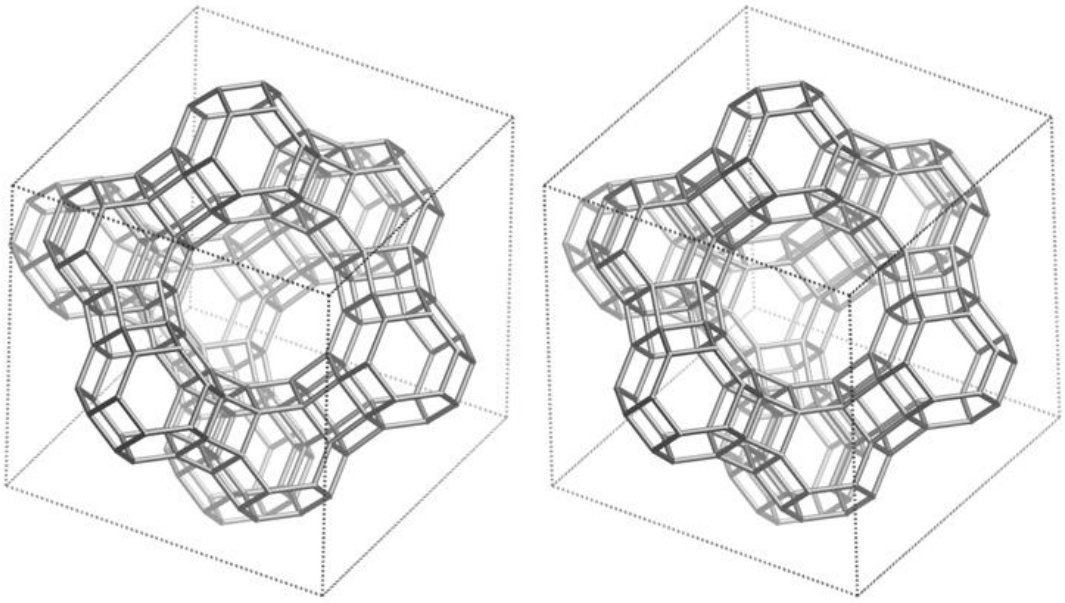

Figure 2.1 Framework of faujasite type (FAU) zeolite (viewed along [111] (l) and [110] (r)). [From Baerlocher et al., 2007, with permission]

Published works on natural tschernichite (natural BEA zeolite) [Boggs et al., 1993, Galli et al., 1995, Alberti et al., 2002] have reported dependence of chemical composition on the crystal size of the mineral. Thus, the larger tetragonal crystals (several mm) have higher Si content in zeolite framework and higher Ca^{2+} ions concentration in channels, whereas small crystals (<0,5 mm) have significantly lower silicon content and higher Mg^{2+} ions concentration in channels [Boggs et al., 1993].

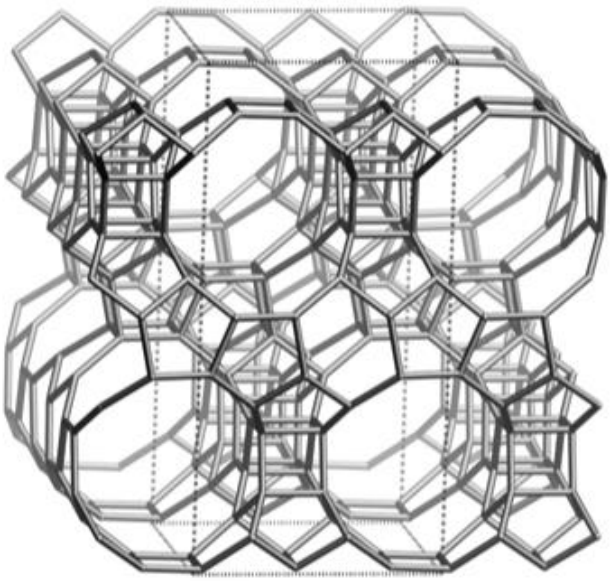

Figure 2.2 Structural framework of BEA zeolite (viewed along [010] [from Baerlocher et al., 2007, with permission]

2.1.2. Mesoporous silica and periodic mesoporous organosilica

Mesoporous silica is a kind of silicon oxide, firstly patented in the late 60-th of XX century [Chiola et al., 1969]. The primary building material is SiO_2. Mesoporous silica is synthesized in a presence of (organic) template, which allows to achieve desired inner-pore structure. Afterwards, template is removed. The mesoporous silica has cubic three-dimensional porous structure, high surface area (>500 m^2/g), pore volume (>0,9 cm^3/g), narrow particle-size distribution, large pores (2-40 nm) is chemically and physically stable, what marks mesoporous silica as a good sorbent [Slowing et al., 2008; Benhamou et al., 2009; Ng et al., 2017; Brankovic et al., 2017]. An example of a template used in the synthesis of mesoporous silica is provided in Figure 2.3.

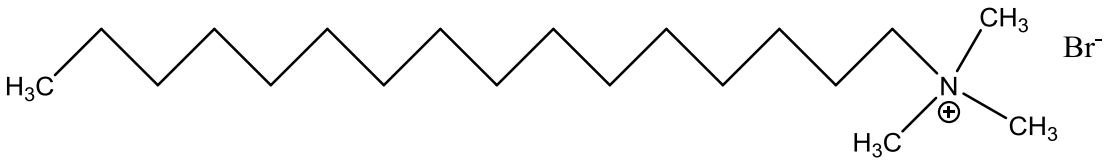

Figure 2.3 Chemical structure of cetyltrimethylammonium bromide (CTAB)

The template is removed by calcination [Liang and Meixner, 2017]. In special cases the template remains in the frame to fulfil the demands to the material.

Periodic Mesoporous Organosilica (PMO-silica) was developed in 1999 [Melde et al., 1999; Inagaki et al., 1999; Asefa et al., 1999]. Since 1999 various organic fragments were combined with mesoporous silica and today PMO is already used in multiple applications, in medicine, adsorption, catalysis etc. PMO combines advantages of mesoporous silica with its ordered pore system and high specific surface area and organic fragments, versatile combination of which allows achieving desired properties for specific applications. Pores of this type of silica are relatively large – 2 – 50 nm. Like mesoporous silica, PMO-silica possesses highly-developed inner-pore system, specific surface area is high (<700 m^2/g) Mesoporous properties of this silica are tailored by the presence of organic fragments in chemical structure.

An example of PMO-silica is shown in Figure 2.4.

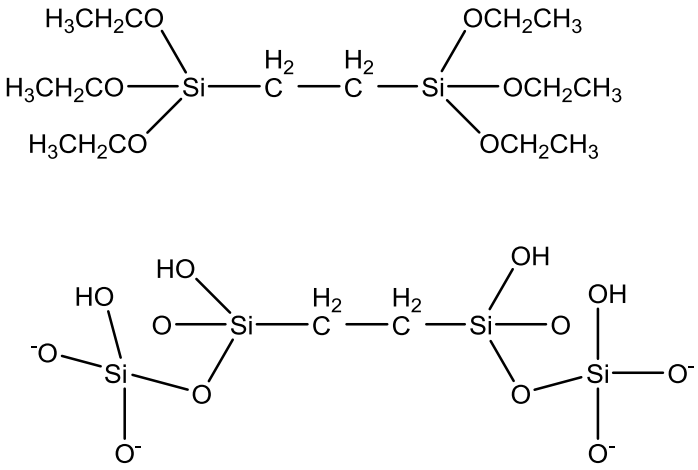

Figure 2.4 Example of PMO-silica fragment structure [from Luo, 2018]

Physical properties, such as point of zero charge may vary significantly from material to material, depending on the composition. PMO-silica like mesoporous silica has a highly developed surface area (800-1300 m^2/g). The presence of organic moiety in the structures of PMO-silica (in the form of functional groups) and in the framework of mesoporous silica impacts the properties of the materials. The hydrophobicity of mesoporous silica is determined by the properties of the template [Luo, 2018].

2.1.3. Aluminium Oxide

Aluminium oxide or alumina is a naturally abundant mineral, that is widely used in different branches of applications due to its low cost and high abundance. On a row with natural minerals, alumina is widely manufactured, which allows controlling properties for the target application.

In environment alumina is wide-spread in three forms:

$\alpha - Al_2O_3$ is the most stable crystallic form of alumina with the rhombohedral (trigonal) crystal structure. It is also known as corundum. The presence of various intrusions of other metals, which define its colour. Saphire, ruby are the examples of corundum with different metals.

The mixture of Na_2O and Al_2O_3 oxides [$Na_2O.11Al_2O_3$] is called diaoyudaoite and is $\beta - Al_2O_3$. Through the heat treatment $\alpha - Al_2O_3$ is transformed into metastable modifications, such as $\gamma - Al_2O_3$ with the cubic crystal structure, which contains molecular water (1-2%) in its structure [Zapolskiy, 1981; Chaliy, 1972]. The modifications of alumina may be transformed into each other, for example $\gamma - Al_2O_3$ transforms into bayerite $\beta - Al(OH)_3$ [Jonsson, 2007]

An amorphous aluminium oxide is a form with poor crystalline structure. In nature, it is abundant in higher soil layers. Due to the poorly structured nature, amorphous alumina has higher physical deformability and may be a subject to structure suppression.
A nonporous alumina is a form with very low porosity and consequently low surface area (0,5-14 m^2/g). Alumina has an amphoteric nature, typical point of zero charge is in a range of pH 8-10, which depends on crystallinity and measurement method [Sposito, 1995].
Aluminium oxide is stable in a pH range 3-12, in extremely acidic and extremely basic conditions aluminium oxide is slightly soluble [Lewis, 2007].

2.2. Pesticides

Pesticides are (organic) substances, used against pests and weeds. Annually around 6 billion tons of pesticides are applied worldwide [Atwood, 2017]. Pesticides like other organic pollutants have high persistence and depending on their structure infiltrate into surface and subsurface waters. There they may persist or may form metabolites [Akesson et al., 2015].
Pesticides in the current work belong to three different classes: insecticides, fungicides and herbicides. Choice of pesticides for the present work was done based on their abundance and persistence in aqueous basins. Table 2.2 provides a summary of physical-chemical parameters of the pesticides, chosen for the present study (data is taken from PPDB).

Table 2.2 Summary of physical-chemical properties of compounds used in the present work [Pesticides Properties Database; Goodwin et al., 2003; Li et al., 2018]

Aqueous Solubility [mg/l] at 20°C	18	100 (150)	184	610	10.500	1.466.561	500.000
Octanol-water partitioning coefficient Kow at 20°C	$7{,}94 \cdot 10^{3}$	$5{,}25 \cdot 10^{3}$	18	3,7	$6 \cdot 10^{-4}$	$2{,}34 \cdot 10^{-2}$	$9{,}77 \cdot 10^{-5}$
Vapor Pressure at 25°C [mPa]	0,018	0,056	$3 \cdot 10^{-7}$	$4 \cdot 10^{-7}$	$1.31 \cdot 10^{-2}$	-	$3{,}10 \cdot 10^{-2}$
Henry's law constant at 25°C [Pa*m³/mol]	$3{,}33 \cdot 10^{-4}$	$9{,}20 \cdot 10^{-5}$	$5 \cdot 10^{-10}$	$1{,}7 \cdot 10^{-10}$	$2 \cdot 10^{-7}$	0,16	$4{,}48 \cdot 10^{-9}$
Dissociation constant (pKa)	2,3	1,09	n/a	n/a [or 11,12]	0,8; 2,2; 5,4; 10,2	1,8; 5,4; 10	<2,0: 2,0; 9,15
Soil adsorption Koc [l/kg]/K_{foc}	1040/-	1086/-	-/393-870	-/109-/411	884-50.660/160 0-60.000	2.002/9.665	600/-
Class	Fungicide	Fungicide	Insecticide	Insecticide	Herbicide	Metabolite of Glyphosate	Herbicide
Name	**Hexaconazole**	**Propiconazole**	**Thiacloprid**	**Imidacloprid**	**Glyphosate**	**AMPA**	**Glufosinate**

2.2.1. Insecticides

Historically insecticides were designed to control insects that are harmful to human or crop. Mode of action of "harmful" insects may be direct, i.e. be dangerous for people or indirect, harming crop, food and textiles.

Neonicotinoids belong to the novel class of insecticides. Neonicotinoids act selectively on nAChRs of invertibrates' central nervous system [Jeschke et al., 2008]. Structural non-similarity of nAChRs of vertebrates and invertebrates explains the high selectivity of neonicotinoids to insects and non-harmful behaviour to mammals and birds. Today neonicotinoids are applied against most of the known crop pest insects [Elbert et al., 2008; Jeschke et al., 2011].

Nowadays seven neonicotinoids are commercially available and represent cyclic [imidacloprid and thiacloprid as five-membered-ring structures and thiamethoxam – six-membered ring structure] and noncyclic structures [Jeschke et al., 2013; Casida et al., 2011; Jeschke et al., 2007].

Neonicotinoids act similarly on target and not-target insects, such as honeybees and wasps [Balança and de Visscher, 1997; Sánchez-Bayo and Goka, 2006].

Nowadays **imidacloprid** is the most widely-distributed insecticide in the world [Simon-Delso et al., 2015]. Imidacloprid is a chloronicotinyl nitroguanidine insecticide with chemical formula: $C_9H_{10}ClN_5O_2$ (Figure 2.5).

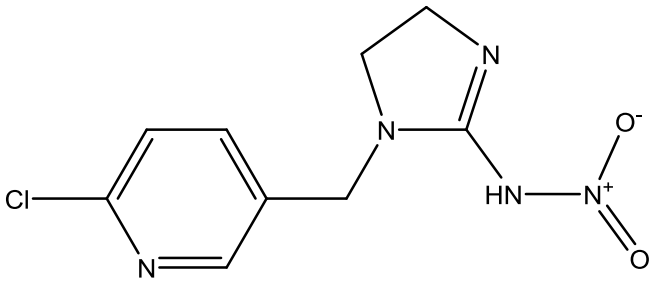

Figure 2.5 Chemical structure of imidacloprid molecule [ChemDrawProfessional 17.1]

Imidacloprid has relatively good water-solubility (610 mg/l), low vapour pressure ($4*10^{-7}$mPa at 25°C, and low volatility (Henry's constant $1,7*10^{-10}$ Pa*m³/mol) [HSDB, US]. Summary of physical-chemical properties of imidacloprid is given in Table 2.2.

The half-life of imidacloprid in soil is 40-190 days depending on presence of the organic substances [Scholz and Spiteller, 1992]. In several studies on 12 soils K_{foc} values of imidacloprid were in a range of 109-411 ml/g, which marks imidacloprid as moderately mobile [PPDB, Univ. of Hertfordshire, 2013].

Imidacloprid undergoes photolytic degradation in water. Hydrolysis of imidacloprid takes place at higher pHs, no hydrolysis is observed under acidic or neutral conditions. Dissociation constant of imidacloprid pKa is at the alkaline conditions (pKa=11,12).

The United States Environmental Protection Agency [U.S. EPA, 2010] classified imidacloprid as non-carcinogenic based on animal studies ["Group E" (noncarcinogenic for humans)]. There is no data on imidacloprid possible carcinogenicity according to the International Agency for Research on Cancer [IARC, 2015]. However, it is classified as potentially toxic for humans [U.S. EPA, 2010]. No data is available on reproductive effects of imidacloprid in humans.

Toxicity to fish is moderately low but rather high for aquatic invertebrates [Kidd and James, 1994].

Thiacloprid or (Z)-[3-[(6-chlor-3-pyridinyl) methyl]-2-thiazolidinylidene]cyanamid is another representing neonicotinoid. Thiacloprid, like imidacloprid, acts as nicotinic acetylcholine receptor (nAChR) agonist [Jeschke et al., 2008]. Thiacloprid's structural formula is depicted in Figure 2.6. Thiacloprid has moderate water solubility (187 mg/l at 20°C); Henry's law constant is of the same order of magnitude as the one of imidacloprid ($4{,}1*10^{-10}$ Pa*m³/mol), which implies non-volatile properties [HSDB, US]. Thiacloprid is slightly mobile (K_{foc}=393-879 ml/g in study on 6 soils). Thiacloprid does not dissociate. Physical properties of thiacloprid are listed in Table 2.2.

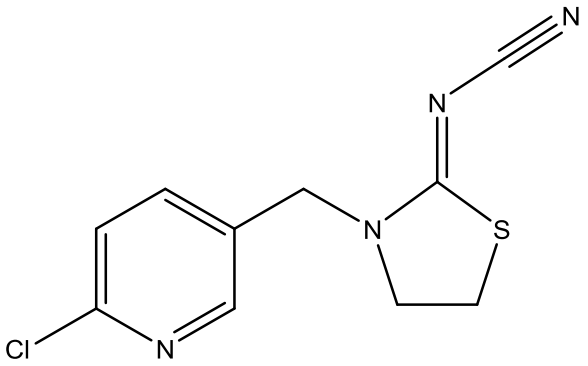

Figure 2.6 Chemical structure of thiacloprid molecule [ChemDrawProfessional 17.1]

Like other neonicotinoids, thiacloprid is a systemic insecticide, performing high toxicity for insecticides and being relatively harmless for mammals. Toxicity for useful insects (for example, bees) is a question of concern. Lethal dosis (LD_{50}) of thiacloprid for bees is determined as 0,0001 μg/μg bee weight [Iwasa et al., 2004].

Degradation time (DT_{50}) of thiacloprid in soil is determined as 15,5 days under typical conditions. In aqueous phase thiacloprid is stable in pH range 5-9, undergoing neither hydrolysis nor photolysis in this range [PPDB, Univ. of Hertfordshire, 2013].

Thiacloprid is classified as possible endocrine disrupter (possible toxicity for liver and thyroid) [Verordnung (EU), 2015].

2.2.2. Azole Fungicides

Azole fungicides belong to the broad-spectrum antifungal compounds used for prevention or curing of fungal deceases [Zarn et al., 2003]. Application mode of azoles is on the crops or on the seeds. Azoles perform both topical and systemic antifungal effect.

Azole fungicides may be divided into two classes: imidazoles and triazoles [Trösken, 2005].

Azole compounds inhibit lanosterol-14α-demethylase (CYP51) [Yoshida, 1988; Podust et al., 2001], which is a cytochrome P450 monooxygenase abundant in fungi, plants, mycobacteria, mammals, including humans [Lepesheva et al., 2003; McLean et al., 2002; Venkateswarlu et al., 1997]. Due to the lipophilic nature of the CYP51 substrate, it is concluded that active sites of an enzyme are penetrated through the membrane [Akhtar et al., 1978].

Propiconazole belongs to the group of triazole fungicides (Figure 2.7). It is a clear-yellowish, highly viscose liquid with a weak characteristic smell. Propiconazole is a systemic foliar fungicide and has different application spheres. It is used as a protecting substance from fungi and viruses for various fruits, cereals, nuts etc. It is also widely-used as wood-preservatives in adhesives, paints, coatings, leather and textiles [EPA, 2016]. Propiconazole is commercially available in a form of stereoisomers mixtures.

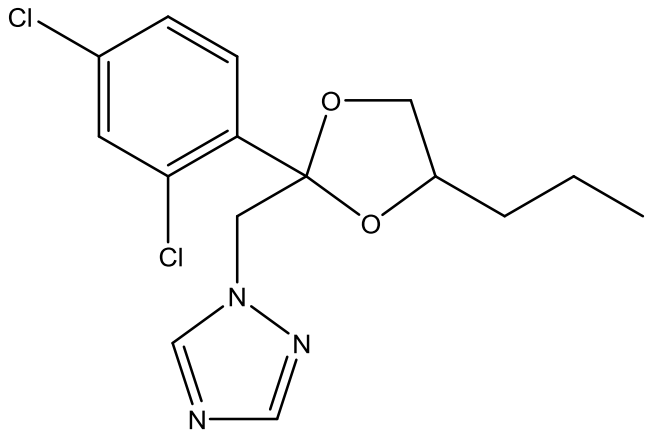

Figure 2.7 Chemical structure of propiconazole molecule [ChemDrawProfessional 17.1]

The mode of action of propiconazole on fungi is demethylation of C-14 during ergosterol biosynthesis, causing accumulation of C-14 methyl sterols. These C-14 methyl sterols slow down the fungal growth

and prevent widening of the fungus. Thus, propiconazole is qualified as fungi-static and not fungicidal (killing fungus) [Tech. inf. Bulletin for Prop. Pest.].

An effect on non-target organisms, such as soil microbes and insects, is very low. No toxic effect was detected for earthworms [Tech. inf. Bulletin for Prop. Pest.].

The pKa value of propiconazole is at 1,09 [PPDB], below it propiconazole is in a protonated form (with protonation at a nitrogen in the triazole moiety), above pKa neutral molecule is a prevailing form of propiconazole.

No hydrolysis of propiconazole at 20°C at three different pHs (5, 7, 9) was observed [Farm chemicals handbook, 1997; U.S. EPA, 1993]. Photolysis of propiconazole was evaluated as 20% in 12 days under daylight. In the presence of natural photosensitizers photodegradation of propiconazole is rather rapid [Tech. inf. Bulletin for Prop. Pest.]. Propiconazole is a non-volatile compound (Henry's law constant $9{,}2*10^{-5}$ Pa*m³/mol).

Water solubility is moderate (moderate-low) (100 mg/l). Due to its affinity to soil rich in organic matter, soil mobility and leaching ability of propiconazole are not high (Koc=1.086 ml/g) [Table 2.2].

According to environmental protection agency propiconazole and its degradation products are supposed not to be carcinogenic [EPA, 2006], however, it is a possible liver and endocrine disruptor.

Hexaconazole is a fungicide from the azole class of pesticides. In early 80-th of 20-th century hexaconazole was used against several fungi species, namely "higher fungi" Ascomycetes and Basidomycetes from Dikarya kingdom [Moore, 1980]. Chemical structure of hexaconazole is presented in Figure 2.8.

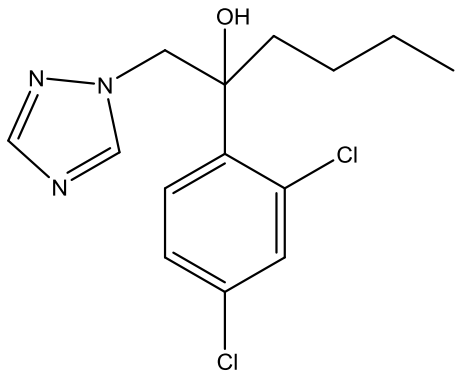

Figure 2.8 Chemical structure of hexaconazole molecule [ChemDrawProfessional 17.1]

Like other azole compounds, hexaconazole has a moderate affinity to the soil with Koc=1.040 ml/g. Hexaconazole has low water solubility (18 mg/l at 20°C, Table 2.2), low volatility (Henry's law constant $3{,}33*10^{-4}$ Pa*m³/mol) [Kamrin, 1997]. Hexaconazole's dissociation constant pKa=2,3. Like for propiconazole, protonation of hexaconazole occurs below pKa at a nitrogen in the triazole moiety; above pH 2,3 hexaconazole is a neutral molecule.

Hexaconazole is known to be stable to hydrolysis, aqueous photolysis (DT50 in days) is moderately fast and takes approximately 10 days. Hexaconazole is persistent in soil under aerobic conditions (DT50 = 225 days) [PPDB, Univ. of Hertfordshire, 2013]. U.S. EPA classifies hexaconazole as possible carcinogen. By decision of EU commission in 2006 it is not used anymore in EU countries as a compound with possible harmful effects even at correct application [Entscheidung 2006/797/EG der Kommission, 2006]. Nevertheless, it is still used in major Asian countries, mainly for rice pest control [Zhang et al., 2015].

2.2.3. Herbicides

Nowadays **phosphonates** are used in different spheres of agriculture [Fest and Schmidt, 1982]. First synthetic phosphonates were synthesized and described in the literature in 1944. 2-Aminoethylphosphonic acid and amino-substituted alkyl-phosphonic acids are typical representatives of this class of compounds [Hildebrand and Henderson, 1983]. Excessive introduction of these compounds in agriculture resulted in their accumulation and pollution of landfills including aquifers.

One of the well-known organophosphorus compounds is glyphosate.

Glyphosate is a broad-spectrum, non-selective systemic herbicide. Due to its efficiency against most of the crop harming plants, glyphosate stays the most widely produced herbicide in the world. It was discovered and patented by John E. Franz from Monsanto company in 1970 [US Patent 3799758, Franz J.E.]. Glyphosate has two main paths to enter the plant: through foliage and partially through roots.

Glyphosate disturbs Shikimate-3-phosphate pathway in plants metabolism by inhibiting the enzyme 5-enylpyruvylshikimate-3-phosphate synthase (EPSPS) and interfering with aromatic amino acids phenylalanine, tyrosine, and tryptophan synthesis [Steinrücken and Amrhein, 1980].

Glyphosate is an organophosphorus compound. It is highly soluble in water (10,5 g/L at 20°C); it has relatively low Kow [log Kow -3,5 at 20] [Schuette, 1998]. Glyphosate molecule has low molecular weight (MW=169,08), carboxylic, amino and phosphonate functional groups. Glyphosate has four acidic constants: (pKa = 0,8; 2,2; 5,4; 10,2, Scheme 2.1) [Goodwin et al., 2003].

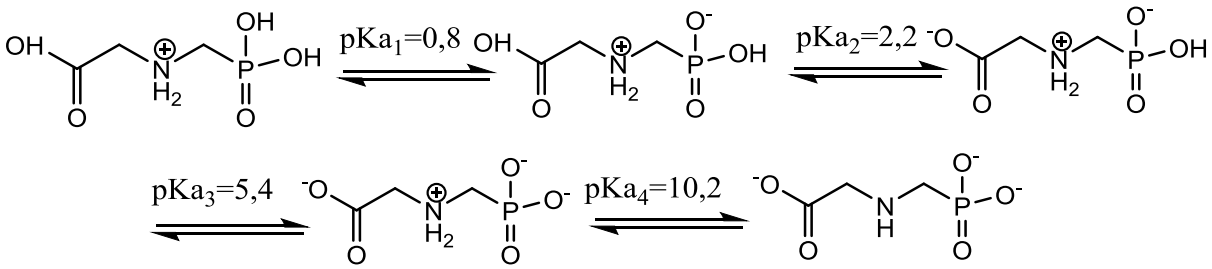

Scheme 2.1 pKa values of glyphosate [from Goodwin et al., 2003]

Summary of the physical properties of glyphosate are presented in Table 2.2. Commercially glyphosate is available in three forms: glyphosate acid, glyphosate isopropylamine salt, glyphosate ammonium salt. High Koc value of glyphosate (884-50.660 ml/g) indicates glyphosate's high affinity to the organic carbon. It may sorb on various minerals in the soil through surface metal coordination. Sorption of glyphosate may cause mobilization of sorbed trace metals by chelation or displacement of ions, such as phosphates. Application of Roundup on agricultural soils caused increased leaching of such metals as Zn, Cu, Ni, P, Al, As, Si [Barret and McBride, 2006]. Another explanation of glyphosate affinity to the soil is the formation of complexes with Ca^{2+}, Cu^{2+}; $Mg^{2+,}$ Fe^{3+}, Al^{3+} [Subramaniam and Hoggard, 1988; McBride, 1991; McBride and Kung, 1989].

Additionally, glyphosate forms inner-sphere complexes with Fe^{3+} and Al^{3+} using phosphonate groups, like phosphate sorption mechanism. Therefore, phosphate is competing with glyphosate for sorption sites [Laitinen et al., 2006].

According to Miles and Moye ,1988 sorption mechanism of glyphosate on soil compartments is mainly due to H-bond formation and inner-sphere complexation with cations (on cations-rich soil).

Nomura and Hilton, 1977 revealed direct proportionality between glyphosate sorption and organic matter content, whereas increasing pH caused lower sorption of glyphosate to the soils.

Glyphosate is stable to aqueous photolysis and hydrolysis [Carlisle and Trevors, 1988; Lund-HØie and Friestad, 1986]. This is due to the lack of absorption bands in UV/VIS spectrum. On the other hand, glyphosate can be a subject for indirect photolysis promoted by $OH^{\cdot}$ Radicals [Manassero et al., 2010; Chen et al., 2012].

Microbial degradation is one of the prevailing pathways of glyphosate degradation in soils [Franz et al., 1997; Laitinen et al., 2006]. The most wide-spread metabolite of glyphosate is AMPA. Another way of metabolization of glyphosate is through plant uptake. In both cases (microbial and plant) glyphosate may undergo two degradation pathways: oxidative cleavage of the C-N bond, producing AMPA or breaking of a C-P bond resulting in sarcosine [Franz et al., 1997].

It is revealed, that glyphosate attenuated in soil does not undergo or undergoes degradation to the lower extent, than freely-dissolved glyphosate. Koc value of glyphosate is high (Koc = 884-50.660; K_{foc} = 1.600-60.000, depending on the soil, [PPDB, Univ. of Hertfordshire, 2013]), thus it is slightly (or non-) mobile. However, due to its pH dependence, glyphosate's sorption on soil is a reversible process. The reversible character of glyphosate sorption conduces its re-mobilization with consequent leaching into lower layers or plant uptake [Salazar and Appleby, 1982].

Nowadays glyphosate is the most prevailing herbicide in the world. Its massive use in agriculture and stability in the environment makes it to the compounds of concern for environment and humans. Various studies concerning its carcinogenicity, toxicity, teratogenicity, mutagenicity were implemented.

Thus, in March 2015 International Agency for Research on Cancer [IARC] has classified it in a category 2A (probably carcinogenic to humans) [IARC, 2015].

Health Canada in April 2017 reported glyphosate as non-genotoxic and probably non-carcinogenic [Health Canada, 2017].

Aminomethylphosphonic acid or AMPA is a metabolite of glyphosate and some other aminophosphonates.

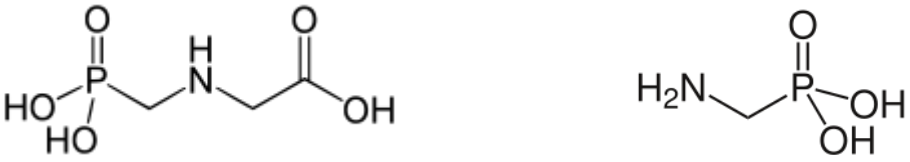

a) b)

Figure 2.9 Chemical structures of a) glyphosate; b) Aminomethylphosphonic acid molecules [ChemDrawProfessional 17.1]

AMPA may be formed through various degradation processes, such as biodegradation by microorganisms: *Escherichia coli, Bacillus megaterium, Streptomyces morookaensis* and some others [Obojska and Lejczak, 2003] and chemical degradation by iron. The microbial degradation of glyphosate is the major degradation pathway leading to AMPA formation in the environment, with chemical and photodegradation pathways being minor ones.

pKa values of AMPA are presented in Scheme 2.3 [Goodwin et al., 2003].

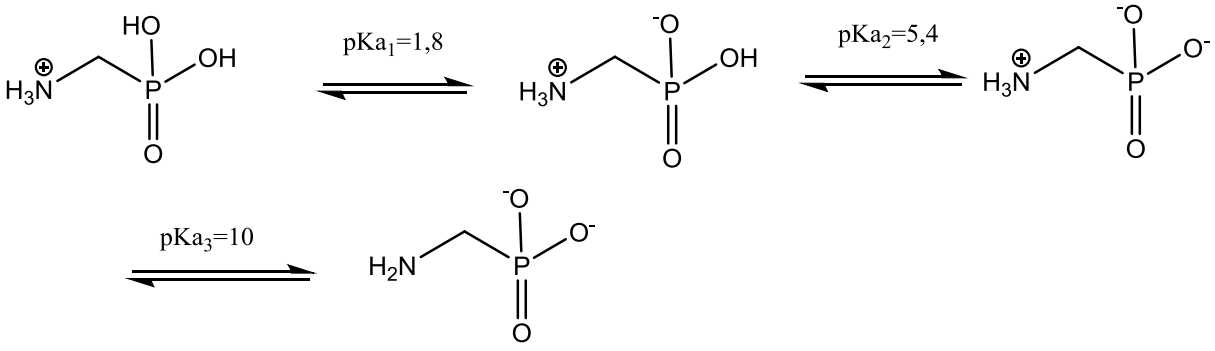

Scheme 2.2 pKa values of AMPA [from Goodwin et al., 2003]

AMPA degradation in soil is slower than that of glyphosate (DT50 under abiotic conditions, field study: 419 days, [PPDB, Univ. of Hertfordshire, 2013]). With Koc value of 2002 ml/g (K_{foc} = 9.664,5 ml/g) it is characterized as slightly (or non-) mobile. Being a degradation product of glyphosate, AMPA is found in the environment in higher concentrations. With a Henry's law constant 0,16 Pa*m³/mol AMPA is

considered moderately volatile. Having very high water-solubility coefficient – 1.466.561 mg/l at 20°C [PPDB, University of Hertfordshire, 2013] and being persistent in water, AMPA is found in groundwaters in high concentration over long periods of time. The Pesticide Properties Database [PPDB, 2016] has classified AMPA as persistent with the half-life (DT50) of 121 days. Major degradation pathway of AMPA is microbial biodegradation, that is directly proportional to temperature and OM content [Simonson et al., 2008]. According to Marrs and Ballantyne, 2004, AMPA has very low acute toxicity, is non-mutagenic.

Glufosinate ammonium

Glufosinate is used on the market as glufosinate ammonium or ammonium-2-amino-4-(hydroxymethyl-phosphinyl)butyrat.

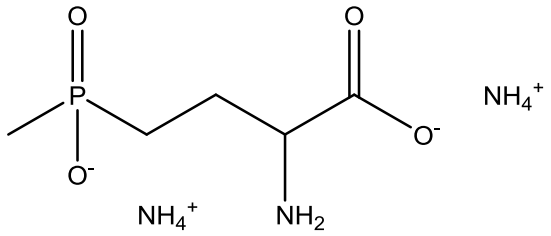

Figure 2.10 Chemical structure of glufosinate ammonium molecule [ChemDrawProfessional 17.1]

Glufosinate ammonium is a non-selective broad-spectrum herbicide, which needs total area coverage. Glufosinate is soluble in water and insoluble in organic (non-polar) solvents [Everman, 2008; Everman et al., 2009; Martinson, 2002]. Glufosinate ammonium affects the glutamine synthetase enzyme and inhibits glutamine amino acid synthesis and ammonia transformation [Everman, 2008]. Accumulated ammonia causes necrosis of the plant with chloroplasts and membranes destruction and leads to the plant death [Everman, 2008]. Glufosinate is classified as low or moderately toxic to mammals. Thus, LD50 for mice is 450 mg/kg and 300 mg/kg for dogs [Sparling, 2016]. U.S. EPA classified glufosinate ammonium as not likely carcinogenic to humans with the very low toxicity of 140 µg/l.

Glufosinate is highly soluble in water: 786 g/l, is non-volatile bioaccumulation of glufosinate is low [Sparling, 2016]. Farm Chemicals Handbook (2002) reports even higher water solubility (1.370 g/l).

Low Henry's law constant $4{,}48*10^{-9}$ Pa*m³/mol indicates non-volatile character of glufosinate.

Under aerobic conditions glufosinate is non-persistent in soil. Half-life in soil is 3-43 days [Jewell and Buffin, 2001]. Half-life in water is longer: around 300 days [Jewell and Buffin, 2001]. Glufosinate does not undergo aqueous photolysis and hydrolysis [PPDB, Univ. of Hertfordshire, 2013].

2.3. Methods

2.3.1. Capillary Electrophoresis (CE)

Capillary Electrophoresis (CE) is a relatively new method, which is widely used for the analysis of peptides, ions and various charged particles. The separation of the charged particles is provided by electric field application. CE is conducted in a very thin capillaries (20-100 µm) (Karcher, 1995) and is applied to the analysis of ions and peptides. An advantage of a thin capillary is equal temperature distribution between its outer and inner parts [Wimmer, 2017]. Thus, the sample in the capillary flows with the same velocity at the walls and in the centre, resulting in an electroosmotic flow (EOF). The advantage of the EOF flow in comparison to the laminar flow, is explained by the even distribution of the sample in the capillary and consequently, better analysis of the compound.

An important factor, affecting the EOF is a pH in the capillary. At high pH solute may achieve high EOF and elute too fast [HP – CE, Agil. Techn. manual]. At low pH, negatively charged surface of the capillary may attract and retain positively charged species. According to Wimmer (2017), for the analysis of glyphosate at very acidic pH (<2) the main obstacle for the analysis was an interaction between capillary silica surface and the molecule of glyphosate due to its protonated state. To avoid that, it was decided to use capillaries with coatings (polyvinyl alcohol (PVA)), preventing glyphosate from the direct interaction with the capillary surface [Wimmer, 2017]. The CE was coupled with ESI-MS and analysis of glyphosate, AMPA, phosphate and glufosinate were conducted using CE-ESI-MS.

The CE separation was conducted on Agilent Technologies 7100 capillary electrophoresis (Waldbronn, DE) with Agilent Technologies massspectrometer (Santa Clara, US-CA), modell 6550 iFunnel Q-ToF LC/MS. Ionisation of the sample was done on Dual-ESI-Ionsource. The Sheath Liquid (SL) was pumped with Agilent 1260 Infinity isocratic pump with flow rate 5 µl/min. For some samples UV-DAD-detection of 7100 CE was used. The 65 cm (CE-MS) or 35 cm (CE-UV) long PVA-capillaries from Agilent (Waldbronn, DE) with 50 µm internal diameter (ID) were used [Wimmer, 2017].

2.3.2. ATR-FTIR

ATR technique is a sampling method, in which infrared beam is getting reflected of the internal surface (ATR crystal), forming evanescent wave, which extends into the sample [Güldenhaupt, 2010]. An advantage of ATR is ability to analyze both liquid and solid samples without pretreatment (pellets formation, pre-concentration etc.).

The qualitative parameter of ATR method is the penetration depth:

$$d_p = \frac{\lambda}{2\pi\sqrt{n_1^2 sin^2\theta - n_2^2}} \quad (2.1)$$

d_p- penetration depth [µm];

θ – angle of the incident radiation [radians];

λ – wavelength of incident radiation [in µm=10000/wavenumber in cm^{-1}];

n_1 – refractive index of ATR crystal;

n_2- refractive index of the sample;

$$l_{eff} = d_p * N_{refl} \quad (2.2)$$

l_{eff} −effective beam pathway [µm];

N_{refl} – number o f reflections (for Bio-ATR II: 9-12) [Brucker Confocheck Benutzerhandbuch]

The effective volume is calculated from the penetration depth and radius of the ATR spot.

$$V_{eff} = \pi r^2 d_p \quad (2.3)$$

r −radius of ATR crystal spot, [mm]

There are several factors, restricting applicability of ATR method. Among them is geometry of the system and crystal material. The most widely used crystals are germanium, sapphire, chalcogenides, silver halides, zinc sulphide, silicon, zinc selenide. BIO ATR cell II with silicon crystal was used in the current work.

Infrared spectra were recorded on a Brucker Vertex80v with LN-MCT Mid VP detector at 22°C temperature (controlled by cooling system) and atmospheric pressure. Spectra were recorded at 400 scan number with optical resolution 4 cm^{-1} mainly in fingerprint region. Opus visual software was used for the spectra interpretation.

2.3.3. Langmuir sorption model

Langmuir, Freundlich and BET (Brunauer-Emmett-Teller) models are the most often used sorption models, used to describe sorption of aqueous or liquid samples on solid materials [Schwarzenbach et al., 2005].

Langmuir model describes sorption on the solid surfaces with the following assumptions:

The surface of the sorbent is homogeneous, i.e. all the sorption sites are equally accessible by sorbate molecule. Maximum one molecule of the sorbate may sorb on one sorption site (mono-layer sorption).

The sorbed molecules don't interact with one another and don't affect the sorption properties of the neighbouring sorption sites [Schwarzenbach et al., 2005].

Langmuir model may be derived from the equation 2.4:

$$S + C_{aq} \overset{K_L}{\leftrightarrow} C_{sorb} \quad 2.4$$

Equation (2.4) depicts sorption of the compound [C] from aqueous phase onto S binding sites of the sorbent. One of the central assumptions of the Langmuir model is an equal activity of all sorption sites S. Equilibrium of the system is described with Langmuir constant:

$$K_L = \frac{C_{sorb}}{S.C_{aq}} \quad 2.5$$

C_{sorb} −sorbed concentration [mg/kg];

$C_{aq}(or\ C_W)$ −aqueous concentration in equilibrium [mg/l];

K_L −Langmuir equation constant [l/kg]

Since at the most one molecule of the compound C may sorb on each sorption site S (monolayer coverage), sorption is limited to C_{sorb_max}:

$$C_{sorb\_max} = S + C_{sorb} \quad 2.6$$

C_{sorb_max} −maximum sorption capacity [mg/kg];

Combining the equations (2.5) and (2.6) gives Langmuir isotherm:

$$C_{sorb} = \frac{K_L.C_{aq}}{1+K_L.C_{aq}} C_{sorb\_max} \quad 2.7$$

In linearized form equation (2.7) transforms into:

$$\frac{C_{sorb}}{C_{aq}} = K_L.(C_{sorb\_max} - C_{sorb}); K_d = \frac{C_{sorb}}{C_{aq}} \quad 2.8$$

K_d – distribution coefficient, which is constant in a linear range [l/kg].

At the low concentrations with $C_{sorb} \ll C_{sorb\_max}$:

$$\frac{C_{sorb}}{C_{aq}} = K_L.C_{sorb\_max} \quad 2.9$$

$$K_d^* = K_L.[C]_{sorb_{max}} \quad 2.10$$

K_d^* - distribution coefficient at low concentrations

2.3.4. Liquid chromatography

Liquid chromatography was performed using an Agilent 1260 infinity device including solvent degasser, binary pump, auto-sampler and column compartment. 3 µL of sample were injected on a Phenomenex Synergi Polar-RP 80A column with 4 µm particle size, 3 mm internal diameter and 150 mm length. Thiacloprid was eluted with isocratic mixture of 50% water and 50% acetonitrile (both acidified with

0,1% formic acid) at 0,6 ml/min for 4 minutes. For propiconazole and hexaconazole water/acetonitrile ratio was 35%/65%.

2.3.5. Mass spectrometry

After liquid chromatography, thiacloprid was detected by tandem mass spectrometry using an Agilent 6490 triple quadrupole mass spectrometer with positive electrospray ionization (ESI+). Ionization was performed applying 12 l/min of nitrogen at 400°C as sheath gas, 16 l/min of nitrogen at 150° C as drying gas, a nebulizer pressure of 35 psi and a capillary voltage of 2500V with 0V for the nozzle. Thiacloprid was then detected using three transitions: one quantifier 253→126 (20 eV collision energy) along with two qualifiers 253→89,9 and 253→98,9 (both with 45 eV collision energy). Propiconazole was detected using two transitions: 342→159 (36 eV collision energy) and 342→69 (24eV collision energy). For hexaconazole detection two transitions were used: 314→159 (30 eV collision energy) and 314→70 (20 eV collision energy).

2.3.6. HPLC

High performance liquid chromatography was performed on Shimadzu LC solution device (with LC-20AD solvent delivery module, DGU-20A_3/DGU-20A_5 on-line degasser, SPD-M20A UV-VIS photodiode array detector, SI C-20A(20AC SIL-20 AHT)20 ACHT autosampler, CBM-20A/20Alite system controller). Reverse phase HPLC was conducted with Agilent column Eclipse Plus C18 (3,5 µm; 4,6*100 mm). Analysis was done using binary gradient mode with total flow 0,4 ml/min, 40% H_2O and 60% MeOH for neonicotinoids and 20% H_2O and 80% MeOH for azole fungicides.

2.3.7. Zeta potential

Zeta potential was measured on Malvern Zetasizer Nano ZSP at room temperature (23°C), with preliminary preparation of sample suspension in water solution by sonication.

2.4. Chemicals

- Agilent 5182-0567, polypropylene 1ml (for glyphosate-containing samples)
- Agilent Technologies 5181-1513, Snap caps, polyethylene olefin

- Al/SiO_2 (labeled TU249C) (synthesized by Yucang Liang at the University of Tübingen, Department of Anorganic Chemistry
- Aluminum oxide Al_2O_3 (Aldrich)
- Aluminum oxide Al_2O_3 (synthesized by Leilei Luo at the University of Tübingen, Department of Anorganic Chemistry)
- Aminomethylphosphonsäure (AMPA) (Sigma)
- BCB 070300 screw cap with septa-silicone
- BCB 1,5 screw neck vials (32*11,6 mm) (HPLC vials)
- Bentonite (Aldrich)
- Calcium chloride dihydrate (Sigma Aldrich)
- Ferrihydrite (synthesized by James Byrne, University of Tübingen, Microbiology Department)
- Fisherbrand 1154-1454 lids
- Glufosinate ammonium (Sigma Aldrich)
- Glyphosate (Sigma Aldrich)
- Hexaconazole (Sigma Aldrich)
- Hydrogen chloride HCl (Merck)
- Imidacloprid (Sigma Aldrich)
- Iron oxide Fe_2O_3 (maghemite) (Aldrich)
- MCM-48 (synthesized by Leilei Luo at the University of Tübingen, Department of Anorganic Chemistry)
- Methanol HPLC grade (Sigma Aldrich, Chromasolv)
- pH 0-14 (step 1) (Chemsolute test) pH strips
- pH 4,0-7,0 (step 0,2-0,3) (M ColorHast) pH strips
- pH 6,5 – 10,0 (step 0,2-0,3) (M ColorHast) pH strips
- pH 6,5 – 10,0 (step 0,3) (Merck) pH strips
- pH 7,5 – 14 (step 0,5) (Alkalit) pH strips
- PMO-silica (synthesized by Leilei Luo at the University of Tübingen, Department of Anorganic Chemistry)
- Potassium Chloride KCl (AppliChem)
- Propiconazole (Sigma Aldrich)
- Safe-lock Eppendorf tubes, 2ml
- SiO_2 (labeled TU243C) (synthesized by Yucang Liang at the University of Tübingen, Department of Anorganic Chemistry)
- Sodium hydroxide NaOH (Merck)

- Suwannee River Humic Acid standard I (SRHA; 2S101H) from the International Humic Substances Society (IHSS).
- Thermo-scientific 2ml, clear, microcentrifuge tubes
- Thiacloprid (Sigma Aldrich)
- Zeolite beta(OH)-III (synthesized at the North-Korean University by Hwa Jun Lee)
- Zeolites (Alfa Aesar)

2.6. Equipment list

Centrifuges:

- Eppendorf 5417 C
- Eppendorf Hermle Z320
- Herolab HiCen 21
- Heraeus Megafuge 1.OR

- US rod: Bandelin sonopuls HD 2200/UW 2200
- Horizontal shaker: IKA-Werke HS501 digital
- CE: Agilent Technologies 7100 capillary electrophoresis
- LC-MS: Agilent Technologies 6490 TripleQuad LC/MS
- HPLC: Shimadzu: Liquid chromatograph: LC-20AD
    - Degasser: DGU-20A_3
    - Diode array detector: SPD-M20A
    - Auto sampler: SIS-20ACHT
- FTIR-ATR: Bruker VERTEX 80v FTIR spectrometer with LN-MCT Mid VP detector with BIO ATR II
- Zeta potential measurements: Malvern Zetasizer Nano ZSP

Chapter 3 Sorption of Neonicotinoid Insecticides on Zeolites

3.1. Introduction

Neonicotinoids are widely-used in agriculture against almost all the known crop pest insects [Elbert et al., 2008; Jeschke et al., 2011]. Now imidacloprid is the most-sold insecticide in the World [Simon-Delso et al., 2015]. Due to their wide distribution and similar effect for target- and non-target organisms [Balança and de Visscher, 1997; Sanchez-Bayo and Goka, 2006], neonicotinoids' environmental fate is a question of concern and was studied by several researchers [De Smedt et al., 2015; Bonmatin et al., 2014]. Attenuation of neonicotinoids through adsorption was studied and reported in the literature [Daneshvar et al., 2007; Liu et al., 2006; Bajeer et al., 2012].

The objective of the present chapter is to study the adsorption of thiacloprid and imidacloprid on the (nano-)zeolites. Zeolites are known as effective adsorbents. A detailed description of zeolites' properties is given in Chapter 2. Although, sorption of imidacloprid on zeolites was studied previously [De Smedt et al., 2015; Rongchapo, 2015], this study focuses on the small zeolite particles (<1µm). The toxicological studies (described in detail in Chapter 9) prompted the choice of the small particle size of the zeolite. The initial choice of the particle size of 100 nm was changed to a larger size of 600-700 nm due the issues with surface charge and aggregation. It was expected to achieve high sorption of imidacloprid and thiacloprid on the zeolites [De Smedt et al., 2015; Rongchapo, 2015].

Ionic strength, the presence of cations and pH are important environmental parameters which may significantly affect the sorption behaviour of organic molecules. Natural waters have high variability of pH (in the range of 4-10). Calcium is abundant in the most water basins. Only a few papers are available on the effect of the ionic strength on Ca^{2+} effect on TC and IC sorption [Li et al., 2003; Muszynsky and Brodawska, 2014]. To fullfil the existent knowledge gap, present work researches the impact of the ionic strength, presence of Ca^{2+} cations, HA presence, competitive sorption, pH factors on neonicotinoids sorption. Many studies show that uncharged molecules are not affected by the ionic strength by the same mechanisms as charged molecules [Alva and Singh, 1991; Clausen et al., 2001; de Jonge and de Jonge, 1999]. Due to the non-charged character of the imidacloprid and thiacloprid molecules, it was not expected to observe high pH effect on their sorption. Ca^{2+} cations were expected to replace some exchangeable cations from the zeolite. The effect of the exchange was investigated under different mechanisms of IC and TC adsorption. Li et al., 2013 reported diminishing effect of Ca^{2+} ions on TC and IC sorption on smectites. Due to the significant difference between clays and zeolites structure and the scarcity of the literature on this topic, it was planned to determine the Ca^{2+} effect on thiacloprid and imidacloprid sorption on zeolites.

Many uncharged organic compounds sorb strongly to the natural organic matter in water and soil. Numerous studies have concluded an increase in organic pollutants sorption with increasing NOM content [Bekbolet et al., 1999; Gonzalez and Ukrainczyk, 1996; Mallawatantri and Mulla, 1992]. Karickhoff, 1979, Schwarzenbach and Westfall, 1981 and Schwarzenbach, 1993 demonstrated, that the organic carbon content of the particles is an important parameter for the sorption of hydrophobic pesticides
Thermodynamically, adsorption on the organic matter is favourable for hydrophobic compounds. Eisenreich demonstrated, that the pesticides with low water solubility readily sorb to the particulate organic carbon [Eisenreich et al., 1981; Nowell et al., 1999].
Considering moderate water solubility of imidacloprid and thiacloprid (Table 2.2), NOM was expected to have only slight effect on the imidacloprid and thiacloprid sorption.
Hence organic pollutants have various sources and are rarely found in nature as single compounds, the competitive sorption of the pesticides should be studied to reveal how the presence of more than one compound impacts the sorption of the target compound. The competitive sorption of imidacloprid and thiacloprid was studied. Since both compounds have similar structures, the competition for the sorption sites was expected, implying a decrease in sorption from the mixture in comparison to the individual pesticide sorption.
One of the objectives of interdisciplinary cooperation project EXPAND was to investigate an effect of sorption of thiacloprid on the mortality and behaviour of *Chironomus riparius* larvae. An effective sorbent for neonicotinoids found in the current experiment was used in the toxicological studies to decrease the bioavailability of the pesticide and in order to change of toxicological effects for the studied organisms. An objective of the toxicological studies [Lorenz et al., 2017b] was to investigate, how the sorption of thiacloprid on zeolites affects the toxicological effects of thiacloprid for *C. riparius* larvae (Chapter 9).

Mass balance

The decrease in the aqueous concentration may be due to the sorption, as well as other processes, such as evaporation, degradation and metabolization etc. To assure, that the decrease in the dissolved concentration results from the sorption, a mass balance was calculated. The elements of the pesticide mass balance include concentration in the aqueous phase after the equilibrium in sorption experiments was reached (Cw_eq), pesticide concentration, that desorbed from the sorbent in water in desorption experiments (Cw_desorb) and pesticide concentration that was extracted from the sorbent with methanol (Cw_extract). Samples from the kinetics experiments were used for the mass balance calculation.

Figure 3.1. depicts the mass balance of IC and TC (a and b, respectively). Extraction was done with methanol for 24 hours.

The recovery rate of pesticides was very high (95-102%). Therefore, for the present experiments decrease in aqueous concentration was primarily due to the sorption processes, side reactions and unexpected loss can be neglected.

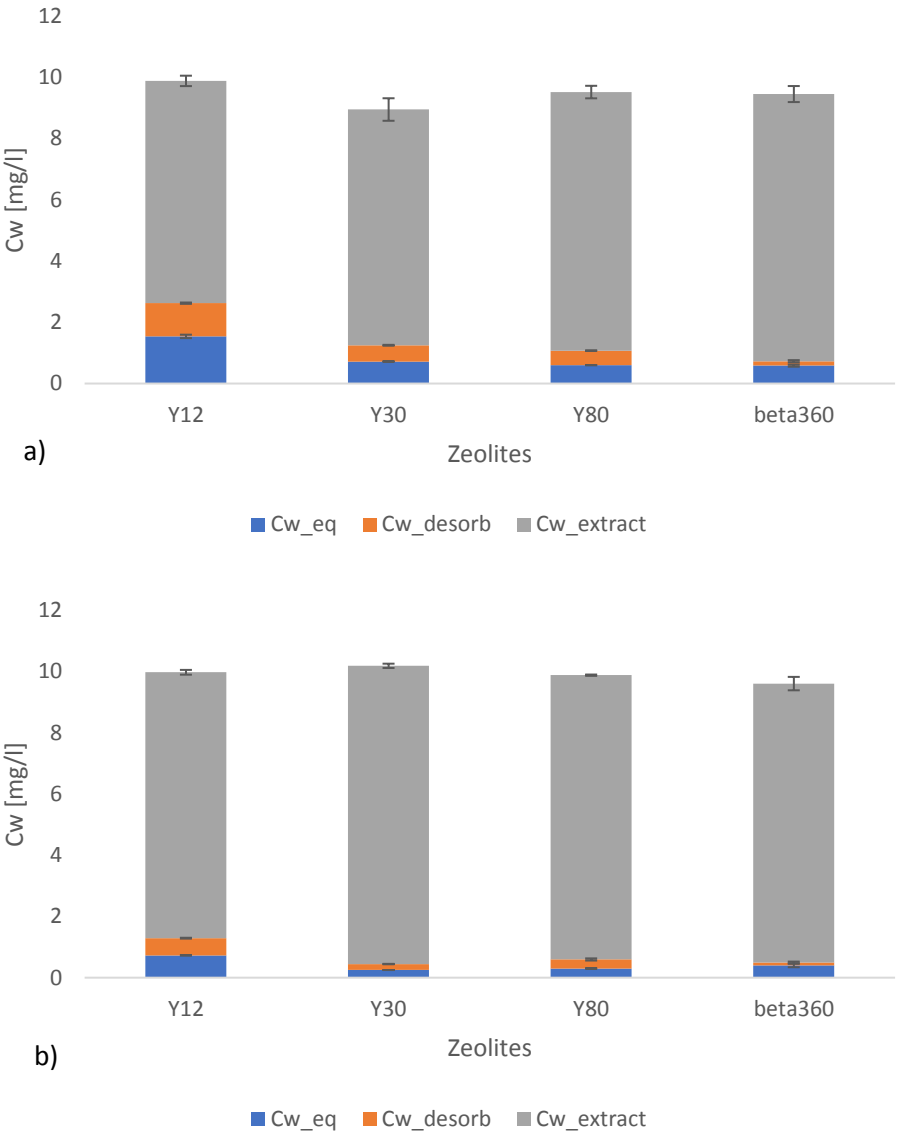

Figure 3.1 Mass balance of a) imidacloprid; b) thiacloprid in sorption on zeolites experiments. An average value of triplicates is presented. Error bars present the standard deviation between the triplicates

3.2. Experimental Part

Experiments were designed and conducted using the batch equilibrium method. Every sample including controls was prepared in triplicates; the reported values are the average of the three measurements. Aliquots of thiacloprid (imidacloprid) and zeolites were mixed in HPLC vials (1,5 ml). Solutions of $CaCl_2$, KCl and humic acid [Suwannee River] were added to the samples at different concentrations. pH was adjusted with HCl and NaOH and measured with a pH electrode. Samples were shaken on the horizontal shaker [IKA] for 60 minutes to reach equilibrium conditions. Thereafter, vials were centrifuged [Heraeus Megafuge 1.OR], and aqueous phase pipetted into the fresh HPLC vials. Imidacloprid and thiacloprid were measured using HPLC technique [Shimadzu], isocratic method, 60% MeOH in the mobile phase. HA concentrations were measured photometrically at 364 nm.

3.3. Results and Discussion

Sorption kinetics of the neonicotinoids imidacloprid and thiacloprid on zeolites

Figure 3.2 shows the sorption kinetics of thiacloprid on various zeolites. In the experiments with Y type zeolites, sorption equilibrium was reached within the first ten minutes.

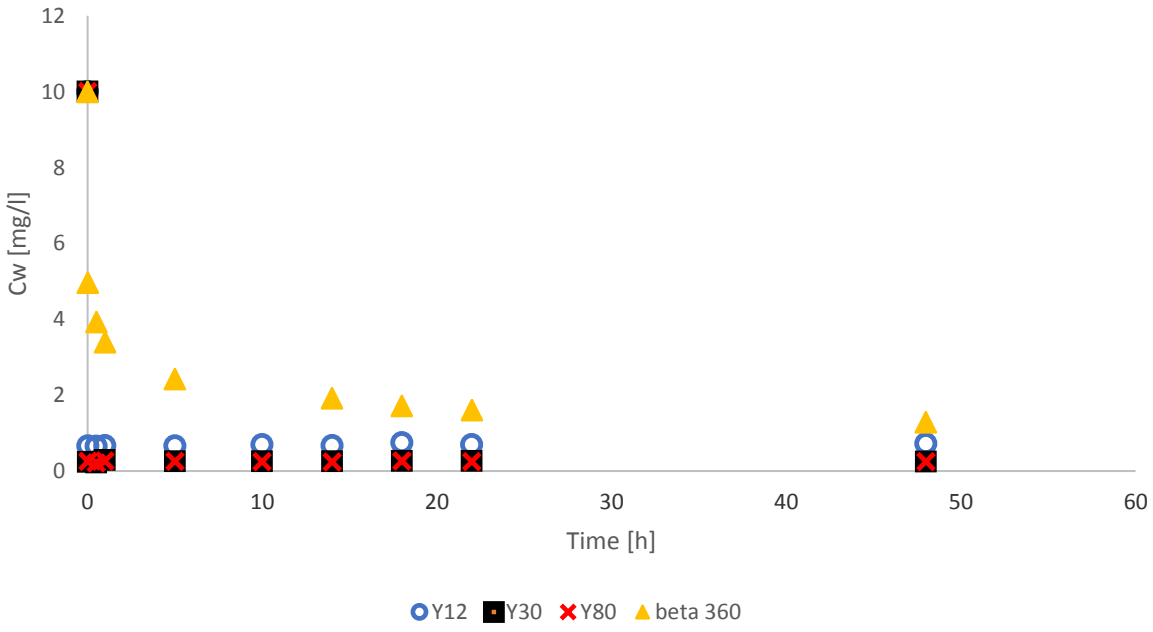

Figure 3.2 Sorption kinetics of thiacloprid on Y30, Y12, Y80, beta360 zeolites [I=0,05 M, T=20°C (room temperature), pH 7]

Sorption of thiacloprid on BEA zeolites was high, but sorption kinetics was noticeably slower on BEA zeolites than on FAU zeolites. Sorption kinetics on BEA zeolites clearly shows, that within 15 hours contact time concentration of freely dissolved thiacloprid was continuously decreasing.

This difference in sorption kinetics can be explained by the different pore size and pore accessibility of Y type and beta type zeolites (Figure 3.3). Zeolite BEA has pores of irregular spherical shape (Figure 3.3), which have different diameters, viewed along different angles (Figure 3.3). The pores of FAU are larger and have the same diameter from every angle, which facilitates the access of neonicotinoids into FAU pores. The access to the BEA pores is more complicated and requires more time until neonicotinoids molecules diffuse into the pores and sorb there.

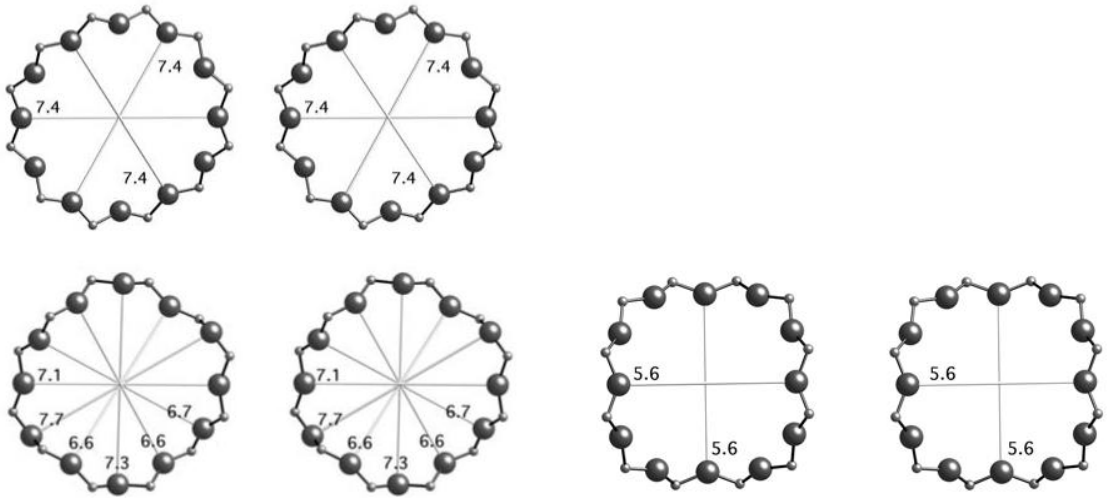

Figure 3.3 The pores of FAU zeolite (viewed along <100>; above), and BEA zeolites (viewed along <100> and <001>; below) [from Baerlocher et al., 2007, with permission]

Desorption kinetics of thiacloprid from the zeolites was fast ($t_{eq} \leq 10$ min), as depicted in Figure 3.4. Comparison of freely dissolved thiacloprid concentration (percentage of total concentration) suggests a reversible character of the sorption. Total concentration in sorption kinetics experiment was concentration measured in controls; total concentration in desorption kinetics experiment was measured as a sum of dissolved concentration and concentration, extracted by methanol out of sedimented particles. Even for beta 360 zeolite desorption equilibrium was reached faster than sorption equilibrium, during following 45 hours freely dissolved concentration of thiacloprid remained unchanged. Equilibrium concentration in desorption experiments was significantly lower than in sorption experiments (in both experiments concentration is presented as % of total concentration). The observed hysteresis between sorption and desorption was caused by the geometry of the pores: it was expected, that the molecules of imidacloprid and thiacloprid access the pores, but their desorption may be complicated by sterically

hindered position of the functional groups of neonicotinoids in the pore, i.e. the neonicotinoid molecule was “trapped” in the pore.

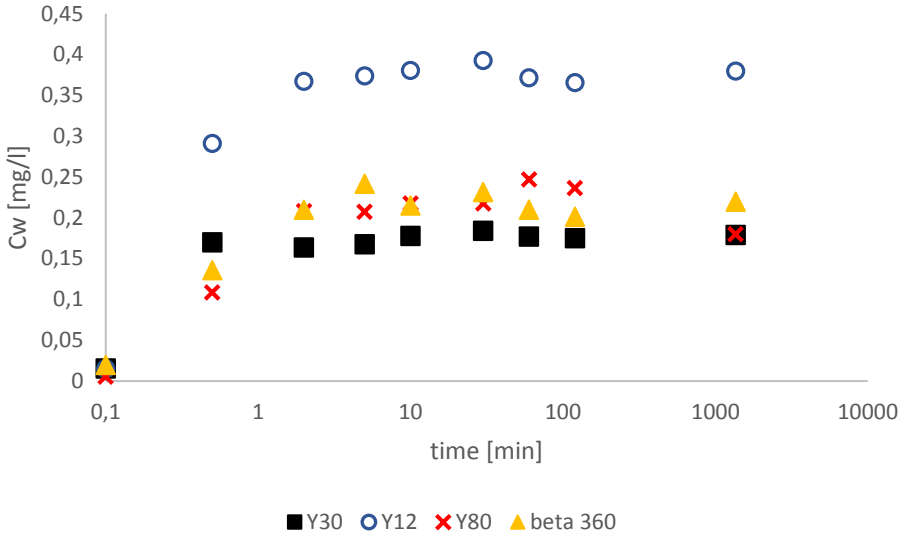

Figure 3.4 Desorption kinetics of thiacloprid on Y12, Y30, Y80 and beta360 zeolites [I=0,05 M (KCl), T=20°C (room temperature), pH 7]

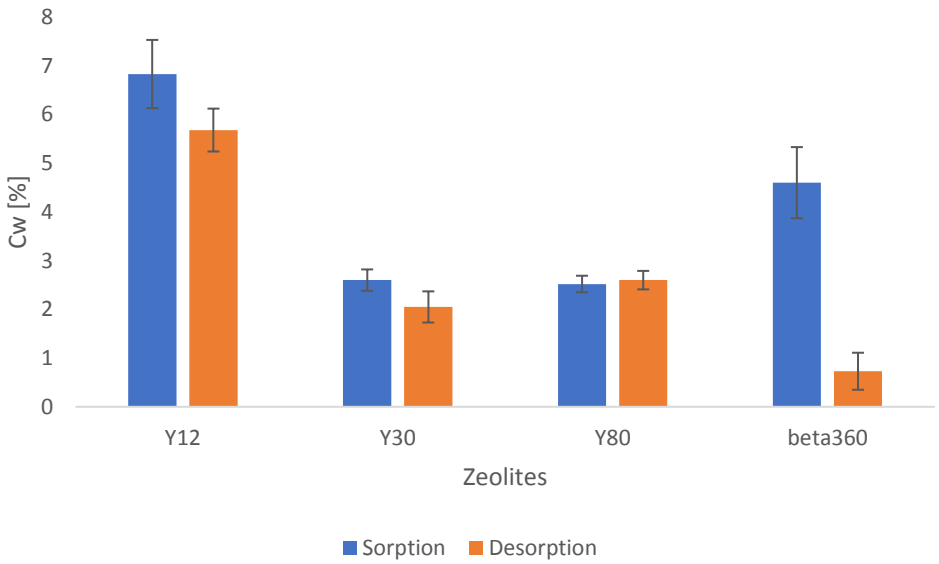

Figure 3.5 Comparison of equilibrium aqueous concentrations of thiacloprid in sorption experiments with Y12, Y13, Y80 and beta360 zeolites. Concentration Cw is depicted in per cent (%) of total thiacloprid concentration

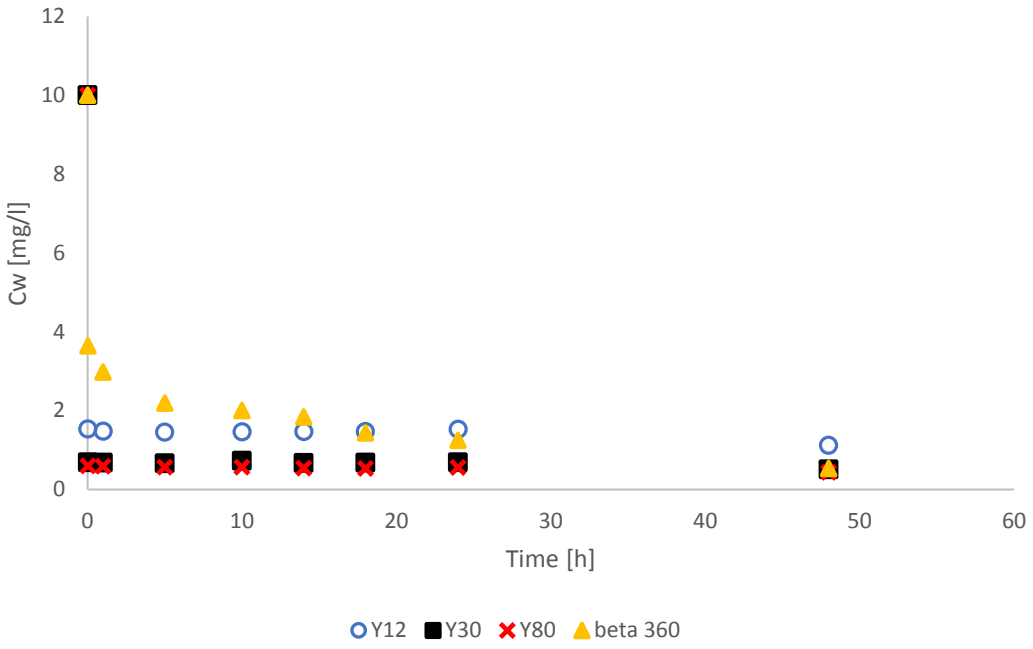

Figure 3.6 Sorption kinetics of imidacloprid on four zeolites (Y12, Y30, Y80, beta360) [I=0,05 M (KCl); T=20°C (room temperature), pH 7]

Sorption kinetics of imidacloprid on zeolites was similar to thiacloprid.

Sorption of imidacloprid on FAU type zeolites was very fast (<10 min). Sorption equilibrium on beta 360 was reached after 24 hours. Such similarity with thiacloprid in sorption behaviour is due to the structural similarity of the thiacloprid and imidacloprid molecules, defining their size [the longest side for each molecule is 0,7 nm by topological measurement, Avogadro 1.90] and space orientation.

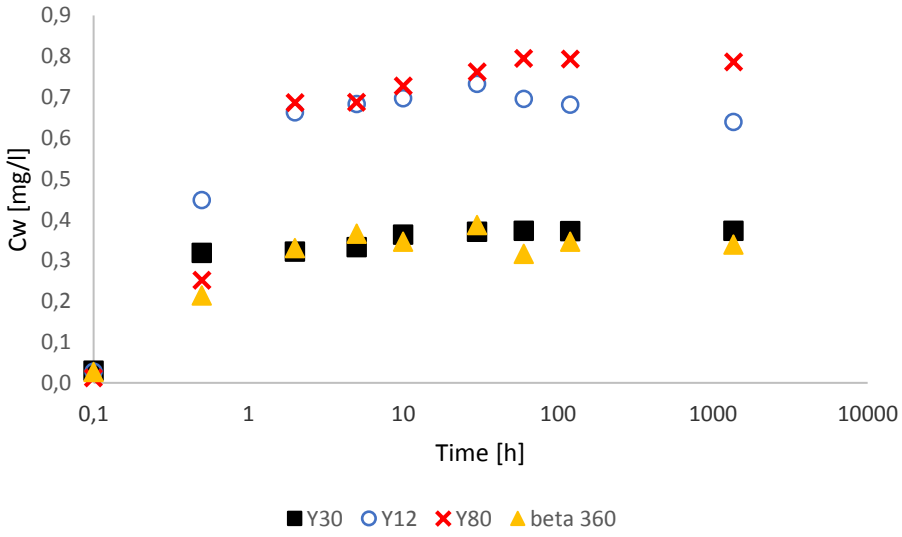

Figure 3.7 Desorption kinetics of imidacloprid on Y12, Y30, Y80 and beta360 zeolites [I=0,05 M (KCl); T=20°C (room temperature), pH 7]

Desorption of imidacloprid from the zeolites was fast (<10 min) (Figure 3.7). Comparison of aqueous concentrations (%) in sorption and desorption experiments prooves the reversibility of sorption on FAU zeolites, which converges with thiacloprid sorption behaviour on the same zeolites (Figure 3.8). Similarly to the desorption of thiacloprid, imidacloprid's desorption rate from beta360 was lower than from the Y zeolites.

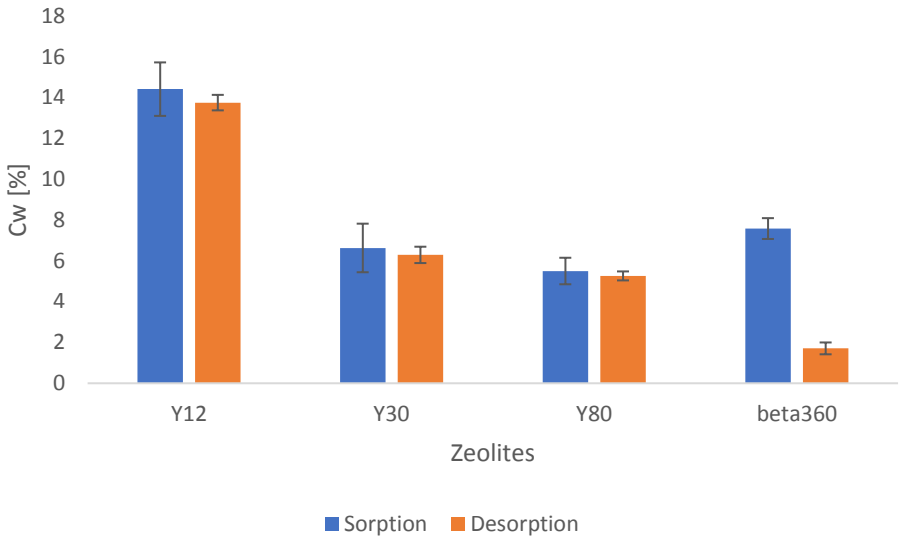

Figure 3.8 Comparison of equilibrium aqueous concentrations of imidacloprid in sorption experiments on Y12, Y30, Y80 and beta360 zeolites. Concentration Cw is depicted in per cent (%) of total imidacloprid concentration

Grathwohl and Reinhard, 1993 discussed the non-equilibrium in contaminant desorption ("Tailing"). They mention, that "Tailing" is independent of the water amount. Using a short period approximation of the diffusion-controlled contaminant uptake and release from a particle (infinite bath) (eq. 3.1), the diffusion rates for sorption and desorption of imidacloprid on beta360 and Y30 were calculated.

$$\frac{M}{M_{eq}} = 6\sqrt{\frac{D_a.t}{a^2.\pi}} - 3\frac{D_a.t}{a^2} \qquad 3.1$$

M —mass of the compound, diffused into the particle after a certain time t;

M_{eq} —contaminant mass, which is in the particle grain under equilibrium conditions;

$\frac{D_a}{a^2}$ —diffusion rate constant;

a — particle radius; [Grathwohl and Reinhard, 1993]

For Y30 diffusion rate constants for sorption and desorption were 0,75 and 0,81 1/h respectively. For beta360 the values of diffusion rate constants (both sorption and desorption) were significantly lower (0,019 and 0,047 1/h), which supports the hypothesis, that the pores of FAU zeolites are easier accessible than the pores of BEA zeolites.

The purpose of the kinetics study primarily was to define suitable experimental conditions to conduct further experiments at equilibrium. Even though the sorption of FAU type zeolites was fast and equilibrium was reached within the first hour, contact time of 24 hours was chosen to have comparable experimental conditions for all the experiments with zeolites, including BEA.

Sorption isotherms. The sorption isotherms of imidacloprid and thiacloprid on the five zeolites were measured under constant pH, ionic strength and temperature. To estimate how the sorption would be affected by environmental factors, effects of the pH, ionic strength, presence of Ca^{2+} cations, NOM and competitive sorption of imidacloprid and thiacloprid on the sorption were determined. Ca^{2+} cations, as well as NOM, are abundant in natural water basins, thus they may have a significant impact on the sorption under natural conditions.

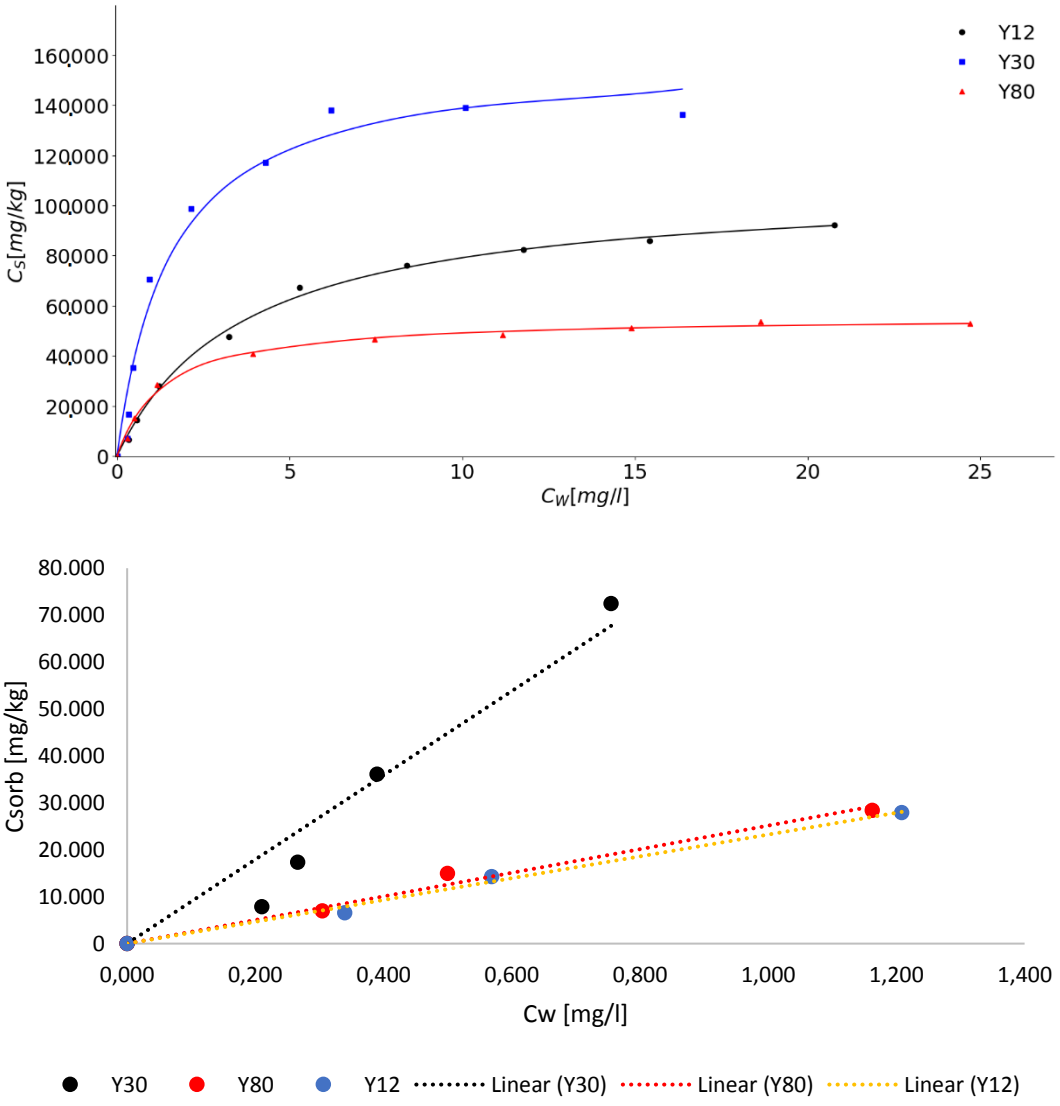

Figure 3.9 Sorption isotherms of thiacloprid on Y12, Y30 and Y80 zeolites [I=0,05 M (KCl), T=20°C (room temperature), pH 7]. Image below – Sorption isotherm of thiacloprid on zeolites at lower concentrations (linear range)

The isotherms are convexly curved and at higher surface coverage tend to reach saturation (Csorb_max).

The linear part of the isotherms in the lower concentration range is presented in Figure 3.9 (below).

The sorption isotherms of imidacloprid with zeolites are also convexly curved, reach saturation concentration Csorb_max at higher concentrations and the Langmuir model parameters were fit to the data (Figure 3.10).

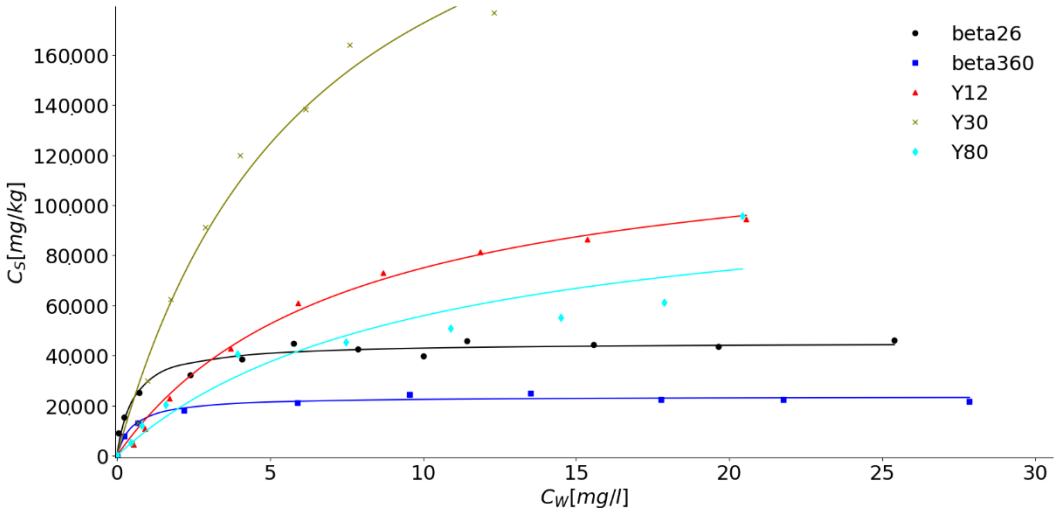

Figure 3.10 Sorption isotherms of imidacloprid on Y12, Y30, Y80, beta 360, beta26 zeolites [I=0,05 M (KCl), T=20°C (room temperature), pH 7]

De Smedt et al., 2015 studied the adsorption of different pesticides including imidacloprid on FAU and BEA zeolites and demonstrated good fit of the Langmuir model to the experimental data of imidacloprid sorption on FAU and BEA zeolites. Csorb_max and K_L determined in the present work are of the same order of magnitude as in De Smedt et al., 2015 The similarity of the experimental conditions (sorption of imidacloprid on BEA and FAU type zeolites from aqueous solutions) determines the similarity of the results obtained by De Smedt and in the current study. An existing deviation between the values is due to the difference in FAU and BEA zeolites, used in the present research and experiments of De Smedt.

The maximum saturation concentration (Csorb_max) of imidacloprid and thiacloprid on five zeolites were experimentally determined and modelled using Python (Nelder-Mead simplex optimization algorithm in SciPy package of Python 2.3). Assuming the monolayer coverage of the zeolite surface with projected molecules, monolayer concentration was empirically calculated using topological polar surface area of IC= 86,3Å²; TC=77,6 Å² and BET specific surface area of zeolites. This data is compiled in

Table 3.1. A high discrepancy between measured data and calculated one points out, that the sorption of neonicotinoids on zeolites occurred on special sorption sites and not on the total surface.

K_d^* is a distribution coefficient calculated from the Langmuir model constants for the low concentrations range (equation (2.10), Chapter 2) Table 3.2 presents comparison of K_d and K_d^* values.

Table 3.1 Measured maximum saturation concentrations for IC and TC on five zeolites and theoretically calculated values of monolayer concentrations [Topological polar surface area of IC=86,3 Å²; of TC=77,6 Å²]

Zeolite	**BET spec. surface area [m²/g]**	**Csorb_monolayer IC [mg/kg]**	**Csorb_monolayer TC [mg/kg]**	**Csorb_max IC [mg/kg]**	**Csorb_max TC [mg/kg]**
Y12	730	$2{,}16*10^{29}$	$2{,}38*10^{29}$	130.654	108.328
Y30	780	$2{,}31*10^{29}$	$2{,}31*10^{29}$	207.816	152.846
Y80	780	$2{,}31*10^{29}$	$2{,}31*10^{29}$	109.858	55.809
Beta 26	685	$2{,}03*10^{29}$	$2{,}03*10^{29}$	44.396	48.804
Beta 360	620	$1{,}84*10^{29}$	$1{,}84*10^{29}$	23.690	27.206

Table 3.2 Comparison of experimentally determined Kd distribution coefficients and Kd values as a product of K_L*Csorb_max for the linear (low) concentration range (csorb<<Csorb_max) [I=0,05 M (KCl), T=20°C 8room temperature), pH 7]*

a) Thiacloprid sorption on five zeolites

Zeolite	K_d [l/kg]	K_d^* [l/kg]
Y12	25.190	29.248
Y30	65.564	118.376
Y80	31.069	40.629
Beta26	31.217	86.147
Beta360	46.226	117.639

b) Imidacloprid sorption on five zeolites

Zeolite	K_d [l/kg]	K_d^* [l/kg]
Y12	12.027	17.638
Y30	19.335	44.394
Y80	14.937	11.315
Beta26	34.244	94.976
Beta360	19.098	44.300

Experimentally determined Kd values are lower than the Kd* values from the Langmuir model, which implies Kd* values from the model are overestimated. A possible explanation is that the values of the model are fitted to the whole range of concentrations (lower and higher concentrations) and present an idealized sorption isotherm. Hence sorption on zeolites was very strong and the slope of the isotherm was steep, it is possible that the linear (low) concentration range was amplified in a model in comparison to the lab data. Moreover, equation 2.10 shows, that Kd^* distribution coefficient is calculated for the low concentrations. From Figure 3.10 it may be seen, that in the studied concentration range saturation plateau is reached very fast. The discrepancy between K_d^* and K_d values can be explained by the non-linear range of concentrations.

Langmuir model implies that all the sorption sites are equal and there is no interaction between sorbed molecules. However, the discrepancy between experimental data and modelled values indicates inequality of the sorption centres. This could be due to the highly developed inner-pore structure of the zeolites and various accessibility of the sorption sites.

Effect of the ionic strength. To examine an effect of ionic strength on the IC and TC sorption, experiments in the presence of 0,01 M; 0,1 M; and 1 M KCl were conducted. Figure 3.11 presents the effect of ionic strength on the Kd value of the neonicotinoid_Y30 system. The Kd values both of thiacloprid and imidacloprid increase with increasing ionic strength, i.e. 0,01 M KCl ≈ 0,1 M KCl < 1M KCl. The K^+ cations may sorb on the zeolite surface through cation exchange mechanism. Li et al., 2004 suggested, that K^+ cations have relative low hydration energy, therefore, a zeolite with K^+ ions surrounding it is being hydrated to a lower extent, which makes it more hydrophobic. Thus, the zeolite's surface is easier approachable for the molecules of neonicotinoids. A similar effect was observed by Muszynski and Brodowska, 2014 for metamitron sorption; Li et al., 2004, for imidacloprid sorption on smectites. However, the K_{OW} values of TC and IC (Table 2.2, Chapter 2) allow to classify them as mildly hydrophobic and mildly hydrophilic respectively. Thus, an explanation, given by Li et al., 2004 for the effect of ionic strength on hydrophobic compounds' sorption is not fully applicable to imidacloprid. For the uncharged

molecules effect of ionic strength was explained by Setchenov salt-effects [from Hefter and Tomkins, 2003].

The Sechenov coefficients were calculated using Salt-effect equation (or Sechenov equation):

$$ln\left(\frac{Z_B^*}{Z_B}\right) = k_{syz}.y \qquad 3.2$$

$Z_B^* \; and \; Z_B$ – solubilities of component B in an electrolyte and in pure water respectively;

y –salt composition.

For Z_B^* and Z_B the equilibrium concentrations were used, for y – ionic strength.

The positive k_{syz} (Sechenov coefficient) implies salting-out effect, i.e. solubility decreases in the presence of salt and sorption increases. The negative k_{syz} implies a salting-in effect or increase of solubility and decrease of sorption.

The calculated Sechenov coefficients were positive (Table 3.3), suggesting the salting-out effect, which implies the solubility of both IC and TC decreases in the systems with higher salt concentrations.

Table 3.3 Sechenov coefficients for imidacloprid and thiacloprid in 0,1 M and 1 M KCl

Ionic strength	K_{syz} thiacloprid [l/mol]	K_{syz} imidacloprid [l/mol]
0,1 M	0,1	0,02
1M	0,14	0,1

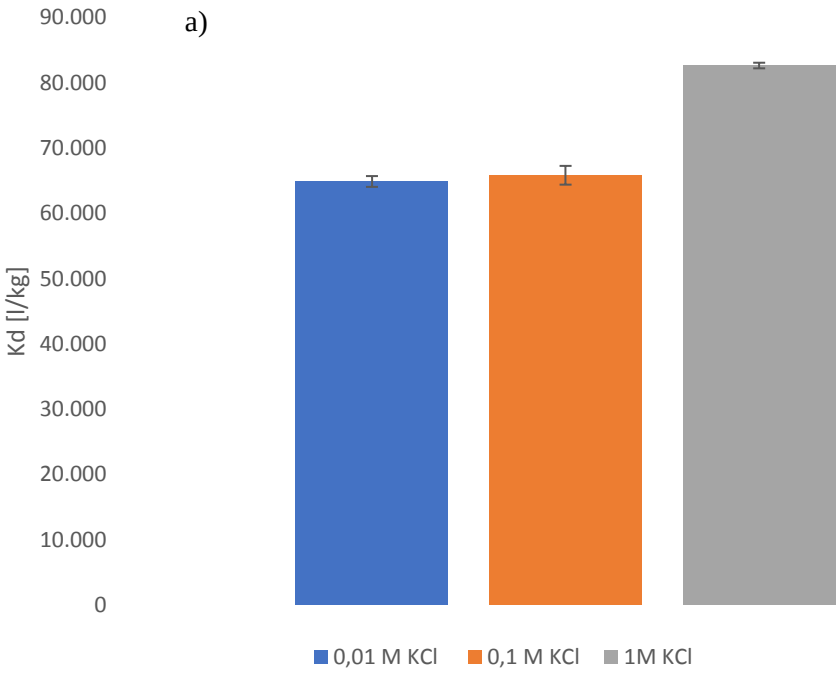

Figure 3.11 Effect of ionic strength on distribution coefficient Kd (=Csorb/Cw) of thiacloprid sorption on zeolite Y30 [T=20°C (room temperature), pH 7]. Error bars present standard deviation between triplicates

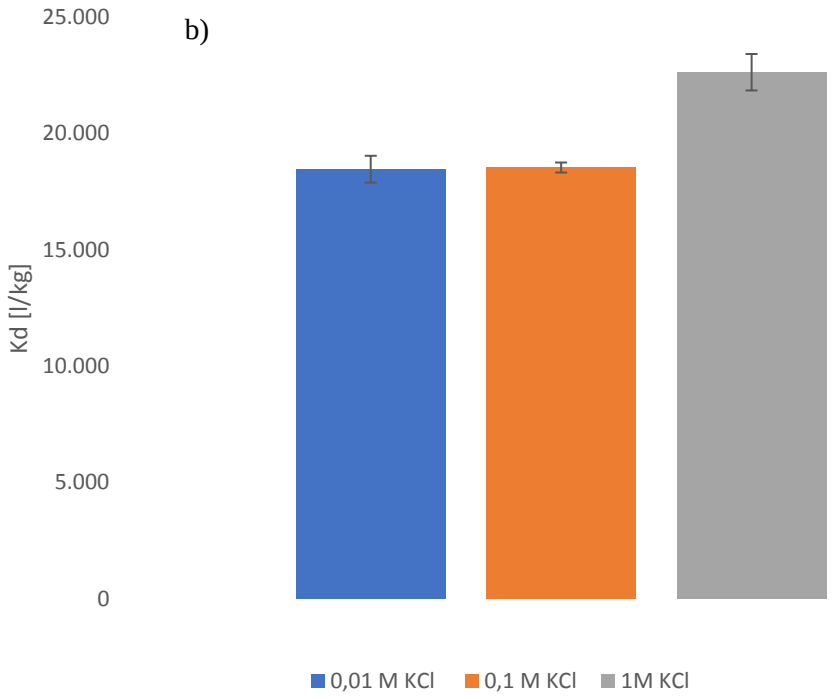

Figure 3.11' Effect of ionic strength on distribution coefficient Kd (=Csorb/Cw) of imidacloprid sorption on zeolite Y30 [T=20°C (room temperature), pH 7]. Error bars present standard deviation between triplicates

Effect of the Ca^{2+} cations. To determine how Ca^{2+} cations affect the sorption of selected neonicotinoids on zeolites, sorption experiments were conducted in the presence of 0,1 M and 1 M $CaCl_2$ concentration at constant pH (7). The results were compared with the ones of sorption studies in the presence of KCl at the equal ionic strength (0,3 M and 3 M), calculated using formula $I = \frac{1}{2}\sum C_i . Z_i^2$. Presence of Ca^{2+} cations had a diminishing effect on neonicotinoids sorption on zeolites at 3 M ionic strength, whereas at I=0,3 M the calculated Kd values (as described above) did not differ significantly. Figure 3.12 depicts Kd values of thiacloprid on Y30 at I=0,3 and 3 M with Ca^{2+} and K^+ ions. Hefter and Tomkins (2003) discuss the ability of some electrolytes to cause salt-in and salt-out in the same system depending on the amount added. Johnston et al, 2001 proposed that the larger enthalpy of hydration of Ca^{2+} (-1515 kJ/mol; K=-304 kJ/mol) restrains access of pesticides' functional groups to the zeolite surface. Besides, large hydration enthalpy promotes lower hydrophobicity of the zeolite, which decreases thiacloprid sorption.

Clausen with co-authors (2001), investigated the diminishing effect of $CaCl_2$ on the sorption of some pesticides, and proposed several hypotheses that explain a decrease in pesticides sorption with $CaCl_2$ addition: a) possible competition between pesticide molecules and Ca^{2+} cations. Due to the smaller size, Ca^{2+} could easily access the inner-pore space and reduce the number of available sorption sites.

b) possible complexation between the pesticides and Ca^{2+}, reducing the amount of sorbed pesticide. Clausen et al., 2001 proposed the present explanation for the anionic pesticides [In the current thesis, complexation between Ca^{2+} cations and anionic glyphosate molecule is discussed in Chapter 6]. Due to the noncharged character of imidacloprid and thiacloprid molecules, such complex formation is less probable and no published data on Ca-IC or Ca-TC complexes are available. Due to the ambiguous effect of different $CaCl_2$ concentration on neonicotinoids sorption, it would be worthwhile to estimate experimentally possible complex formation, or measure the surface population of zeolite to clarify, whether Ca^{2+} sorbed on the surface.

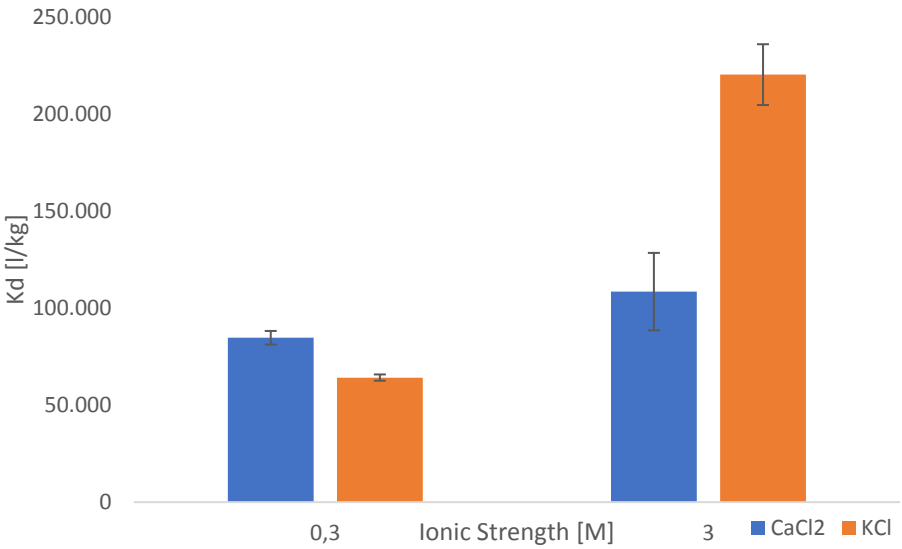

Figure 3.12 Effect of Ca^{2+} cations on Kd values of thiacloprid sorption on Y30 [T=20°C (room temperature), pH 7]. Error bars present standard deviation between triplicates

Effect of pH. The pH values of environmental aqueous systems vary in a broad pH range (the extreme conditions of very acidic or basic pH are not considered here). The pH was not expected to strongly affect TC and IC. To prove this hypothesis, sorption of imidacloprid and thiacloprid at three different pHs (pH 5, 7 and 8,5) was investigated and the sorption isotherms were obtained

Figure 3.13 depicts three sorption isotherms at pH 5, pH 7 and pH 8,5 on the example of thiacloprid and Y30. No significant effect of pH on sorption isotherm was detected. In all three cases, Csorb_max was 163±1 g/kg with a slight difference in the Langmuir adsorption constant, K_L. The adsorption capacity Csorb_max and Langmuir constant K_L values are summarized in Table 3.4.

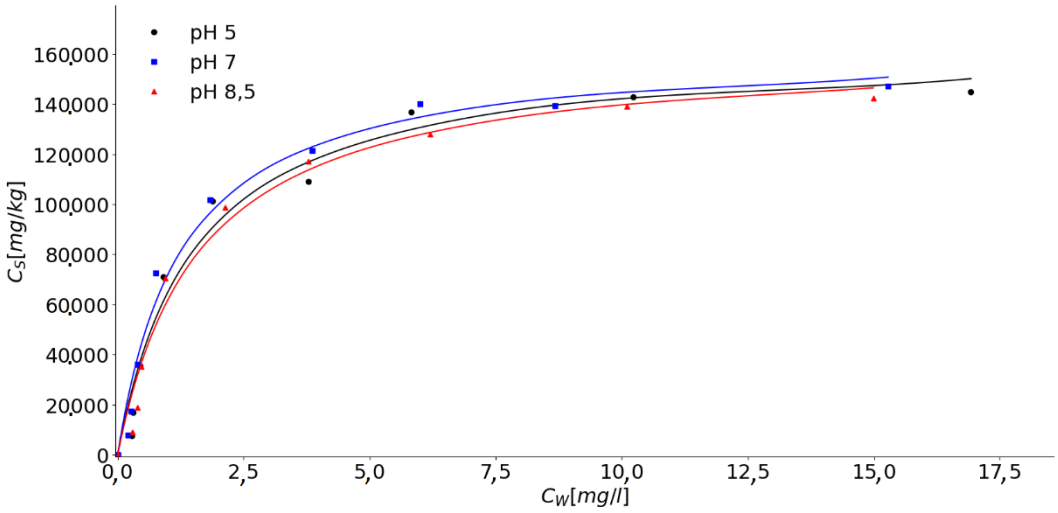

Figure 3.13 Effect of pH on the thiacloprid sorption on Y30 [I=0,05 M (KCl), T=20°C (room temperature), pH 7]

Table 3.4 Comparison of the Langmuir model parameters for the sorption isotherms of thiacloprid on Y30 at three different pHs

pH	Csorb_max [mg/kg]	K_L [l/mg]
5	163.510	0,661
7	163.228	0,79
8,5	162.220	0,618

Dependence of imidacloprid and thiacloprid sorption on pH was described in literature [Zahoor, 2011; Ping et al., 2010]. They have reported a decrease in sorption with higher pH. Zahoor, 2011 determined lower sorption at alkaline conditions. However, such trend was observed only at pH above 8,5; below pH 8 sorption extent stayed unchanged. Such decrease in sorption at higher pH may be due to the change in surface properties of the sorbent, as well as the proximity of pKa value of imidacloprid (11,12, Table 2.2, Chapter 2). Since in the present study the highest pH, at which sorption was studied, was pH 8,5, no additional conclusions about the effect of a strongly alkaline environment of thiacloprid and imidacloprid sorption on zeolites were done.

Independence of the neonicotinoids' sorption on zeolites from pH in the present work may be explained through stability of thiacloprid molecule, uncharged in the studied pH range. The pzc of zeolites is at pH 2-3, which implies that in the studied pH range zeolite surface is negatively charged. Haderlein, 1992 suggested that independence of sorption from pH may be explained in two ways: either surface speciation of the sorbent does not play a role for the sorption, or sorption takes place at the sorption sites, which are not affected by pH. In the current study surface speciation was not expected to affect

the sorption. Possibly, the sorption involved pyridine and imidazolidine ring and exchangeable cations on the zeolite surface [Liu et al., 2002]. The surface charge of zeolite with pH increase is getting more negatively charged (the point of zero charge was determined experimentally by titration, PZC<pH3), i.e. the Al-OH and Si-OH surface groups are getting deprotonated. This would cause the decrease of H-bond formation between the nitrogen of pyridine and imidazolidine rings and zeolite surface. Missing effect of pH suggests that sorption sites (exchangeable cations) were still available for the IC and TC sorption (the sorption mechanism of neonicotinoids on zeolites is discussed below).

Effect of humic acids (HA). HA are abundant in environment and may significantly affect the sorption of pesticides [Karickhoff, 1979, Schwarzenbach and Westfall, 1981 and Schwarzenbach, 1993]. Sorption of imidacloprid and thiacloprid on zeolites in the presence of 10 mg/l Suwannee River humic acid standard was investigated. Figure 3.14 depicts Kd values of thiacloprid on three zeolites with an addition of HA and without HA.

The results are presented as an average value of triplicates. No statistically significant effect of HA on Kd values was observed.

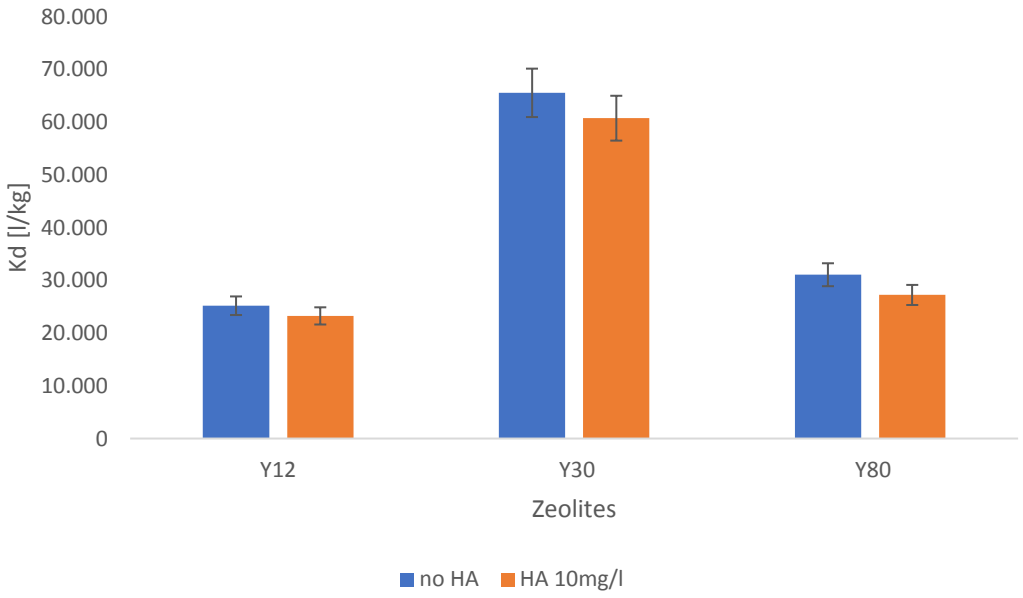

Figure 3.14 Comparison of Kd values of thiacloprid sorption on zeolites without HA and in the presence of 10 mg/l HA (Suwannee River Humic Acid Standard) [I=0,05 M (KCl), T=20°C (room temperature), pH 7], the standard deviation is calculated between triplicates

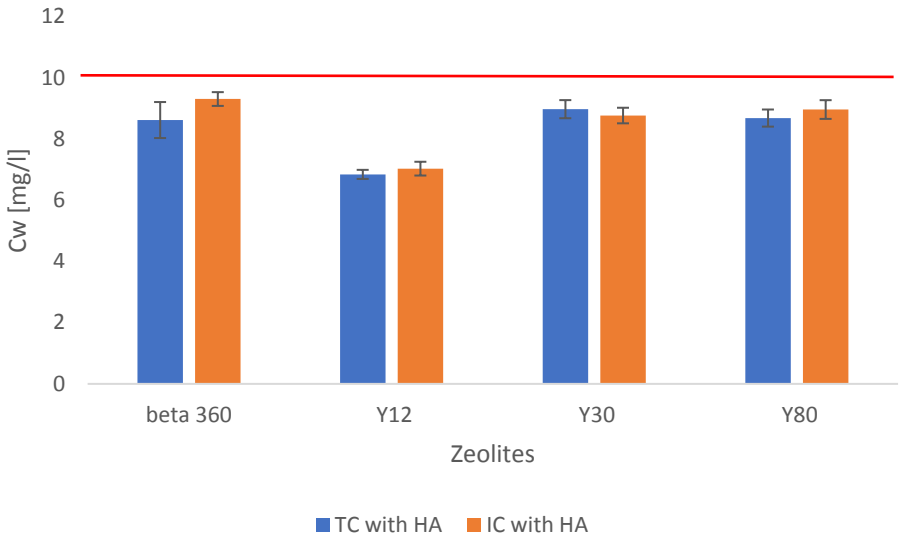

Figure 3.15 Aqueous concentration of humic acid (Cw_tot=10 mg/l) in samples with IC and TC (Cw_tot=10 mg/l), the standard deviation is calculated between triplicates

As it can be seen in Figure 3.15 that HA underwent sorption, which is shown as aqueous concentration decrease from 10 to 8-9 mg/l. Both in the presence of imidacloprid and thiacloprid HA sorption was comparable, causing equal HA equilibrium concentrations.

Generally, the sorption of hydrophobic pesticides to the substrates containing organic matter (OM) is a partitioning process between water (polar phase) and organic matter (nonpolar phase). Schwarzenbach and Westfall, 1981 proposed the correlation between organic carbon (K_{OC}) and octanol-water partitioning coefficient (K_{OW}):

$$logK_{OC} = 0{,}72 * (K_{OW} + 0{,}49) \quad 3.3$$

Another correlation was proposed by Karickhoff, 1981:

$$K_{OC} = 0{,}41 * K_{OW} \quad 3.4$$

Assuming $K_{OC} \approx K_{OW}$, the distribution coefficient of contaminant (pesticide) between the particles with HA (K_{OC} [l/kg]) and the aqueous phase is given by equation (3.5).

$$K_{OC} = \frac{K_d}{f_{oc}} \quad 3.5$$

K_d −distribution coefficient soil/water [l/kg];

f_{OC} −fraction of organic carbon [-];

$\left[1 - \frac{f_{sorb}}{f_{diss}}\right], f_{sorb}\ and\ f_{diss}$ are sorbed and dissolved fractions

Using fractions of humic acid in sorbed and dissolved forms, the distribution coefficients for thiacloprid and imidacloprid were calculated and compared with the experimentally measured K_d values in the presence of HA [Table 3.5].

Table 3.5 Comparison of the calculated K_{OC} distribution coefficients, considering calculated HA input to the sorption (eq. 3.11) and experimentally measured Kd distribution coefficients for thiacloprid

	K_{OC} [l/kg]	K_d [l/kg]
beta360	14.384	13.009
Y12	16.669	16.226
Y30	60.757	52.608
Y80	31.024	27.234

All the calculated values were slightly higher than the experimentally measured, predicting an increase in the sorption with HA addition.

Hence sorption of HA did not affect the Kd values of neonicotinoids significantly, it was assumed, that HA adsorption did not modify sorption sites on which IC and TC were adsorbed. Garbarini and Lion. 1986 postulated adsorption of organic pollutants mainly on the organic fraction of the soil and have concluded, that the higher OM content will bind more organic compounds. It was unexpected not to measure any effect of the HA presence, since the calculated K_{OC} prognosticated an increase in neonicotinoids sorption through the sorption to HA. Alternatively, HA could cause a decrease in IC and TC in the case, when both HA and neonicotinoid molecules would sorb to the same sorption sites. To predict the sorption mechanism of HA is always complicated since different HAs have a rather complex and different structures [Rahman et al., 2010; Klucakova, 2018; Baglieri et al., 2014]. Rahman, 2010 demonstrated complex formation between some environmentally abundant metals (Fe^{3+} and Cd^{2+}) and humic acids. Kostic et al., 2011 reported complex formation between HA and HA ligands and Cu^{2+} and Pb^{2+} cations. HA could form bonds with the cations on the zeolite surfaces and reduce sorption of IC and TC. The molecule dimensions measurement, implemented in Avogadro 1.90, resulted in the maximum length of TC and IC of 0,7 nm, whereas the average size of OM varies in 1,4-10 nm range for single crystals [Baalousha et al., 2006], whereas depending on the solution conditions HA is present in the form of agglomerates (100-1000 nm) [Klucakova, 2018]. With the pore size of the zeolites 0,74 and 0,6 nm for FAU and BEA respectively, neonicotinoid molecules are expected to diffuse into pores (pore-filling limited sorption and desorption of pesticides on zeolites was discussed above), whereas HA is more probable to sorb on the outer surface, not affecting IC and TC sorption within the pores. Therefore, because of the size-exclusion effect, the sorption sites of TC and IC stayed unaffected, resulting in equal distribution coefficients in the presence and absence of HA. To prove the proposed hypothesis, it is reasonable to investigate the mechanism of Suwannee River Humic Standard interaction with the zeolites and determine exact sorption sites, on which sorption takes place.

Competitive sorption of imidacloprid and thiacloprid. In nature pesticides are rarely present independently, as a single compound, but rather as a mixture of several compounds. It was important to estimate how the presence of other compounds influences the sorption of studied pesticide. Sorption of two neonicotinoids with similar structures was investigated to reveal possible competitive sorption. Imidacloprid and thiacloprid were added to the zeolites in equal quantities; the obtained sorption isotherms were compared with the sorption isotherms of single compounds.

Figure 3.16 presents experimental data on the competitive sorption of imidacloprid and thiacloprid on the Y30 zeolite. Sorption isotherms of individual compounds, imidacloprid and thiacloprid in a mixture, as well as the sum of two compounds in the mixture are depicted. IC and TC in mixture compile exactly the half of the sorption isotherms of the individual compounds. Sorption isotherm composed of two compounds in the mixture correlates well with the sorption isotherms of individual compounds and fall in the middle between IC and TC. Csorb_max and K_L parameters are summarized in Table 3.6.

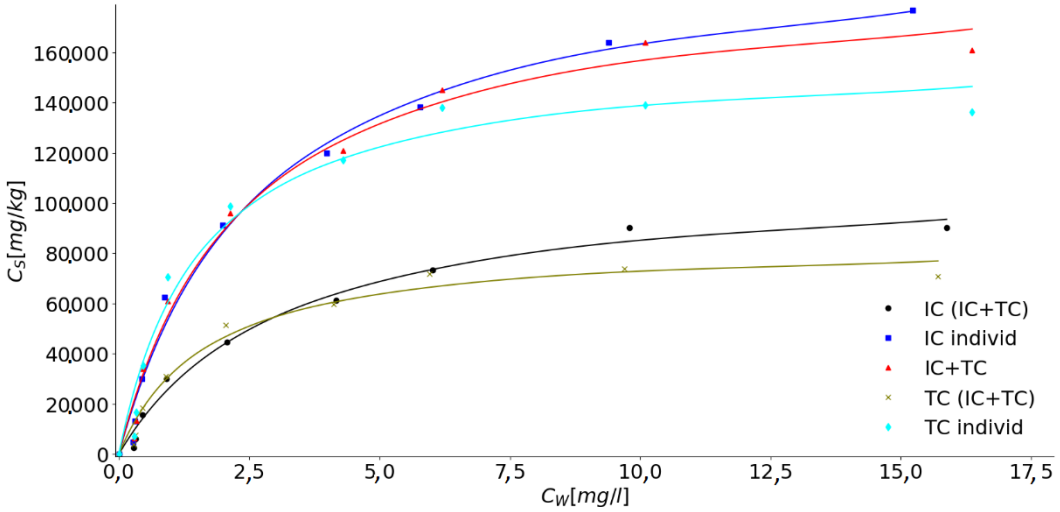

Figure 3.16 Competitive sorption of imidacloprid and thiacloprid on Y30 [I=0,05 M (KCl), T=20°C (room temperature), pH 7]

Table 3.6 Csorb_max and K_L parameters of individual TC and IC sorption isotherms and of the compounds in the mixture (1:1)

	Csorb_max [mg/kg]	K [l/mg]
IC (IC+TC)	107.346	0,346
IC (individ)	207.810	0,369
IC+TC	184.036	0,477
TC (IC+TC)	80.474	0,69
TC (individ)	160.336	0,64

The obtained results clearly reveal the competitive sorption character of imidacloprid and thiacloprid, i.e. both compounds compete for the same sorption sites at the mineral surface. The maximum adsorption capacity of the mixture is shown to be equal to the one of the individual compounds. Various authors studied sorption of organic compounds from the mixture, containing several molecules, potentially expected to compete for the sorption sites. [Traina and Onken, 1991; Brusseau, 1991]. Traina and Onken, 1991, studying competitive sorption of aromatic N-heterocycles and pyrene by smectites revealed additive sorption of organic compounds, i.e. two or more organic compounds sorbed additionally to each-other. Cumulative, or additive sorption is possible, when the compounds are sorbed to the different sorption sites and the presence of one compound does not intersect with the presence of another compound. The values from Table 3.6. demonstrate a decrease of Langmuir parameters approximately by ½ in the samples with both compounds in comparison to the individual compounds. This points out the competitive character of IC and TC sorption and suggests, that imidacloprid and thiacloprid sorb on the same sorption sites and in a sorbed form don't show an additive effect of sorbed compounds. The competitive sorption of TC and IC confirms the proposed above size-exclusion effect, supporting HA sorption on external sorption sites and TC and IC – on the internal sorption sites.

3.4. Sorption mechanism of neonicotinoids on the zeolites

Sorption mechanisms of various pesticides were widely studied and reported in the literature (Goulson and Kleijn, 2013; Inyang and Dickenson, 2015; Xiao and Pignatello, 2015). The authors have proposed following mechanisms to explain sorption of pesticides on various substrates: hydrogen bonding, van der Waals forces, hydrophobic partitioning, p-π and π-π EDA (Electron donor-acceptor) interactions, cation bridging, coulombic forces and complex formation.

Liu et al., 2002 proposed the following mechanism of imidacloprid sorption: C=N group of the pyridine ring forms a coordinated bond with the sorbent surface. Therefore, N of pyridine group is expected to coordinate with exchangeable cations on the zeolite surface or with OH- groups of Si-OH on the zeolite surface. Coordination between N and exchangeable cations may be a direct bonding between a cation and N electron pair (demonstrated on N of pyridine ring in Scheme 3.1.a. Moreover, C=N of imidazolidine ring may participate in analogous interactions. Both nitrogen atoms are assumed to have equiprobable chances of both pathways. Additionally, the pesticide molecules can bind to the exchangeable cations on the zeolite surface indirectly through the water bridges (Scheme 3.1.b.). Three mechanisms of cation- pesticide coordination were proposed and described by Rausell-Colom and Serratosa, 1987: i) direct coordination between cations and pesticide moieties; ii) coordination to the cations through the water bridges; iii) proton acceptance from the water coordinated around cations.

Liu et al., 2002 proposed H-bond formation between Cl^- of imidacloprid and thiacloprid molecule with hydrogens on the clay surface. Analogously, the bond formation between Cl^- anions of neonicotinoid molecule and hydrogens on the zeolite surface is expected. However, in the studied pH range (5-9) zeolite surface is negatively charged (PZC determined experimentally at <pH 3), thus the density of the surface hydrogens is not high and the bonding to the exchangeable cations is more probable.

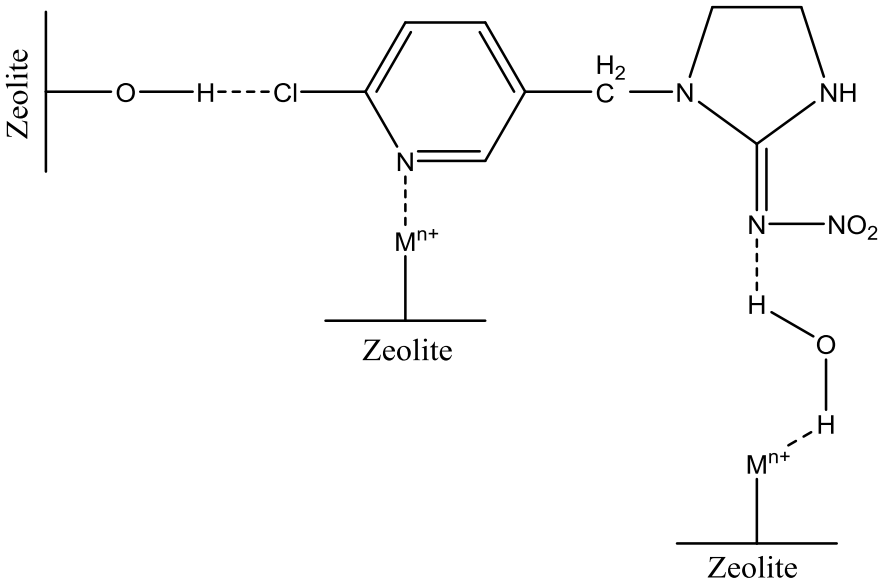

a)

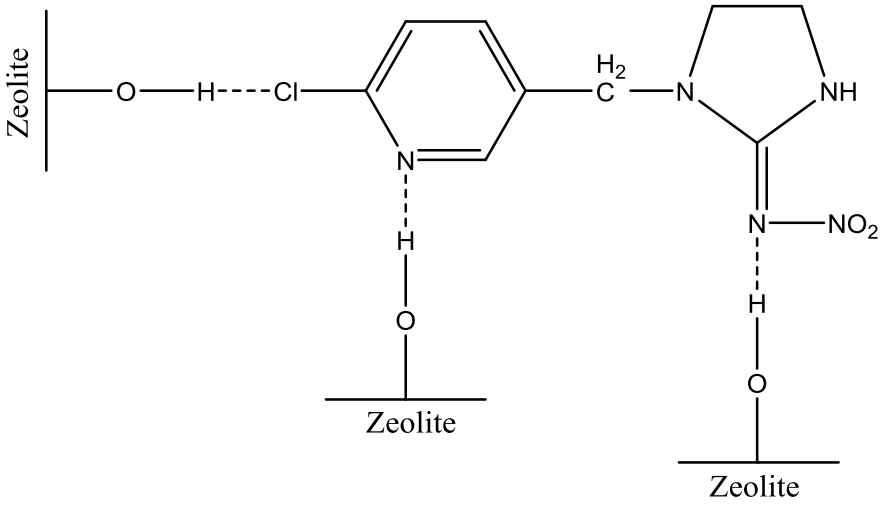

b)

Scheme 3.1 Possible interactions between neonicotinoid imidacloprid and zeolite surface: a) coordination of C=N group (of pyridine and imidazolidine ring) with exchangeable cations of zeolites. b) hydrogen bond formation between Al-O-H, Si-O-H groups of the zeolites and N atoms of IC and TC molecules

3.5. Conclusions

The sorption of both neonicotinoids on FAU type zeolites was significantly faster than on BEA type zeolites. The comparison of two types of zeolites reveals a significant difference in the pore geometry, but similar chemical properties (chemical composition, PZC). It was concluded, that due to the smaller pores and their different orientation along 110 and 010 axes (Chapter 2), the access to the pores for imidacloprid and thiacloprid is more complicated and takes more time. Assuming pore-filling process to be a limiting factor for contaminant uptake for infinite bath approach, the diffusion rate for thiacloprid sorption to Y30 and beta360 zeolites was calculated, which resulted in significantly lower values for the sorption on BEA zeolites. The desorption from BEA zeolites was not fully-reversible. Due to the sterically hindered position of TC and IC molecules within the pores of BEA, part of the sorbed compound did not desorb.

The experiments with different ionic strength concentrations (0,01 M; 0,1 M; 1 M) demonstrated an increase in sorption with increasing ionic strength. Applying the Sechenov equation, the salting-out effect was determined, which explained the decrease in solubility and respectively an increase in sorption with salt addition. The presence of Ca^{2+} cations at 0,3 M ionic strength did not have a significant effect on the sorption, whereas at 3 M ionic strength sorption decreased. The possibility of Ca^{2+} adsorption to the zeolite surface, as well as possible complex formation between Ca^{2+} cations and neonicotinoid molecules, were considered. An absence of clear effect of Ca^{2+} on the sorption suggested the necessity of additional experiments: an ion analysis of the samples in the presence of Ca^{2+} cations to evaluate the presence of Ca^{2+} sorption ; experimentall investigation of Ca^{2+}-IC and Ca^{2+}-TC complexes formation. Without these results and due to the lack of literature data on Ca^{2+}-IC and Ca^{2+}-TC complexes, these two hypotheses still need confirmation.

As was expected, pH did not affect the sorption of neonicotinoids. The molecules of IC and TC in the studied pH range are non-charged; the surface of the zeolite is negatively charged in the studied pH range. The proposed sorption mechanism (coordinated bonds between the nitrogen of pyridine and imidazolidine rings) and exchangeable cations on the zeolite sorption seems not to be affected by the pH change.

Experiments in the presence of organic matter (Suwannee River HA) unexpectedly provided no effect of HA on IC and TC sorption. Based on the calculated K_{OC} distribution coefficients, a slight increase in neonicotinoids sorption was expected. Whereas measured distribution coefficients in the presence of HA were non-elevated, comparing to the samples without HA, it was concluded, that no additional sorption of IC and TC on HA took place. Thus, zeolites act as effective sorbents of IC and TC in the environments with HA present. An absence of decrease in IC and TC sorption implies, that there is no competition between neonicotinoids and HA for the sorption sites. Due to the size exclusion (huge

difference in the molecule size of neonicotinoids and HA), HA sorbed predominantly on the outer surface of zeolite, whereas IC and TC diffused into the pores and occupied sorption sites, unattainable for HA. The similar size and structure of TC and IC and their access to the pores of zeolites implies competitive sorption between two pesticides. The sorption of IC and TC in the competitive study decreased in comparison to the sorption of the single component. Therefore, the presence of the second neonicotinoid in the aqueous system can diminish sorption of the studied component by all the equal conditions.

The proposed sorption mechanism of imidacloprid and thiacloprid on zeolites surface is coordination between N atom of pyridine group with silanol groups on the zeolite surface; or coordination to the exchangeable cations on the zeolite surface either directly or through the water bridges. Additionally, hydrogen bond may be formed with Cl atom of imidacloprid and thiacloprid.

In conclusion, zeolites are effective sorbents of neonicotinoids (imidacloprid and thiacloprid), which productively reduce the concentration of freely-dissolved insecticides. This results in a diminished bioavailability of the pesticide for the environment and may alter the toxicological effect for the studied system. Due to the reversibility of the process (for FAU), it is concluded, that no chemical degradation of the compound in zeolite took place and the contaminant desorbs at the changed equilibrium conditions.

An effect of thiacloprid's sorption on FAU and BEA zeolites on *Chironomus riparius* mortality, investigated by Lorenz et al., 2017b is described in chapter 9.

Chapter 4 Sorption of Neonicotinoids on MCM-48, PMO-silica and Al_2O_3

4.1. Introduction

This chapter presents the results of the sorption experiments of imidacloprid and thiacloprid on the three different materials. The sorption materials (mesoporous silica MCM-48, periodic mesoporous organosilica PMO-silica and amorphous alumina Al_2O_3 particles) were synthesized by Luo, 2018 within the scope of EXPAND project. The summary of the particle properties, characterized by Luo, 2018 is presented in Chapter 2, Table 2.1.

One of the main pathways of the pesticides into the environment is transport in the aqueos phase. This makes an understanding of the physical processes playing role in the pesticide transport a very important problem. Sorption on the sediments and dispersed particles modifies the distribution of the pesticides [De Smedt et al., 2015; Derylo-Marczewska et al., 2010] and pesticides' bioavailability [Sims et al., 1991]. The objective of the present study is to investigate the sorption of neonicotinoids imidacloprid and thiacloprid on MCM-48, PMO-silica and Al_2O_3, quantify changes in the aqueous concentration of neonicotinoids during sorption and evaluate the effect of environmental parameters on the process. Analogously to Chapter 3, an effect of pH, ionic strength, presence of Ca^{2+} cations and competitive sorption were investigated.

4.2. Experimental part

The experiment was conducted using batch sorption equilibrium technique with chosen particles and IC and TC. Every sample was prepared in triplicates, the average of the three measurements were used as a reported value. Aliquots of neonicotinoids (imidacloprid and thiacloprid) and particles suspensions (MCM-48, PMO-silica, nonporous Al_2O_3) were mixed in HPLC vials (BCB 1,5 ml, screw). Aliquots of $CaCl_2$, KCl and NOM [Suwannee River Humic Acid] were added to the samples. pH was adjusted by HCl/NaOH titration and measured with a pH electrode. Samples were shaken for 24 h on a horizontal shaker, centrifuged, aqueous phase separated from the sedimented particles and pipetted into fresh HPLC vials. Imidacloprid and thiacloprid were measured with HPLC method (Chapter 2), isocratic method, 60% MeOH in the mobile phase. NOM concentrations were measured photometrically at the wavelength 364 nm.

4.2.1. Sorption of imidacloprid and thiacloprid on the mesoporous silica MCM-48

As described in Chapter 2, mesoporous silica is synthesized in a presence of (organic) template which allows achieving desired inner-pore structure. Due to its physical properties (Table 2.1., Chapter 2), mesoporous silica is known as an effective sorbent of organic pollutants [Brankovic et al., 2017; Ng et al., 2017; Benhamou et al., 2009]. Thus, mesoporous silica MCM-48 was chosen for the present study as a prospectively effective sorbent for thiacloprid and imidacloprid.

The sorption experiment of neonicotinoids imidacloprid and thiacloprid on MCM-48 mesoporous silica was conducted using two different setups: a) single compounds sorption experiments with IC and TC and b) sorption experiments with a binary mixture of IC and TC at similar total concentrations (1:1 mixture). Langmuir model parameters were fitted to the experimental data. Figure 4.1. presents sorption isotherms of single components for experimental setups a) and b) as well as the sum of the two components for the setup b). Sorption isotherms generally were convexly curved, but at the higher end of the concentration range studied (aqueous equilibrium concentrations 12-16 mg/l) surface saturation of the sorbent was not achieved by the end of experiment. Table 4.1. summarizes modelled Langmuir equation constants of the fitted isotherms.

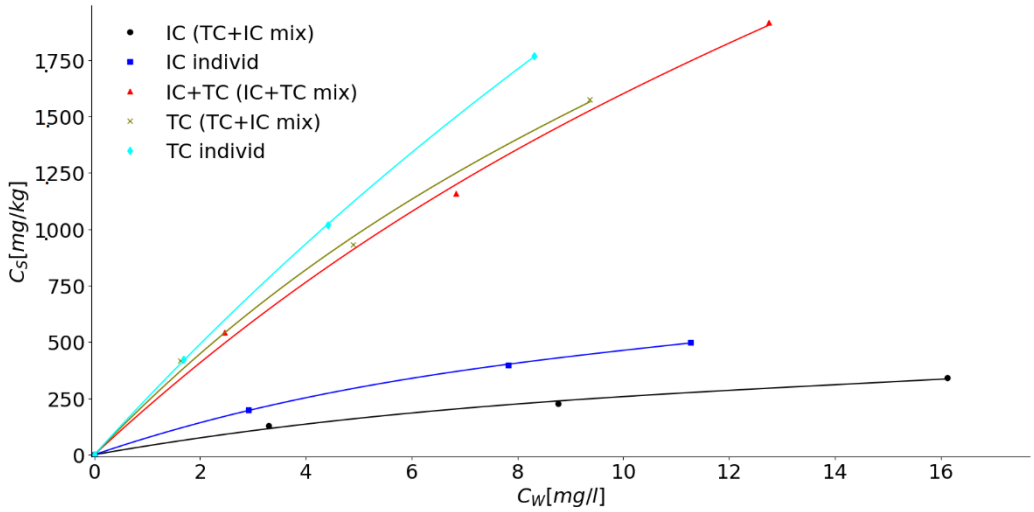

Figure 4.1 Sorption isotherms of imidacloprid and thiacloprid (individual compounds, mixture [1:1] and the sum of two compounds in the mixture) [I=0,1 M (KCl), T=20°C (room temperature), pH 7]

Table 4.1 Summary of Langmuir model constants for the sorption of imidacloprid and thiacloprid on MCM-48 as individual compounds and from the 1:1 mixture (I=0,1 M (KCl), T=20°C, pH 7)]

	Csorb_max [mg/kg]	K_L [l/mg]
IC individ	1.060	0,08
IC (IC+TC mix)	659	0,065
TC individ	9.960	0,026
TC (IC+TC mix)	4.853	0,05
IC+TC (from IC+TC mix)	5.993	0,037

As can be seen from Figure 4.1. individual compound sorption of neonicotinoids is much lower on MCM-48 mesoporous silica than on zeolites [comparison of Csorb_max in Table 4.1 and Table 3.1 in Chapter 3]. Popat et al., 2012 studied the sorption of imidacloprid on several types of mesoporous silica nanoparticles with different pore sizes and determined that MCM-48 experiment provides the highest sorption results.

The MCM-48 particles in the present research contained cetyltrimethylammonium bromide, a template used in the synthesis of these mesoporous materials [Luo, 2018].

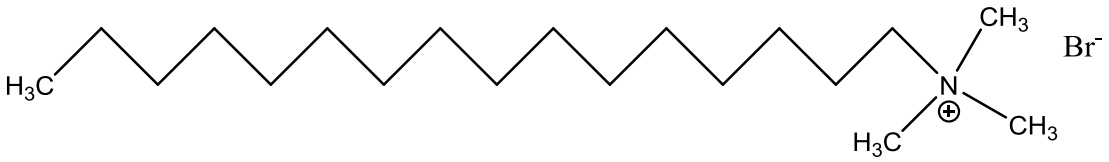

Figure 4.2 Chemical structure of cetyltrimethylammonium bromide (CTAB) [ChemDrawProfessional 17.1]

Due to its long C-C chain, cetyltrimethylammonium bromide occupies pore channels of the MCM-48 which may enhance the sorption of IC and TC on the MCM-48 through the interactions with the hydrophobic tail of the CTAB molecule.

To test this hypothesis, sorption experiments with calcined MCM-48 particles were performed. Calcination, i.e. heating MCM-48 particles at 540 °C for 4 hours, completely removes the organocationic templates [Liang and Meixner, 2017]. Sorption isotherms of imidacloprid on MCM-48 and calcined MCM-48 are presented in Figure 4.3. Sorption on the calcined particles was lower in the absence of the template. This can be explained by chemical interaction between the template and pesticides molecule, namely the hydrophobic interactions. Imidacloprid and thiacloprid sorb on non-polar surface sites of MCM-48. This is also supported by difference in imidacloprid and thiacloprid sorption. Thiacloprid's higher Kow value and lower water solubility (Table 2.2, Chapter 2) than the values of imidacloprid, explains its higher sorption capacity on MCM-48. Furthermore, calcination is known to cause shrinkage

of some pores [Erdem et al., 2015; Johansson, 2010; Lowe and Baker, 2014], making them inaccessible for the neonicotinoid molecules. The measured sorption after calcination in the absence of CTAB template involves a different type of interaction [Kd=50 l/kg for calcined MCM-48], without chemical interaction with the surface, and solely involving physical pore-filling.

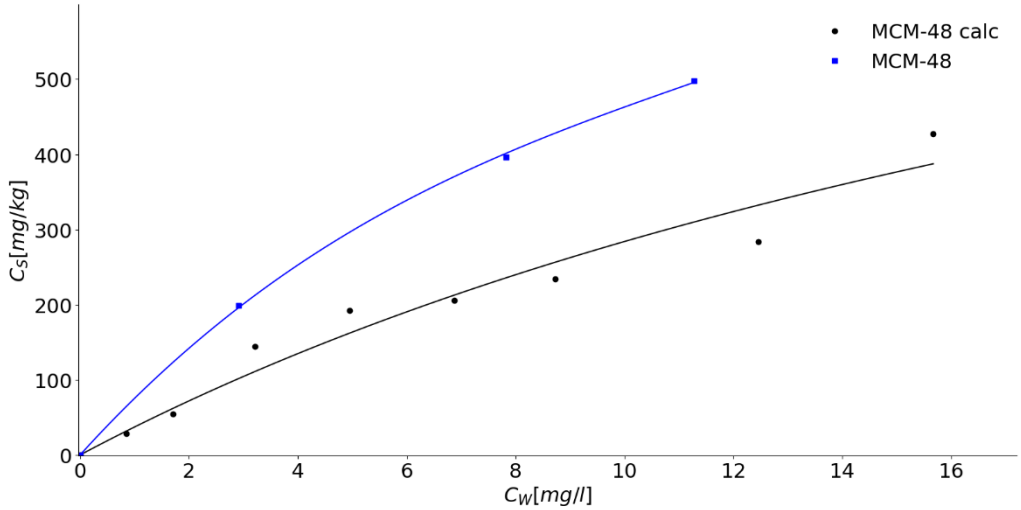

Figure 4.3 Sorption isotherms of imidacloprid on MCM-48 and MCM-48 calcined [I=0,1 M (KCl), T=20°C (room temperature), pH 7]

Effect of competitive sorption of neonicotinoids was already discussed in Chapter 3 (Figure 3.16). The competitive sorption diminished sorption of imidacloprid and thiacloprid implying sorption of both compounds on the same sorption sites. In the experiments with mesoporous silica sorption of IC and TC from the mixture was also lower, than of the individual compound (Figure 4.1.). Summary of Csorb_max values is presented in Table 4.1. It is obvious that the sorption of imidacloprid on the MCM-48 is significantly lower than of thiacloprid. The results of the competitive sorption of IC and TC on PMO-silica shown in Figure 4.5 indicate the difference in TC and IC sorption extent.

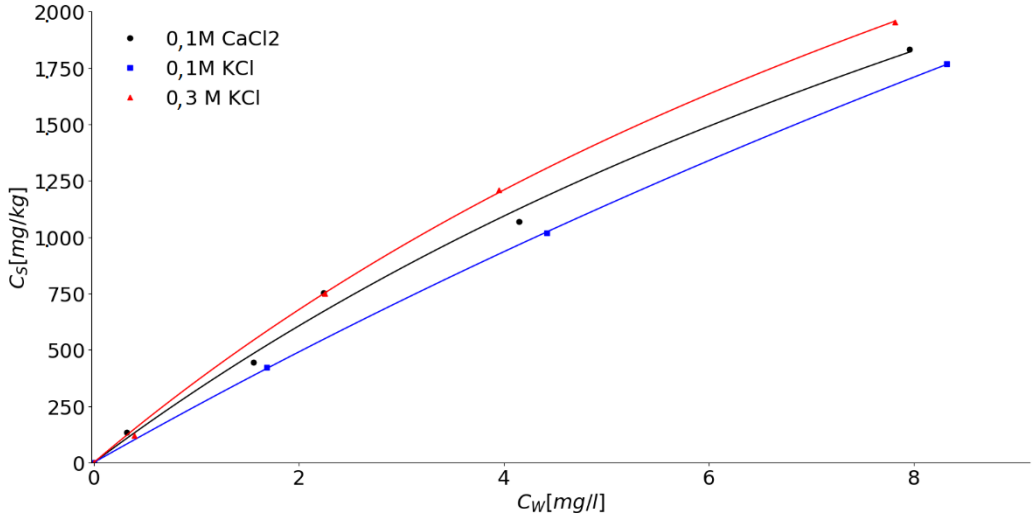

Figure 4.4 Effect of KCl and $CaCl_2$ on thiacloprid sorption on MCM-48 [I=0,1 M (KCl), T=20°C (room temperature), pH 7]

The standardized electrolyte for the most batch sorption experiments is 0,01 M $CaCl_2$ M [de Jonge and de Jonge, 1999]. However, it was proven by multiple researchers, that Ca^{2+} cations may enhance or reduce sorption of some pesticides in the environment mainly by complex formation [Jonsson, 2007; Pessagno et al., 2008; Madsen et al., 1978], shielding of the sorbent surface from the pesticide functional groups due to the Ca^{2+} presence [Johnston et al., 2001]. Impact of ionic strength on uncharged molecules is lower than on the charged ones [Alva and Singh, 1991; Clausen et al., 2001; de Jonge and de Jonge, 1999]. The experiments in the presence of 0,1 M $CaCl_2$, 0,1 M KCl, 0,3 M KCl were conducted to investigate the effect of Ca^{2+} cations and ionic strength on the sorption. An example of the Langmuir isotherms from the experiment of sorption on MCM-48 in the presence of 0,1M $CaCl_2$, 0,1M KCl, 0,3M KCl is shown in Figure 4.4. The Langmuir model fitted to the three sets of data (Langmuir model is described in Chapter 2). The constants of the Langmuir model are summarized in Table 4.2.

Table 4.2 Comparison of experimentally determined Kd distribution coefficients and Kd values as a product of K_L*Csorb_max for the linear (low) concentration range (Csorb<<Csorb_max) for thiacloprid sorption on MCM-48 [I=0,1 M (KCl, T=20°C (room temperature), pH 7]*

	Csorb_max [mg/kg]	K_L [l/mg]	K_d^* [l/kg]	K_d [l/kg]
0,1 M $CaCl_2$	5.566	0,061	340	352
0,1 M KCl	9.960	0,026	259	258
0,3 M KCl	5.583	0,069	385	316

Two sorption experiments at 0,3 M ionic strength calculated by formula $I = \frac{1}{2}\sum C_i . Z_i^2$, where C_i – is the concentration of the ion, Z_i – charge of the ion (0,1 M $CaCl_2$ and 0,3 M KCl) resulted in the Langmuir equation coefficients, deviating from one another by 0,4% and 13% (Csorb_max and K_L respectively). At the constant ionic strength sorption was unaffected by Ca^{2+} ions. Possible explanation of the effect of Ca^{2+} cations presence on thiacloprid and imidacloprid sorption on zeolites was discussed in the Chapter 3. One of the two possible mechanisms is competition between Ca^{2+} cations and neonicotinoid molecules for the sorption sites [Clausen et al., 2001]. Ca^{2+} cations, due to their small size can easily enter the pores of MCM-48 (2,2 nm in diameter, Table 2.1, Chapter 2). As was discussed above, sorption of imidacloprid and thiacloprid to MCM-48 was mainly due to the interactions with non-polar sites on MCM-48 surface and pesticide molecule. Thus, even if Ca^{2+} cations diffused into the MCM-48 pores, but did not bind to the CTAB, neonicotinoid's sorption would be unaffected by the presence of Ca^{2+} cations. Another mechanism of possible effect of Ca^{2+} on IC/TC sorption, discussed in Chapter 3, is a complex formation between Ca^{2+} and pesticide molecule [Clausen et al., 2001]. However, the absence of Ca^{2+} cations effect on imidacloprid and thiacloprid sorption on MCM-48 negates the possibility of complex-formation. The results of the experiment on MCM-48 can clarify the results of the sorption experiment on zeolites, indicating that the effect of Ca^{2+} cations on the sorption is not due to the complex formation, but due to the sorption/interaction of Ca^{2+} with zeolite surface and alteration of the sorption sites of imidacloprid and thiacloprid.

In the 0,1 M KCl, calculated Csorb_max was 79% higher, than in 0,1 M $CaCl_2$ and 0,3 M KCl; K_L – 58% lower. Adamczyk et al., 1999; Mandal and Moulik, 1982 discussed an effect of ionic strength on CTAB and concluded, that increase of ionic strength causes a reduction in the solution surface tension, i.e. CTAB solubility increases. The altered solubility of CTAB affected its interactions with neonicotinoid molecule. Therefore, the difference between the sorption of neonicotinoids on MCM-48 at 0,1 M and 0,3 M is caused by changes in surface tension.

4.2.1.a. Conclusions

Sorption of imidacloprid and thiacloprid on MCM-48 is mainly due to the hydrophobic interactions between CTAB template and neonicotinoid molecule. It was shown that sorption on calcinated MCM-48 results in significantly lower sorption than on non-calcinated MCM-48 (Kd=50 l/kg for TC on MCM-48 calcined vs 250 l/kg on MCM-48). The proposed sporption mechanism on calcined MCM-48 is physical process without chemical interaction with the surface due to the CTAB template removal and pore shrinkage.

Ionic strength impacts the sorption of neonicotinoids to MCM-48 due to the change in CTAB water solubility. It may be concluded, that the studied interaction between neonicotinoids and mesoporous silica may be affected by different salt concentrations and cause changes in the sorption extent. No effect of Ca^{2+} cations was registered, implying no complex-formation between neonicotinoids and Ca^{2+}, which brings new insights to the interpretation of the sorption experiment results of IC and TC on zeolites (Chapter 3). It implies that the abundance of Ca^{2+} in the environment won't alter neonicotinoids sorption and their bioavailability for the target and non-target organisms. Interactions of thiacloprid and imidacloprid with MCM-48 were similar for both compounds. Thus, the competitive sorption affects the sorption of a single compound and consequently alters its bioavailability in the environment.

4.2.2. Sorption of imidacloprid and thiacloprid on the periodic mesoporous organosilica PMO-silica (LL-17)

PMO-silica combines advantages of mesoporous silica with its ordered pore system and high specific surface area and organic fragments, facilitating high binding capacity of organic molecules. PMO-silica is favourable for the removal of pesticides from the aqueous environments [Ganiyu et al., 2014; Huq et al., 2001]. The objective of present study is to use PMO-silica, synthesized by Luo, 2018 as sorbent for imidacloprid and thiacloprid, estimate and quantify the sorption of neonicotinoids on PMO-silica. This would provide an information, to which extent concentrations of neonicotinoids in water can be reduced by PMO-silica with the consequent effect on their bioavailability and accessibility for target and non-target organisms. Whereas competitive sorption was pronounced in the sorption on zeolites and MCM-48, competitive sorption of imidacloprid and thiacloprid on PMO-silica was investigated. Since organic matter is abundant in the water systems and may affect the sorption, it was intended to investigate sorption on PMO-silica in the presence of Suwannee River Humic Acid (HA).

Figure 4.5 presents sorption isotherms of the fitted Langmuir model (Chapter 2, equations (2.4) - (2.10)) to the results of competitive sorption experiment. For both neonicotinoids, sorption isotherms are convexly curved. Langmuir equation constants obtained for thiacloprid and imidacloprid are presented in Table 4.3.

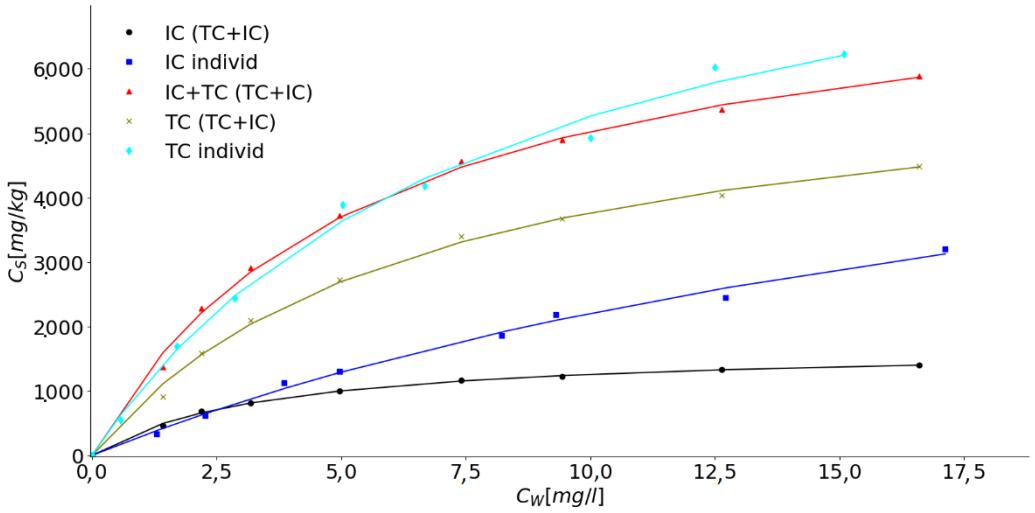

Figure 4.5 Sorption isotherms of thiacloprid and imidacloprid (as individual compounds, mixture (1:1) and sum of the compounds in mixture) [I=0,1 M (KCl), T=20°C (room temperature), pH 7]

Table 4.3 Comparison of Langmuir model constants for imidacloprid and thiacloprid sorption on PMO-silica (as individual compounds and from the mixture with similar concentrations) [I=0,1 M (KCl), T=20°C (room temperature), pH 7]

	Csorb_max [mg/kg]	K_L [l/mg]
IC individ	7.545	0,04
IC (IC+TC mix)	1.689	0,29
TC individ	9.599	0,12
TC (IC+TC mix)	6.252	0,15
IC+TC (from IC+TC mix)	7.843	0,18

The results presented in Figure 4.1 and Figure 4.5 (Tables 4.1. and 4.3) show that sorption of thiacloprid on both PMO and MCM-48 is higher than of imidacloprid (comparison of Langmuir equation coefficients). In the sorption from the mixture, neither of the components reaches Csorb_max of the individual compound. Imidacloprid's Csorb_max in the presence of TC is only 22% of Csorb_max of the individual IC, whereas thiacloprid's Csorb_max in a mixture composes 65% of its Csorb_max as an individual compound. This agrees with the previously observed higher sorption of thiacloprid than imidacloprid.

There are two possible explanations of the different IC and TC sorption on PMO-silica. The first hypothesis is that Imidacloprid and thiacloprid are sorbed to the different sorption sites. However, it is contradicted by the reduction of sorption measured in the presence of co-sorbent. The second hypothesis is that the sorption of imidacloprid and thiacloprid on PMO-silica is driven by hydrophobicity. Imidacloprid's water solubility is 610 mg/l at room temperature, whereas thiacloprid's water solubility is three

times lower – 185 mg/l (Table 2.2, Chapter 2). This leads to greater sorption of thiacloprid than imidacloprid from the water solutions on the surface of PMO-silica. The distribution coefficients (Kd) of imidacloprid, thiacloprid and propiconazole sorption on PMO-silica (propiconazole sorption on PMO-silica is discussed in Chapter 5) are 8.012 l/kg for propiconazole, 850 l/kg for thiacloprid and 292 l/kg for imidacloprid. Insofar, increasing hydrophobicity results in the higher sorption of pesticides.

Effect of humic acid (HA). Being an important part of soils and aqueous systems, organic matter is known to significantly affect sorption of organic pollutants [Schwarzenbach et al., 1993; Karickhoff et al., 1979; Schwarzenbach and Westfall, 1981] and hence change their distribution and the toxicity in the environment. Therefore, for the scope of the present study, it was essential to evaluate the effect of humic acids presence on imidacloprid and thiacloprid sorption on the PMO-silica.

Comparison of distribution coefficients (Kd) for IC_PMO-silica in the presence of different HA concentration is presented in Figure 4.6

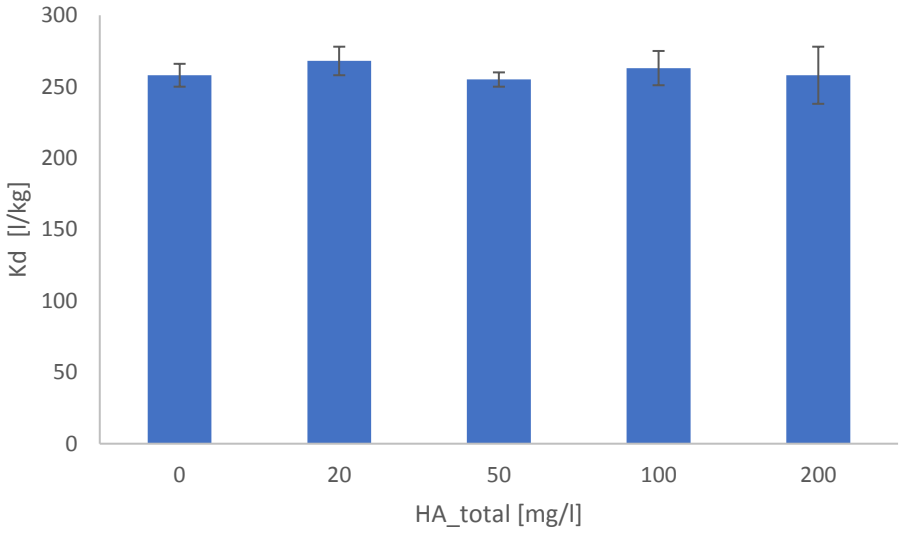

Figure 4.6 Distribution coefficients for IC sorption on the PMO-silica in the presence of various HA concentrations [I=0,1M (KCl), T=20°C (room temperature), pH 7, IC_tot=10 mg/l, PMO-silica=1 g/l]. Error bars represent standard deviation between triplicates

The concentrations of HA were measured photometrically, all the HA in four samples was non-sorbed and present in the aqueous phase (apart from 20 mg/l total concentration sample, where 10% were sorbed). The fractions of sorbed and dissolved HA are summarized in Table 4.4.

Table 4.4 The fractions of sorbed and dissolved HA in different samples [I=0,1 M (KCl), T=20°C (room temperature), pH 7, IC_tot=10 mg/l, PMO-silica=1 g/l]

HA_tot concentration [mg/l]	f_{sorb} [%]	f_{diss} [%]
20	10,2	89,8
50	0	100
100	0	100
200	0	100

Using a similar approach, as was used in Chapter 3 (eq. 3.5), the K_{OC} values for the samples in the presence of various concentrations of HA were calculated.

Calculated assuming $K_{OC} \approx K_{OW}$ values of K_{OW} and K_d values are almost identical.

Table 4.5 Comparison of calculated K_{OC} and experimentally measured Kd values for the sorption of imidacloprid on PMO-silica in the presence of various concentrations of HA [I=0,1 M (KCl), T=20°C (room temperature), pH 7, IC_tot=10 mg/l, PMO-silica=1 g/l]

HA_tot concentration [mg/l]	K_{OC} [l/kg]	Kd [l/kg]
20	302	268
50	255	255
100	263	263
200	258	258

Figure 4.7 depicts sorption isotherms of HA on PMO-silica in the presence of imidacloprid and thiacloprid. An average Kd value is 50 l/kg, indicating low sorption.

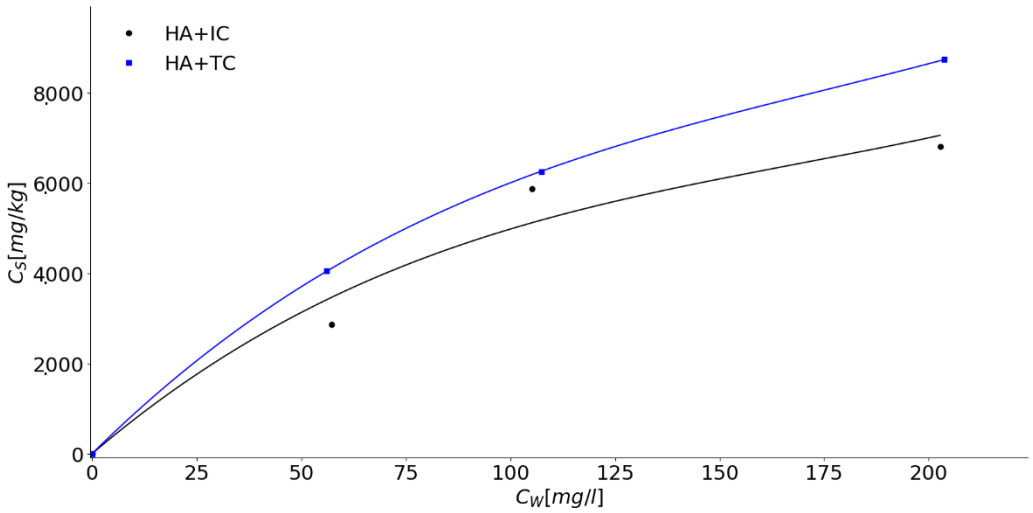

Figure 4.7 Sorption isotherms of HA on PMO-silica in the presence of thiacloprid and imidacloprid [I=0,1 M (KCl), T=20°C (room temperature), pH 7]

A comparison of the distribution coefficients of imidacloprid and K_{OC} values, considering fractions of sorbed and dissolved organic matter, did not reveal any effect of HA presence on imidacloprid sorption (Figure 4.6). The conclusions from the experiment of HA effect on IC and TC sorption on zeolites (Chapter 3), proposed the size-exclusion effect, i.e. neonicotinoids and humic acids sorbed to the different sorption sites of zeolites, not interfering with each other.

Thiacloprid and imidacloprid sorption on the PMO-silica was hydrophobicity-driven, implying an absence of chemical interaction with the surface. According to the results, depicted in Figure 4.7, PMO-silica's surface does not posess sorption sites for the hydrophilic HA, which supports the hydrophobicity-driven character of the sorption on PMO-silica.

4.2.2.a. Conclusions

Low sorption rates of the neonecotinoids on both PMO-silica and MCM-48 prompted no need for further toxicological studies of the imidacloprid and thiacloprid with these sorbents. The competitive sorption of imidacloprid and thiacloprid was revealed, implying that in the nature in the presence of the second pesticide sorption of the thiacloprid (or imidacloprid) would be diminished. An increase in hydrophobicity in a row imidacloprid < thiacloprid < propiconazole resulted in the increased sorption (sorption of propiconazole on PMO-silica is discussed in Chapter 5 and Chapter 8). No effect of HA (Suwannee River Humic acid) on the neonicotinoid sorption on PMO-silica was observed. Therefore, sorption of IC and TC on PMO-silica in the environment is not expected to be affected by HA presence.

4.2.3. Sorption of imidacloprid and thiacloprid on the alumina Al_2O_3

There are few available studies of imidacloprid or thiacloprid sorption on alumina [Clausen et al., 2001]. Multiple researchers investigated sorption of imidacloprid on soil, containing aluminium oxide [Jeong and Selim, 2010; Kandil et al., 2015]. Clausen et al., 2001 concluded, that alumina is a poor sorbent for non-charged pesticides. The motivation to investigate sorption of neonicotinoids on amorphous aluminium oxide (synthesized by Luo, 2018, properties are described in Table 2.1, Chapter 2) was caused by nano-Al_2O_3 interest for the toxicological studies on *Chironomus riparius* larvae [Lorenz et al., 2017a]. Several papers revealed toxic effects of nano-Al_2O_3 on the aqueous organisms [Oberholster et al., 2011; Li et al., 2011; Zhu et al., 2009]. It was decided to investigate, how nano-Al_2O_3 would influence the mortality of *Chironomus riparius* through direct effect and interaction with thiacloprid. The sorption of thiacloprid on the Al_2O_3 was studied to provide information, whether Al_2O_3 decreases bioavailability of thiacloprid for *C. riparius* and alters thiacloprid's toxicological effects. Figure 4.8. depicts sorption

isotherm of thiacloprid on Al_2O_3 (nano-)particles. In the concentration range 5-8000 µg/l average sorbed concentration was 0,346 ±0,03 µg/l (average of 10 samples).

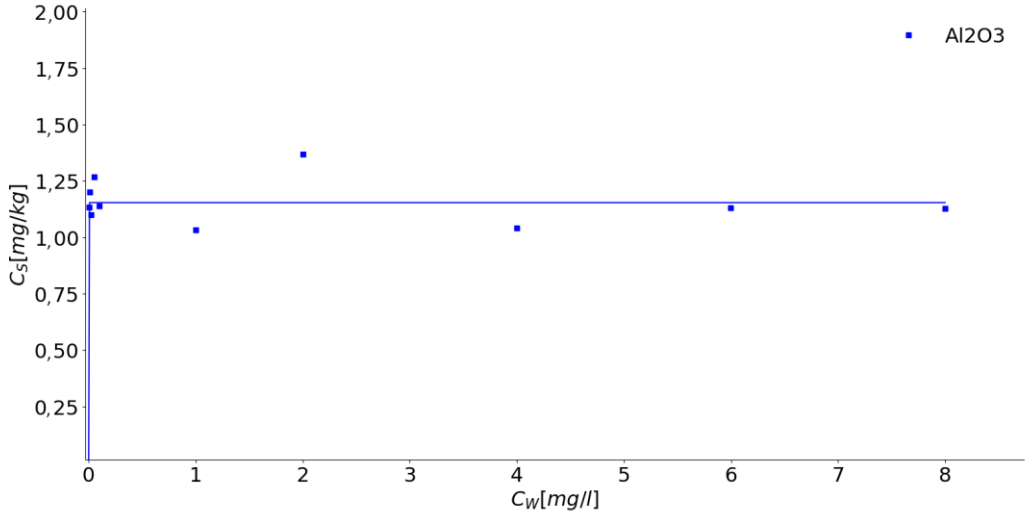

Figure 4.8 Sorption isotherm of thiacloprid on Al_2O_3 particles. [I=0,1 M (KCl), T=20°C (room temperature), pH 8,5]

Table 4.6. summarizes the BET specific surface area, pore size and Csorb_max for thiacloprid sorption on eight sorbents. Sorption of thiacloprid on Al_2O_3 is very low in comparison to the rest of the sorbents used in this study. Out of all the sorbents that were applied, Al_2O_3 has the lowest surface area (9 m^2/g), lowest pore volume (0,015 cm^2/g at relative pressure 0,974) (Table 2.2, Chapter 2).

Table 4.6 Comparison of BET, pore size and Csorb_max for thiacloprid sorption on eight sorbents

Sorbent	**BET spec. surface area [m^2/g]**	**Pore size [nm]**	**Csorb_max [mg/kg]**
Al_2O_3	9	- (nonporous)	1,154
Y12	730	0,74	108.328
Y30	780	0,74	152.846
Y80	780	0,74	55.809
Beta 26	685	0,5-0,6	48.804
Beta 360	620	0,5-0,6	27.206
MCM-48	1.150	2,2	9.960
PMO-silica	1.050	1,9	9.599

Csorb_max value for thiacloprid decreases in a row:

Y30 > Y12 > Y80 > beta26 > beta360 > MCM-48 > PMO-silica >Al_2O_3

The comparison of the properties of the materials used as sorbents provides the following conclusions for the observed order of sorption capacity. Very low sorption of imidacloprid and thiacloprid on alumina implies low affinity to the aluminol groups and significantly higher affinity to silanol groups, which is supported by high sorption on aluminium – deficient zeolites. Clausen [Clausen et al., 2001] suggested that aluminium oxide is a much weaker sorbent for non-charged molecules than silica. In the present work sorption on zeolites was significantly higher, than on mesoporous silica and periodic organosilica. Thus, the high specific surface area of the material contributes to the high sorption. However, MCM-48 and PMO-silica provide lower sorption of thiacloprid than zeolites, although BET of zeolites is lower than that of MCM-48 and PMO-silica. Preliminary experiments conducted with FAU zeolite with SiO_2/Al_2O_3 ratio of 1,5 (the results are not discussed in the present work) have shown very low sorption of both IC and TC, therefore, the high SiO_2/Al_2O_3 ratio was important for thiacloprid and imidacloprid sorption. On the contrary, sorption on beta360 (SiO_2/Al_2O_3 = 360) was lower, than on Y30 (SiO_2/Al_2O_3 = 30). It is suggested, that the limiting factor for the proposed order of the sorbents was the pore size. The sorption on the zeolites, controlled by pore-filling process, is discussed in Chapter 3. Thus, IC and TC molecules diffuse into the pores of zeolites (BEA: 0,5-0,6 nm; FAU: 0,74 nm), whereas MCM-48 and PMO-silica possess larger pores (2,2 and 1,9 nm respectively), which results in weaker bonding and respectively lower sorption. The studied alumina is a nonporous material, with no diffusion possible, which results in a very low sorption of thiacloprid.

4.2.3.a. Conclusions

The sorption of thiacloprid on Al_2O_3 is very low: 0,346 ±0,03 µg/l (average of 10 samples within the total thiacloprid concentration range 5-8000 µg/l). The comparison of the sorption extent of thiacloprid on eight sorbents brings the conclusion, that the sorption of noncharged molecules of thiacloprid (and imidacloprid) depends on the chemical composition of the sorbent, namely TC and IC have higher affinity to silanol groups, than to aluminol groups. The high SiO_2/Al_2O_3 ratio is determined by the lower number of aluminol groups and results in higher sorption than on alumina-rich zeolites. The sorption is typically high on the materials with the high specific surface area. The pore geometry and size are very important for the sorption of IC and TC. Thus, the sorption on the materials with pore size close to the molecule size of the contaminant (here: IC and TC) results in sorption, limited by the pore-filling

process, and higher sorption in comparison to the materials with pores much bigger, than the contaminant molecules. The sorption on PMO-silica, MCM-48 was mainly due to the hydrophobic interactions with no chemical interaction with the surface. Due to the significantly larger pores than the size of IC and TC molecules, the “trapping” of neonicotinoids in the pores of the material was not considered.

The low sorption of thiacloprid on nonporous alumina suggests, that the bioavailability of the studied compound in the environment would not be lowered through sorption on alumina and the possible changes in thiacloprid toxicity for target and non-target compounds should be referred to the alternative effects, and not to the sorption.

The discussion of the toxicological effects of thiacloprid and alumina is provided in Chapter 9.

Chapter 5 Sorption of Propiconazole on PMO-silica (LL-17)

5.1. Introduction

Propiconazole is a broad-spectrum fungicide, used against fungal diseases of different plants. Propiconazole inhibits the steroid demethylation, disrupting the biosynthesis of ergosterol [Garrison et al., 2011]. Hexaconazole is another azole fungicide with a similar mode of action. Hexaconazole is not used anymore in EU countries due to possible harmful effects even at the approved application levels [Entscheidung 2006/797/EG der Kommission, 2006]. However, it is still used in some Asian countries against fungal decease of rice [Zhang et al., 2015] and oil palm trees [Muhamad et al., 2012]. Description of propiconazole and hexaconazole properties and their mode of action is given in Chapter 2 (2.2 Pesticides).

Due to the wide use of propiconazole and its stability, different researchers found increased concentrations of this compound in different aqueous systems [Kahle et al., 2008; Kreuger, 1998; Kronvang et al., 2003]. These often occurences of elevated concentrations of propiconazole in aqueous environments can not be explained by the typical pathway mechanisms because of its moderately low water solubility (100 mg/l). Wu et al., 2003 proposed, that the mobility of propiconazole is explained by its sorption on the small particles (<2 μm), which are carried with the water flow into the water basins.

An objective of the present study was to acquire a deep understanding of the sorption of propiconazole and hexaconazole on the periodic mesoporous silica (PMO-silica, particle size: 360 nm) and propose a sorption mechanism. The PMO-silica sorbent is described in Chapters 2 and 4. In addition, an effect of glucose on the sorption of propiconazole was studied as relevant to toxicological studies.

Environmental factors, such as pH, ionic strength, the presence of co-sorbents is known to alter the sorption of some compounds [Pusino et al., 2003; de Jonge and de Jonge, 1999; Clausen et al., 2001]. As discussed in Chapter 3, the sorption of the non-charged molecules is stronger influenced by the ionic strength and pH, than the sorption of the non-charged molecules [Alva and Singh, 1991].

Copper cations (Cu^{2+}) are known to affect sorption of some pesticides through complexation or competitive sorption [Dousset et al., 2007; Martell and Motekaitis, 1988; Subramanian and Hoggard, 1988]. The common sources of Cu^{2+} cations in water include Cu-containing waste, such as sewage sludge, swine and poultry manure [Fjallborg and Dave, 2003; Lv et al., 2018] and application of Cu-based fungicides on the vineyards against fungal diseases of grapes, such as mildew [Arias et al., 2006].

To evaluate the possible effects of the environmental factors on sorption of propiconazole, the experiments were conducted using different concentrations of KCl, Cu^{2+} cations, co-sorbent (hexaconazole) and different pHs.

As a part of the EXPAND project, this study evaluated effectiveness of PMO-silica as a sorbent of propiconazole, the potential to decrease the bioavailability of propiconazole in the aqueous systems, and applicability to toxicological studies.

5.2. Experimental part

The batch equilibrium method was used for the sorption experiments. The pH of pesticide solution and PMO-silica suspension were adjusted by titration (HCl/NaOH) without buffers. The aliquots of pesticides (propiconazole and hexaconazole solutions) and PMO-silica suspension were mixed in LC-MS vials. Aliquots of $CuCl_2$, KCl were added to the samples. The samples were prepared in LC-MS glass vials (Fisherbrand), were shaken for 24 h on the horizontal shaker, centrifuged and pipetted into fresh LC-MS screw vials. Samples were prepared in triplicates. Concentrations of propiconazole and hexaconazole were measured with LC-MS method (method description is provided in Chapter 2).

5.3. Results and discussion

Sorption isotherms of propiconazole on mesoporous PMO-silica particles were determined and the Langmuir model parameters were fitted to the experimental data. The Langmuir model is described in Chapter 3. To comply with the toxicological studies (on *Laccaria bicolor, Amanita muscaria, Genococcum geophilum*) conducted by Früh [Doctoral thesis, in preparation] sorption isotherms were also determined in MMN medium [Marx, 1969] with two glucose concentrations [5 g/l; 10 g/l]. All three sorption isotherms were determined at pH 5,8 to meet the conditions of the toxicological study. Figure 5.1 shows fitted sorption isotherms for three settings.

Sorption of propiconazole on PMO-silica did not vary significantly with the glucose concentration, which suggests that it has no significant effect on the sorption. Thus, the further sorption experiments with propiconazole and PMO were conducted in aqueous suspensions and the results were referred to the conditions of the toxicological experiments.

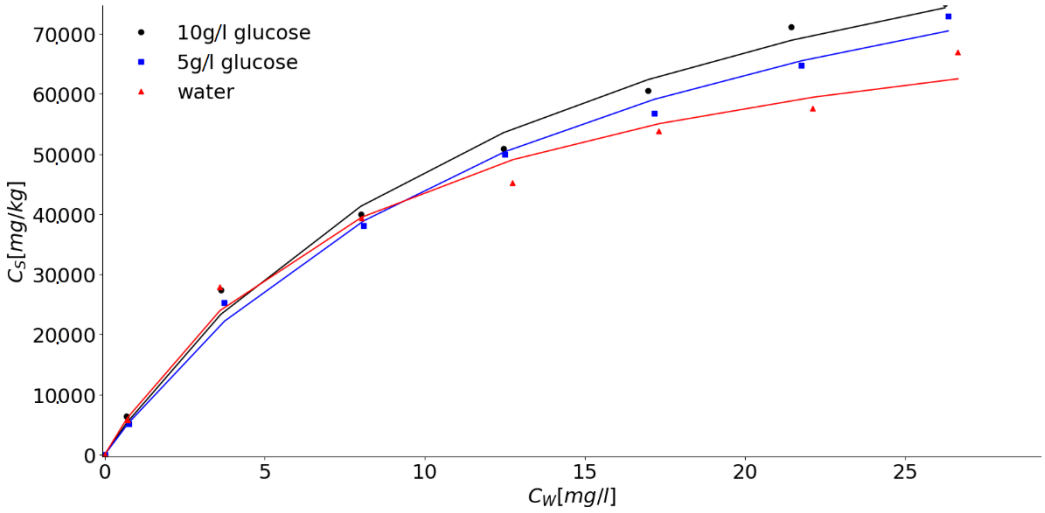

Figure 5.1 Sorption isotherms of propiconazole on PMO-silica particles suspended in MMN medium with varying concentrations of glucose (5g/l, and 10 g/l glucose; [I=0,05 M (KCl); T=20°C, pH 5,8]

Kinetics of the propiconazole sorption on PMO was monitored over 36 hours (Figure 5.2). Significant concentration changes occurred within the first thirty minutes of the reaction, with slight fluctuations (within standard deviation range) during the whole experiment.

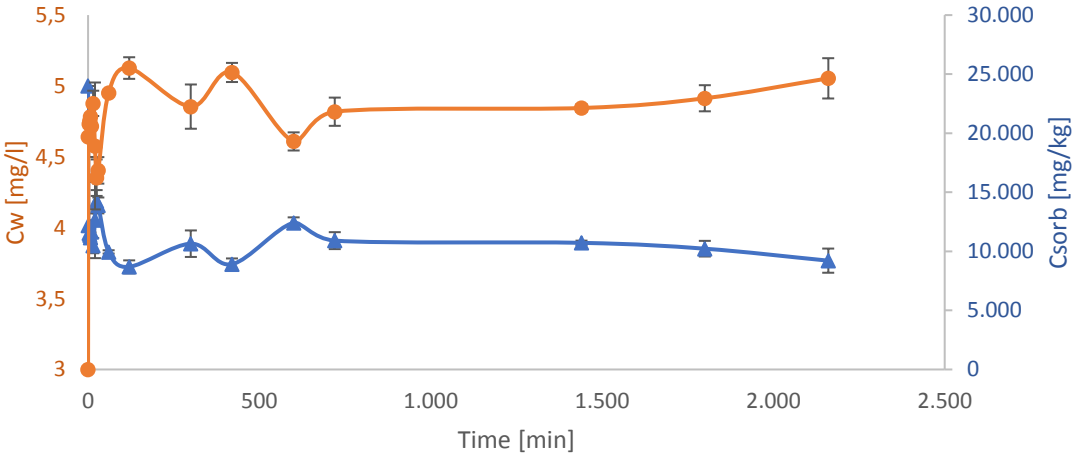

Figure 5.2 Kinetics of the propiconazole sorption on PMO- silica particles [I=0,05 M (KCl), T=20°C (room temperature), pH 7]. Error bars present the standard deviation between triplicates

To assess the effect of changing envoronmental conditions on the interactions between propiconazole and PMO-silica, the sorption was carried under conditions of different pHs and ionic strength. Sorption experiments were conducted at three different pH values (5,8; 7,8; 9,2) with a) no background electrolyte. The calculated ionic strength ($I = \frac{1}{2}\sum C_i . Z_i^2$) was I=0,1- 0,15 mM (added HCl and NaOH). In the setup b) 50 mM KCl were used as a background electrolyte.

Figure 5.3. depicts the comparison of Kd values of propiconazole sorption on PMO-silica at 3 different pHs (5,8; 7,8; 9,2) and different ionic strengths: 0,1-0,15 mM – blue bars and 50 mM – orange bars. The Kd values were determined for propiconazole equilibrium concentration Cw=4 mg/l. The sorption isotherm depicted in Figure 5.1. shows, that at Cw=4 mg/l sorption isotherm is linear and is not concentration-dependent. In the presence of 50 mM KCl the Kd values at all the three pH values are 4864±297 l/kg, whereas in the system with no electrolyte (I=0,1-0,15 mM) increase in pH results in lower Kd values (Figure 5.3). Thus, the increase of the pH from pH 5,8 to 7,8 resulted in Kd decrease by 8%, from pH 7,8 to 9,5 – Kd decrease by 22%. Sorption of propiconazole in the presence of background electrolyte was lower compared to the lower ionic strength (0,1-0,15 mM).

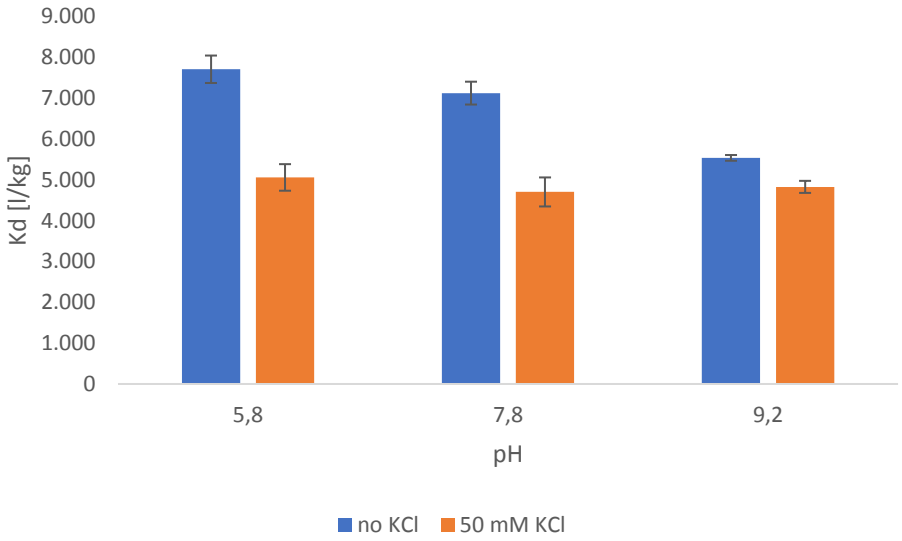

Figure 5.3 Comparison of the distribution coefficients of propiconazole sorption on PMO at pH 5,8; 7,8; 9,2 without background electrolyte (I=0,1-0,15 mM) and with 50 mM KCl [T=20°C (room temperature), Cw=4 mg/l, 0,1 g/l PMO-silica]. Error bars present the standard deviation between triplicates

The point of zero charge of PMO-silica was measured on Malvern Zetasizer below pH 3 [Grünhage, 2017]. With increasing pH, the particles surface is getting more negative. As propiconazole is uncharged its sorption should not be affected by electrostatic interactions. For an uncharged molecule, an effect of electrolyte concentration may be explained by salt-effects.

The most common way to account for the salt-effects (salting-in or salting-out) is Sechenov equation (eq. 5.1)

$$ln\left(\frac{Z_B^*}{Z_B}\right) = k_{syz}.y \quad 5.1$$

$Z_B^* \; and \; Z_B$ solubilities of component B in an electrolyte and in pure water respectively;

y —salt composition

For Z_B^* and Z_B the equilibrium concentrations were used, for y – ionic strength.

The Sechenov parameters k_{syz} for three pH values are summarized in Table 5.1. All the calculated values are negative, implying salting-in effect [Hefter and Tomkins, 2003], i.e. at higher salt concentration (50 mM KCl) solubility of propiconazole increased, resulting in lower sorption.

Table 5.1 Summary of Sechenov parameters for propiconazole sorption on PMO-silica at three pHs [I=50 mM KCl] (eq. 5.1)

	pH 5,8	pH 7,8	pH 9,2
k_{syz} [l/mol]	-4,6	-4,7	-1,2

The salting-in effect at pH 5,8 and pH 7,8 was more pronounced than at pH 9,2. For the non-charged molecule of propiconazole and PMO-silica with PZC below 3, pH was not expected to alter the sorption. The possible explanation of a decrease in Kd values at higher pH is the salting-in effect. To adjust pH of propiconazole and PMO-silica to higher pH (pH 9,2) more titrant (NaOH) was used, resulting in higher ionic strength. Therefore, ionic strength without BG electrolyte is different at three pHs. With increasing ionic strength, the solubility of propiconazole increases and it results in lower sorption at pH 9,2. Thus, the measured salting-in effect at pH 9,2 is lower, than at pHs 5,8 and 7,8, where the difference in ionic strengths is higher than at pH 9,2. The stability of silica particles was also considered. The solubility of amorphous silica (glass) in NaOH at high pH (or high NaOH concentrations) increases significantly [Eikenberg, 1990; Nibori et al., 2000]. Above pH 10,5 silica dissolves, resulting in dimers, trimers and tetramers formation. However, at pH below pH 10 polymerization is insignificant [Eikenberg, 1990]. Pham et al., 2012 investigated the stability of mesoporous silica and concluded the relatively high solubility (30-42%) of various mesoporous silica types in the pH range 7-9,2. The solubility of PMO-silica, used in our study was not investigated, thus slight dissolution should not be totally neglected, especially assuming, that over-titration took place. The dissolution of the PMO-silica surface would decrease the number of sorption sites for propiconazole and consequently, result in the lower sorption.

Effect of Cu^{2+} cations on sorption. Copper-based fungicides are widely used against various fungal diseases in agriculture and poultry [Arias et al., 2006; Ewing et al., 1998; Berenstein et al., 2017; Wang et al., 2018; Pose-Juan et al., 2009]. This results in high concentrations of Cu^{2+} cations in the environment, including aqueous systems. The presence of Cu^{2+} may influence the sorption of studied compounds [Arias et al., 2006]. To study how Cu^{2+} would affect propiconazole sorption on PMO-silica and

propiconazole's bioavailability, sorption experiments of propiconazole on PMO-silica were conducted in the presence of 17 mM $CaCl_2$.

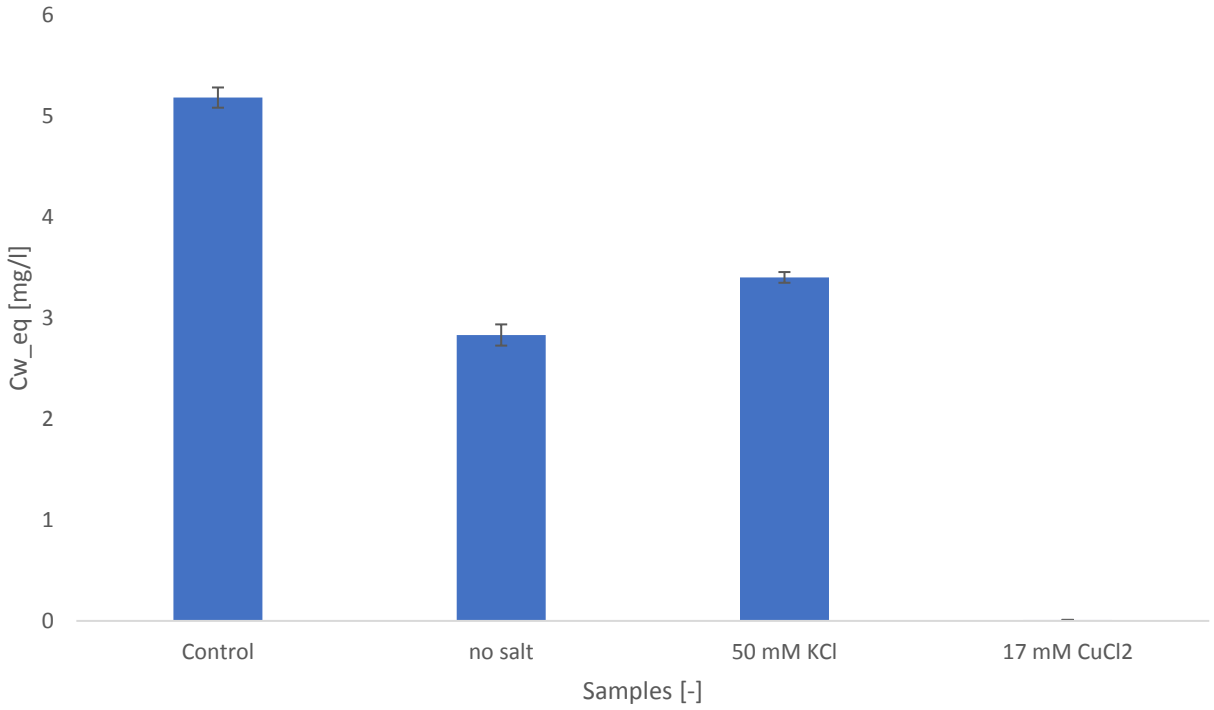

Figure 5.4 Comparison of the equilibrium concentrations of propiconazole sorption on PMO [pH 5,8; T=20°C (room temperature), 5,18 mg/l propiconazole (control); 0,1 g/l PMO-silica; a) with no BG electrolyte (I=0,1-0,15 mM); b) 50 mM KCl; c) 17 mM $CuCl_2$]. Error bars present the standard deviation between triplicates

Figure 5.4. depicts the equilibrium concentrations (Cw_eq) of propiconazole sorption on PMO-silica. The results indicate highly increased Kd values in the presence of copper. Aqueous concentration of propiconazole in the presence of 17 mM $CaCl_2$ was slightly below LOQ but above the LOD. Therefore $\lim_{Cw\_eq \to 0} K_d = \infty$, since $K_d = Csorb_{eq}/Cw_{eq}$. Increase in Kd values may be explained through the complex formation between Cu^{2+} ions and propiconazole. Complex formation between triazole fungicides and copper is well documented in the literature [Arias et al., 2006; Dytrtova et al., 2011]. A formation of the Cu-propiconazole complex goes by tetrahedral coordination around Cu-core with two triazole and two chloride ligands bonding [Evans et al., 2010]. Therefore, complexation takes place between 2 molecules of propiconazole and one cation of copper (Figure 5.5).

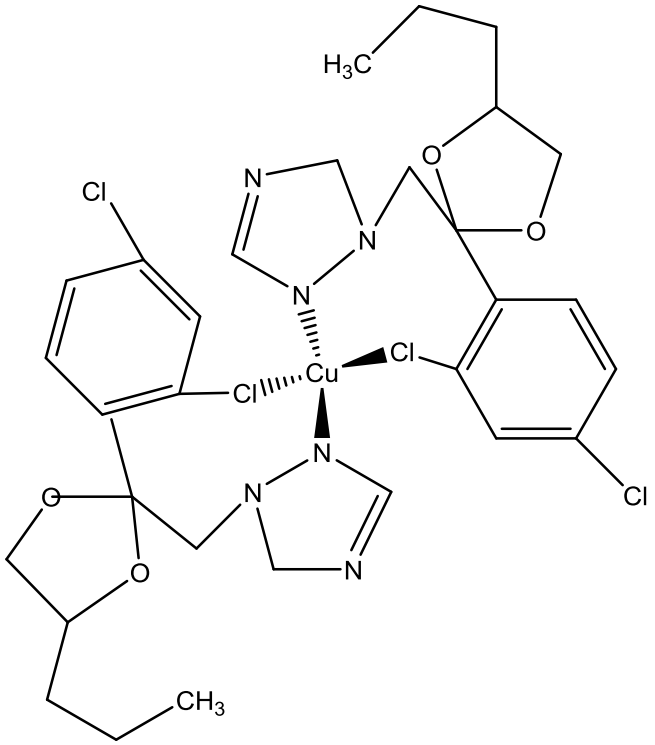

Figure 5.5 Schematic view of the complex between 1 Cu^{2+} cation and 2 propiconazole molecules [ChemDrawProfessional 17.1]

Several authors investigated sorption of Cu^{2+} cations on mesoporous silica and periodic mesoporous organosilica and have concluded the high Cu^{2+} adsorption on different types of silica [Knight et al., 2018; Oravec et al., 2014; Lee et al., 2015; Northcott et al., 2010]. Sheals [Sheals et al., 2003; Sheals et al., 2001] and Maqueda [Maqueda et al., 2002] described the complexation of glyphosate by Cu^{2+} on the water-mineral surface. Assuming the possibility of propiconazole complexation by Cu^{2+} sorbed to the surface of PMO-silica would explain the significant decrease of freely-dissolved concentration of propiconazole. 17 mmol/l dissolved Cu^{2+} cations could bind up to 34 mmol/l propiconazole (roughly 11.642mg/l propiconazole). Calculated value exceeds the initial concentration of propiconazole by four orders of magnitude, which explains almost complete removal of propiconazole from the dissolved state. To approve the hypothesis of propiconazole-Cu^{2+} complexation on the water-particles surface it is necessary to implement ion analysis of the solution and quantify the freely-dissolved and sorbed Cu^{2+} concentration.

Sorption of hexaconazole on PMO-silica. All the above-described experiments were also conducted for hexaconazole. In general, the results for hexaconazole were very similar to the sorption of propiconazole at all conditions studied. Figure 5.6 depicts the sorption isotherms of hexaconazole and propiconazole on PMO-silica. The Langmuir equation parameters are summarized in Table 5.2.

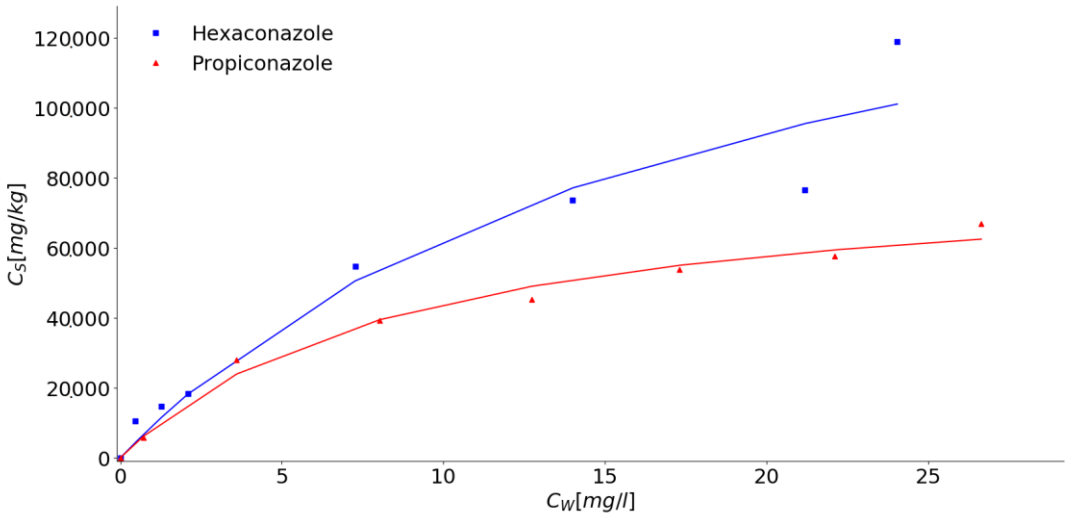

Figure 5.6 Comparison of sorption isotherms of propiconazole and hexaconazole on PMO-silica [I=0,05 M (KCl), T=20°C (room temperature), pH 5,8, 0,1 g/l PMO-silica]

Table 5.2 Comparison of the Langmuir equation coefficients of hexaconazole and propiconazole sorption on PMO-silica [I=0,05 M (KCl), T=20°C (room temperature), pH 5,8]

	Csorb_max [mg/kg]	K_L [l/kg]
Hexaconazole	187.330	0,054
Propiconazole	83.494	0,11

The maximum sorption capacity Csorb_max) of hexaconazole is significantly higher, than Csorb_max of propiconazole. The higher sorption of hexaconazole on PMO-silica may be explained by the difference in hydrophobicity. The hydrophobicity effect of pesticides sorption on PMO-silica was discussed in Chapter 4.

It was proposed, that the sorption decrease in the row: propiconazole-thiacloprid-imidacloprid is due to the increasing water solubility and K_{OW} value decrease (Table 2.2, Chapter 2). Hexaconazole's water solubility is 18 mg/l, K_{OW} is higher, than of propiconazole (Table 2.2, Chapter 2). The hypothesis of increasing sorption with higher hydrophobicity explains significantly higher sorption of hexaconazole on PMO-silica, compared with propiconazole sorption.

5.5. Sorption mechanism of azole fungicides on PMO-silica

Being hydrophobic both hexaconazole and propiconazole incline to participate in hydrophobic interactions. Chemical structures of propiconazole, hexaconazole and periodic mesoporous organosilica (PMO) fragment are presented in Figure 5.7.

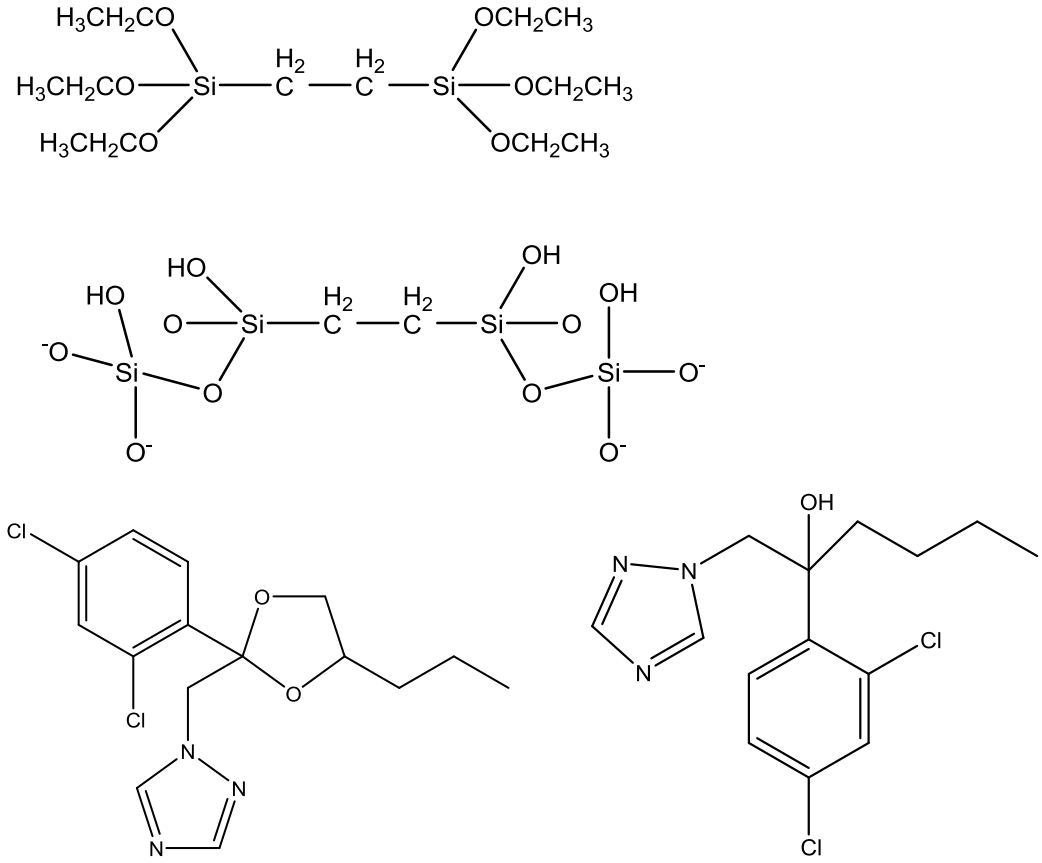

Propiconazole *Hexaconazole*

Figure 5.7 Example of periodic mesoporous silica (PMO-silica) fragment structure [Luo, 2018]; Propiconazole; Hexaconazole

Point of zero charge of PMO-silica was measured using potentiometric titration method and estimated below pH 3 [Grünhage, 2017]. Therefore, in the entire studied pH range surface of PMO-silica was negatively charged due to the dissociation of surface functional groups [Villegas et al., 2017; Otero et al., 2013; Schwarz et al., 1984]. Several sorption mechanisms are possible, considering the surface properties of PMO-silica and propiconazole molecule properties. As was discussed in Chapter 4 and 5, the sorption of the pesticides (imidacloprid, thiacloprid, propiconazole, hexaconazole) on PMO-silica is increasing with the decreasing water solubility and increasing Kow constant. Thus, the present work suggests, that the pesticides sorption on PMO-surface is mainly determined by hydrophobicity. The Cl-

substituents possess strong electron-accepting properties, which decreases electron density of the aromatic rings and make them to strong electron-acceptors [Li and Flood, 2008]. Thus, the aryl rings may participate in π-π EDA interactions with PMO (for example, with non-polar functional groups of PMO-silica and aromatic ring).

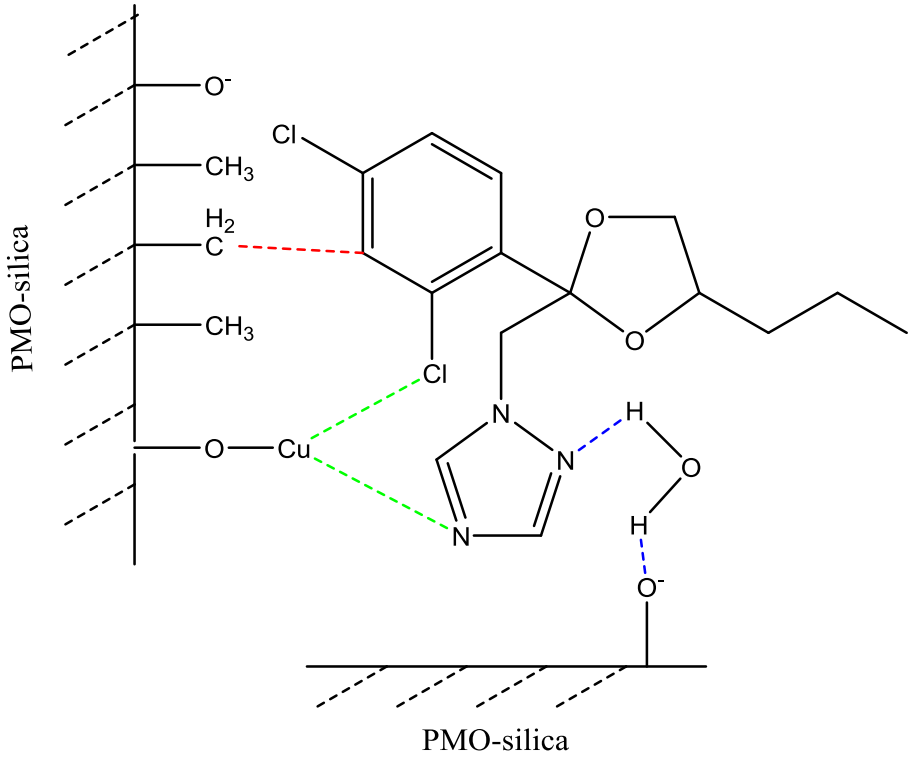

Figure 5.8 Possible interactions between azole compounds (on the example of propiconazole) with PMO surface (represented schematically with functional groups). Blue dotted lines represent hydrogen bonds. Dashed red lines represent EDA interactions. Green dotted lines – complexation with surface Cu^{2+}

The properties of triazoles were described by Juricek et al., 2011. Being nitrogen-rich, triazole is a strongly electron-deficient heterocycle. Triazole can serve as a metal coordinator [cation-N(triazole), being a ligand or cation receptor], participate in hydrogen bond formation ([hydrogen-N(triazole), anion-N(triazole)] [Crowley et al., 2010; Camponovo et al., 2009; Li et al., 2007]. There are several published works, which describe extensively hydrogen-N(triazole) and anion-N(triazole) interactions [Li and Flood, 2008; Hua and Flood, 2010]. Russell et al., 1968 studied sorption of 3-aminotriazole on montmorillonite clay and concluded that 3-aminotriazole may be adsorbed as a triazolium cation, formed under the effect of highly-polarized interlamellar water. PMO surface does not possess exchangeable cations, thus mainly hydrogen-N(triazole) and anion-N(triazole) interactions are expected between triazole moiety and PMO surface. The hydrogen-N(triazole) bond is expected between azole

molecules and the surface of PMO-silica through the water bridges (Figure 5.8) [Li et al., 2007]. In the presence of $CaCl_2$ or $CuCl_2$, the triazole moiety may coordinate with the divalent cation, sorbed on the PMO-surface (green dotted lines in Figure 5.8). The complex between the propiconazole and Cu^{2+} cations, sorbed on the surface of PMO-silica was proposed in Figure 5.5.

5.6. Conclusions

The sorption of propiconazole and hexaconazole on PMO-silica was high. The sorption increased in a row: imidacloprid<thiacloprid<propiconazole<hexaconazole, implying significant effect of hydrophobicity on sorption on PMO-silica. The proposed sorption mechanism of azole fungicides on PMO-silica involved hydrogen-N(triazole) and anion-N(triazole) bond formation. Additionally, aryl-ring was suggested for anion-π EDA interactions. The Cu-propiconazole complex-formation on the surface water-PMO-silica was proposed. I.e. it was suggested, that Cu^{2+} sorbs to the PMO-silica and through complex-formation facilitates propiconazole sorption. The proposed complex involves 1 atom of Cu^{2+} and two molecules of propiconazole, Cu^{2+} coordinated two Cl atoms and two N atoms of triazoles. An increase in ionic strength results in the salting-in effect (calculated with Sechenov equation), i.e. the solubility of propiconazole increased and sorption decreased. The decrease in sorption at high pH (pH 9,2) in comparison to the lower pH (pH 5,8 and 7,8) in the absence of BG electrolyte can be explained through ionic strength increase, which diminishes the sorption. The pH increases in the presence of BG electrolyte does not have a significant effect on sorption. Thus, it may be concluded, that both presence of Cu^{2+} cations and ionic strength impact the sorption of propiconazole on PMO-silica, changing fungicide's bioavailability and toxicological effect for the environment, namely for target and non-target organisms in aqueous systems. Overall, PMO-silica is an effective sorbent of propiconazole and hexaconazole and may be used for the toxicological studies.

Additionally, sorption of propiconazole in MMN medium in presence of glucose was studied and no measured effect of glucose presence on sorption was determined. Therefore, implementation of toxicological studies in MMN medium should not affect the effectiveness of PMO-silica as a sorbent of propiconazole.

Chapter 6 Sorption of Glyphosate on Alumina (Al_2O_3) Particles

6.1. Introduction

Glyphosate is one of the most widespread herbicides. Due to its popularity and recently raised concerns of potential health impacts, glyphosate was intensively studied in the recent years. Its environmental fate was investigated by various researchers [Schuette, 1998; Aparicio et al., 2013; Manassero et al., 2010; Wang et al., 2016; Rueppel et al., 1977]. One of the research questions, addressed in the studies is sorption of glyphosate on various substrates [Ololade et al., 2013; Hance, 1976; Wang et al., 2005; Munira and Farenhorst, 2017; de Jonge and de Jonge, 1999; Glass, 1987]. In most of the studies, sorption experiments were conducted on different types of soils or clay minerals. Some authors have emphasized the high relevance of iron oxides [Miles and Moye, 1988; Rampazzo et al., 2013; Ololade et al., 2013; Sheals, 2002] and aluminium oxides [Morillo et al., 2000] as soil constituents for glyphosate adsorption.

Several papers describe the mechanism of glyphosate interaction with metal oxides (mostly, goethite and hematite). Barja and dos Santos Afonso, 1998; Sheals et al., 2002; Gimsing et al., 2004 conclude that the interaction with the oxide surface involves phosphonate group of glyphosate. Additionally, amine and carboxylic groups may form outer sphere complexes. Dideriksen and Stipp (2003) demonstrated the interaction of hydroxyls of phosphonate group with the mineral surface. They proposed that carboxyl can form mono- and bidentate bounds, additionally fixing glyphosate molecule on the oxide surface [Dideriksen and Stipp, 2003]

The motivation of the present study is to investigate the interactions of glyphosate with the mineral species abundant in the soil. The sorption experiments were designed to be conducted on the material with high sorption capacity of glyphosate and determine the impact of environmental factors on glyphosate sorption. Amorphous aluminium oxide particles were chosen as a sorbent of glyphosate due to their high binding capacity of glyphosate, determined in the preliminary experiments. So far, sorption of glyphosate on amorphous alumina of (nano-)size has not been studied explicitly. However, some works indicated a positive effect of alumina presence in soils on glyphosate sorption [Morillo et al., 2000; Orcelli et al., 2018].

In the present study, alumina was chosen as a sorption material as an important constituent of soils and sediments. pH was expected to affect glyphosate sorption due to the glyphosate's speciation (Scheme 6.1). Various ions such as Cu^{2+} and Ca^{2+} were expected to affect glyphosate's sorption through the complexation [Maqueda et al., 2002; Martell and Motekaitis, 1988; Subramanian and Hoggard, 1988; Dousset et al., 2007; Barret and McBride, 2006]. Phosphate and glyphosate are known to

compete for the same sorption sites [Borggaard and Gimsing, 2008], building strong Al-O-P bonds; therefore, the addition of phosphate was targeted to reveal competitive sorption. To reveal the significance of the molecule charge and structure on the sorption, sorption of glufosinate ammonium and the main metabolite of glyphosate – AMPA were studied.

6.2. Experimental setup

Experiments were designed and conducted in a batch equilibrium method. Every sample including controls was prepared in triplicates; the reported values are the average of the three measurements. Aliquots of glyphosate and alumina were mixed in Eppendorf tubes (2 ml). Solutions of $CaCl_2$, $CuCl_2$, KCl and K_2HPO_4 were added to the samples at different concentrations. pH adjustment was done by titration with HCl/NaOH in the absence of buffers. In the earlier experiments, pH was measured using pH strips (Merck, Darmstadt, DE) to prevent any contact of glyphosate with glass surfaces and possible loss due to sorption of the pesticide. After it was proven, that the sorption of glyphosate on the pH electrode is negligibly low in comparison to the total glyphosate concentration, pH was measured with a pH electrode, providing higher precision. Samples were shaken on the horizontal shaker for 24 hours to reach equilibrium conditions. Subsequently, Eppendorf tubes were centrifuged and decanted into polypropylene vials. Glyphosate, as well as phosphate concentrations were measured by capillary electrophoresis coupled to mass spectrometry (experimental conditions are described in Chapter 2).

6.3. Results and Discussion

Langmuir sorption model was fitted to the experimentally obtained data.

To evaluate the impact of the pH on the sorption, sorption isotherms of glyphosate on alumina were obtained at three different pH levels [pH 5; pH 7; pH 8,5]. The resulted isotherms are presented on Figure 6.1. Impact of pH was studied without the addition of background electrolyte; therefore, an ionic strength was determined by the amount of added NaOH/HCl during the pH adjustment. The ionic strength was calculated using formula $I = \frac{1}{2}\sum C_i . Z_i^2$, where C_i – is the concentration of the ion, Z_i – charge of the ion. The amount of added HCl and NaOH varied slightly from experiment to experiment, resulting in 0,04 – 0,1 mM ionic strength. At pH 7 sorption isotherm has the steepest slope and the higher sorbed concentrations were reached at lower equilibrium concentrations; at pH 5 sorption isotherm is more gradual, however, reaches the higher sorbed concentrations; the lowest and slowest sorption was observed at pH 8,5, at which both the slope and maximum sorbed concentration are lower than at pH 5 and pH 7. Langmuir equation coefficients are summarized in Table 6.1.

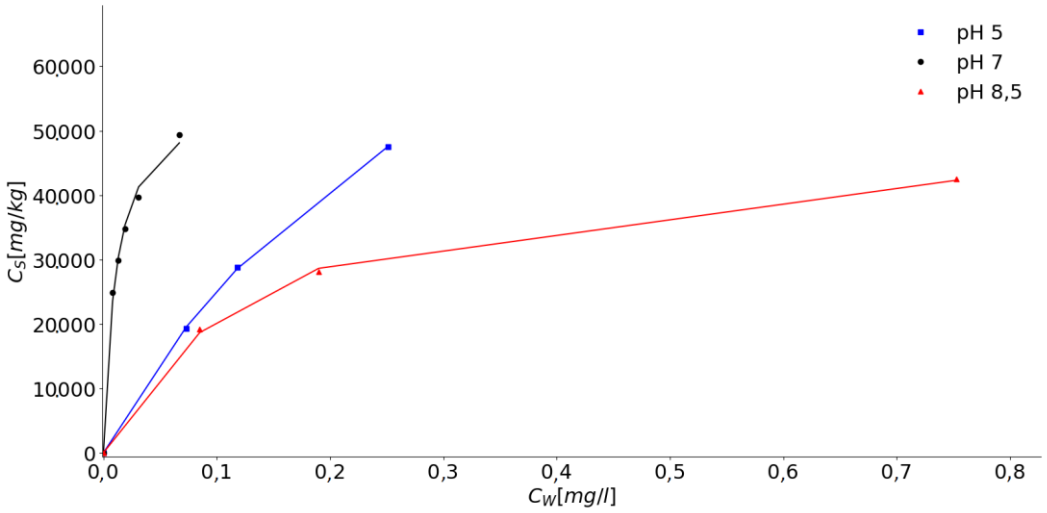

Figure 6.1 Sorption isotherm of glyphosate on Al_2O_3 particles [I=0,04-0,1 mM, T=20°C (room temperature), pH 5; 7; 8,5]

Table 6.1 Langmuir equation parameters (Csorb_max and K_L) of the sorption of glyphosate to Al_2O_3 at pH 5, pH 7, pH 8,5 [I=0,04-0,1 mM, T=20°C (room temperature)]

Langmuir parameters	*pH 5*	*pH 7*	*pH 8,5*
Csorb_max [mg/kg]	114.984	*55.456*	*48.738*
K_L [l/mg]	*2,80*	*91,9*	*7,14*

The point of zero charge (PZC) of the aluminium oxide was at pH = 9 as determined by Guluzada and Grünhage [Appendix, Figure_I; Grünhage, 2017]. These values correlated well with the ones estimated by Sposito, 2008. Therefore, in the pH range pH 5 – 8,5 the positive charge of the Al_2O_3 particles decreases to zero. The pH increase results in deprotonation of glyphosate. Its third pKa_3 is 5,4 [Scheme 6.1, Goodwin et al., 2003]. Therefore, during increasing pH from 5 to 7, glyphosate changes its anionic charge from z = -1 to -2. Thus, at the pH 7, the maximum sorbed concentration is reached at the lower equilibrium concentrations. The surface charge of alumina decreases with pH and at pH 8,5 it is close to zero, i.e. the surface is uncharged. At pH 7 alumina's surface charge is lower, than at pH 5, implying weaker electrostatic interactions, which results in the lower sorption at higher pH. However, even at pH 8,5 the sorption of glyphosate on alumina is relatively high (Csorb_max=48.738 mg/kg). Thus, sorption of glyphosate on alumina is determined not only by electrostatic interactions. Jonsson, 2007 explained it by the covalent bonding between the glyphosate molecule (through phosphonate group) and functional groups of the alumina surface. Mui et al., 2016 studied the adsorption of the humic acids (negatively charged above the pH 4) and made similar conclusions to the ones presented in the current work. According to Mui et al., 2016, at pH 5 adsorption of humic acids (HA) to the alumina surface is

favourable for the electrostatic interactions. However, at the pH>PZC the electrostatic barrier between the negatively charged alumina and HA inhibited the sorption of HA on the aluminium oxide surface.

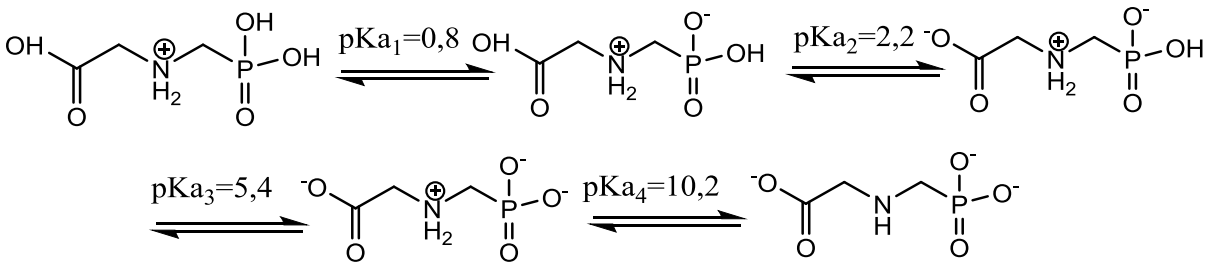

Scheme 6.1 pKa values and species of glyphosate [Goodwin et al., 2003]

Borggaard and Gimsing (2008) determined a decrease of glyphosate sorption on aluminium and iron oxides at higher pHs, which was explained by the negative charge of both the sorbent and sorbate. Gimsing et al., 2004 measured two-times higher sorption of glyphosate at pH 6 in comparison to pH 8 and explained It by the change in the surface charge of the sorbent.

Effect of ionic strength. To estimate an effect of ionic strength on the sorption of glyphosate, experimental isotherms were constructed for the cases of 0,5; 5 and 50 mM KCl presence. The comparison of the Langmuir equation coefficients at different electrolyte concentrations (Table 6.2) and (Table 6.1) reveals a decrease in Csorb_max with increasing ionic strength. K^+ and Cl^- build the electric double-layer on the mineral's surface. The higher ionic strength causes a steeper decrease of the potential and thus a lower zeta potential [Vindvogel, 1992]. For the negatively charged molecule of glyphosate higher zeta potential determines higher electrostatic interactions and thus more favorable conditions for the sorption.

Alumina particles are positively charged at pH 5. Figure_I in the Appendix depicts PZC of aluminium oxide in MilliQ water, in a solution of 5 mM KCl or 1,7 mM $CaCl_2$. The point of zero charge in 5 mM KCl solution is slightly lower than in MilliQ water. The comparison of the values summarized in Table 6.2. demonstrates, that Csorb_max decreased by 39 % from 0,5 mM to 5 mM KCl and by only 19 % when increasing the KCl concentration from 5 mM to 50 mM, which is explained by partial dissociation of the electrolyte at higher concentrations. Orcelli et al., 2018 observed decrease of the PZC of goethite with increasing sodium chloride concentration. In the same work there was suggested an interaction between Cl^- ions and positively charged sites on the sorbent surface, whcih reduced the zeta potential of the material.

The decrease in zeta potential results in the lower positive charge of the surface and lower sorption of negatively charged glyphosate [Orcelli et al., 2018]. Johnson and Pytkowicz (1979) and Degreve and da

Silva (2000) proposed, that at high concentration [0,7 M NaCl] of sodium chloride approximately 10% of the salt are present undissociated as ion pairs. Therefore, the high decrease in the PZC charge is not expected at higher concentrations of electrolyte.

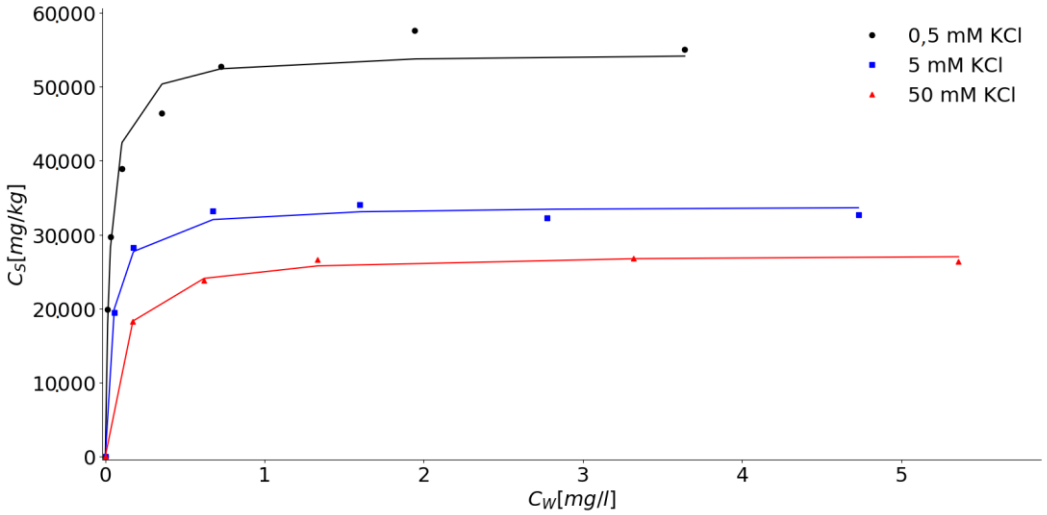

Figure 6.2 Sorption isotherms of glyphosate on Al_2O_3 particles [KCl as BG electrolyte; T=20°C (room temperature), pH 5]

Table 6.2 Langmuir equation parameters (Csorb_max and K_L) of the glyphosate sorption on Al_2O_3 at different KCl concentrations

KCl concentration [mM]	*0,5*	*5*	*50*
Csorb_max [mg/kg]	54.597	*33.919*	*27.453*
K_L [l/mg]	*33,52*	*25,27*	*11,54*

Moreover, an increase in the ionic strength of the solution causes the compression of the diffused layer around the alumina particles. This results in a lower zeta-potential of the surface, which decreases the repulsion between the particles and facilitates their aggregation [Mui et al., 2016]. Therefore, at the higher ionic strength, the number of the surface sites on the alumina surface is lower due to the aggregation, which inhibits the sorption of glyphosate.

However, there is no univocal explanation in the literature of the ionic strength effect on glyphosate sorption. De Jonge and de Jonge, 1999 studying sorption of glyphosate to the sandy loam soil, measured an increase in the sorption with increasing ionic strength (applying $CaCl_2$, NH_4Cl and KCl as electrolytes). They explained it by the slight pH decrease with the addition of electrolytes. Gimsing and Borggaard, 2001 did not measure a significant effect of ionic strength (0,01 M $CaCl_2$, 0,1M KCl and 0,01 M KCl). Orcelli et al., 2018 determined a decrease with increasing ionic strength, concluding that glyphosate sorbs to goethite through the phosphonate groups forming outer-sphere complexes. Miles and Moye, 1988 reported enhanced desorption of glyphosate from different sorbents (silica, alumina,

clay minerals, soils) with increasing pH and ionic strength, which correlates with the results of the present research. They proposed, that in the presence of the electrolyte, negatively charged ions compete with glyphosate for the sorption sites.

Therefore, the negative effect of ionic strength on the glyphosate sorption on alumina in the present study is explained by the several factors:

a) Competition between Cl^- anions and glyphosate molecule (z=-1) for the positive sorption sites;
b) The decrease of the zeta potential of alumina surface with the addition of electrolyte resulting in the lower electrostatic interactions between alumina and glyphosate;
c) The lower zeta potential of the aluminium oxide surface results in the lower repulsion forces and aggregation of alumina into bigger particles, reducing the total amount of accessible sorption sites.

Effect of Ca^{2+} and Cu^{2+} cations. To investigate the effect of the divalent ions on glyphosate sorption, experiments were conducted in the presence of $CaCl_2$ and $CuCl_2$ [1,7 mM] at pH 5 and the results were compared with the sorption in the presence of 5 mM KCl at the similar pH values. The choice of ions was justified by the common occurrence in the environment. The most abundant cations in water are calcium (Ca^{2+}), magnesium (Mg^{2+}), sodium (Na^+) and potassium (K^+). Calcium ions are often present in nature as a constituent of limestone rocks; e.g. seawater contains 0,15% calcium chloride. Copper ions are often present in the high concentrations from such sources as application of fertilizers, mildew removal sprays in the vineyards, sewage sludge and other Cu-containing waste [Fjallborg and Dave, 2003; Arias et al., 2006; Lv et al., 2018]. Moreover, multiple researchers described complex formation between glyphosate and Ca^{2+} and Cu^{2+} cations. Thus, it was expected, that Cu^{2+} and Ca^{2+} can affect the sorption of glyphosate, as well as its bioavailability.

The sorption isotherms in the presence of $CaCl_2$ and $CuCl_2$ are depicted in Figure 6.3 (a, b); a summary of the Langmuir parameters is presented in Table 6.3.

a)

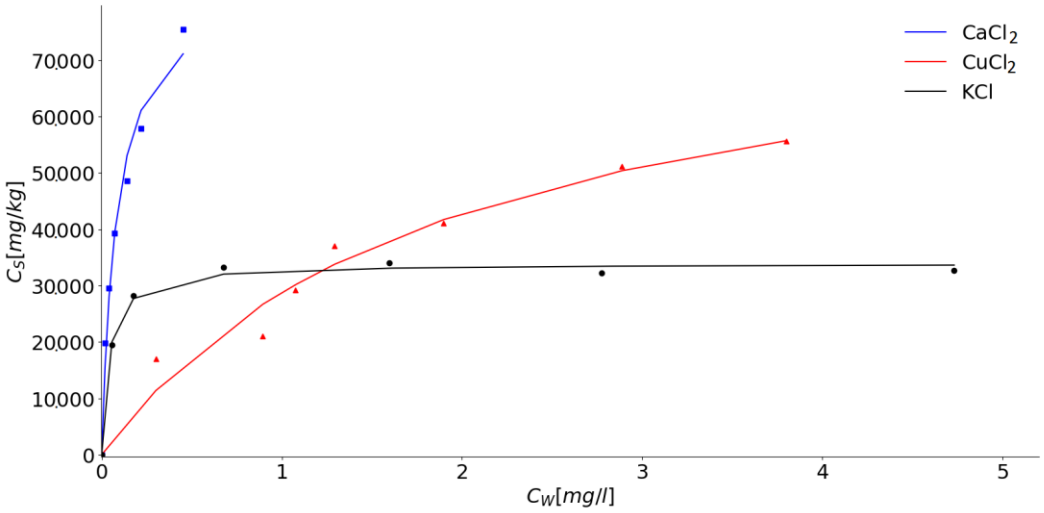

b)

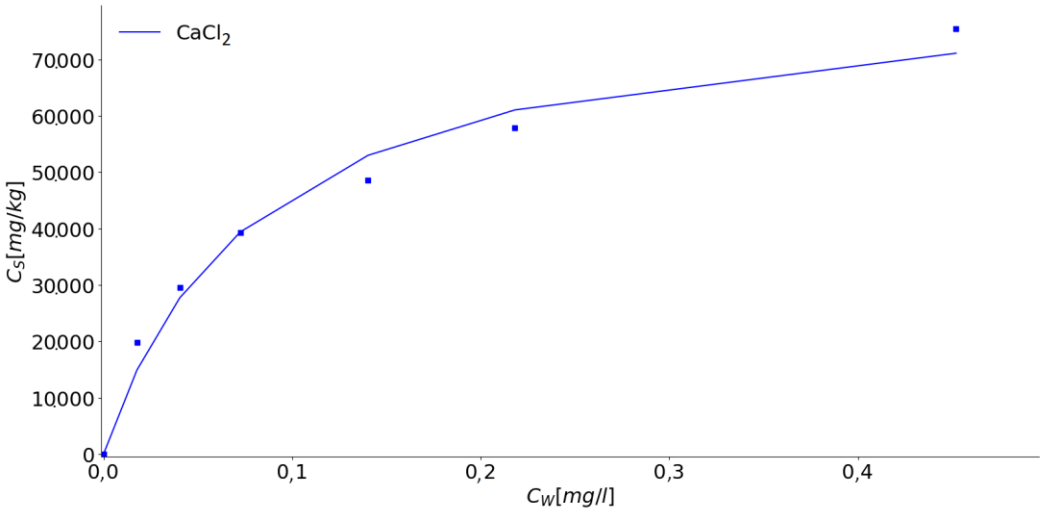

Figure 6.3 Sorption isotherm of glyphosate on Al_2O_3 particles [a) 1,7 mM $CaCl_2$, 1,7 mM $CuCl_2$, 5 mM KCl; b) 1,7 mM $CaCl_2$, T=20°C (room temperature), pH 5]

Table 6.3 Langmuir equation parameters (Csorb_max and K_L) of the sorption of glyphosate on Al_2O_3 in the presence of different cations [I=5 mM, T=20°C (room temperature), pH 5]

I=5 mM	*K^+*	*Ca^{2+}*	*Cu^{2+}*
Csorb_max [mg/kg]	*33.919*	*84.027*	*84.048*
K_L [l/mg]	*25,27*	*12,18*	*0,52*

The presence of Ca^{2+} and Cu^{2+} produced similar adsorption capacities (Csorb_max) as the result of the experiment. Martell and Motekaitis (1988) and Subramanian and Hoggard (1988) demonstrated

strong coordination bonds of glyphosate with metal ions and concluded the strong chelating behavior of glyphosate. Dousset et al., 2007 studied the effect of copper on glyphosate's mobility in soils and suggested that in the presence of copper ions glyphosate may build complexes in aqueous environments. Barret and McBride also observed a higher mobility of glyphosate because of complex formation with Cu [Barret and McBride, 2006].

High hydration enthalpy for copper and its ionic size promotes coordination of glyphosate, which effectively decreases the concentration of free glyphosate in solution. However, Maqueda et al., 2002 proposed that sorption of the glyphosate-copper complex occurs which increases glyphosate's overall sorption in comparison to free glyphosate. Mattos et al., 2017 investigated the sorption of glyphosate on clay, treated with various ions (Na^+, Ca^{2+}, Zn^{2+}, Cu^{2+} and Al^{3+}), and concluded, that the binding increased with the increase in cation charge. Sheals et al., 2003 demonstrated the direct formation of glyphosate-Cu^{2+} ternary surface complexes at the water-goethite interface at pH 4. According to ATR-FTIR and EXAFS results, Sheals et al., 2003 proposed that the phosphonate group of glyphosate forms inner-sphere monodentate bonds with the mineral surface, whereas the carboxylate and amine group coordinate Cu^{2+}, forming a 5-membered chelate ring. Similar results were provided by Jonsson, 2007 who studied complexation of glyphosate with Cd^{2+} cations and proposed the formation of two five-membered chelate rings between glyphosate and Cd^{2+} (1:1 complex). Sheals et al., 2001 studied glyphosate-copper complexes in the aqueous solutions and concluded the formation of 1:1 complexes, suggesting copper(II) to be at the center of a Jahn-Teller octahedron with all three functional groups (amine, carboxylate and phosphonate) being involved in the coordination sphere in two five-membered chelate rings. Thus, Cu^{2+} ions coordinate glyphosate both on the surface of the mineral and in the aqueous solution. Madsen et al., 1985 determined the complex formation constants (K_{ML}) of glyphosate with divalent cations by potentiometric titration. The reported log K_{ML} values as 11,92 and 3,25 for Cu(II) and Ca(II) 1:1 complexes with glyphosate respectively [Madsen et al., 1978]. Pessagno et al., 2008 demonstrated, that the strength of the complexes increases in a row mono-<di-<tri-valent ions. They suggested that Cu^{2+} forms a stronger complex with glyphosate than Ca^{2+}. Similar conclusion was made by Glass, 1984 who measured an increase in glyphosate complexation by the ions in the row Na^+<Ca^{2+}<Mg^{2+}<Cu^{2+}<Fe^3. In general, the presence of both Ca^{2+} and Cu^{2+} ions in the present work significantly affected the Csorb_max values [Table 6.3], decreasing the concentration of freely-dissolved glyphosate. The modelled maximum sorbed concentrations in the presence of both cations are close to each other [Table 6.3]. However, Csorb_max is reached faster in the presence of Ca^{2+} ions than in the presence of Cu^{2+} ions [K_L in the presence of Ca^{2+} and Cu^{2+} are 12,18 and 0,52 l/mg respectively]. To explain the deviation between two values further investigations are required which would determine experimentally the complex formation constants by potentiometric titrations.

To learn more about the **effects of the sorbate´s charge and structure** on the adsorption mechanisms, adsorption experiments with glufosinate and AMPA were carried out. Glufosinate's sorption on Al_2O_3 was negligibly low (approximately 2-6% of initial concentration were sorbed, which are in the error range of the method) in comparison to the glyphosate sorption.

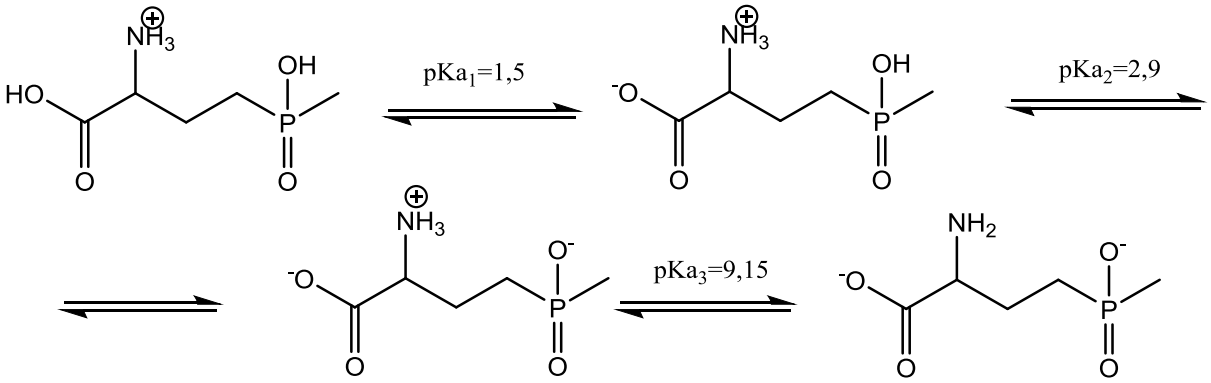

Scheme 6.2 Speciation scheme of glufosinate [from Li et al., 2018]

Li et al., 2018 determined the protonation constants of glufosinate in aqueous solutions using NMR spectroscopy and direct calorimetry. Scheme 6.2. depicts this speciation. Thus, at pH 5 glufosinate has 2 negative charges (on phosphinic and carboxylic groups) and one positive charge on the primary amine. In the present study, glufosinate ammonium was used (Figure 6.4)

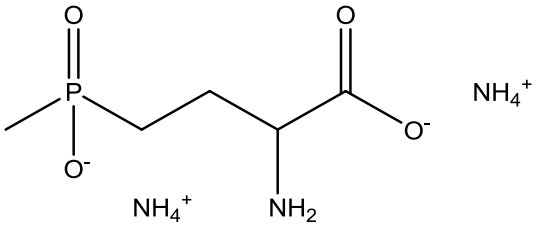

Figure 6.4 Chemical structure of glyphosate ammonium molecule at pH 5 [ChemDrawProfessional 17.1]

As it has been discussed above and proved by various scientists, glyphosate's binding to the mineral surface primarily involves the phosphonate group. The presence of the phosphinate group in the glufosinate molecule and not a phosphonate group seems to inhibit the sorption of glufosinate. McBride (1989), explaining sorption mechanism of glyphosate on goethite, suggested relocation of the proton from amino-group to the phosphonate group with the further H-bond formation between the glyphosate and goethite surface. In glufosinate molecule, such relocation of the proton is not expected, due to the presence of primary amine group and its spatial isolation from the phosphinate group. The low sorption of glufosinate on alumina, observed in the present study, can be explained by specific type of interaction between the phosphonate group of glyphosate through the hydrogen bonding to the

mineral surface, described previously by McBride (1989). Additionally, glufosinate possesses much higher aqueous solubility (500 g/l for glufosinate and 10 g/l for glyphosate, Table 2.2, Chapter 2), which emphasizes difficulties in glufosinate attenuation by adsorption from aqueous solution. Laitinen et al., 2008 investigated glufosinate-ammonium sorption on soils and measured 4 times higher sorption of glyphosate in comparison to glufosinate, mentioning high mobility and low sorption of glufosinate.
The main metabolite of glyphosate AMPA sorbed to alumina particles to a significantly higher extent than glufosinate. AMPA's sorption isotherm is depicted in Figure 6.5.

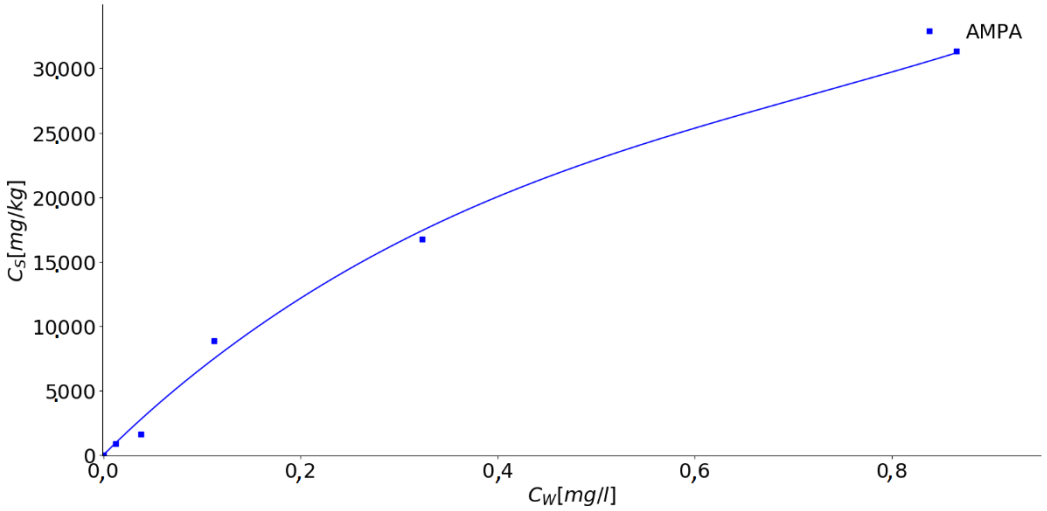

Figure 6.5 Sorption isotherm of AMPA on Al_2O_3 [0,5 mM KCl, T=20°C (room temperature), pH 5]. Csorb_max=59.171 mg/kg; K_L=1,29 l/mg]

The high sorbed concentration for AMPA is reached at higher equilibrium aqueous concentrations than for glyphosate (K_L(glyphosate)>>K_L(AMPA)) [Table 6.2. and Figure 6.5.].

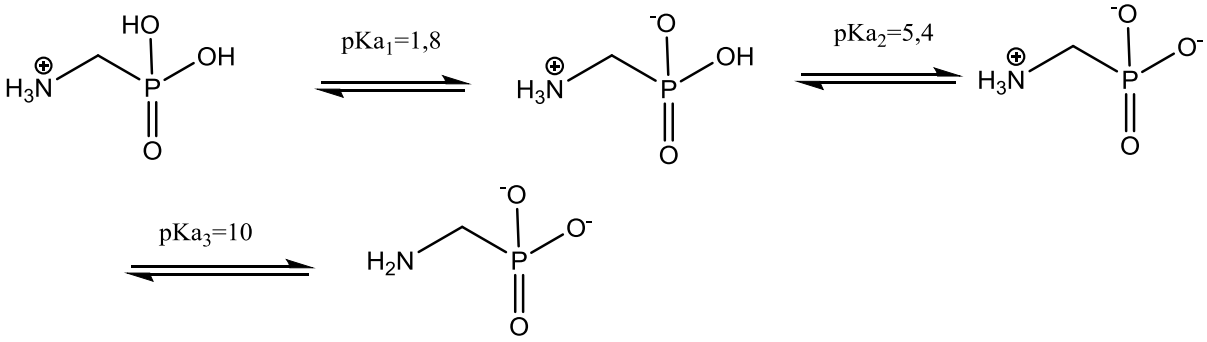

Scheme 6.3 pKa values and species of AMPA [from Goodwin et al., 2003]

pKa values of AMPA [Scheme 6.3] demonstarte, that at pH 5 AMPA molecule carries one negative charge (phosphonate group), which is compensated by protonated amine-group, resulting in total zero

charge of the molecule. At the same pH, glyphosate has total z=-1 charge (2 negative and 1 positive charge). It is expected that both AMPA and glyphosate molecules form monodentate complexes between the phosphonate group and alumina surface (the structure is described in detail in Chapter 7). As was suggested by McBride, 1989 and discussed above, the proton from the amino-group may migrate to the phosphonate group and promote the H-bonding which is missing in the glufosinate binding mechanism. Moreover, glyphosate can form outer-sphere complexes using the negative charge of the carboxylic group (Scheme 7.4, Chapter 7). Csorb_max values for both molecules are in the same order of magnitude: 59.171 mg/kg and 54.597 mg/kg for AMPA and glyphosate, respectively. However, K_L values differ significantly: 1,29 and 33,52 l/mg for AMPA and glyphosate [Figure 6.5., Table 6.2]. Thus, the structure of the glyphosate molecule conduces the maximum sorbed concentration to be reached already at lower aqueous equilibrium concentrations.

The sorption results on alumina nanoparticles show increased sorption of the components in the row: glufosinate<AMPA<glyphosate. This emphasizes the importance of the chemical structure of glyphosate for the interactions with alumina surface and supports the sorption mechanism of glyphosate through the phosphonate group.

Competitive adsorption of glyphosate and phosphate. Numerous researchers have investigated the competitive sorption of phosphate and glyphosate. Gimsing et al., 2004 and Gimsing and Borggaard, 2001 concluded that phosphate and glyphosate compete for the same sorption sites (the study was done on soils and goethite), proposing that the phosphonate group of the glyphosate is involved in the interaction. They determined glyphosate-soil complexes to be monodentate, whereas phosphate-soil complexes were characterized as bidentate, which explained the almost two-times higher sorption of glyphosate, however stronger sorption of phosphate due to the higher affinity of phosphate to the soil components [Gimsing et al., 2007]. The authors also determined the competitive character of glyphosate and phosphate sorption, emphasizing phosphate's ability to replace adsorbed glyphosate. Zheng et al., 2012 visualized phosphate inner sphere complexes with gamma-alumina at pH 4 and pH 9 using ATR-FTIR.

In the present study, 3 different concentrations of phosphate in the form of K_2HPO_4 [10, 50 and 100 nM] were added to the aqueous solution of glyphosate (23,66 µM). The objective of the present experiment was to verify whether glyphosate's adsorption on alumina involves the phosphonate functional group and whether both compounds compete for the same sorption sites. To revise whether phosphate can cause glyphosate's desorption or vice versa, two setups, differing in the order of components addition, were tested: a) Glyphosate was added to alumina; thereafter phosphate was added to the glyphosate-alumina suspension; b) Phosphate was added to alumina; thereafter glyphosate was added to the glyphosate-alumina suspension.

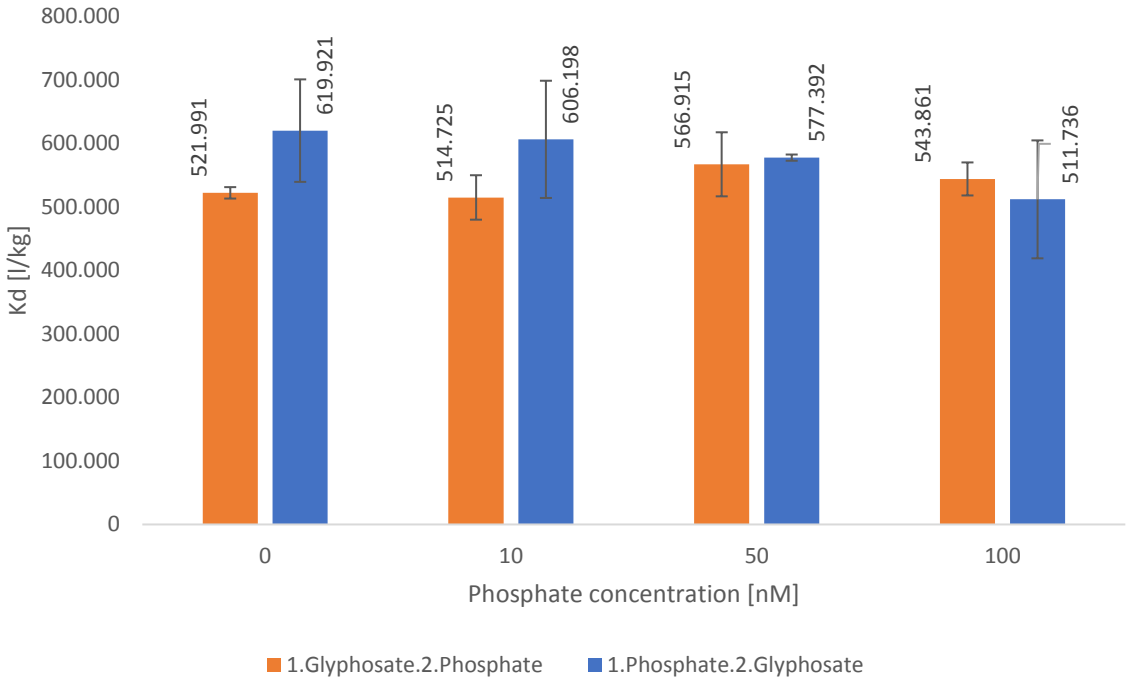

Figure 6.6 Comparison of the Kd values of glyphosate sorption on Al_2O_3 with different phosphate concentrations. Initial glyphosate concentration in all the samples was 23,66 µM (4 mg/l) – linear range of the sorption isotherm (Figure 6.1) [I=0,04 - 0,1 mM; T=20°C (room temperature), pH 5]. Error bars present standard deviation between triplicates

The concentration of phosphate (measured with CE) in all the samples, after equilibrium was reached, was below LOQ, indicating almost quantitative adsorption of phosphate to Al_2O_3. A negligible response of the glyphosate distribution coefficient on the phosphate presence (Figure 6.6.) may be explained by the significantly lower concentrations of phosphate in comparison to glyphosate. In literature, competitive sorption between phosphate and glyphosate was studied with equal or similar concentrations of both compounds. For the present study phosphate concentration was chosen based on environmental relevance, representing concentrations frequently observed in nature. However, such a pronounced difference in concentrations of glyphosate and phosphate did not provide data on phosphate effect on glyphosate's sorption.

To compare calculated maximum sorbed concentration Csorb_max at pH 5 (Table 6.1) with the cumulative concentrations of glyphosate and phosphate in the competitive sorption experiments and to reveal how far the total sorption capacity was reached, concentrations of the sorbed glyphosate and sorbed phosphate in mmol/l were calculated. Considering monodentate glyphosate_alumina binding and bidentate phosphate_alumina binding (i.e. phosphate occupies two sorption sites) the calculated concentrations were summarized and compared with Csorb_max in mmol/kg. The results are summarized in Table 6.4.

Table 6.4 Comparison of the total sorbed concentration of glyphosate and phosphate and calculated Csorb_max at pH 5 and I=0,04-0,1 mM. Cw_tot_glyphosate=23,66 µM, Cw_tot_phosphate: 0,01 µM; 0,05 µM; 0,1 µM. After equilibration, the concentration of phosphate in the samples was below LOQ. a) 1. Glyphosate; 2. Phosphate were added to alumina; b) 1. Phosphate; 2. Glyphosate were added to alumina.

a)

Concentration of added phosphate [µmol/l]	Csorb_glyphosate [mmol/kg]	Csorb_phosphate [mmol/kg]	Csorb_glyphosate+2·Csorb_phosphate [mmol/kg] *	Csorb_max [mmol/kg]
0	232,24	-	232,24	680
0,01	232,16	0,056	232,28	
0,05	232,57	0,281	233,13	
0,1	232,41	0,562	233,53	

b)

Concentration of added phosphate [µmol/l]	Csorb_glyphosate [mmol/kg]	Csorb_phosphate [mmol/kg]	Csorb_glyphosate+2·Csorb_phosphate [mmol/kg]	Csorb_max [mmol/kg]
0	232,93	-	232,93	680
0,01	232,8	0,056	232,9	
0,05	232,66	0,281	233,2	
0,1	232,08	0,562	233,2	

***** p*hosphate is counted twice due to the formation of bidentate complexes and occupation of two sorption sites by one molecule*

The total sorbed concentration of phosphate and glyphosate in all the experiments is 233±0,5 mmol/l, which is three times lower than calculated Csorb_max in the sorption isotherm experiments at pH 5 (680 mmol/kg).

Overall, no effect of phosphate on glyphosate sorption was observed. This result contradicts literature findings (see above), however can be explained by the fact that the concentration of the added phosphate composed <0,2% of the total added glyphosate. Secondarily, the added concentration of glyphosate was in the linear range of the sorption isotherm (Figure 6.1), thus, saturation had not yet been reached. Therefore, no competition of phosphate and glyphosate for the sorption sites could be registered.

Similar sorption experiments conducted by Grünhage, 2017 showed lower sorption of glyphosate on alumina than described so far. Additionally, the pH effect on the glyphosate sorption deviated from the

one shown in Figure 6.1, reaching the highest sorption at pH 8,5 [Figure 6.7]. Moreover, Grünhage (2017) conducted experiments in the presence of background electrolyte (0,5 mM KCl), whereas initial experiments (Figure 6.1) were carried out without electrolyte, therefore ionic strength was determined after pretreatment of the components with HCl and NaOH (I=0,04-0,1 mM).

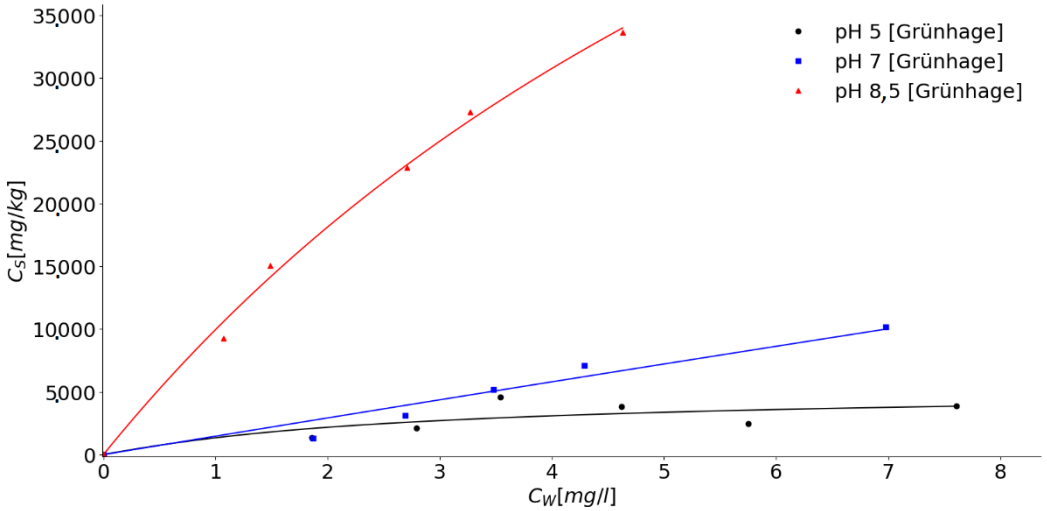

Figure 6.7 Sorption isotherm of glyphosate on Al_2O_3 particles [I=0,5 mM KCl; T=20°C (room temperature), pH 5; 7; 8,5]. The experiment was conducted by Grünhage, 2017

The effect of ionic strength on the sorption has been depicted and described above [Figure 6.2, Table 6.2]. A decrease in pH causes an increase in the alumina's zeta potential, not changing the position of the shear plane. pH affects the surface charge and thus the zeta potential but also the formation of the Helmholtz double layer by KCl on the aluminium oxide nanoparticles. Even though there is a discrepancy in explanation of ionic strength on glyphosate sorption, the works of various authors [Sposito, 2008; Jonsson, 2007; Borggaard and Gimsing, 2008; Gimsing et al., 2004; Orcelli et al., 2018] come to the same understanding of the pH effect on glyphosate sorption on metal (Al and Fe) oxides. These works demonstrated a decrease in sorption with increasing pH, which agrees with the pattern obtained in our experiment (Figure 6.1). Jonsson (2007) discussed strong covalent bonding between glyphosate and alumina, which explains the sorption of glyphosate to alumina at higher pH (8,5-9). Nevertheless, Jonsson also reported higher sorption at lower pHs due to the electrostatic interactions. Significantly, all the above -mentioned studies were conducted in the presence of BG electrolytes (0,01 M – 0,1 M KCl, NaCl or $CaCl_2$). The deviation of the results in Figure 6.7. from the published data was not fully clarified.

The detailed discussion of the possible parameters that could cause a strong deviation between the two experiments is presented by Grünhage, 2017. pH effect, agglomeration of the particles, human factor, different laboratory ware material, water filters, chemicals batches were thoroughly discussed and controlled to exclude an error. None of the above-mentioned parameters could cause such pronounced difference. Initial concentrations in the samples were controlled by using samples without adsorbent. Even though the results obtained by different human operators vary, the discrepancy is not large enough to explain the deviation from the published data. Amorphous alumina is an unstable material, changing its surface properties depending on the ultrasonication time, hydration time and undergoes mechanical transformations [Luo, 2018]. The samples in Grünhage's, 2017 experiments were left on the horizontal-shaker for 12 hours, whereas the samples in the present were shaken for 24 hours on the overhead-shaker. Thus, it is possible that in the experiments, discussed in the present work, a higher amount of Al^{3+} ions were released into the solution. Jonsson, 2007 studied the formation of Al^{3+}-Gly complexes in aqueous solutions and proposed several types of complexes ($AlHGly^{+}$; AlGly; $AlHGly_2^{2+}$; $AlGly_2^{3-}$) depending on pH [Jonsson, 2007]. Jonsson, 2007 concluded, that Al-Gly complexes contain a maximum of two coordinated glyphosate ligands. Therefore, the presence of Al^{3+} in the solution could potentially increase the complexation of glyphosate and decrease its equilibrium concentration in a freely-dissolved form. Moreover, Jonsson discussed the dissolution of Al^{3+} from the alumina surface under acidic conditions. In the pH range investigated here, the solubility of the mineral should not be significant (log $S_{Al}<10^{-5}$ M) [Jonsson, 2007]. However, the possible excessive titration in some experiments could cause increased dissolution of the mineral.

6.4. Conclusions

Study of glyphosate sorption on alumina nanoparticles revealed high sorption of the herbicide. The high affinity of glyphosate to aluminol groups was expected and reported in works of different authors [Martell and Motekaitis, 1988; Glass, 1984; Orcelli et al., 2018].

An increase in ionic strength caused a decrease in glyphosate sorption on alumina. Several reasons for this behavior were found:

a) Competition between Cl^- anions and glyphosate molecule (z=-1) for the positive sorption sites;
b) The decrease of zeta potential of alumina surface with the addition of electrolyte resulting in the lower electrostatic interactions between alumina and glyphosate;
c) The lower zeta potential of the aluminium oxide surface results in the lower repulsion forces and aggregation of alumina into bigger particles, reducing the total amount of accessible sorption sites.

To clarify how bivalent cations [Ca^{2+} and Cu^{2+}] affect the sorption of glyphosate, 1,7 mM $CaCl_2$ and 1,7 mM $CuCl_2$ were added to glyphosate_alumina. It was expected that complexation would increase with the increase in cation charge [Mattos et al., 2017], thus Csorb_max values for glyphosate sorption on alumina were expected to increase in the presence of $K^+<Ca^{2+}\approx Cu^{2+}$. It was concluded, that both Ca^{2+} and Cu^{2+} cations form complexes with glyphosate which decreases freely dissolved concentration of glyphosate, causing significantly higher Csorb_max values [Table 6.3]. Strong coordination bonds of glyphosate with metal ions were reported in the literature [Martell and Motekaitis, 1988; Glass, 1984; Subramanian and Hoggard, 1988]. Glass, (1984) reported an increase in glyphosate complexation in a row $Na^+<Ca^{2+}<Mg^{2+}<Cu^{2+}<Fe^{3+}$. The results of the present study correlated with the published data, emphasizing the significance of the cations' charge for the complex formation. However, complex formation was assumed relying on the published data and solely on the glyphosate concentration measurements. To estimate the complex-formation in the described experiment it is suggested to measure complex formation experimentally, determining complex formation constants. Additionally, the surface charge of alumina after addition of glyphosate in the presence of Ca^{2+} and Cu^{2+} should be monitored in the future experiments.

As was expected, the pH effect was pronounced for the glyphosate sorption due to the glyphosate's speciation change at different pH values. However, since experiments at different pH values were conducted in the absence of background electrolyte, the pretreatment of Al_2O_3 and glyphosate, i.e. titration with HCl and NaOH determined the ionic strength of the mixture. Since ionic strength strongly affected the Csorb_max, an effect of pH in the presence of background electrolyte caused more complicated dependence of the sorption on the pH. As was demonstrated by Grünhage, 2017 the initial anion population of the alumina surface altered the pH dependence of the glyphosate sorption. To prove proposed explanation of the pH effect in the presence of background electrolyte, the following experiments must be conducted: groups on the alumina surface at different pHs in the presence and absence of electrolyte should be experimentally distinguished. Additionally, sorption at different pHs in the presence of higher KCl concentration (50 mM) should be studied to verify proposed explanation.

To study how the charge of the sorbate impacts adsorption mechanism, sorption of glufosinate ammonium and AMPA were investigated. Presence of phosphinate group in the glufosinate molecule instead of phosphonate group in the glyphosate and AMPA is responsible for the different sorption mechanism in glufosinate and glyphosate. McBride (1989) discussed a possibility of proton migration from amino-group to the phosphonate group and formation of H-bonds between glyphosate and goethite surface. Glufosinate ammonium sorption was very low, which correlated with the published data. Laitinen et al., 2008 reported four times lower sorption of glufosinate ammonium on the soils in comparison with glyphosate. They suggested that glufosinate ammonium sorption follows a different pathway than glyphosate and takes place on the cation exchange sites of the soils. Applying the mechanism suggested

by McBride (1989) to the present study and not expecting such migration in the glufosinate molecule may explain the high difference between glyphosate's and glufosinate's sorption. AMPA molecule at pH 5 demonstrated significant sorption, the mechanism of the sorption is expected to be like the glyphosate's, involving the phosphonate group. A missing carboxylic group suggests that only one bound between AMPA molecule and alumina is formed, whereas glyphosate additionally to phosphonate bond can form outer-sphere complexes involving the carboxylic group. These results emphasized the importance of electrostatic interactions between negatively charged glyphosate and positively charged alumina surface, as well as the significance of phosphonate group, responsible for the coordinated bond formation, for the glyphosate adsorption.

Expected sorption mechanism of glyphosate on alumina was through the phosphonic group like the sorption mechanism of phosphate. Thus, the competitive sorption of glyphosate and phosphate was investigated. Quantitative adsorption of added phosphate was measured [0,01 µM, 0,05 µM, 0,5 µM]. Sorbed concentration of glyphosate in all the samples was 232,48±0,3 mmol/kg, which was lower than the calculated Csorb_max [608 mmol/kg] and the chosen glyphosate concentration [23,66 µM or 4 mg/l] was in the linear range of the sorption isotherm. To study whether phosphate or glyphosate sorbs predominantly and whether desorption of one compound by another is possible, both components were added in two different orders: glyphosate + phosphate and phosphate + glyphosate. Due to the high difference between introduced phosphate and glyphosate concentrations (phosphate composed ~0,2% of glyphosate total concentration), it is difficult to make any conclusions concerning the mutual influence of both compounds. The extensive investigation of the phosphate effect on the glyphosate sorption on alumina is needed. It is reasonable to choose comparably similar phosphate and glyphosate concentrations and conduct an experiment in the concentration range reaching sorption saturation and not only in a linear range of the sorption isotherm.

To clarify the deviation of the results, obtained by Grünhage, 2017, from the published data, it is suggested to conduct sorption experiments at three pHs in the presence of three various electrolyte concentrations.

It was concluded, that glyphosate's aqueous concentration decreases significantly in the presence of amorphous aluminium oxide nanoparticles. Different environmental factors influence the sorption, however measured sorption in all the experiments indicates effectiveness of alumina as a sorbent of glyphosate, which affects glyphosate's distribution in the environment and its availability for the target and nontarget organisms.

Chapter 7 ATR-FTIR Analysis of Glyphosate Sorption on Al_2O_3

To explain mechanism of glyphosate sorption on aluminium oxide, FTIR spectra of glyphosate at different pHs were obtained. The peaks were identified and correlated with the appropriate functional groups. The results were compared and correlated with the literature [Barja and Dos Santos Afonso, 1998; Piccolo and Celano, 1993]. Figure 7.1 depicts spectra of glyphosate at four pH values with the corresponding functional groups. Every pH value represents different speciation form of glyphosate (Scheme 6.1, Chapter 6).

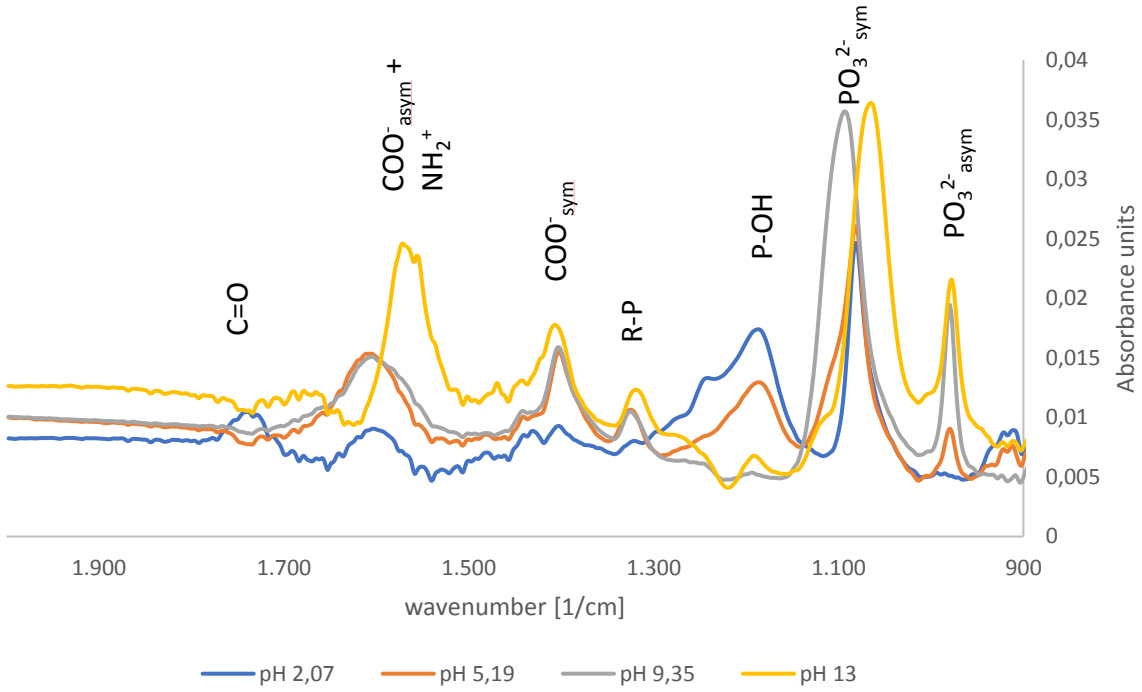

Figure 7.1 FTIR spectra of glyphosate at 4 pH values, representing different speciation forms [scan number: 400, 2000-800 cm^{-1}, glyphosate concentration 7g/l, 50 mM KCl; BG: MilliQ water with 50 mM KCl]

Table 7.1 Peaks [wavenumber, cm^{-1}] corresponding to the functional groups in glyphosate molecule [data is taken from Barja and dos Santos Afonso, 1998][Δ-bending, υ-stretching]

Functional group	Wavenumber [cm^{-1}]
υ(C=O)	1.736
$\Delta(NH_2)+\upsilon_{asym}(COO)$	1.616
$\upsilon_{sym}(COO)$	1.403
υ(R-P)	1.320
υ(P-OH)	1.190
$\upsilon(P-O)_{sym}$	1.093
$\upsilon(P-O)_{asym}$	979

At pH 13 slight shift in $\upsilon(P\text{-}O)_{sym}$ vibrational stretching to the lower wavenumber is observed. Similar shifts in the phosphonate peaks with increasing pH were reported in the literature [Xu et al., 2016, Sheals et al., 2002]. Sheals et al., 2002 related shift of the P-O to the lower wavenumber to the full deprotonation of the phosphonate group. The work also described hydrogen bonding between the amino group and the phosphonate group. Thus, at the pH values below the pKa_4 value (10,2) $P\text{-}O^-$ may still interact with hydrogen of the amino-group, however above pH 10,2 molecule is fully deprotonated, and a slight shift of the peaks takes place.

The results of the glyphosate spectra at different scan numbers indicate an optimum at scan number 400. Scan number 32 gives poor peak intensity (broad bands), whereas a further increase in scan number (above 400) does not provide much higher intensity, however, requires a longer time for each measurement. Figure 7.2. depicts exemplary glyphosate spectra at pH 2,07 at four different scan numbers.

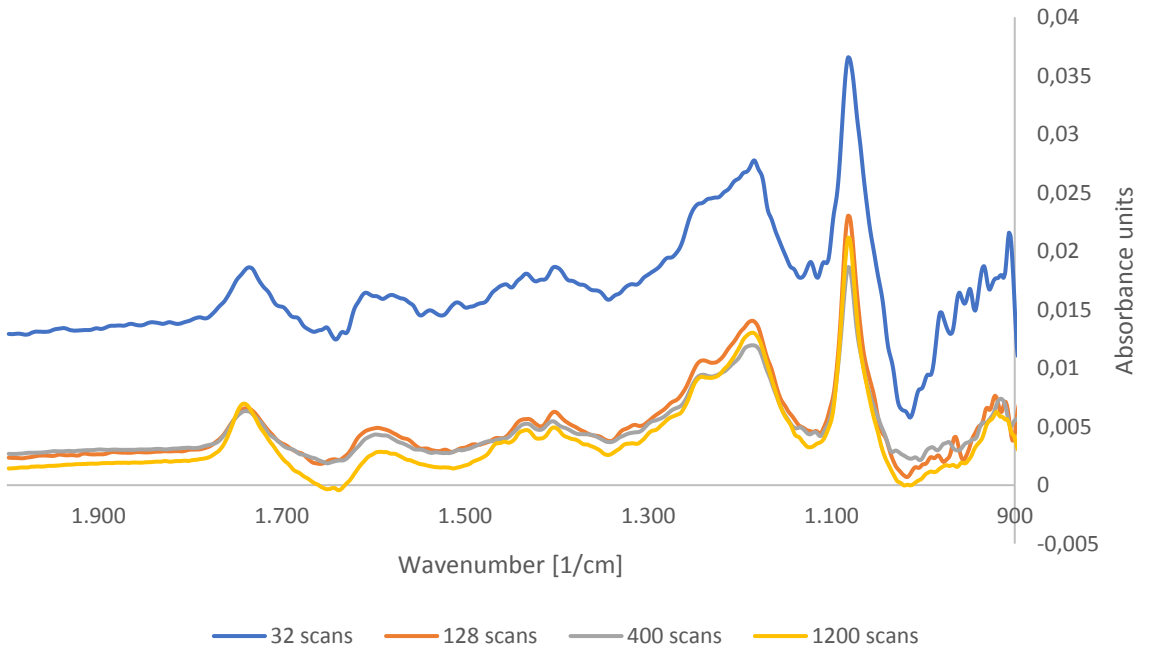

Figure 7.2 FTIR spectra of glyphosate at pH 2,07 [scan number: 32; 128; 400; 1200; 2000-800 cm^{-1}, glyphosate concentration 7 g/l, 50 mM KCl; BG: MilliQ water with 50 mM KCl]

Spectra of different glyphosate concentrations were obtained to define the lowest concentration, at which all the peaks are distinguishable (LOD). As it may be seen in Figure 7.3, both 3 g/l and 2 g/l concentrations may still be referred to glyphosate with the most functional groups still distinguishable. However, the resolution and the intensity of the peaks is much poorer, some peaks (P-OH) are lost. Thus, 2 g/l is the lowest acceptable concentration for reliable glyphosate characterization.

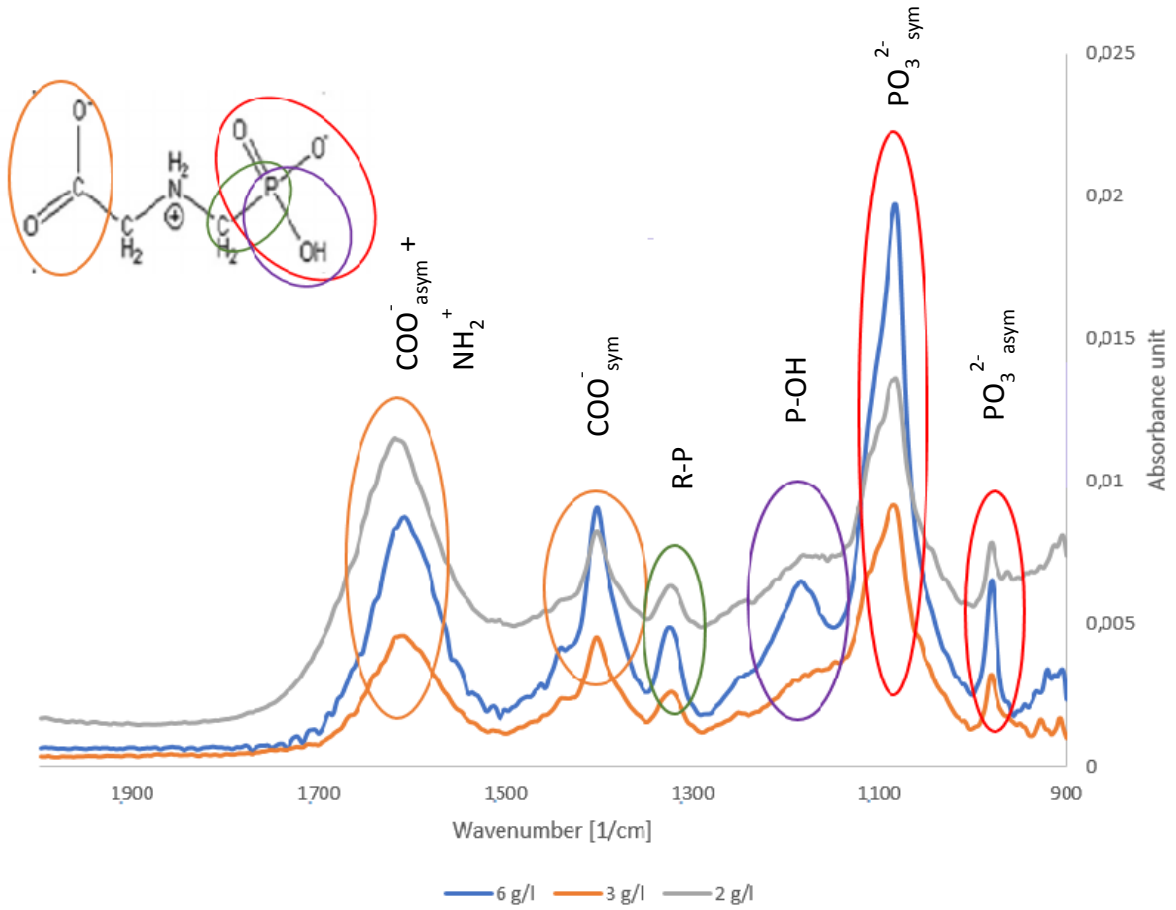

Figure 7.3 FTIR spectra of glyphosate at pH 5,2 [scan number: 400, 2000-800 cm^{-1}, glyphosate concentrations: 2, 3, 6 g/l, 50 mM KCl, BG: MilliQ water with 50 mM KCl]

Sorption experiment of glyphosate on Al_2O_3 was conducted in ATR cell and spectra of glyphosate were taken at different times. Figure 7.4 performs six spectra, including BG water, spectrum of 7g/l glyphosate at pH 9,2 (BG: H_2O with KCl), spectrum of 7g/l glyphosate after 80 minutes in contact with Al_2O_3 (BG: H_2O with KCl on Al_2O_3), as well as spectra of 70 mg/l glyphosate on Al_2O_3 and as a reference compound. Most of the peaks stay unchanged, however, peak at 1093 cm^{-1} corresponding to the symmetrical stretching of PO_3^{2-} group is getting broader at the concentration 70 mg/l after 1,5 h contact with Al_2O_3. This implies, that sorption of glyphosate on alumina involves phosphonate group. The most probable is an inner-sphere complex formation. Zheng et al., 2012 studied sorption of phosphate on alumina and suggested the formation of either nonprotonated monodentate complex or nonprotonated bidentate binuclear complex at higher pH levels (pH 9). For the glyphosate sorption on alumina, similar complexes are expected to be formed (Scheme 7.1). The monodentate complex is sterically preferable since free rotation around single Al-O bond facilitates hydrogen bonding interactions. The higher probability of the monodentate complex formation was also suggested by Sheals et al., 2002 who

demonstrated intra-molecular hydrogen bond formation between phosphonate oxygen and amino group hydrogen.

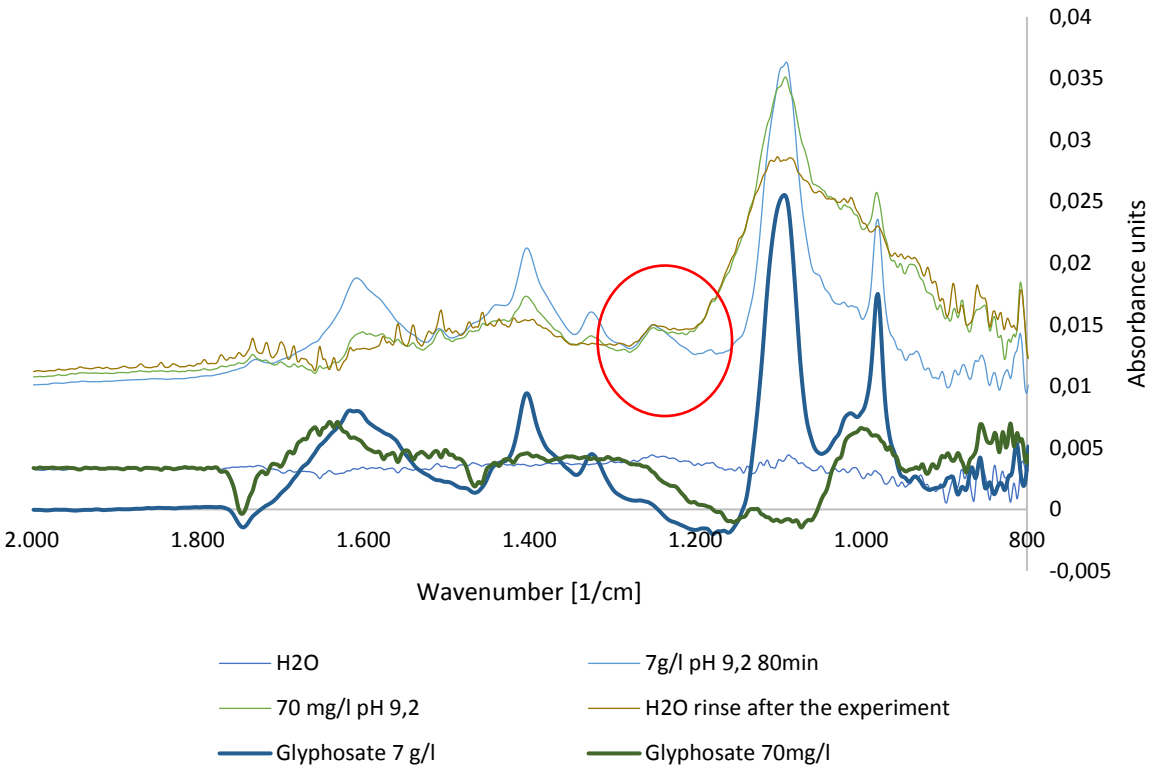

Figure 7.4 FTIR spectra of the glyphosate sorption on Al_2O_3 [scan number: 400, 2000-800 cm^{-1}, pH 9,2, glyphosate concentrations: 7 g/l and 70 mg/l, 50 mM KCl, BG: MilliQ water with 50 mM KCl on Al_2O_3 surface]

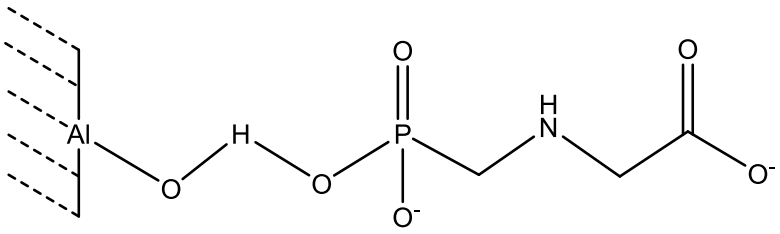

a) nonprotonated monodentate complex

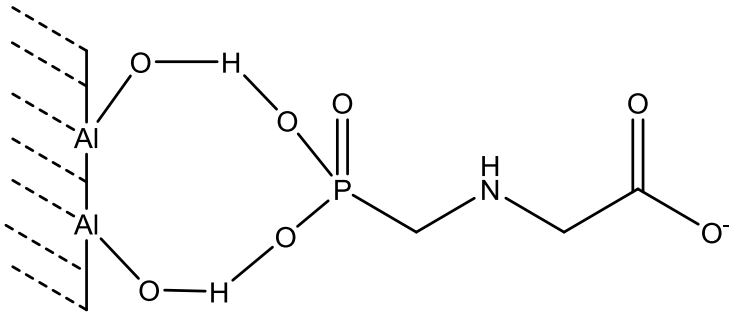

b) nonprotonated bidentate binuclear complex

Scheme 7.1 Possible structure of inner-sphere complex between alumina and glyphosate at pH 9

Zheng et al., 2012 studied phosphate sorption to alumina surface and proposed hydrogen bonding of phosphate to an inner-sphere complex. They concluded, that at pH 9 nonprotonated or monoprotonated surface complex between phosphate and aluminium is expected, suggesting hydrogen bonding to the HPO_4^{2-} anion.

At pH 9 the surface of the formed complex is non-protonated, implying the negative charge of the surface. Therefore, electrostatic interactions between glyphosate and alumina are not favoured. Even though the sorption of glyphosate above pH 8,5 is lower than at pH 5 and pH 7 (Figure 6.1, Chapter 6), it is still high which is explained through the specific interactions. McBride et al., 1989 studied the complexation of glyphosate with iron Fe(III) and suggested, that the complex of Fe^{3+} with glyphosate (z=-2 with a proton on the amine group) is unstable. It may cause the migration of the proton from the amino group to the phosphonate group and result in the terdentate Fe-Glyphosate complex, in which Fe is bridged with phosphonate group through the hydrogen bridges.

Therefore, at pH 9 the binding of glyphosate to alumina according to McBride is depicted in Scheme 7.1. This correlates with Sheals et al., 2002 who discusses the mobility of the proton from amino-group at higher pH.

Damonte et al., 2007 suggested that glyphosate's interaction with alumina involves phosphonate and carboxylic moieties.

Additionally, an absorbance peak at 1240 cm^{-1} in the spectra of glyphosate with aluminium oxide may be seen, which is missing in the spectrum of glyphosate without alumina. This peak was assigned to the C-O stretch of carboxylic group. From the Figure 7.1 it is evident, that such peak is present only in a spectrum of glyphosate at pH 2,07 since only at that pH -COOH group is protonated and this induces a C-O bond stretching. The appearance of the same peak during an interaction of glyphosate with alumina implies a possibility of interaction between $-C-O^-$ and the surface of alumina. According to Sheals [Sheals et al., 2002], glyphosate may form intra-molecular hydrogen bonds. At the studied pH, the $C-O^-$ group could bind to the H^+ proton from NH_2^+ group (Scheme 7.2) since at higher pH, protons of amino-group are getting mobile.

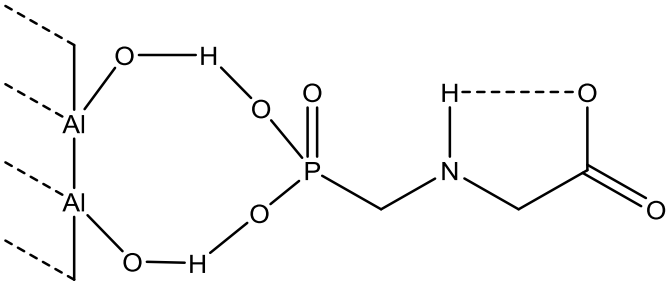

or

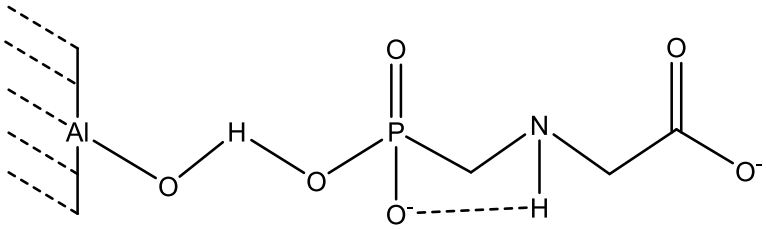

Scheme 7.2 Possible glyphosate intra-molecular hydrogen bond formation between COO^- and NH_2^+ groups

A missing peak at 1240 cm^{-1} in glyphosate spectrum without alumina suggests, that intra-molecular hydrogen bond formation between functional groups of glyphosate is caused by the specific geometry of the molecule in the presence of aluminium oxide particles. It is reasonable to expect glyphosate to have not a linear configuration, but the bent one instead. At such geometry O^- ion is expected to interact either with the alumina positively-charged surface sites, or hydrogen from the amino group. Both interactions would cause C-O stretching, observed at 1240 cm^{-1}. Since no significant change in the peak at 1616 cm^{-1} corresponding to the amino group bending was detected, interaction of COO^- with Al_2O_3 is a more probable explanation for the peak emergence. Alternatively, carboxyl-group may stabilize glyphosate-alumina complex through the outer-sphere bond formation with the other alumina particles (Scheme 7.3). Damonte et al., 2007 studying sorption of glyphosate on montmorillonite, proposed complexation of glyphosate with the metal cations on the clay surface through water bridges as the dominant adsorption mechanism. Both carboxyl- group and alumina surface at pH 9 are negatively charged. The expected interactions between both groups involve water bridges, promoting binding of negatively charged carboxyl group on the negatively charged alumina.

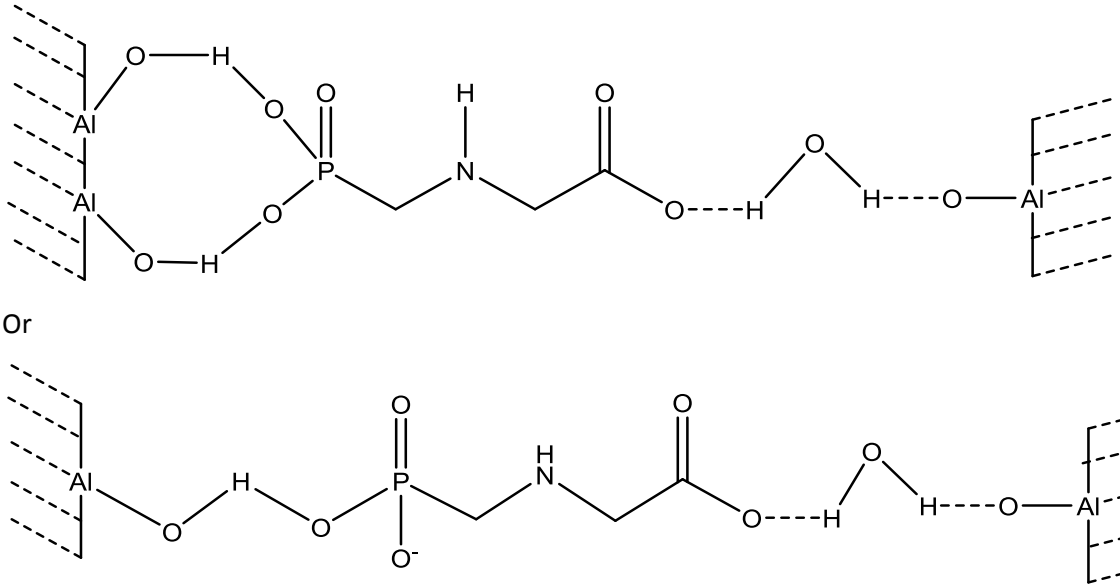

Or

Scheme 7.3 Formation of the complex between glyphosate and aluminium oxide surface a) inner-sphere complex formation through phosphonate group; b) outer-sphere complex formation through the water-bridges

Based on the ATR-FTIR results and the previous studies it was concluded, that glyphosate sorbs to the alumina nanoparticles primarily through the phosphonate group forming either nonprotonated monodentate complex or nonprotonated bidentate binuclear complex. According to McBride (1989), it is expected, that proton from amino group migrates to the phosphonate group, decreasing repulsion between deprotonated glyphosate and negatively charged alumina and promoting adsorption. Secondarily, peak at 1240 cm^{-1}, corresponding to the C-O stretching, implies the carboxyl group interaction with the aluminium oxide surface through the water bridges, which correlates with data, published in the literature [Damonte et al., 2007].

Chapter 8 ATR-FTIR Analysis of Neonicotinoids and Triazole Fungicides

ATR-FTIR analysis was used to provide an in-depth explanation of neonicotinoids and azole fungicides sorption. The primary goal was to make peak assignment of the pesticide's spectra. The ATR-FTIR technique was applied to revealing intensity changes in the peaks assigned to the functional groups, resulting from the interaction between the sorbent surface and studied pesticides.

8.1. Peak assignment of ATR-FTIR spectra

Unlike for glyphosate, there is not much literature available on ATR-FTIR analysis of the aqueous solutions of the chosen neonicotinoids or triazoles. The probable reason is moderate to low water solubility of these compounds. To obtain significant spectral features, reference spectra in methanol solution were recorded (Figure 8.1). Literature data on imidacloprid FTIR analysis in polar protic solvents are available and peaks in the present work were referenced using these spectra [Quintas et al., 2004; Aregahegn, 2017]. No published data was found on FTIR analysis of thiacloprid. Figure 8.1 demonstrates similarity in some peaks of IC and TC spectra (bands at 1108 cm^{-1}, 1461 cm^{-1}, 1572 cm^{-1}, peak assignment is given in Table 8.1), which are assigned to the common moieties of imidacloprid and thiacloprid molecules. Specific functional groups, characteristic for only one of these two neonicotinoid compounds were also assigned (Figure 8.1, Table 8.1).

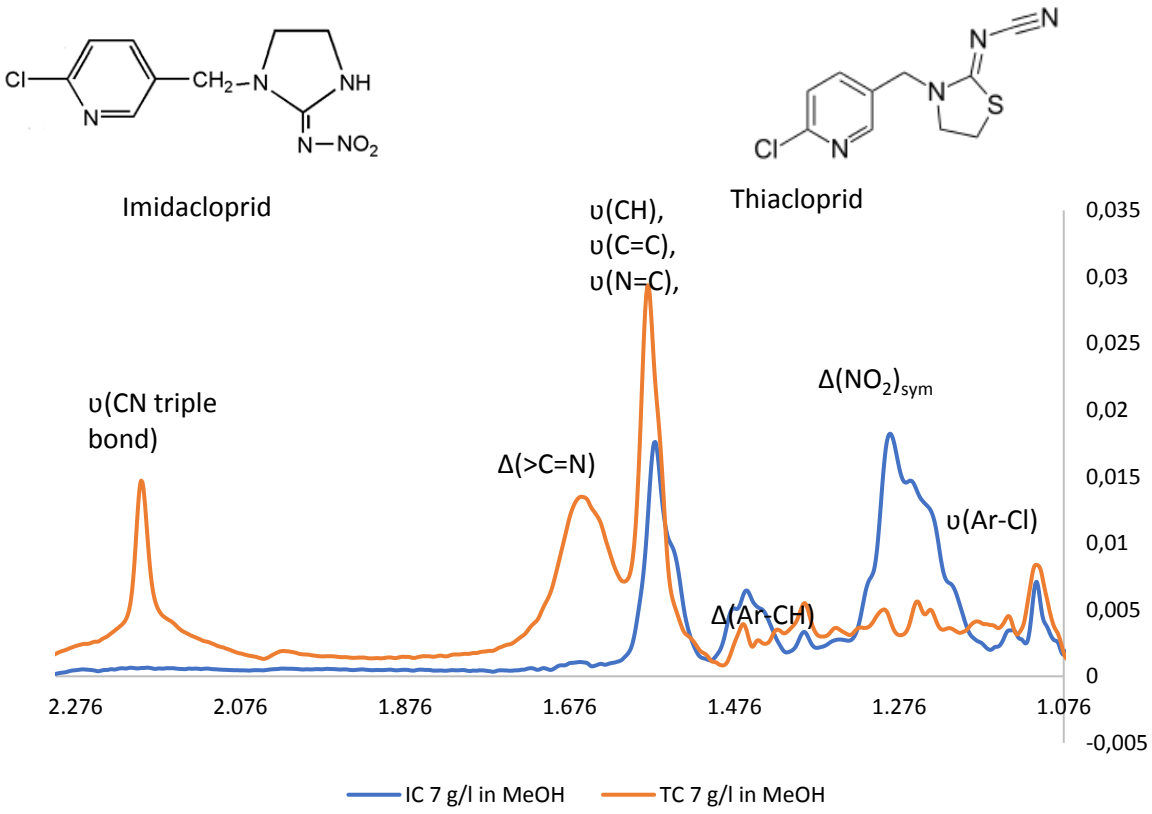

Figure 8.1 FTIR spectra of methanolic imidacloprid and thiacloprid solutions [22°C, 400 scan number, IC, TC concentrations: 7 g/l; BG: MeOH HPLC grade]

Table 8.1 Peak assignment [wavenumber, cm^{-1}] of functional groups of neonicotinoids imidacloprid and thiacloprid [data was taken from Quintas et al., 2004] [Δ-bending, υ-stretching]

Functional group	Wavenumber [cm^{-1}]
υ(CN triple bond) (TC)	2.196
Δ(>C=N)	1.662
υ(CH- of pyridine group), υ(C=C), υ(N=C),	1.572
Δ(Ar-CH)	1.461; 1.386
υ $(NO_2)_{sym}$ (IC)	1.286
υ(aryl-Cl)	1.108

The detection limit was determined as 0,5 g/l for imidacloprid, using spectra of imidacloprid different concentrations in MeOH. Using a saturated solution of imidacloprid in water (0,62 g/l), aqueous FTIR spectra of imidacloprid was obtained (Figure 8.2). A clear difference in spectra at 128 and 400 scan numbers is seen. However, an increase of the scan number to 1200 did not provide a further improvement of peak intensity and resolution. Therefore, scan number 400 was used for further experiments with imidacloprid. Nonetheless, even at high scan numbers peaks corresponding to the functional

groups show relatively low intensity, only slightly higher than the noise. Though the comparison of Figures 8.1 and 8.2 proves correct peak assignment in Figure 8.2, such a low peak intensity may complicate the statistical significance of the results.

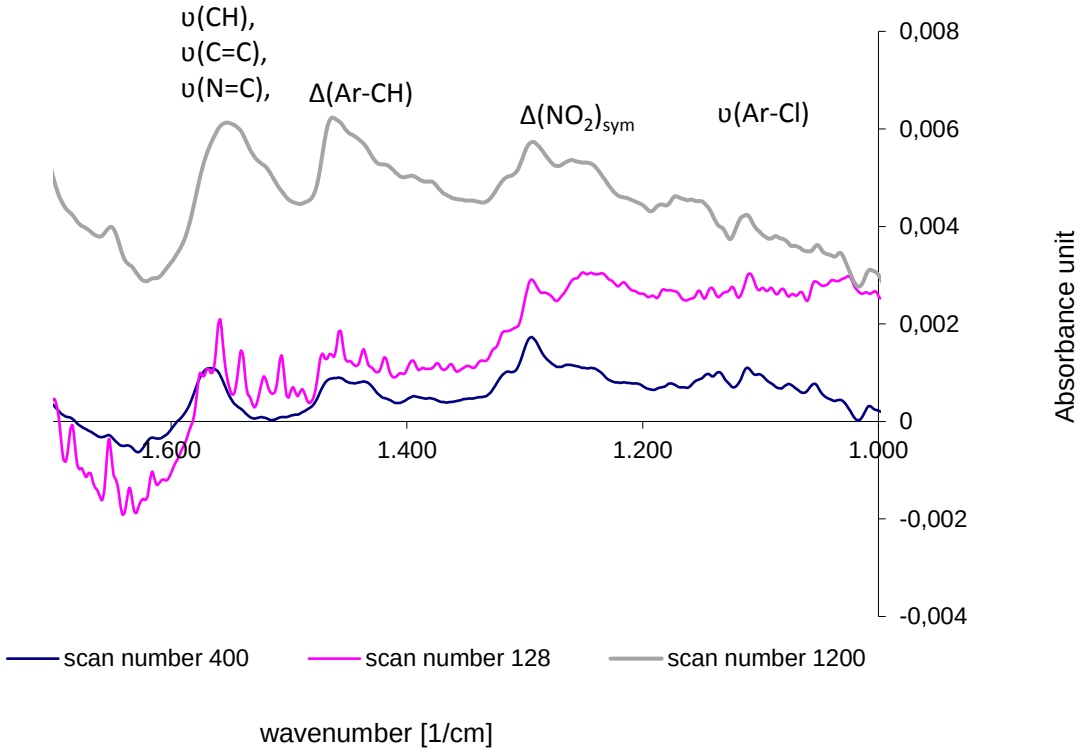

Figure 8.2 FTIR Spectra of a saturated aqueous solution of imidacloprid [22°C, 128, 400, 1200 scan number, IC concentration: 0,62 g/l BG: MilliQ water]

However, because of the sorption it was expected to obtain significantly higher IC concentrations in the ATR-cell, than 0,62 g/l and subsequently, higher intensity.

Thus, for the sorption on beta26 (sorption isotherm, Figure 3.10, Chapter 3) the sorbed concentration in equilibrium (use Csorb_max) would be 44 g/kg (Table 3.1., Chapter 3). Using equation 8.1. the bulk density of zeolites (average value) was calculated ρ_{bulk}=0,945 kg/l; sorbed concentration of imidacloprid – 37,8 g/l.

$$\rho_{bulk} = (1 - n).\rho \qquad 8.1$$

$$\rho_{bulk} - \text{bulk density } \left[\frac{\text{kg}}{\text{l}}; \frac{\text{g}}{\text{cm}^3}\right];$$

$$\rho - \text{density; } 2{,}0 - 2{,}16 \left[\frac{\text{kg}}{\text{l}}; \frac{\text{g}}{\text{cm}^3}\right];$$

$$n - \text{porosity; } 0{,}55\ [-]$$

Therefore, the total concentration of imidacloprid in the ATR cell was expected to be equal to 38,42 g/l, which would be enough to obtain peaks with high enough intensities to interpret which functional groups were involved in the sorption mechanism.

8.2. Peak assignment of ATR-FTIR spectra of azole fungicides

Spectra of hexaconazole and propiconazole in methanol (HPLC grade) were recorded (Figure 8.3). Multiple peaks were distinguished. The bands were assigned to the functional groups according to literature data [Aziz et al., 2014; Best et al., 2014]. Figure 8.3 depicts spectra of hexaconazole and propiconazole in MeOH. Peak assignment is summarized in Table 8.2.

Unexpectedly high peak intensities were obtained for the spectra of propiconazole in water (oversaturated solutions of propiconazole in water (<0,5 g/l) were used). Oversaturated solutions were prepared because of the low water solubility of propiconazole. Higher than required mass of propiconazole was deliberately added to water and the sample was ultrasonicated. The excessive propiconazole droplets were expected to precipitate and the solution was used for the ATR measurements. Figure 8.4. depicts spectra of propiconazole in water and 10 g/l propiconazole solution in MeOH. Similar magnitude of the peaks' intensities for propiconazole aqueous concentration <0,5 g/l and solution in methanol 10 g/l implies the presence of non-dissolved propiconazole droplets in the ATR cell. While propiconazole is soluble in methanol, its water solubility is only ~ 100 mg/l. Therefore, presence of non-dissolved propiconazole droplets (propiconazole at room temperature is a viscous liquid) enhances peak performance and makes them comparable with significantly higher concentrations of the methanol solution. To obtain the spectrum of pure propiconazole, viscous liquid (propiconazole) was placed into ATR cell. The obtained spectrum is presented in Figure 8.3. a. Alignment of the peak-intensities in the pure compound and in the solution confirms that the oversaturated aqueous solution contained pure propiconazole droplets, resulting in the high intensity of the peaks and their correlation with the literature values [Aziz et al., 2014].

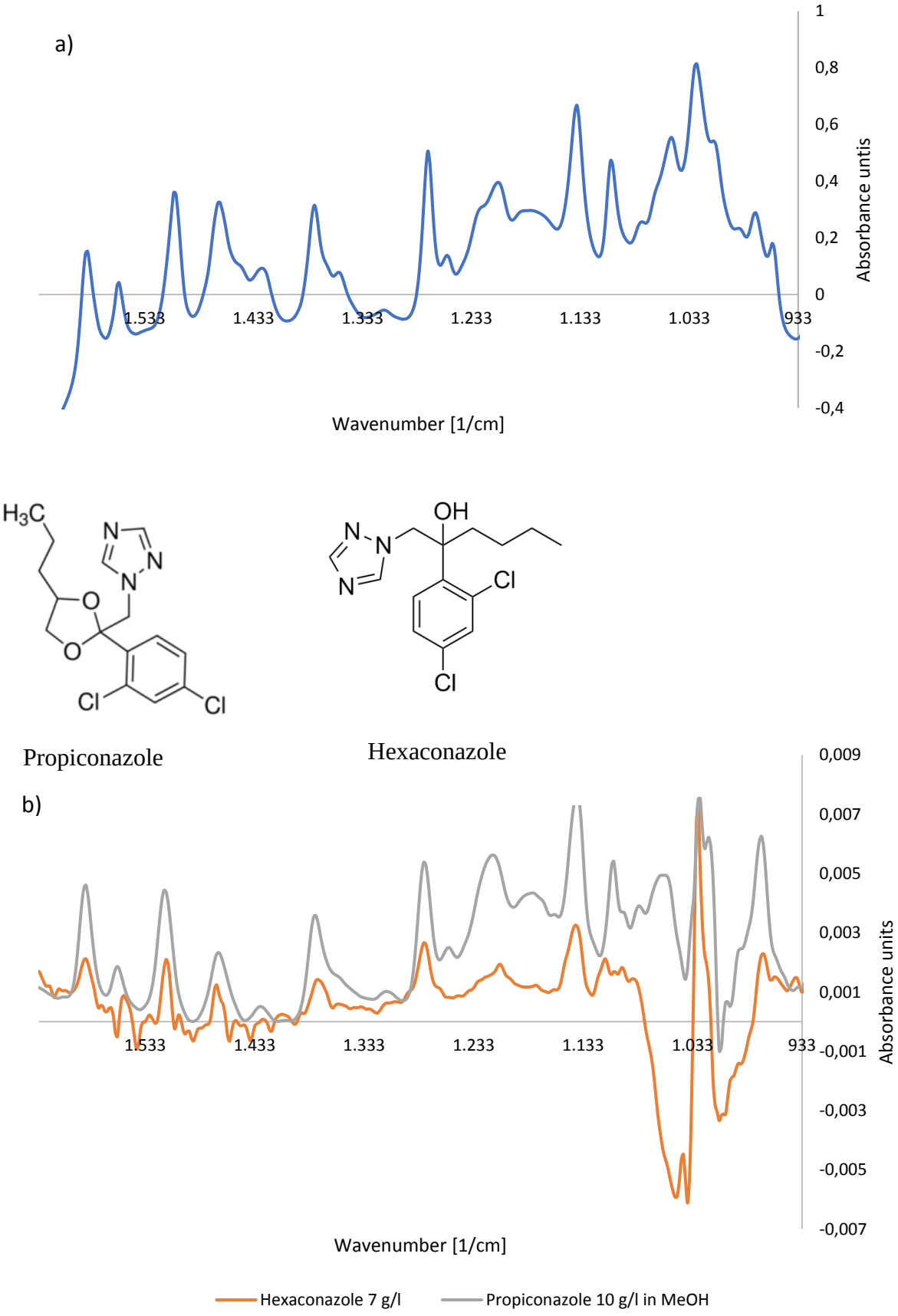

Figure 8.3 a) The spectrum of pure liquid propiconazole; b) spectra of hexaconazole and propiconazole standards in MeOH [22°C, 400 scan number, Hex: 7 g/l, Prop: 10 g/l; BG: MeOH HPLC grade]

Both compounds have similar peaks regarding the identical groups.

Table 8.2 Peak assignment [wavenumber, cm^{-1}] of functional groups of propiconazole [data was taken from Aziz et al., 2014] [Δ-bending, υ-stretching]

Functional group	Wavenumber [cm^{-1}]
υ(C=C aryl)	1.589
ΔNH, υ(C=N), υ(N=N)	1.570-1.515
Δ(CH)	1.465
υ(C-N aryl)	1.351
Δ(CH in a plane)	1.276
υ(aryl-Cl)	1.105
υ(C-O)	1.260-1.000
Ring disruption	970; 1.025

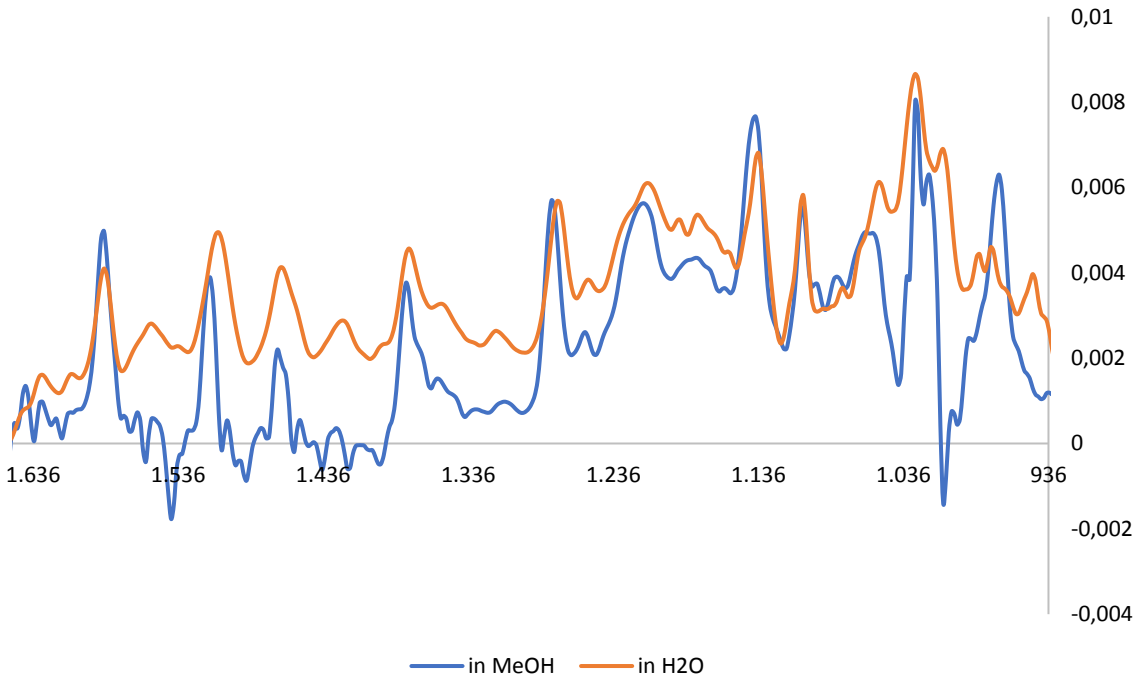

Figure 8.4 Spectra of propiconazole in water and methanol [22°C, 400 scan number, propiconazole concentration in H_2O: <0,5 g/l; in MeOH: 10g/l]

8.3. Formation of mineral layers at the ATR cell to determine sorption kinetics

After pesticides' spectra were assigned and characterized, the target was to characterize an interaction between the sorbent surface and pesticide. To conduct real-time measurements of pesticide interactions with mineral surface, the layer of the sorbent particles on the ATR crystal should be prepared. The number of beam reflections within the Bio-ATR II cell is 9-12, the effective beam pathway 5,7 – 7,7 µm, which was calculated using penetration depth equation (eq. 2.1, Chapter 2), multiplied by reflections number. The effective volume, which would be penetrated by evanescent beam was calculated using equation 2.2 (Chapter 2). The value was used to estimate the thickness of the layer, using density of the particles (for zeolites: 0,945 g/cm³ with the porosity 0,55). Thus, the layer of the particles should be minimum 0,64 µm thick to achieve the spectrum of the compound on the particles.

The suspension of the sorbent particles was injected into ATR measuring-spot (20 µl). After the liquid evaporated, pesticide solution was injected into the injection pipe (using flow-through set-up) [Xue, 2018]. The obtained spectrum of pesticide was expected to provide an information on the interactions between the particles surface and pesticide's functional groups.

Image 8.1 Bio-ATR II cell. The layer of the particles is prepared in the ATR measuring spot (silicon crystal). The lid of the ATR cell is fixed using screws. The solution (1. Blank and 2. Pesticide is injected through the injection pipe

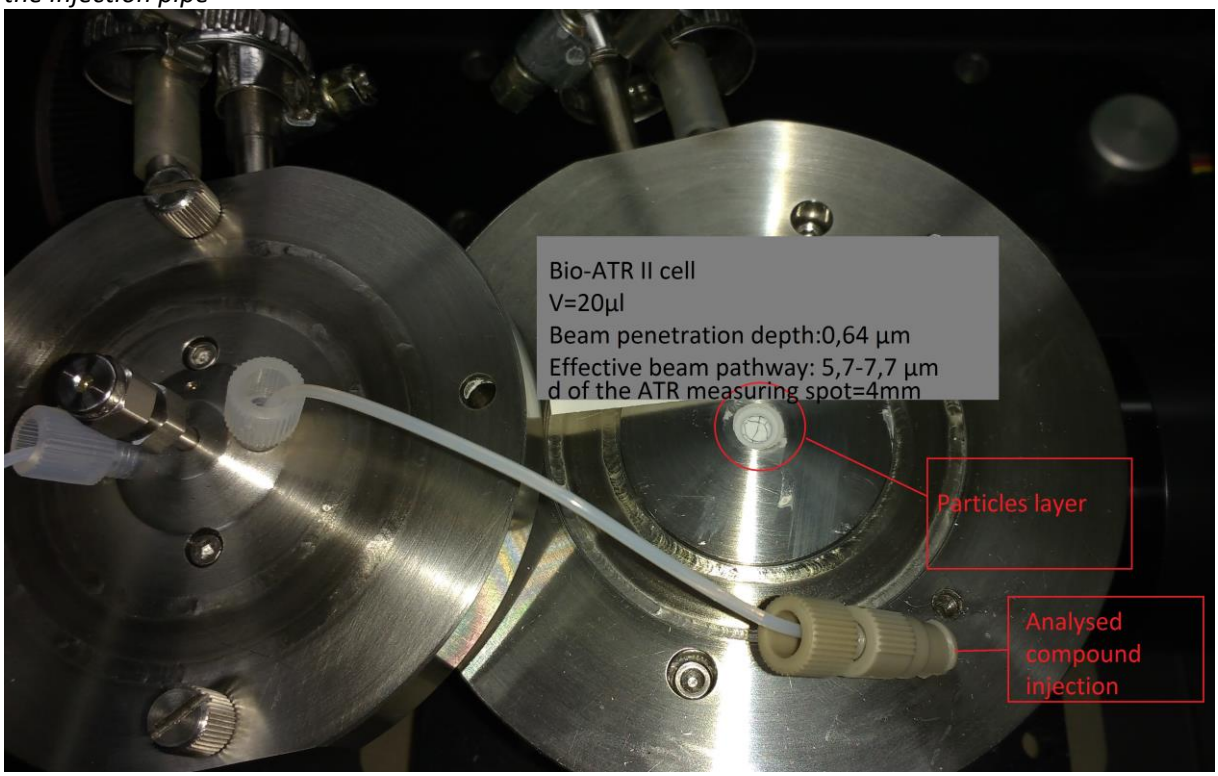

Both PMO-silica particles and several zeolites used for the sorption experiments of azole fungicides and neonicotinoids had a small particle size (ensure the possibility of the uptake by the studied organisms for the toxicological studies), high specific surface area, high porosity and consequently low bulk density (Table 2.1, Chapter 2). Due to the low bulk density and small particle size, it was difficult to obtain a stable layer for the analysis.

The main difficulty, that arose during layer preparation for the ATR-FTIR sorption mechanism analysis was the instability of the particles layer.

A summary of all the modifications for layer preparation is given below.

[particles= PMO-silica, zeolites (β and Y type)]

a) particles at pH 3 (close to the pzc of both PMO and zeolites), pH 5, pH 7, pH 9 without background electrolyte;
b) particles mixed with alumina (50:50%; 30:70%; 10:90%) at pH 9 (close to the pzc of Al_2O_3), at pH 3 (close to the pzc of both PMO-silica and zeolites), at pH 5 without KCl. Motivation: Al_2O_3 layer was successfully obtained for the glyphosate experiments and alumina has acted as a weak adsorbent for neonicotinoids and azole fungicides, and thus, would not interfere with sorption on PMO-silica and zeolites;
c) a) and b) in the presence of 50 mM KCl; 1,7 mM $CaCl_2$;
d) addition of montmorillonite and hectorite clays as fixators (10, 30, 50%);
e) addition of PVA was regarded ineffective since vinyl acetate monomer (diameter of the molecule; 0,47 nm) might access pores of zeolites (pore diameter: 0,74 nm) and of PMO (pore diameter: 1,9 nm) and hence compete for sorption sites with pesticides;
f) suspensions of the particles in methanol were prepared. Due to the low surface tension of methanol, evaporation of methanol distributed particles beyond the ATR-crystal and did not form a homogeneous layer (Image 8.2);
g) addition of gelatin was unsuccessful since pesticide molecules interacted with proteins of gelatin, the concentration of the pesticide was reduced, and it was impossible to distinquish reduction through interaction with proteins from sorption on the particles;
h) an addition of agaritine instead of gelatin, didn't result in interaction with pesticide molecules due to agaritin's composition, containing sugars and no peptides. However, an addition of agar-agar to the particles produced faulty results:
    - 0,18% Agar-agar: congelation happened around separate nuclei, what caused inhomogeneous congelation and appearance of the faults on the dry layer;
    - 1,8% Agar-agar: after drying out layer was solid, without faults. However, material shrank with dehydration; as a result, obtained layer covered only 75% of the ATR-crystal surface;

- Attempt to measure sorption mechanism over wet agar particles composite (to avoid shrinkage after drying) resulted in non-fully congealed agar fractures, concentrated around the particles. Thus, the surface of the composite on the ATR-crystal was inhomogeneous and was partially washed out by water injection in the flow-through mode. Applying steady-state mode resulted in some material loss through wiping water with paper tissues and destroyed the layer solidity. It is concluded, that agar-particles composites had weak contact with the ATR-crystal.

All the above-mentioned experiments did not provide a durable solid layer of the particles to record distinguishable spectra of the pesticides and consequently, did not provide practical support to theoretically expected sorption mechanism. Problems with the layer could be separated into two groups:

I. The appearance of the faults in the process of dehydration (Image 8.3)

II. Removal of the particles through the injection of the water due to the loose character of the particles (Image 8.4).

Image 8.2 Layer Y30 in methanol, pH 6. Methanol evaporation distributed particles unevenly, not providing solid layer

Image 8.3 Layer Y30_Al2O3 (50%:50%) (exemplary), pH 6. The layer obtained faults after drying out

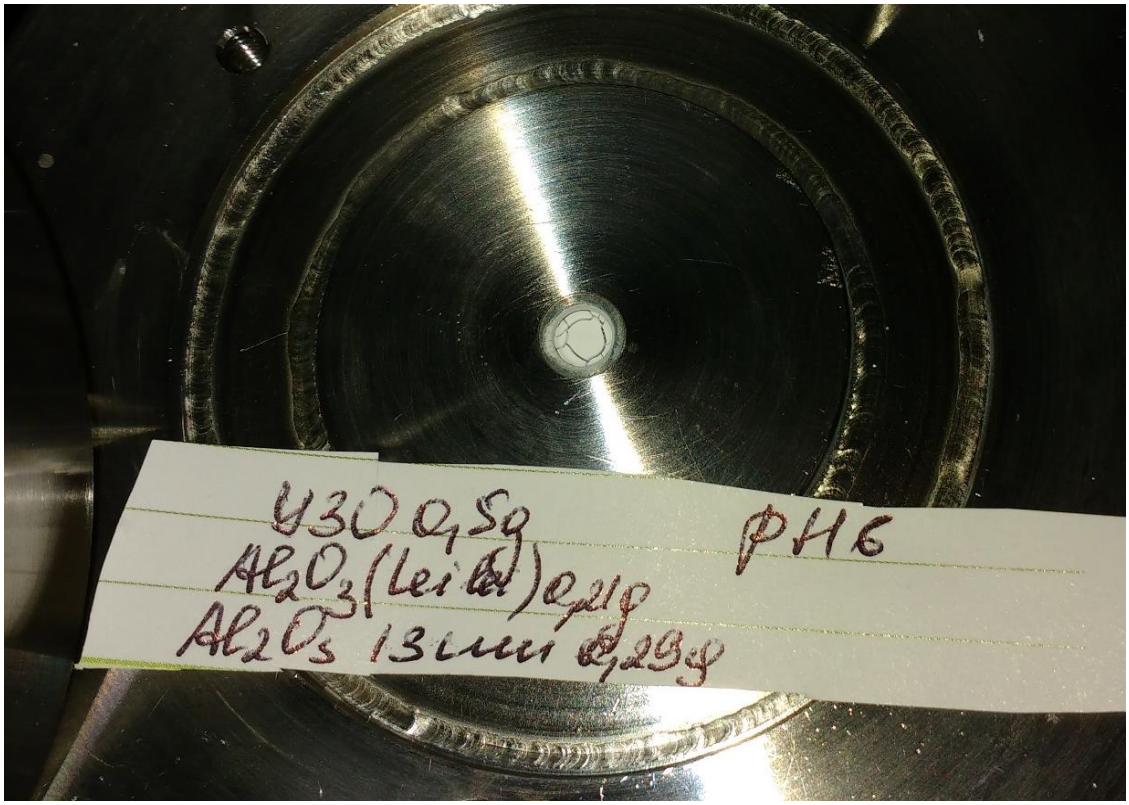

Image 8.4 Layer Y12:Al2O3 (50%:50%) (exemplary), pH 9. The layer was damaged through imidacloprid injection

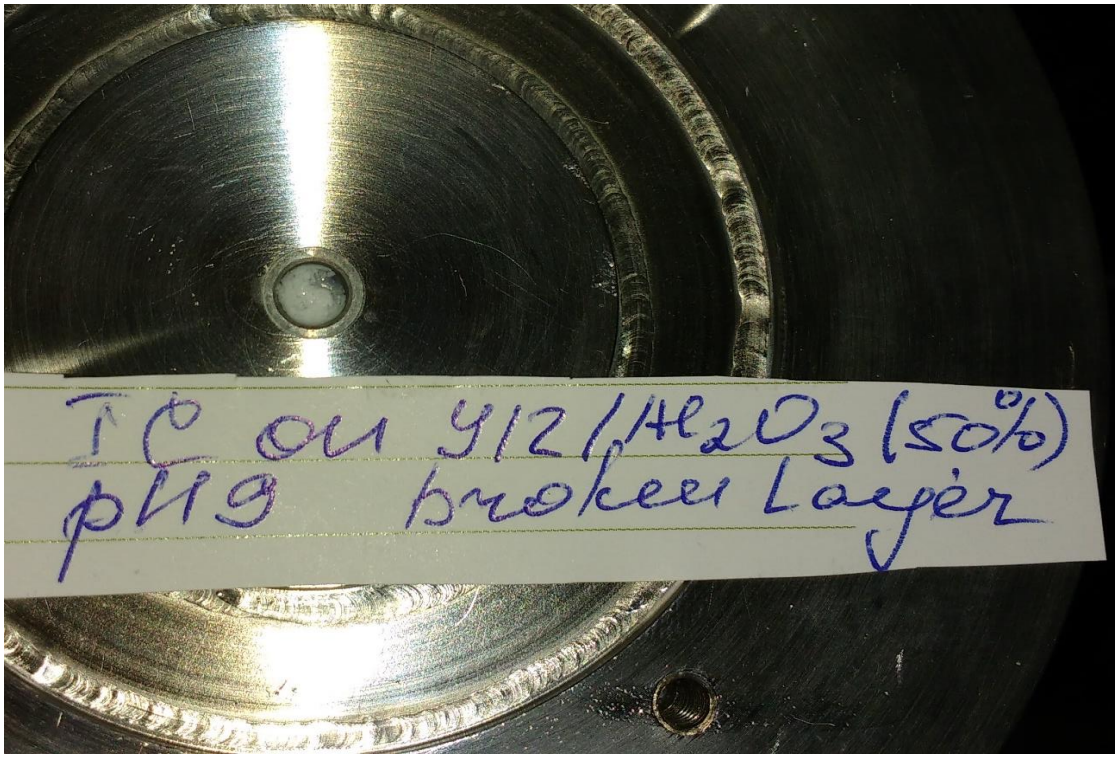

In conclusion, all the attempts to get a stable layer of the particle, applicable for the “in-situ” ATR analysis of imidacloprid sorption on zeolites, as well as sorption of propiconazole on PMO-silica were not effective. Whereas particles layers were not obtained, no ATR-FTIR data was achieved to support the proposed sorption mechanisms (Chapter 3 and Chapter 5). For the future research, it is recommended to establish a method, which would allow getting experimental data to interpret the sorption mechanisms of propiconazole and imidacloprid on the chosen sorbents.

Chapter 9 Toxicological Significance of the Sorption of Thiacloprid_Y30, Thiacloprid_Al_2O3 and Propiconazole_LL-17

9.1. Introduction

The current chapter presents the results of an interdisciplinary study (EXPAND) and reveals the significance of sorption experiments for the objectives of the project. The experiments described here were conducted by several researchers [Lorenz, 2017, Früh, in preparation, Wicht, 2018, Guluzada, present work]. The results of the sorption experiments [Guluzada] of thiacloprid on alumina and zeolites were used for the toxicological studies on *Chironomus riparius* larvae [Lorenz, 2017]. Alumina and zeolites were chosen as examples of very low and very high thiacloprid sorption, to investigate how these two conditions affect the insecticide bioavailability and toxicological effects for *C. riparius* larvae.
The results of propiconazole sorption experiments on PMO-silica [Guluzada] were applied to the toxicological studies on three fungi: *Laccaria bicolor, Amanita muscaria, Cenococcum geophilum* [Früh, in preparation]. Due to the high sorption of propiconazole on PMO-silica (Chapter 5), it was expected to observe modified bioavailability of propiconazole in the presence of PMO-silica and consequently, the change in toxicology for the studied species. The analysis of biotransformation products was conducted by Wicht, 2018.

9.2. The significance of the thiacloprid_Al_2O_3 sorption experiment for the toxicological effect on the midge *Chironomus riparius*

It was intended to clarify, whether Al_2O_3 affects thiacloprid uptake by non-target organisms, namely *Chironomus riparius* larvae [Lorenz et al., 2017a]. Sorption of thiacloprid on Al_2O_3 was studied in the presence of *Chironomus riparius* larvae. The results were compared with the experiments in the absence of larvae (Figure 9.1). The detailed description of sample preparation and toxicological study procedure is given in Lorenz et al., 2017a.

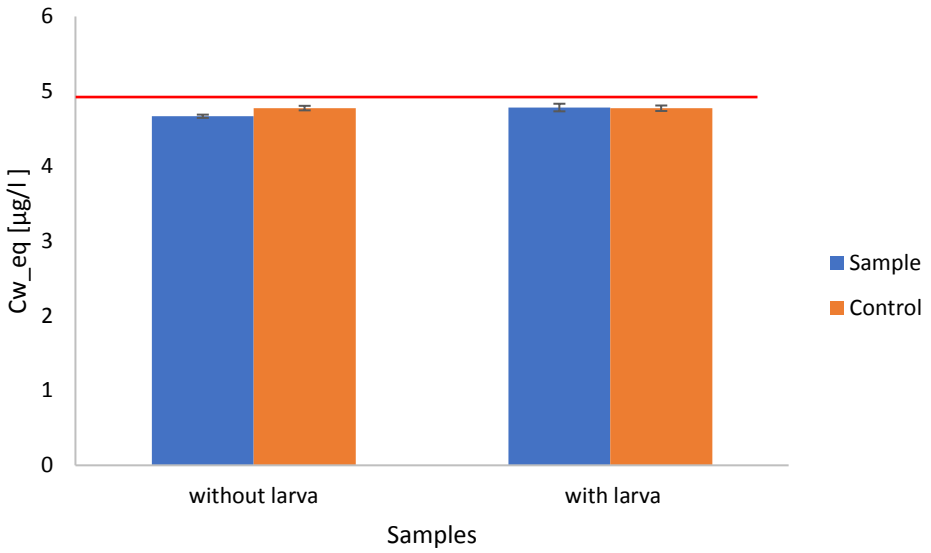

Figure 9.1 Comparison of the thiacloprid equilibrium aqueous concentrations (Cw_eq) in the systems with and without larvae. Sample: 5µg/l with 1g/l Al_2O_3; Control – TC in H_2O without particles) [T=20°C (room temperature), pH 8,6. The red line presents TC concentration in controls. Error bars present standard deviation between triplicates

No effect of the larva presence on the sorption was determined, excluding the binding of thiacloprid to the organic tissues of the larvae.

Sorption experiments were conducted on untreated Al_2O_3 and alumina nanoparticles, excreted from the larvae. Very low sorption of thiacloprid on alumina was discussed in Chapter 4. It was concluded, that due to the low specific surface area, the non-porous character of the material and low affinity of thiacloprid to aluminol groups (reported in the literature, Clausen et al., 2001), Al_2O_3 is ineffective sorbent of thiacloprid and does not change the bioavailability of thiacloprid in the environment through sorption. The sorption of thiacloprid on the alumina nanoparticles excreted from *C. riparius* larvae was low (100% of TC initial concentration were detected in the aqueous phase), demonstrating unchanged sorption properties of the particles past digestion tract of the larva (Figure 9.2).

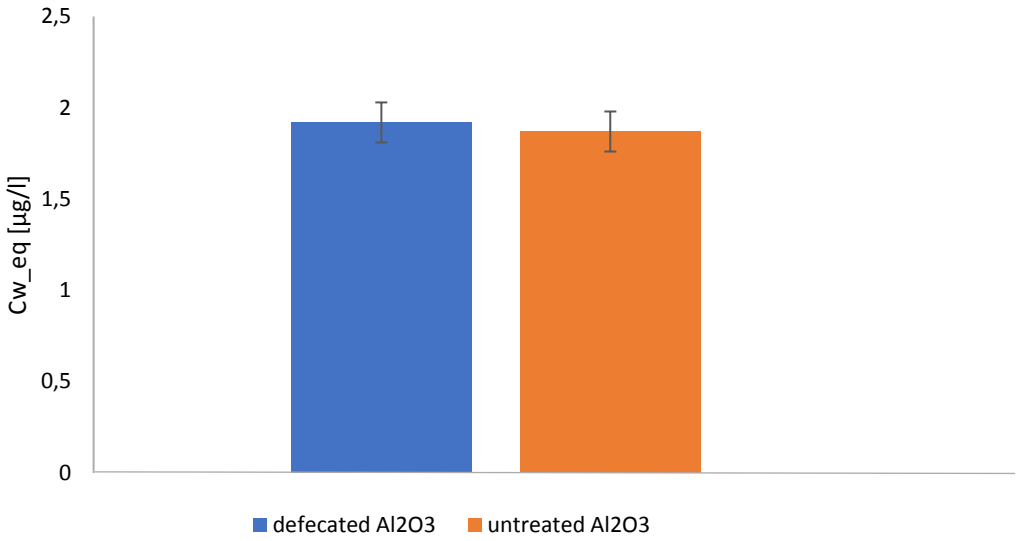

Figure 9.2 Comparison of the thiacloprid equilibrium concentration (Cw_eq) in the sorption experiments with untreated and defecated alumina. Al_2O_3 were swallowed by C. riparius, excreted into filtered and dechlorinated water within 24 hours after swallowing. Sample: 2 µg/l with 1 g/l Al_2O_3; Control – TC in H_2O without particles) [T=20°C (room temperature), pH 8,6]. Error bars present standard deviation between triplicates

Addition of thiacloprid in the absence of alumina and in mixture with 300 mg/l and 1000 mg/l Al_2O_3 nanoparticles to the *C. riparius* larva revealed the decrease in thiacloprid concentration in larval tissues [Lorenz et al., 2017a].

Lorenz et al., 2017 demonstrated, that the mortality of *C. riparius* significantly decreased with the Al_2O_3 introduction to the system.

Mortality of larva was not affected by the presence of alumina without thiacloprid.

A decrease in the mortality rate of *C. riparius* with increasing alumina concentration in thiacloprid_Al_2O_3 mixture, to which larva were exposed implies a protective effect of alumina particles [Lorenz et al., 2017a]. Multiple published works explained such effect by a reduction in bioavailability of the pesticide, namely by sorption [Nowack and Bucheli, 2007; Baun et al., 2008]. In the present work sorption of thiacloprid on alumina, untreated and defecated, was very low (Figure 9.1 and 9.2). It was explained by the effect of Al_2O_3 on the physical-chemical properties of the digestive tract of the larva, or formation of physical barrier, protecting intrinsic organs from the direct contact with thiacloprid [Lorenz et al., 2017a].

Lorenz et al., 2017a concluded, that the bioavailabilty of the pesticide (thiacloprid) and its toxicological effects for the target and non-target species may be impacted by different interaction mechanisms between particles and pesticides. Even though thiacloprid's sorption on alumina was very low, aluminium oxide particles diminished the mortality of studied organisms through the physical barrier formation and alteration of thiacloprid's bioavailability for these organisms [Lorenz et al., 2017a].

9.3. The significance of the thiacloprid_zeolites sorption experiments for the toxicological effect on the midge *Chironomus riparius*

In Chapter 3 high sorption extent of thiacloprid on zeolites was demonstrated (Figure 3.9, Table 3.1). It was suggested, that due to the high sorption of thiacloprid, zeolites are the effective sorbents of thiacloprid and may affect its bioavailability and toxicity for the aqueous organisms. Additionally, due to the small particle size, zeolites with the sorbed thiacloprid are expected to be consumed (swallowed) by the organisms.

Lorenz et al., 2017b investigated the environmental significance of thiacloprid sorption on zeolites (Y30 and beta26).

Using equation (9.1) [Schwarzenbach et al., 2005], three different concentrations of zeolites, needed for the sorption of 97%, 60%, 30% of thiacloprid concentrations, were calculated.

$$r_{SW} = \frac{\frac{1}{f_w} - 1}{K_d} \tag{9.1}$$

r_{SW} −adsorbent concentration [mass of the sorbent per aqeous phase volume]

f_w −fraction of adsorbate in the aqueous phase

K_d −distribution coefficient between solid and aqueous phases

The Kd values were determined experimentally (Table 3.2, Chapter 3). Ingestion of the zeolites by *C. riparius* larva was confirmed by LA-ICP-MS technique [Lorenz et al., 2017b]. Being sediment dwelling and detritus-feeding larva, *C. riparius* could ingest zeolites deposited on the substratum [Lorenz et al., 2017b]. Both beta26 and Y30 zeolites applied solely did not have any significant effect on larval mortality.

This can be explained by the relatively high particle size of both zeolites (Table 2.1, Chapter 2, Table_I, Appendix). The primary beta26 particle size (Image I B., Appendix) was determined to be less than 100 nm, however, beta26 particles tend to form very stable agglomerates in the micrometre range, which made the cell uptake less probable and neutralized the possible negative effect of particles for the organisms. Lehman and Larsen, 2014 investigated the safety of larger size zeolites to water remediation and reported their non-toxic character for the organisms.

Lorenz et al., 2017b measured a pronounced negative effect on behaviour and life length of the larva. As has already been discussed in part 9.1 of the present chapter, thiacloprid, as an agonist of the acetylcholine receptor, affects the central nervous system of *Chironomus riparius* [Elbert et al., 2008].

Thiacloprid increased mortality and caused convulsions of organisms [Lorenz et al., 2017a, b.]. The presence of three concentrations of zeolites diminished mortality of *C. riparius* larvae [Lorenz et al., 2017b]. As was expected, high sorption of thiacloprid on zeolites changed its bioavailability and reduced the toxicity for non-targed organisms (*C. riparius*).

Thus, two different mechanisms of the effect of thiacloprid toxicity for *C. riparius* were determined. No sorption of thiacloprid on alumina nanoparticles was measured. However, the presence of Al_2O_3 in the system decreased the toxicity of thiacloprid, probably due to the physical barrier formation in the digestive tract of *C. riparius* larvae, which prevented it from the direct contact with thiacloprid. The presence of zeolites diminished toxicity of thiacloprid, which was caused by a decrease in insecticide's bioavailability through adsorption [Lorenz et al., 2017b].

9.4. The significance of the propiconazole sorption on PMO-silica for the toxicological effect on the ectomycorrhizal fungi *(Laccaria bicolor, Amanita muscaria, Cenococcum geophilum)*

The effect of PMO-silica LL-17 nanoparticles, propiconazole and propiconazole with PMO-silica on the ectomycorrhizal fungi was studied [Früh, in preparation]. Chapter 5 discusses the sorption of propiconazole on PMO-silica in water and liquid MMN medium. High sorption of propiconazole both in water and medium was determined (Figure 5.1, Chapter 5). The analysis of the samples prepared by Früh (in preparation) with and without fungi revealed a significant effect of the fungi on the propiconazole concentration (Figure 9.3). All the samples inoculated with ectomycorrhizal fungi (*A. muscaria*) independently from the nanoparticles (NP) concentration did not contain propiconazole after 7 days contact time. In the systems without fungi propiconazole attenuation was proportional to the NPs concentrations. The propiconazole concentration did not change with time (samples were taken at days 0 and 7) (Figure 9.3).

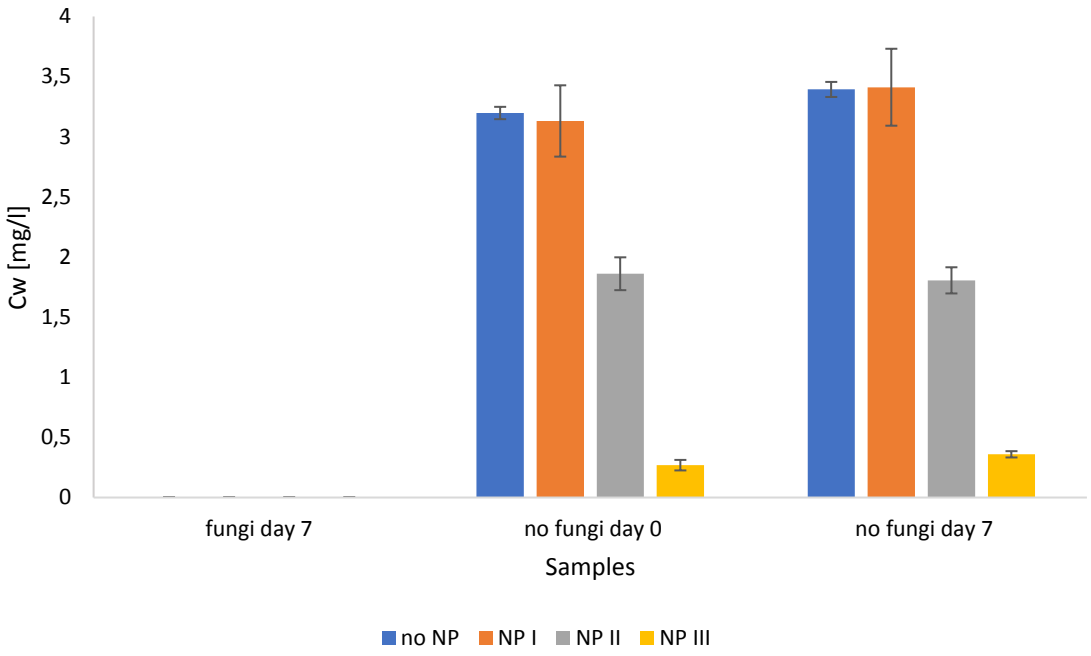

Figure 9.3 Propiconazole concentration in the systems with and without ectomycorrhizal fungi (Amanita muscaria) and different PMO-silica NPs concentrations (NP I=0,032 g/l; NP II= 0,129 g/l; NP III = 0,519 g/l). Concentrations in the presence of fungi were below LOD of the method. Samples prepared by Früh [Doctoral thesis, in preparation]. The error bars present the standard deviation between triplicates

The total attenuation of propiconazole in the samples containing fungi (concentrations in samples were below the LOD of the method) should be referred to the fungal effect on propiconazole. Früh (in preparation) confirmed propiconazole attenuation in the presence of three ectomycorrhizal fungi *(Laccaria bicolor, Amanita muscaria, Cenococcum geophilum)* (Figure 9.4).

Several researchers investigated the possibility of bioremediation and biotransformation of azole compounds by fungi. Woo et al., 2010 studied remediation of tebuconazole and propiconazole impregnated in wood by *Trametes versicolor* and *Fomitopsis.* Woo measured the attenuation of 53% and 54 % tebuconazole (0,771 kg/m³) by *T. versicolor* and *F. palustris* respectively after 21 days of fungal growth. *Trametes versicolor* attenuated 75% of propiconazole (1,39 kg/m³), whereas *F. palustris* did not affect propiconazole abundance significantly [Woo et al., 2010]. Kim et al., 2002 distinguished the following degradation products of propiconazole: 1-[[2(2,4-dichlorophenyl)-2-(1,2,4-triazole -1-yl) ketone (DP-1), 1-(2,4-dichlorophenyl)-2-(1,2,4-triazole-1- yl) ethanol (DP-2) and 1-[[2(2,4-dichlorophenyl)-4-hydroxypropyl-1,3-dioxolane-2-yl]methyl]1*H*-1,2,4-triazole (DP-3 and DP-4). To explain significant depletion in propiconazole concentration in the samples in the presence of ectomycorrhizal fungi (Figure 9.3 and 9.4) Wicht, 2018 analyzed the samples for the presence of propiconazole metabolites with HPLC-MS. Her work revealed the presence of the following propiconazole biotransformation products: BTP 2.1,

BTP 2.2, BTP 2.3, BTP 3, BTP 4 [Konwick et al., 2006; Rosch et al., 2016], [from Vialaton et al., 2001]), [Wicht, 2018].

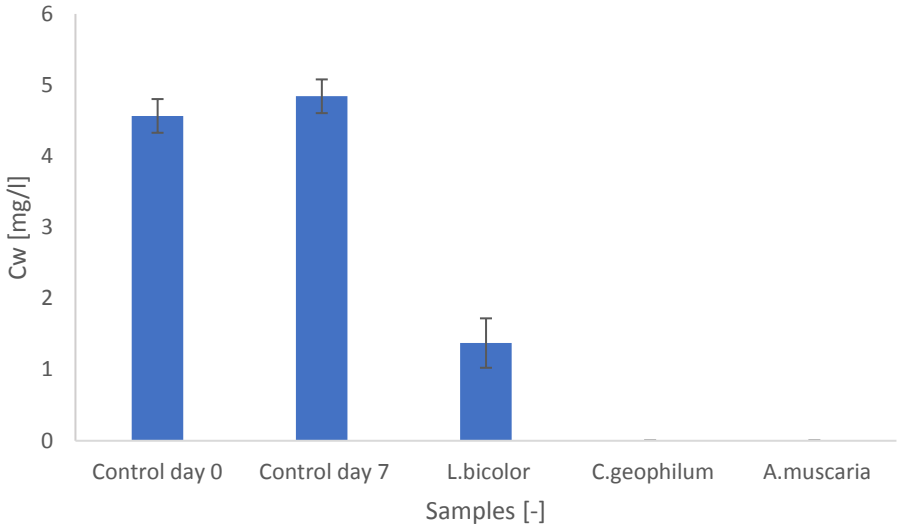

Figure 9.4 Propiconazole concentration in the presence of three ectomycorrhizal fungi (Laccaria bicolor, Amanita muscaria, Cenococcum geophilum) without PMO-silica. Concentration in controls depicts initial concentration of propiconazole in samples. Concentrations in the presence of fungi C. geophilum and A. muscaria after 7 days were below LOD of the method. Samples prepared by Früh [Doctoral thesis, in preparation]. Standard deviation is calculated from triplicates

The rate and extent of biotransformation reported by Woo et al., 2010 and in the present work differ significantly: *F. palustris* did not transform propiconazole after 21 days, *T. versicolor* – 75% of propiconazole after 21 days; in the present work *C. geophilum* and *A. muscaria* caused biotransformation of ~100% of propiconazole already after 7 days, *L. bicolor* – 72 % of propiconazole after 7 days [Woo et al., 2010]. The reported difference can be explained by the different bioactivity of the applied fungi, different experimental setups and conditions, which affected the fungi.

Moreover, Früh (in preparation) revealed an impact of propiconazole sorption on fungal growth. Früh, (in preparation) determined a positive effect of the increase in the particle-associated propiconazole and decrease in free propiconazole induced by PMO-silica addition on fungi growth on agar plates. Thus, the fungus diameter on agar was obviously larger in the presence of sorbed propiconazole instead of freely-dissolved propiconazole. However, the results in the liquid MMN medium were not strongly pronounced and reproducibility was low [Früh, in preparation].

Conclusively, collaborative work revealed a significant effect of particle-associated propiconazole for the non-target ectomycorrhizal fungi [Früh, in preparation; Wicht, 2018; Guluzada, present work]. The work proved the formation of propiconazole degradation products (biotransformation, but not phototransformation) in the presence of fungi [Wicht, 2018]. The sorption of propiconazole on PMO-silica decreased pesticide's toxicity through the lower bioavailability, which caused an increase in the fungal growth.

Chapter 10 Conclusions and Outlook

The objectives of the present work were:

a) To investigate the sorption of the pesticides on the model particles and estimate the impact of environmental conditions on the sorption process;
b) To suggest the sorption mechanisms;
c) As a part of interdisciplinary project EXPAND, to evaluate the effect of the pesticides' adsorption on their bioavailability and toxicological effects for the target and non-target organisms.

The present work demonstrated, that the sorption mechanisms of non-charged and ionizable organic molecules in their pKa range differ significantly and involve different processes.

The comparison of the infrared spectra (IR) of glyphosate without particles and in the presence of Al_2O_3 particles at pH 9 revealed broadening of the peak at 1093 cm^{-1}, referred to the symmetrical stretching of PO_3^{2-} group [Barja and dos Santos Afonso, 1998]. Based on ATR-FTIR experimental data it was proposed, that the sorption of glyphosate involves phosphonate group and results in either nonprotonated monodentate complex or nonprotonated bidentate binuclear complex. Alteration of the peak at 1240 cm^{-1} suggests outer-sphere coordination of carboxylic oxygen with alumina surface through water bridges.

The sorption of neonicotinoids on the zeolites is limited by pore-filling process. The pore size and pore geometry were demonstrated as important factors for imidacloprid and thiacloprid sorption. The sorption of TC and IC on zeolites (with pore diameter 0,5-0,74nm) was significantly higher than on MCM-48 and periodic mesoporous organosilica (PMO-silica) (pore diameter 2,2 nm and 1,9 nm respectively). Hence, it was proposed, that the pores, which are slightly larger than the molecule, facilitated the pore-filling with subsequent "trapping" of organic molecules in the pores. The presence of organic functional groups on the surface of PMO-silica and in MCM-48 (CTAB template) indicated, that sorption on these surfaces was hydrophobicity driven. This was supported by the comparison with the propiconazole and hexaconazole sorption on PMO-silica. It was also discussed, that the shape of the pores affects the sorption of organic molecules. Thus, the kinetics experiments of thiacloprid and imidacloprid sorption on FAU and BEA zeolites demonstrated the faster sorption on FAU zeolites with a spherical form of the pores (0,74 nm in diameter), than on BEA type zeolite with deformed spherical shape and smaller diameter (0,5 – 0,65 nm).

According to Liu et al., 2002, sorption mechanism of imidacloprid on the silica surface involves C=N (from pyridine group) coordination with the surface silanol groups. It was proposed that the sorption mechanism of thiacloprid and imidacloprid on zeolites involves coordination of C=N group (imidazolidine and pyridine rings) with exchangeable cations of zeolites; hydrogen bond formation between

silanol groups of the zeolites and N atoms of IC and TC molecules; hydrogen bonding between Cl- of the neonicotinoid molecule and the hydrogens on zeolite surface.

An interpretation of the sorption mechanism of non-charged neonicotinoids (IC and TC) on zeolites was done without experimental data from ATR-FTIR. No data concerning the sorption mechanism was obtained, since no stable particles layer, necessary for the "In-situ" analysis in the ATR cell, was obtained. The instability of the particles layer was explained by high porosity, low density and small particle size of the studied zeolites.

The sorption of propiconazole and hexaconazole on PMO-silica was primarily explained by low solubility and high K_{OW} values of these compounds. The sorption of pesticides increased in a row: imidacloprid < thiacloprid < propiconazole < hexaconazole. The aryl ring may participate in π-π EDA interactions with PMO-silica. Multiple studies show, that sorption of triazole-containing compounds involves N of triazoles and enforces the interaction of strongly electron-deficient heterocycles with the sorbent, resulting in metal coordination (cation-N(triazole)) or H-bond formation (anion-N(triazole) and hydrogen-N(triazole)) [Crowley et al., 2010, Camponovo et al., 2009, Li et al., 2007]. Dioxolane moiety of propiconazole could participate in EDA interactions with the PMO-silica surface. Due to the high porosity, low density and small particle size, no effective layer for ATR-FTIR analysis was achieved. Therefore, the proposed sorption mechanism was not experimentally proven.

The variation of environmental parameters revealed several important effects on the sorption. The presence of Ca^{2+} and Cu^{2+} affected the sorption of both non-ionogenic and ionizable pesticides. An increase in sorption of both propiconazole and glyphosate as examples of a non-charged and negatively charged molecule at the studied conditions suggested the complex-formation with the cations on the surface of the sorbent, i.e. sorption of the cations on the surface of PMO-silica and alumina was proposed. Glyphosate complexes with Ca^{2+} and Cu^{2+} were extensively described in literature [Maqueda et al., 2002; Mattos et al., 2017], including the direct formation of glyphosate-Cu^{2+} ternary surface complexes on the mineral (goethite) surface [Sheals et al., 2003] There is scarce information available on surface complexation of propiconazole with cations. Evans et al., 2010 described the complexes of tebuconazole and propiconazole with divalent cations (Zn^{2+}, Cu^{2+}) in the aqueous phase.

In the present dissertation, the complex-formation of propiconazole with Cu^{2+} on the PMO-silica surface was proposed, which explains an increased adsorption in the presence of $CuCl_2$ under assumption of Cu^{2+} adsorption on the PMO-silica. To support this hypothesis, in the future experiments it is needed to quantitatively determine concentration of sorbed and freely-dissolved Cu^{2+} cations.

The presence of Ca^{2+} cations diminished imidacloprid and thiacloprid sorption. It was suggested, that Ca^{2+} could occupy some sorption sites, or replace the exchangeable cations on the zeolites surface and hence, reduce the number of sorption sites of imidacloprid and thiacloprid. The hypothesis of complex formation between Ca^{2+} and imidacloprid (thiacloprid) was rejected due to missing effect of Ca^{2+}

cations on imidacloprid (and thiacloprid) sorption on MCM-48. Sorption of imidacloprid and thiacloprid was mainly due to the hydrophobic interactions with the surface, therefore presence of Ca^{2+}, even considering its sorption, did not affect the sorption mechanism of imidacloprid and thiacloprid. The complex formation, if there was any in the sorption on zeolites, should also take place in the sorption experiments on MCM-48. Because of no effect of Ca^{2+} cations on the sorption of imidacloprid and thiacloprid on MCM-48, it was concluded, that no complex-formation between the studied neonicotinoids and Ca^{2+} takes place. This is supported by the lack of published literature describing such complex-formation.

The pH variation in the pH range 5-9 affected the sorption of ionizable pesticide, whereas sorption of non-charged molecules was not affected by the pH in the studied pH range. The lowest sorption of glyphosate on alumina was measured at the highest studied pH (8,5), close to the point of zero charge of alumina. It was proposed, that at this pH the interaction between negatively charged glyphosate molecule (z=-2) and partially negative alumina surface cause unfavourable electrostatic conditions. A similar conclusion was made by Borggaard and Gimsing, 2008 who observed the lowest sorption of glyphosate on aluminium and iron oxides at the highest pH (pH 8) and explained it through the repulsion between a mineral surface and pesticide molecule.

In this study, the presence of phosphate did not diminish the glyphosate sorption. The proposed sorption mechanism of glyphosate on alumina involves the phosphonate group and it was expected to observe the competition between glyphosate and phosphate for the same sorption sites [Gimsing et al., 2004; Gimsing and Borggaard, 2001]. It was proposed, that the missing qualitative effect of the phosphate on glyphosate sorption was due to the large difference in the chosen concentrations (glyphosate's concentration was three orders of magnitude higher than the concentration of phosphate) and additionally, studied glyphosate concentration was in the linear range of the sorption isotherm.

The competitive nature of imidacloprid and thiacloprid sorption suggested their sorption to involve similar mechanisms and proposed the sorption on the same sorption sites.

Whereas humic acid (Suwannee River Humic Acid) did not alter the sorption of imidacloprid and thiacloprid, it was proposed, that the sorption of neonicotinoid molecules on zeolites were not affected due to the size-exclusion effect. Because of their small molecule size, imidacloprid and thiacloprid molecules were able to diffuse into the pores of zeolites, whereas humic acids sorbed mainly on the outer surface.

Summarizing the results of the effects of all above-mentioned environmental factors, it is concluded, that:

a) Sorption of both ionizable and non-ionogenic pesticides on the minerals in the environment is affected by various environmental factors;

b) The mechanism of the sorption of charged and non-charged molecules involves different mechanisms. For charged molecules, electrostatic interactions significantly affect the sorption, whereas for the non-charged molecules π-π EDA interaction is more probably involved in the bond formation. Sorption of neonicotinoids on the zeolites was limited by pore-filling process. Sorption of four non-charged molecules (neonicotinoids and azole fungicides) on the PMO-silica and MCM-48 was hydrophobicity driven. Sorption of ionizable molecules is strongly affected by the pH change in their pKa range.

c) The sorption of the pesticides on chosen particles was high even under the limiting conditions.

The recent conclusion lead to the following implications:

- An interaction between the zeolites and neonicotinoids reduces the concentration of freely-dissolved pesticides, which affects their bioavailability for the aquatic organisms and modifies the toxicity of the systems. This was demonstrated by Lorenz et al., 2017 b, who investigated an effect of thiacloprid sorption on *Chironomus riparius* and reported a decrease in thiacloprid's toxicity for *Chironomus riparius* through its sorption on the zeolites.
- Sorption of propiconazole and hexaconazole on PMO-silica results in lower aqueous concentrations and changes the toxic effects and bioavailability. This was studied and confirmed by the work of Früh (Doctoral thesis, in preparation), who observed a decreased toxicity of propiconazole for ectomycorrhizal fungi *Laccaria bicolor, Amanita muscaria, Cenococcum geophilum* due to propiconazole sorption on the PMO-silica.
- Sorption of glyphosate on alumina decreases its freely-dissolved concentration and affects the bioavailability of glyphosate and its effects on the aqueous organisms.

For future research, which will further investigate the impact of the pesticides' sorption on natural or synthetic (nano-)particles the following suggestions were done:

1. The sorption mechanism of neonicotinoids and azole fungicides on the chosen sorbents should be determined experimentally, using, for example, ATR-FTIR. To avoid the problems with the particles layer formation, like in the present work, the sorbents with similar properties, but with the higher density or larger particle size should be chosen.
2. Investigating an effect of di- and trivalent cations on the sorption and expecting the complex-formation between the pesticide molecule and the added cation, it is recommended to determine complex formation experimentally and estimate the complex formation constants. Additionally, the aqueous complexes should be distinguished from the complexes on the water-sorbent surface.

3. To evaluate the effect of phosphate on glyphosate sorption, it is necessary to conduct the experiment at the comparably equal concentrations of both compounds and in the saturation range of the isotherm.

Appendix

Table_ I Zeolites' particle size measurements [Mastersizer Hydro 2000]. Provided values are d(90).*

**d(90) – 90% of all the particles have size lower or equal to the provided value.*

	Particle size [µm]				
Zeolite	Original	Dry milling	Wet milling at pH 4	Wet milling at pH 8	After sedimen-tation
Y12	8,906	6,476	3,811	3,695	0,545
Y30	5,838	4,401	1,198	1,20	0,691
Y80	31,17	6,487	1,224	1,204	0,596
Beta 360	-	1,16	1,15	1,141	0,581

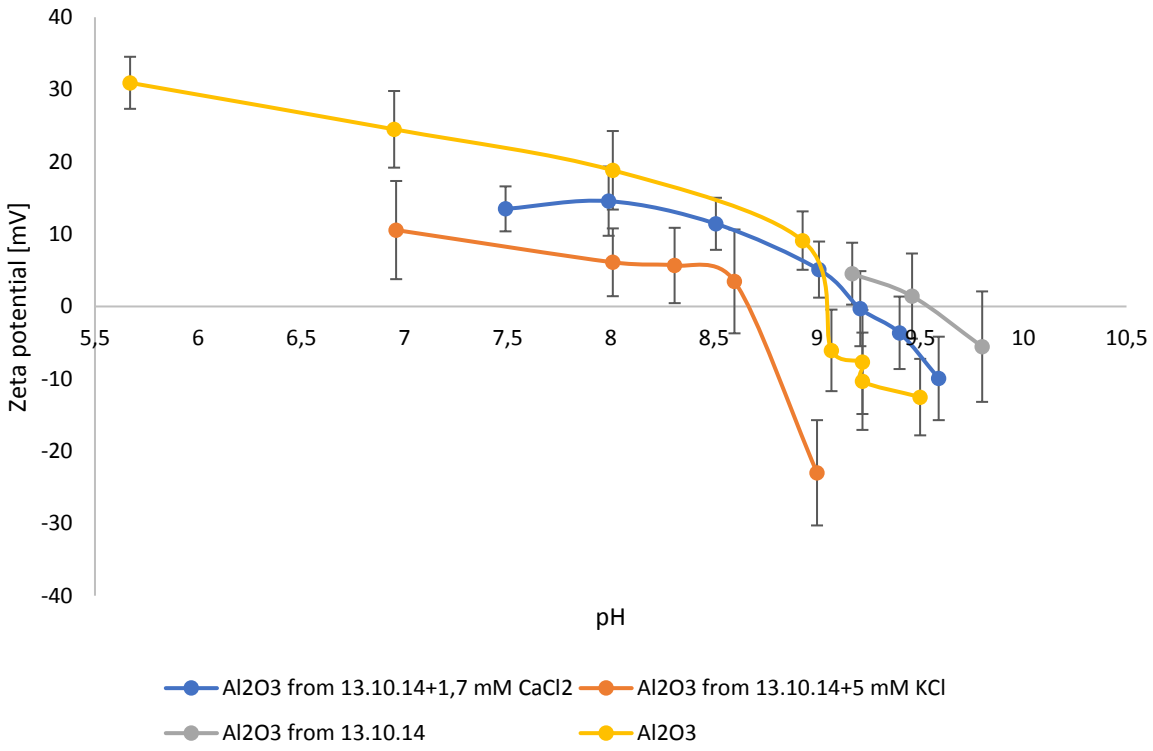

Figure_ I Point of zero charge of Al_2O_3. Measrements conducted on Malvern Zetasizer Hydro 2000

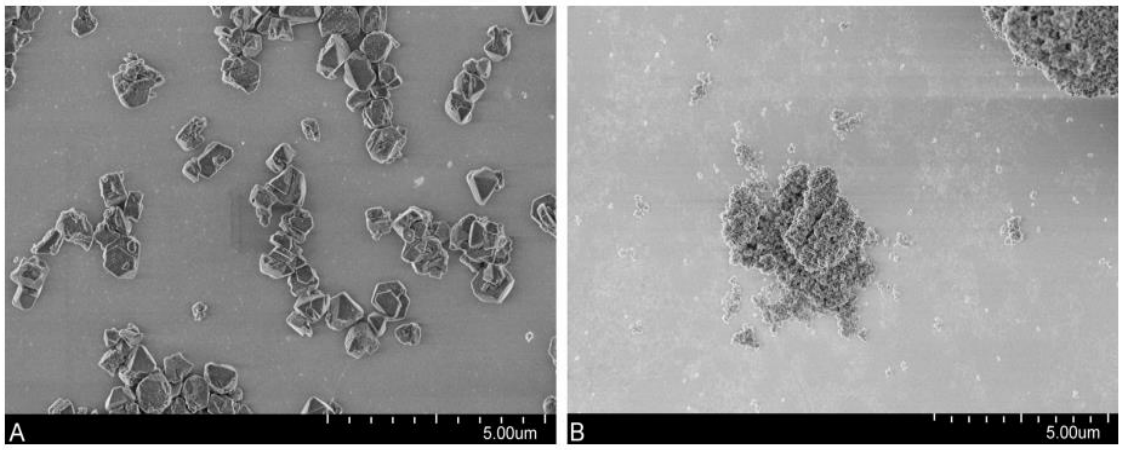

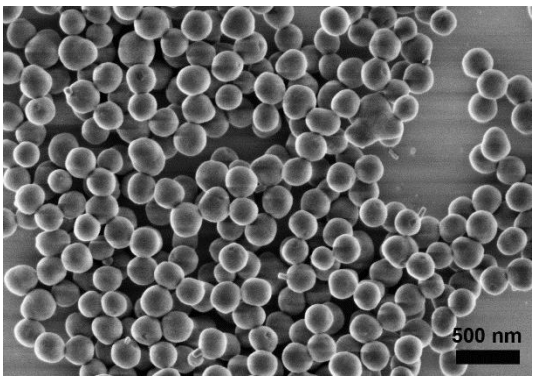

C

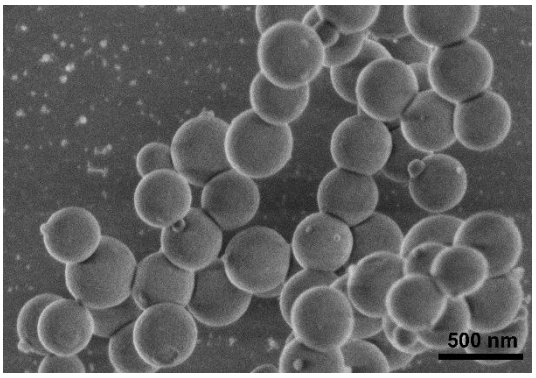

D

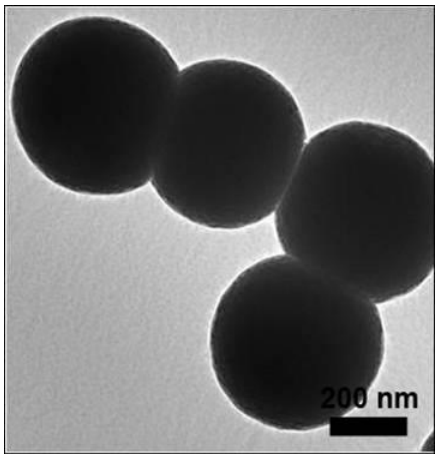

E

Image I. *SEM images of: A) Y30 zeolite (after milling and settling); B) calcined beta26 (H-Beta(OH)-III. TEM images of C) MCM-48; D) LL-17; E) Al_2O_3 [Luo, 2018]*

Literature

Adamczyk, Z., Para, G., Warszynski, P. (1999). “Influence of ionic strength on surface tension of cetyltrimethylammonium bromide”. Amer. Chem. Soc., Langmuir, V. 15 (24), pp. 8383-8387.

Akesson, M., Sparrenbom, C.J., Dahlqvist, P., Fraser, S.J. (2015). „On the scope and management of pesticide pollution of Swedish groundwater resources: The Scanian example”. Ambio, V. 44(3), pp. 226-238.

Akhtar, M., Alexander, K., Boar, R.B., McGhie, J.F. and Barton, D.H. (1978). “Chemical and enzymic studies on the characterization of intermediates during the removal of the 14alpha-methyl group in cholesterol biosynthesis. The use of 32-functionalized lanostane derivatives”. Biochem. J., V. 169, pp. 449-463.

Albers, C.N., Banta, G.T., Hansen, P.E., Jacobsen, O.S. (2009). „The influence of organic matter on sorption and fate of glyphosate in soil-comparing different soils and humic substances”. Environ. Pollut. V. 157 (10), pp. 2865-2870.

Alberti, A., Cruciani, G., Galli, E., Merlino, S., Millini, R., Quartieri, S., Vezzalini, G., and Zanardi, S. (2002). “Crystal structure of tetragonal and monoclinic polytypes of tschernichite, the natural counterpart of synthetic zeolite beta”. J. Phys. Chem, V. B106, pp. 10277-10284.

Alebrahim, M. A. (2013). “ATR-FTIR and Raman imaging to study permanent and primary teeth from different places and ages”, Doctoral thesis, Friedrich-Schiller-University of Jena.

Alva, A.K., Singh, M. (1991). “Sorption-desorption of herbicides in soil as influenced by electrolyte cations and ionic strength”. J. Environ. Sci. Health., V. B 26, pp. 147–163.

Aparicio, V.C., Geronimo, E. de, Marino, D., Primost, J., Carriquiriborde, P., Costa, J.L. (2013). “Environmental fate of glyphosate and aminomethylphosphonic acid in surface waters and soil of agricultural basins”. Chemosphere, V. 93 (9), pp. 1866-1873.

Aregahegn, K.Z., Shemesh, D., Gerber, R.B., Finlayson-Pitts, B. J. (2017). “Photochemistry of thin solid films of the neonicotinoid imidacloprid on surfaces”. Environ. Sci. Technol, V. 51 (5), pp. 2660-2668.

Arias, M., Paradelo, M., López, E., Simal-Gándara, J. (2006). “Influence of pH and Soil Copper on Adsorption of Metalaxyl and Penconazole by the Surface Layer of Vineyard Soils”. Journal of Agricultural and Food Chemistry, V. 54 (21), pp. 8155-8162.

Asefa, T., MacLachlan, M.J., Coombs, N. and Ozin, G.A. (1999). “Periodic mesoporous organosilicas with organic groups inside the channel walls”. J. Nature, V. 402, pp. 867-871.

Atwood, D. (2017). “Pesticides industry and sales and usage”. Biol. Econ. Anal. Div., US. EPA, Washington, accessed 5 November 2018. https://www.epa.gov/sites/production/files/2017-01/documents/pesticides-industry-sales-usage-2016_0.pdf

Aziz, S.G., Elroby, S.A., Alyoubi, A., Osman, O.I., Hilal, R. (2014). “Experimental and theoretical assignment of the vibrational spectra of triazoles and benzotriazoles. Identification of IR marker bands and electric response properties”. J. Mol. Model., V. 20 (3), p. 2078.

Baalousha, M. (2009). “Aggregation and disaggregation of iron oxide nanoparticles: Influence of particle concentration, pH and natural organic matter”. Sci. Total Environ., V. 407, pp. 2093-2101.

Baalousha, M., Motelica-Heino, M., and Le Coustumer, P. (2006). “Conformation and size of humic substances: effects of major cation concentrate ion and type, pH, salinity, and residence time”. Coll. Surf. V. A 272, pp. 48–55.

Baerlocher, C., Meier, W. M., Olson, D.H. (2007). “Atlas of Zeolite Framework Types”, Elsevier Science, Amsterdam, 6-th edition.

Baglieri, A., Vindrola, D., Gennari, M., Negre, M. (2014). “Chemical and spectroscopic characterization of insoluble and soluble acid fractions at different pH values”. Chem. Biol. Technol. Agric., V. 1 (9), pp. 1-11.

Bajeer, M.A., Nizamani, S.M., Sherazi, S.T.H., Muhammad, I.B. (2012). “Adsorption and leaching potential of imidacloprid pesticide through alluvial soil”. Am. J. Anal. Chem., V. 3 (8), pp. 604-611.

Balança, G., de Visscher, M.N. (1997). “Effects of very low doses of fipronil on grasshoppers and non-target insects following field trials for grasshopper control”. Crop Prot., V. 16, pp. 553–564.

Barja, B.C., Dos Santo Afonso, M. (1998). “An ATR-FTIR study of glyphosate and its Fe(III) complex in aqueous solution”. Environ. Sci. Technol., V. 32, pp. 3331-3335.

Barrett, K. A. and McBride, M. B. (2006). “Trace Element Mobilization in Soils by Glyphosate”. J. Soil Sci. Soc. Am., V. 70, pp. 1882–1888.

Barrett, K.A., McBride, M.B. (2005). “Oxidative Degradation of Glyphosate and Aminomethylphosphonate by Manganese Oxide”. Env. Sci. Tech., V. 39 (23), pp. 9223-9228.

Baskaran, S., Kookana, R.S. & Naidu, R. (1997). “Determination of the insecticide imidacloprid in water and soil using high-performance liquid chromatography”. J. Chromat. A, V. 787 (1-2), pp. 271-275.

Battaglin, W.A., Meyer, M.T., Kuivila, K.M., Dietze, J.E. (2014). “Glyphosate and Its Degradation Product AMPA Occur Frequently and Widely in U.S. Soils, Surface Water, Groundwater, and Precipitation”. JAWRA, V. 50 (2), pp. 275-290.

Baun, A., Sørensen, S.N., Rasmussen, R., Hartmann, N.B., Koch, C.B. (2008). “Toxicity and bioaccumulation of xenobiotic organic compounds in the presence of aqueous suspensions of aggregates of nano-C_{60}”. Aquatic Toxicol., V. 86, pp. 379-387.

Baur, W.H. (1964). “On the cation and water positions in faujasite”. Am. Miner., V. 49, pp. 697-704.

Bekbolet, M., Yenigun, O., Yucel, I. (1999). "Sorption studies of 2,4-D on selected soils”. Water Air Soil Pollut., V. 111, pp. 75-88.

Benhamou, A., Baudu, M., Derriche, Z., Basly, J.P. (2009). "Aqueous heavy metals removal on amine-functionalized Si-MCM-41 and Si-MCM-48”. J. Hazard. Mat., V. 171 (1-3), pp. 1001-1008.

Benhamou, A., Baudu, M., Derriche, Z., Basly, J.P. (2009). „Aqueous heavy metals removal on amine-functionalized Si-MCM-41 and Si-MCM-48”. J. Hazard. Mat., V. 171 (1-3), pp. 1001-1008.

Berenstein, G., Nasello, S., Beiguel, A., Flores, P., Di Schiena, J., Basack, S., Hughes, E.A., Zalts, A., Montserrat, J.M. (2017). “Human and soil exposure during mechanical chlorpyrifos, myclobutanil and copper oxychloride application in a peach orchard in Argentina”. Sci. Total Environ., V. 586, pp. 1254-1262.

Bergerhoff, G., Baur, W.H., Nowacki, W. (1958). “Über die Kristallstrukturen des Faujasite“. Neues Jahrb. Miner. Monatsh., pp. 193-200.

Bergerhoff, G., Koyama, H., Nowacki, W. (1956). “Zur Kristallstrukturen des Faujasite“. Experimenta, Basel, V. 12, pp. 418-419.

Bernasconi, S. (2003). “Liquid Phase Nitration of Toluene and 2-Nitrotoluene using Acetyl Nitrate: Zeolite BEA as para-selective Catalyst”, diss. ETH# 15325, Zurich.

Best, N.B., Hartwig, T., Budka, J.S., Bishop, B.J., Brown, E., Potluri, D.P., Cooper, B.R., Premachandra, G.S., Johnston, C.T., Schulz, B, (2014). "Soilless plant growth media influence the efficacy of phytohormones and phytohormone inhibitors." PLoS ONE, V. 9 (12), e107689.

Boggs, R.C., Howard, D.G., Smith, J.V., and Klein, G.L. (1993). “Tschernichite, a new zeolite from Goble, Columbia County, Washington”. Am. Miner., V. 78, pp. 822-826.

Bol’shakov, D.S.; Amelin, V.G. (2016). “Determination of pesticides in environmental materials and food products by capillary electrophoresis”. J. Anal. Chem., V. 71, pp. 965–1013.

Bonmatin, J.-M., Giorio, C., Girolami, V., Goulson, D., Kreutzweiser, D.P. (2014). “Environmental fate and exposure; neonicotinoids and fipronil”. Env. Sci. Pollut. Res., V. 22 (1), pp. 35-67.

Borggaard, O.K., Gimsing, A.L. (2008). “Fate of glyphosate in soil and the possibility of leaching to ground and surface waters: a review”. Pest Man. Science, V. 64 (4), pp. 441-456.

Brankovic, M.D., Zarubica, A.R., Andjelkovic, T.D., Andjelkovic, D.H. (2017). “Mesoporous silica (MCM-41): synthesis/modification, characterization and removal of selected organic micro-pollutants from water”. Advanced Technol., V. 6 (1), pp. 50-57.

Brucker Confocheck Benutzerhandbuch, Brucker Optik GmbH, pp. 43-71.

Bruins, A. P. (1991). "Mass spectrometry with ion sources operating at atmospheric pressure". Mass. Spec. Rev., V.10 (1), pp. 53-77.

Brusseau, M.L. (1991). "Cooperative sorption of organic chemicals in systems composed of low organic carbon aquifer materials”. Environ. Sci. Technol., V. 25, pp. 1501-1506.

Buchholz, A. (2009). “Redox reactions and phase transformation processes at iron mineral surfaces studied by compound specific isotope analysis”. Doctoral thesis, Eberhard-Karls University Tübingen.

Cadkova, E., Komarek, M., Kaliszova, R., Szakova, J., Vanek, A., Bordas, F., Bollinger, J.-C. (2013). “The influence of copper on tebuconazole sorption onto soils, humic substances, and ferrihydrite”. Environ. Sci. Pollut. Res., V. 20, pp. 4205-4215.

Calvet, R. (1989). “Adsorption of organic chemicals in soils”. Env. Health Persp. V. 83, pp. 145–177.

Camponovo, J., Ruiz, J., Cloutet, E., Astruc, D. (2009). “New polyalkynyl dendrons and dendrimers: “Click” chemistry with azidomethylferrocene and specific anion and cation electrochemical sensing properties of the 1,2,3-Triazole containing dendrimers”. Chem.–Eur. J., V. 15 (12), pp. 2990–3002.

Carlisle, S.M., Trevors, J.T. (1988). “Glyphosate in the environment”. Water Air Soil Pollut., V. 39 (3-4), pp. 409-420.

Casida, J. E. (2011). “Neonicotinoid metabolism: compounds, substituents, pathways, enzymes, organisms, and relevance”. J. Agric. Food Chem., V. 59, pp. 2923–2931.

Caullet, P., Guth J.L., Hazm, J., Lamblin, J.M., Gies, H. (1991). “Synthesis, characterization and crystal structure of the new clathrasil phase octadecasil”. J. Eur. Solid State Inorg. Chem., V. 28, pp. 345-361.

Chaliy, V.P. (1972). „Gidrookisi metallov“. Kiev, “Naukova dumka”, p. 160. [Чалый В. П., Гидроокиси металлов. Киев "Наукова думка". 1972 С. 160.]

Chaplain, V., Mamy, L., Vieublé-Gonod, L., Mougin, C., Benoit, P., Barriuso. E., Nélieu, S. (2011). “Fate of pesticides in soils: toward an integrated approach of influential factors, pesticides in the modern World - risks and benefits”. Dr. Margarita Stoytcheva (Ed.), InTech, pp. 535-560.

Chauhan, S.S., Srivastava, A., Chandra Srivastavab, P., Verma, A. (2013). “Sorption – desorption of imidacloprid insecticide on Indian soils of five different locations”. Eur. J. of Soil Sci., V. 2, pp. 107-113.

Chen, J.Q., Hu, Z.J., Wang, N.X. (2012). “Photocatalytic mineralization of glyphosate in a small-scale plug flow simulation reactor by UV/TiO2”. J. Env. Sci. Health, V. 47 (6), pp. 579-588.

Chernushevich, I.V., Loboda, A.V., Thomson B.A. (2001). “An introduction to quadrupole-time of flight mass spectrometry”. J. Mass Spec., V. 36 (8), pp. 849-865.

Chiola, V., Ritsko, J. E., Vanderpool, C. D. (1971). "Process for producing low-bulk density silica." Application No., Publication No. US 3556725 A.

Clausen, L., Fabricius, I. (2001). “Atrazine, isoproturon, mecoprop, 2,4-D, and bentazone adsorption onto iron oxides”. J. Environ. Qual., V. 30, pp. 858–869.

Clausen, L., Fabricius, I., Madsen, L. (2001). “Adsorption of pesticides onto quartz, calcite, kaolinite, and alpha-alumina”. J. Environ. Qual., V. 30, pp. 846–857.

Corma, A. (2003). “State of the art and future challenges of zeolites as catalysts”. J. Catal., V. 216 (1-2), pp. 298-312.

Cornell, R.M., Schwertmann, U. (2004). “The iron oxides: structure, properties, reactions, occurrences and uses”. Wiley VCH., Wiley online library, 2-nd edition.

Crowley, J.D. and Bandeen, P.H. (2010). “A multicomponent CuAAC “click” approach to a library of hybrid polydentate 2-pyridyl-1,2,3-triazole ligands: new building blocks for the generation of metallosupramolecular architectures”. Dalton Trans., V. 39, pp. 612–623.

Crowley, J.D., Bandeen, P.H., Hanton, L.R. (2010). “A one pot multi-component CuAAC “click” approach to bidentate and tridentate pyridyl-1,2,3-triazole ligands: Synthesis, X-ray structures and copper(II) and silver(I) complexes”. Polyhedron, V. 29, pp. 70–83.

Camponovo, J., Ruiz, J., Cloutet, E., Astruc, D. (2009). “New polyalkynyl dendrons and dendrimers: “Click” chemistry with azidomethylferrocene and specific anion and cation electrochemical sensing properties of the 1,2,3-Triazole containing dendrimers”. Chem.–Eur. J., V. 15 (12), pp. 2990–3002.

Li, Y., Huffman, J. C., Flood, A.H. (2007). “Can terdentate 2,6-bis(1,2,3-triazol-4-yl)pyridines form stable coordination compounds?”. Chem. Commun., V. 26., pp. 2692–2694.

Crowley, P.D., Gallagher, H.C. (2014). “Clotrimazole as a pharmaceutical: past, present and future”. J. Appl. Microbiol., V. 117 (3), pp. 611-617.

Da Cruz, L., de Santana, H., Zaia, C.T.B.V., Zaia, D.A.M. (2007). „Adsorption of glyphosate on clays and soils from Parana state: Effect of pH and competitive adsorption of phosphate”. Braz. Arch. Biol. Technol., V. 50, pp. 385-394.

Dachs, J., Mejanelle, L. (2010). “Organic pollutants in coastal waters, sediments and biota: A relevant driver for ecosystems during the Anthropocene?”. Estuar. Coast., V. 33., pp. 1-14.

Damonte, M., Torres Sanchez, R.M., dos Santos Afonso, M. (2007). “Some aspects of the glyphosate adsorption on montmorillonite and its calcined form”. Appl. Clay Sci., V. 36, pp. 86-94.

Daneshvar, N., Aber, S., Khani, A., Khataee, A.R. (2007). “Study of imidaclopride removal from aqueous solution by adsorption onto granular activated carbon using an on-line spectrophotometric analysis system”. J. Hazard. Mat., V. 144 (1-2), pp. 47-51.

De Jonge, H., de Jonge, L.W. (1999). “Influence of pH and solution composition on the sorption of glyphosate and prochloraz to a sandy loam soil”. Chemosphere, V. 39 (5), pp. 753-763.

De Smedt, C., Ferre, F., Leus, K., Spanoghe, P. (2015). „Removal of pesticides from aqueous solutions by adsorption on zeolites as solid adsorbents”. Adsorp. Sc. And Tech., Vol. 33 (5), pp. 457-485.

De Wilde, T., Spanoghe, P., Ryckeboer, J., Jaeken, P. and Springael, D. (2009). “Sorption characteristics of pesticides on matrix substrates used in biopurification systems”. Chemosphere, V. 75 (1), pp. 100-108.

Degrève, L., da Silva, F.L. (2000). “Detailed microscopic study of 1 M aqueous NaCl solution by computer simulations”. Journal of Molecular Liquids, V. 87 (2-3), pp. 217-232.

Derylo-Marczewska, A., Blachnio, M., Marczewski, A.W., Swiatowski, A., Tarasiuk, B. (2010). “Adsorption of selected herbicides from aqueous solutions on activated carbon”. J. Therm. Anal. Calorim., V. 101, pp. 785-794.

Dideriksen, K., Stipp, S.L.S. (2003). „The adsorption of glyphosate and phosphate to goethite: a molecular-scale atomic force microscopy study”. Geoc. et Cosm. Acta, V. 67 (18), pp. 3313-3327.

Dousset, S., Jacobson, A. R., Dessogne, J.-B., Guichard, N., Baveye, P. C., Andreux, F. (2007). “Facilitated Transport of Diuron and Glyphosate in High Copper Vineyard Soils”. Environmental Science & Technology, V. 41 (23), pp. 8056-8061.

Dytrtova, J.J., Jakl, M., Schröder, D., Cadkova, E., Komarek, M. (2011). “Complexation between the fungicide tebuconazole and copper(II) probed by electrospray ionization mass spectrometry”. Rapid Commun. Mass Spectrom., V. 25, pp. 1037-1042.

Eikenberg, J. (1990). “On the problem of silica solubility at high pH”. Paul-Scherrer-Institut, PSI-Bericht #74.

Eisenreich, S.J., Looney, B.B., Thornton, J.D. (1981). “Airborne organic contaminants in the Great Lakes ecosystems”. Environ Sci. Technol., V. 15, pp. 30-38.

Elbert, A., Haas, M., Springer, B., Thielert, W., Nauen, R. (2008). “Applied aspects of neonicotinoid uses in crop protection”. Pest. Manag. Sci., V. 64, pp. 1099–1105.

Entscheidung 2006/797/EG der Kommission vom 22. November 2006 über die Nichtaufnahme von Ammoniumsulfamat, Hexaconazol, Natriumtetrathiocarbonat und 8-Hydroxyquinolin in Anhang I der Richtlinie 91/414/EWG des Rates und den Widerruf der Zulassungen für Pflanzenschutzmittel mit diesen Wirkstoffen, Amtsblatt der Europäischen Union, V. 324, pp. 8-10.

Environmental Protection Agency. Reregistration Eligibility Decision: Propiconazole. (July 2006), accessed 2 November 2018, <http://www.epa.gov/oppsrrd1/REDs/propiconazole_red.pdf>

Erdem, S., Erdem, B., Öksüzoglu, R.M., Cital, A. (2015). „Effect of calcination temperature on the structural and magnetic properties of Ni/SBA-15 nanocomposite". J. Por. Mat., V. 22 (3), pp. 689-698.

EU Regulatory & Evaluation Data as published by EC, EFSA (DAR & Conclusion dossiers), EMA / EU Annex III PIC DGD / EU MRL Database, accessed 2 November 2018, <https://www.efsa.europa.eu/en/publications>

Evans, P. D., Schmalzl, K. J., Forsyth, G. M., Fallon, G. D., Schmid, S., Bendixen, B., Heimdal, S. (2010) "Formation and Structure of Metal Complexes with the Fungicides Tebuconazole and Propiconazole", J. Wood Chem. Technol., V. 27 (3-4), pp. 243-256.

Everman, W. (2008). "Influence of Environmental and Physiological factors on Glufosinate and Glyphosate Weed Management". PhD thesis, North Carolina State University, Raleigh.

Everman, W.J., Mayhew, C.R., Burton, J.D. York, A.C., Wilcut, J.W. (2009). C-glufosinate in glufosinate-resistant corn, goose grass (Eleusine indica), large crabgrass (Digitaria sanguinalis), and sicklepod (Senna obtusifolia). Weed Science, V. 57, pp. 1–5.

Ewing, H.P., Pesti, G.M., Bakalli, R.I., Menten, J.F. (1998). "Studies on the feeding of cupric sulfate pentahydrate, cupric citrate, and copper oxychloride to broiler chickens". Poult. Sci., V. 77 (3), pp. 445-448. "Farm Chemicals Handbook" (1997). Meister Publishing Co., Willoughby, Ohio.

"Farm Chemicals Handbook" (2002). Meister Publishing Co., Willoughby, OH., p. C 214.

Federal Register, n.d. (1995). "Imidacloprid; Pesticide Tolerances", V. 60 (128), pp. 34943-24945.

Feltham, H., Park, K., Goulson, D. (2014). "Field realistic doses of pesticide imidacloprid reduce bumblebee pollen foraging efficiency". Ecotox., V. 23, pp. 317–323.

Fernández De La Mora, J. (2007). "The Fluid Dynamics of Taylor Cones". Ann. Rev. Fluid Mech., V. 39, pp. 217–243.

Fernandez-Bayo, J.D., Nogales, R., Romero, E. (2007). "Improved retention of imidacloprid (Confidor((R))) in soils by adding vermicompost from spent grape marc". S. Tot. Environ., V. 378 (1-2), pp. 95-100.

Fest, C., Schmidt, K.-J. (1982). "Organophosphorus pesticides". Springer-Verlag. Berlin.

Fetter, C.W. (2001). "Applied hydrogeology". 4-th edition. Waveland Press, Inc., Illinois.

Finden, D.A.S. (1984). "Light-induced reduction of natural iron (III) oxide and its relevance to phytoplankton". Nature, V. 309, pp. 783-784.

Fjallborg, B., Dave, G. (2003). "Toxicity of copper in sewage sludge". Environ. Intern., V. 28 (8), pp. 761-769.

Fogel, M.N., Schneider, M.I., Desneux, N., González, B., Ronco, A.E. (2013). "Impact of the neonicotinoid acetamiprid on immature stages of the predator Eriopis connexa (Coleoptera: Coccinellidae)". Ecotox., V. 22, pp. 1063–1071.

Franz, J.E. (1974). "N-phosphonomethyl-glycine phytotoxicant compositions", issued 1974-03-26, assigned to Monsanto Company, US Grant US3799758A.

Franz, J.E., Mao, M.K. and Sikorski, J.A. (1997). "Glyphosate: A Unique Global Herbicide; Am. Chem. Soc., Washington, DC, Chapter 4, pp. 65-97.

Freuze, I., Jadas-Hecart, A., Royer, A., Communal, P.Y. (2007). “Influence of complexation phenomena with multivalent cations on the analysis of glyphosate and aminomethylphosphonic acid in water”. J. Chromatogr. A, V. 1175 (2), pp. 197-206.

Früh, E. (in preparation). “Fungicide, nanoparticles, and their combined effect on ectomycorrhizal fungi as non-target organisms”, Doctoral thesis, University of Tübingen.

Galli, E., Quartieri, S., Vezzalini, G. and Alberti, A. (1995). “Boggsite and tschernichite-type zeolites from Mt. Adamson, Northern Victoria Land (Antarctica)”. Eur. J. Mineral., V. 7, pp. 1029-1032.

Goodwin, L., Startin, J.R., Keely, B.J., Goodall, D.M. (2003). “Analysis of glyphosate and glufosinate by capillary electrophoresis - mass spectrometry utilizing a sheathless microelectrospray interface”. Journal of Chromatography, V. A 1004, pp. 107 – 119.

Ganiyu, S., Bispo, C., Bion, N., Ferreira, P., Batonneau-Gener, I. (2014). “Periodic mesoporous organo-silicas as adsorbents for the organic pollutants removal in aqueous phase”. Micropor. Mesopor. Mat., V. 200, pp. 117-123.

Gao, J., Powers, K., Wang, Y., Zhou, H., Roberts, S.M., Moudgil, B.M., Koopman, B., Barber., D.S (2012). “Influence of Suwannee River humic acid on particle properties and toxicity of silver nanoparticles”. Chemosphere, V. 89 (1), pp. 96-101.

Garbarini, D.R., Lion, L.W. (1986). “Influence of the nature of soil organics on the sorption of toluene and trichloroethylene”. Environ. Sci. Technol, V. 20 (12), pp. 1263-1269.

Garrison, A.W., Avants, J.K., Miller, R.D. (2011). “Loss of propiconazole and its four stereoisomers from the water phase of two soil-water slurries as measured by capillary electrophoresis”. J. Environ. Res. Public Health., V. 8 (8), pp. 3453-3467.

Gimsing, A. L. & Borggaard, O. K. (2010) “Effect of Phosphate on the Adsorption of Glyphosate on Soils, Clay Minerals and Oxides”. International Journal of Environmental Analytical Chemistry, V. 82 (8-9), pp. 545-552.

Gimsing, A. L., Borggaard, O. K. (2001). “Effect of KCl and $CaCl_2$ as background electrolytes on the competitive adsorption of glyphosate and phosphate on goethite”. Clays and Clay Miner., V. 49 (3), pp. 270-275.

Gimsing, A. L., Borggaard, O. K., Bang, M. (2004). “Influence of soil composition on adsorption of glyphosate and phosphate by contrasting Danish surface soils”. Eur. J. Soil Sci., V. 55 (1), pp. 183-191.
Gimsing, A. L., Szilas, C., Borggaard, O. K. (2007). “Sorption of glyphosate and phosphate by variable-charge tropical soils from Tanzania”. Geoderma, V. 138 (1-2), pp. 127-132.

Gioia, R., Dachs, J., Nizzetto, L., Berrojalbiz, N., Galban-Malagon, C., Del Vento, S., Mejanelle., L., Jones, K.C. (2011). „Sources, transport and fate of organic pollutants in the oceanic environment”. In book: “Persistent pollution – past, present and future”, Chapter 8, Springer Verlag, Berlin, Heidlberg.

Glass, R.L. (1984). “Metal complex formation by glyphosate”. J. Agric. Food Chem., V. 32 (6), pp.1249-1253.

Glass, R.L. (1987). “Adsorption of glyphosate by soils and clay minerals”. J. Agric. Food Chem., V. 35 (4), pp. 497-500.

Gonzalez, J.M., Ukrainczyk, L. (1996). "Adsorption and desorption of nicosulfuron in soils". J. Environ. Qual., V. 25, pp. 1186-1192.

Gonzalez-Pradas, E., Villafranca-Sanchez, M., Socias-Viciana, M., Fernandez-Perez, M., Urena-Amate, M.D. (1999). “Preliminary studies in removing atrazine, isoproturone and imidacloprid from water by natural sepiolite”. J. Chem. Technol. Biotechnol., V. 74, pp. 417-422.

Gorth, D.J., Rand, D.M., Webster, T.J. (2011). “Silver nanoparticle toxicity in Drosophila: size does matter”. Int. J. Nanomed., V. 6, pp. 343-350.

Goulson, D., Kleijn, D. (2013). “REVIEW: an overview of the environmental risks posed by neonicotinoid insecticides.” J. Appl. Ecol., V. 50, pp. 977-987.

Grathwohl, P., Reinhard, M. (1993). “Desorption of trichloroethylene in aquifer material: rate limitation at the grain scale”. Environ. Sci. Technol., V. 27 (11), pp. 2360-2366

Grim, R. E. (1968). “Clay Mineralogy”. McGraw-Hill Book Company, New York, 2-nd edition.

Grünhage, V.M. (2017). “Glyphosatsorption an Al_2O_3-Nanopartikeln und weiteren Mineralien“. Bachelor thesis, University of Tübingen.

Guisnet, M., Gilson, J.-P. (2002) Zeolites for Cleaner Technologies. Imperial College Press, London.

Güldenhaupt, J. (2010). “ATR-FTIR-spektroskopische Untersuchungen von membrangebundenem Ras“, Doctoral thesis., University of Bochum.

Guzman, K.A.D.; Finnegan, M.P.; Banfield, J.F. (2006). “Influence of surface potential on aggregation and transport of titania nanoparticles”. Environ. Sci Tech., V. 40, pp. 7688-7693.

Haderlein, S.B. (1992). “Die Bedeutung mineralischer Oberflächen für die Mobilität von substituierten Nitrophenolen und Nitrobenzolen in Böden und Grundwasser“. Diss ETH #9744.

Hance, R.J. (1976). “Adsorption of glyphosate by soils”. Pest. Man. Science. V. 7 (4), pp. 363-366.
Hanns, B., Gottfried, K. (1968). "Process for producing silica in the form of hollow spheres". US Patent, Appl. No. US 342525, Publication No. US 3383172.

Hazardous Substances Databank (HSDB), Imidacloprid; U.S. Department of Health and Human Services, National Institutes of Health, National Library of Medicine accessed 6 November 2018, <http://wayback.archiveit.org/org350/20180125173245/https://toxnet.nlm.nih.gov/newtoxnet/hsdb.htm.>

Health Canada (2017). “Re-evaluation Decision RVD2017-01, Glyphosate”.

Hefter, G.T., Tomkins, R.P.T. (2003). “The experimental determination of solubilities”. John Wiley & Sons, Ltd, Chichester, West Sussex.
High Performance Capillary Electrophoresis (2017). Agilent Technologies manual, Germany.

Hilderbrand, R.L., Henderson, T.O. (1983). “Phosphonic acids in nature. In The role of phosphonates in living systems”. C.R.C. Press. Inc. Boca Raton, Florida.

Hillier, S. (2003). “Clay Mineralogy, Encyclopedia of sediments and sedimentary rocks”. Kluwer Acad. Publishers, Dordrecht.

Hua, Y., Flood, A.H. (2010). “Click chemistry generates privileged CH hydrogen-bonding triazoles: the latest addition to anion supramolecular chemistry”. Chem. Soc. Rev., V. 39, pp.1262–1271.

Huq, R., Mercier, L., Kooyman, P.J. (2001). “Incorporation of cyclodextrin into mesostructured silica”. Chem. Mat., V. 13 (12), pp. 4512-4519.

IARC-Presseerklärung vom 20. März 2015. “IARC Monographs Volume 112: evaluation of five organophosphate insecticides and herbicides”.

Inagaki, S., Guan, S., Fukushima, Y., Ohsuna, T., Terasaki, O. (1999). “Novel mesoporous materials with a uniform distribution of organic groups and inorganic oxide in their frameworks”. J. Amer. Chem. Soc., V. 121 (41), pp. 9611-9614.

Inyang, M., Dickenson, E. (2015). “The potential role of biochar in the removal of organic and microbial contaminants from potable and reuse water: a review.” Chemosphere, V. 134, pp. 232-240.

Ispas, C., Andreescu, D., Patel, A., Goia, D.V., Andreescu, S., Wallace, K.N. (2009). “Toxicity and developmental defects of different sizes and shape nickel nanoparticles in zebrafish”. Environ. Sci. Technol., V. 43, pp. 6349-6356.

Iwasa, T., Motoyama, N., Ambrose, J.T., Michael Roe, R. (2004). “Mechanism for the differential toxicity of neonicotinoid insecticides in the honey bee Apis mellifera”. Crop Prot., V. 23, pp. 371–378.

Janusz, W., J. Patkowski und S. Chibowski (2003). „Competitive adsorption of Ca(II) and Zn (II) ions at monodispersed SiO2/electrolyte solution interface“. J. Colloid Interface Sci., V. 266, pp. 259–268.

Jeong, C.Y., Selim, M. (2010). “Modeling adsorption-desorption kinetics of imidacloprid in soils”. Soil Sci., V. 175 (5), pp. 214-222.

Jeschke, P., Koichi, M. (2007). “Five-membered compounds - imidacloprid and thiacloprid”. Mod. Crop Prot. Compd., Wiley-VCH, Weinheim, 1-st edition, pp. 981–994.

Jeschke, P., Nauen, R., Beck, M.E. (2013). “Nicotinic acetylcholine receptor agonists: a milestone for modern crop protection”. Angew. Chem. Int. Ed. Engl., V. 52 (36), pp. 9464-9485.

Jeschke, P., Nauen, R., Schindler, M., Elbert, A. (2011). “Overview of the status and global strategy for neonicotinoids”. J Agric. Food Chem., V. 59, pp. 2897–2908.

Jeschke, P; Nauen, R. (2008). “Neonicotinoids-from zero to hero in insecticide chemistry”. Pest. Man. Sci., V. 64, pp. 1084–1098.

Jewell, T. and Buffin, D. (2001). “Health and environmental impacts of glufosinate ammonium. Pesticide action network UK. Report” Prepared for Friends of the Earth UK. Pesticide Action Network UK, London, GB.

Johansson, E.M. (2010). “Controlling the pore-size and morphology of mesoporous silica”. Doctoral thesis, Linköping University.

Johnson, K. S., & Pytkowicz, R. M. (1979). “Ion association of chloride and sulphate with sodium, potassium, magnesium and calcium in seawater at 25°C”. Marine Chemistry, V. 8, pp. 87-93.

Johnston, C.T., De Oliveira, M.F., Teppen, B.J., Sheng, G., Boyd, S.A. (2001). “Spectroscopic study of nitroaromatic-smectite sorption mechanisms”. Environ. Sci. Technol., V.35, pp. 4767-4772.

Jonsson, C. (2007). “Modeling of glyphosate and metal-glyphosate speciation in solution and at solution-mineral interfaces”. Doctoral thesis, Umea University.

Jonsson, C.M., Persson, P., Sjöberg, S., Loring, J.S. (2008). “Adsorption of glyphosate on goethite (α-FeOOH): Surface complexation modeling combining spectroscopic and adsorption data”. Environ. Sci. Technol. V. 42 (7), pp. 2464-2469.

Jönsson, J., Camm, R., Hall, T. (2013). “Removal and degradation of glyphosate in water treatment: A review”. J. Wat. Sup: Res. And Tech. – Aqua, V. 62 (7), pp. 395-408.

Jorgenson, J.W.; Lukacs, K.D. (1981). “Zone electrophoresis in open-tubular glass capillaries”. Anal. Chem., V. 53, pp. 1298–1302.

Juricek, M., Kouwer, P.H.I., Rowan, A.E. (2011). “Triazole: a unique building block for the construction of functional materials.” Chem. Commun., V. 47, pp. 8740-8749.

Kagabu, K., Azuma, A., Nishimura, K. (2002). “Insecticidal and neuroblocking activities of thiacloprid and its acyclic analogues and their related cyanoguanidine derivatives”. J. Pestic. Sci., V. 27, pp. 267–271.

Kahle, M., Buerge, I.J., Hauser, A., Muller, M.D., Poiger, T. (2008). “Azole fungicides: Occurrence and fate in wastewater and surface waters”. Environ. Sci. Technol., V. 42, pp. 7193–7200.

Kamrin, M. A. (1997). **“**Pesticide Profiles: Toxicity, Environmental Impact, and Fate”, CRC Press, Boca Raton, Florida.

Kandil, M.M., El-Aswad, A.F., Koskinen, W.C. (2015). “Sorption-desorption of imidacloprid onto a lacustrine Egyptian soil and its clay and humic acid fractions”. J. Environ. Sci. Health. B., V. 50 (7), pp. 473-483.

Karcher, S.J. (1995). “2-Recombinant DNA cloning”. Molec. Biol., A Proj. Appr., pp. 45-134.

Karickhoff, S.W. (1981). “Semi-empirical estimation of sorption of hydrophobic pollutants on natural sediments and soils”. Chemosphere, V. 10, pp. 833-846.

Karickhoff, S.W. (1984). “Organic pollutant sorption in aquatic systems”. J. Hydraulic Eng., V. 110, pp. 707-735.

Karickhoff, S.W., Brown, D.S., Scott, T.A. (1979). “Sorption of hydrophobic pollutants on natural sediments”. Water Res., V. 13 (3), pp. 241-273.

Karickhoff, S.W., Morris, K.R. (1985). “Sorption dynamics of hydrophobic pollutants in sediment suspensions”. Environ. Tox. Chem., V. 4, pp. 469-479.

Kidd, H., James, D. (1994). “Agrochemicals Handbook”. Royal Society of Chemistry, Cambridge, England, 3-rd edition.

Kim, I.S., Beaudette, L.A., Shim, J.H., Trevors, J.T., Suh, Y.T. (2002). “Environmental fate of the triazole fungicide propiconazole in a rice-paddy-soil lysimeter.” Plant Soil, V. 239, pp. 321-331.

Klucakova, M. (2018). “Size and charge evaluation of standard humic and fulvic acids as crucial factors to determine their environmental behavior and impact”. Front Chem., V. 6, pp. 235-241.

Knight, A.W., Tigges, A.B., Ijgren, A.G. (2018). “Adsorption of copper(II) on mesoporous silica: the effect of nano-scale confinement”. Geochem. Trans., V. 19, pp. 1-13.

Kollmeyer, W.D.; Flattum, R.F.; Foster, J.P.; Powell, J.E.; Schroeder, M.E.; Soloway, S.B. (1999). "Discovery of the nitromethylene heterocycle insecticides". In Yamamoto, I., Casida, J.E. “Nicotinoid Insecticides and the Nicotinic Acetylcholine Receptor”. Springer-Verlag., Tokyo. pp. 71–89.

Konwick, B. J., Garrison, A. W., Avants, J. K., Fisk, A. T. (2006). “Bioaccumulation and biotransformation of chiral triazole fungicides in rainbow trout (Oncorhynchus mykiss)”. Aquatic Toxicol., V. 80 (4), pp. 372-381.

Kostic, I., Andelkovic, T., Nikolic, R., Bojic, A., Purenovic, M., Blagojevic, S., Andelkovic, D. (2011). “Copper(II) and lead(II) complexation by humic acid and humic-like ligands”. J. Serb. Chem. Soc., V. 76 (9), pp. 1325-1336.

Kottke, I., M. Guttenberger, R. Hampp and F. Oberwinkler (1987). "An in vitro method for establishing mycorrhizae on coniferous tree seedlings." Trees-Struct. Function, V. 1 (3), pp. 191-194.

Kreuger, J. (1998). “Pesticides in stream water within an agricultural catchment in southern Sweden, 1990–1996”. Sci. Total Environ., V. 216, pp. 227–251.

Kronvang, B., Laubel, A., Larsen, S.E., Friberg, N. (2003). “Pesticides and heavy metals in Danish streambed sediment”. Hydrobiologia, V. 494, pp. 93–101.

Kummer, N.-A. (2003). “Zeolith-gestürzte Katalysatoren zur Hydrodehalogenierung und Hydrierung von Schadstoffen im Grundwasser“, Forschungsvorhaben Safira.

Laitinen, P., Siimes, K., Eronen, L., Rämö, S., Welling, L., Oinonen, S., Mattsoff, L. and Ruohonen-Lehto, M. (2006). “Fate of the herbicides glyphosate, glufosinate-ammonium, phenmedipham, ethofumesate and metamitron two Finnish arable soils”. Pest Manag. Sci., V. 62, pp. 473–491.

Laitinen, P., Siimes, K., Rämö, S., Jauhiainen, L., Eronen, L., Oinonen, S., Hartikainen, H. (2008). “Effects of soil phosphorus status on environmental risk assessment of glyphosate and glufosinate-ammonium”. J. Environ. Qual. V. 37 (3), pp. 830-838.

Le Page, M., Beau, R., Duchene, J. (1970). "Porous silica particles containing a crystallized phase and method". US Patent, Application No. US 3493341D, Publication No. US 3493341.

Lee, J.-Y., Chen, C.-H., Cheng, S., Li, H.-Y. (2015). “Adsorption of Pb(II) and Cu(II) metal ions on functionalized large-pore silica”. Int. J. Environ. Sci. Technol., V. 13, pp. 65-76.

Lehman, S.E., Larsen, S.C. (2014). “Zeolite and mesoporous silica nanomaterials: greener syntheses, environmental applications and biological toxicity”. Environ. Sci.: Nano, V. 1, pp. 200–213.

Lepesheva, G.I., Virus,C. and Waterman, M.R. (2003). “Conservation in the CYP51 family. Role of the B' helix/BC loop and helices F and G in enzymatic function”. Biochem., V. 42, pp. 9091-9101.

Lewis, R.J. (2007). “Hawley's Condensed Chemical Dictionary”. John Wiley & Sons, Inc. New York, 15-th edition.

Li, H., Sheng, G., Teppen, B.J., Johnston, C.T., Boyd, S.A. (2003) "Sorption and desorption of pesticides by clay minerals and humic acid-clay complexes". Soil Sci. Soc. Am J., V. 67, pp. 122-131.

Li, H., Teppen, B.J., Johnston, C.T., Boyd, S.A. (2004) "Thermodynamics of nitroaromatic compound desorption from water by smectite clay". Environ. Sci. Technol., V. 38 (20), pp. 5433-5442.

Li, Q., Liu, B., Mu, W., Yu, Q., Tian, Y., Liu, G., Yang, Y., Li, X., Luo, S. (2018). “Protonation states of glufosinate in aqueous solution”. J. Solut. Chem., V. 47, pp. 705-714.

Li, Y., Flood, A.H. (2008). “Pure C-H hydrogen bonding to chloride ions: a preorganized and rigid macrocyclic receptor”. Angew. Chem., V. 47 (14), pp. 2649-2652.

Li, Y., Flood, A.H. (2008). “Strong, size-selective, and electronically tunable C-H---halide binding with steric control over aggregation from synthetically modular, shape-persistent [3,4]triazolophanes”. J. Am. Chem. Soc., V. 130 (136), pp. 12111–12122.

Hua, Y., Flood, A.H. (2010). “Click chemistry generates privileged CH hydrogen-bonding triazoles: the latest addition to anion supramolecular chemistry”. Chem. Soc. Rev., V. 39, pp. 1262–1271.

Li, Y., Huffman, J. C., Flood, A.H. (2007). “Can terdentate 2,6-bis(1,2,3-triazol-4-yl)pyridines for m stable coordination compounds?”. Chem. Commun., V. 26., pp. 2692–2694.

Li, Y., Yu, S., Wu, Q., Tang, M., Pu, Y., Wang, D. (2011). “Chronic Al_2O_3-nanoparticle exposure causes neurotoxic effects on locomotion behaviours by inducing severe ROS production and disruption of ROS defence mechanisms in nematode Caenorhabditis elegans”. J. Hazard. Mat., V. 219, pp. 221-230.

Liang, Y., Meixner, M. (2017). Organoidium-modified monodisperse ellipsoid-/platelet-like periodic mesoporous silicas”. Dalton Transact., V. 46 (23), pp. 7495-7505.

Libau, F. (1985). “Structural Chemistry of Silicates”. Springer-Verlag, Berlin.

Lindemann, S., Simgen, H. (2014). “Krypton assay in xenon at the ppq level using a gas chromatographic system and mass spectrometer”. Eur. Phys. J., V. 74., pp. 2746-2753.

Liu, Q., Barron, V., Torrent, J., Qun, H., Yu, Y. (2010). “The magnetism of micro-sized hematite explained”. Phys. Earth Planet. Inter., V. 183, pp. 387-397.

Liu, W., Zheng, W., Gan, J. (2002). “Competitive sorption between imidacloprid and imidacloprid-urea on soil clay minerals and humic acids”. J. Agric. Food Chem, V. 50, pp. 6823-6827.

Liu, W., Zheng, W., Ma, Y., Liu, K.K. (2006). “Sorption and degradation of imidacloprid in soil and water”. J. Environ. Sci. Health B., V. 41 (5), pp. 623-634.

Lorenz, C.S., Wicht, A.-J., Guluzada, L., Crone, B., Karst, U., Lee, H.J., Triebskorn, R., Haderlein, S.B., Huhn, C., Köhler, H.-R. (2017.b). “Nano-sized zeolites as modulators of thiacloprid toxicity on Chironomus riparius”. PeerJ, V. 5 (7):e3525.

Lorenz, C.S., Wicht, A.-J., Guluzada, L., Luo, L., Jäger, L., Crone, B., Karst, U., Triebskorn, R., Anwander, R., Haderlein, S., Huhn, C., Köhler, H.-R. (2017a). “Nano-sized Al_2O_3 reduces acute toxic effects of thiacloprid on the non-biting midge Chironomus riparius”. PLoS ONE, V. 12 (5), pp. 1-13.

Lowe, J.B., Baker, R.T. (2014). “Deformation of ordered mesoporous silica structures on exposure to high temperatures”. J. Nanomat., V. 2014, pp. 1-13.

Löwenstein, W. (1954). “The distribution of aluminium in the tetrahedra of silicates and aluminates”. Am. Mineral., V. 39, pp. 92-98.

Lund-HØie, K., Friestad, H.O. (1986). “Photodegradation of the herbicide glyphosate in water”. Bull. Env. Cont. Toxic., V. 36 (1), pp. 723-729.

Luo, L. (2018). “Monodisperse mesoporous silica nanoparticles: preparation, characterization and application”. Doctoral thesis, University of Tübingen.

Lv, X.M., Li, J., Chen, H., Tang, H.J. (2018). “Copper wastewater treatment with high concentration in a two-stage crystallization-based combined process”. Environ. Technol., V. 39 (18), pp. 2346-2352.

Madsen, H.E.L., Christensen, H.H., Gottlieb-Petersen, C. (1978). „Stability constants of copper (II), zinc, manganese (II), calcium and magnesium complexes of N-(phosphonomethyl)glycine (glyphosate)”. Acta Chem Scand., V. 32, pp. 79-83.

Maini, S., Medrzycki, P., Porrini, C. (2010). “The puzzle of honey bee losses: a brief review”. Bull. Insectol., V. 63, pp. 153–160.

Mallawatantri A.P., Mulla, D.J. (1992). "Herbicide adsorption and organic carbon contents on adjacent low-input versus conventional farms". J. Environ. Qual., V. 21, pp. 546-551.

Mamy, L., Barriuso, E., Gabrielle, B. (2005). “Environmental fate of herbicides trifluralin, metazachlor, metamitron and sulcotrione compared with that of glyphosate, a substitute broad spectrum herbicide for different glyphosate-resistant crops”. Pest Manag. Sci., V. 61 (9), pp. 905-916

Manassero, A., Passalia, C., Negro, A.C., Cassano, A.E., Zalazar, C.S. (2010). “Glyphosate degradation in water employing the H_2O_2/UVC process”. Wat. Res., V. 44 (13), pp. 3875-3882.

Mandal, A.B., Moulik, S.P. (1982). “Interaction of cetyltrimethylammonium bromide and sodium dodecyl-sulfate in electrolyte and nonelectrolyte environments”. In: Mittal, K.L., Fendler, E.J. (eds). “Solution behaviour of surfactants”. Springer, Boston, MA.

Manukaju, J.U. (2013). “Industrial potential of some clay deposits in Kogi State North Central Nigeria”. Am. J. Eng. Res., V. 2, pp. 33-38.

Maqueda, C., Morillo, E., Undabeytia, T. (2002). “Cosorption of glyphosate and copper(II) on goethite”. J. Soil Sci., V. 167 (10), pp. 659-665.

Marrs, C.T., Ballantyne, B. (2004). “Pesticide toxicology and international regulation”. John Wiley&Sons, London.

Martell, A.E., Motekaitis, R.J. (1988). “The determination and use of stability constants”. VCH Publishers, New York, 216 pages.

Martinson, K.B., Sothern, R.B., Koukkari, W.L., Durgan, B.R., Gunsolus, J.L. (2002). “Circadian response of annual weeds to glyphosate and glufosinate”. Chronobiol. Intern., V. 19, pp. 405–422.

Marx, D. H. (1969). "The influence of ectotrophic mycorrhizal fungi on the resistance of pine roots to pathogenic infections. I. Antagonism of mycorrhizal fungi to root pathogenic fungi and soil bacteria." Phytopathol., V. 59, pp. 153-163.

Masters, A.F., Maschmeyer, T. (2011). “Zeolites – From curiosity to cornerstone”. Micropor. Mesopor. Mat., V. 142, pp. 423-438.

Matsumoto, T. (2013). “Short- and long-term effects of neonicotinoid application in rice fields, on the mortality and colony collapse of honeybees (Apis mellifera)”. J. Apic. Sci., V. 57, pp.21–35

Mattos, R., Khan, S., Hussain, S., Simoni, J.D. (2017). “Quantitation and adsorption of glyphosate using various treated clay”. J. of Research in Phys. Chem. & Chem. Physics, V. 231 (11-12), pp. 1815-1829.

McBride, M., Kung, K.-H. (1989). “Complexation of glyphosate and related ligands with iron (III)”. J. Soil Sci. Soc. Amer., V. 53, pp. 1668-1673.

McBride, M.B. (1991). “Electron spin resonance study of copper ion complexation by glyphosate and related ligands”. J. Soil Sci. Soc. Am., V. 55, pp. 979–985.

McLean, K.J., Marshall, K.R., Richmond, A., Hunter, I.S., Fowler, K., Kieser, T., Gurcha, S.S., Besra, G.S., Munro, A.W. (2002). “Azole antifungals are potent inhibitors of cytochrome P450 mono-oxygenases and bacterial growth in mycobacteria and streptomycetes”. Microbiol., V. 148, pp. 2937-2949.

Melde, B.J., Holland, B.T., Blanford, C.F., Stein, A. (1999). “Mesoporous sieves with unified hybrid inorganic/organic framework”. Chem. Mater., V. 11, pp. 3302-3308.

Miles, C.J., Moye, H.A. (1988). “Extraction of glyphosate herbicide from soil and clay minerals and determination of residues in soils”. J. Agric. Food Chem., V. 36, pp. 486-491.

Mogusu, E.O., Wolbert, J.B., Kujawinski, D.M., Jochmann, M.A., Elsner, M. (2015). “Dual element ((15)N/(14)N, (13)C/(12)C) isotope analysis of glyphosate and AMPA by derivatization-gas chromatography isotope ratio mass spectrometry (GC/IRMS) combined with LC/IRMS”. Anal. Bioanal. Vhem., V. 407 (18), pp. 5249-5260.

Moore, R.T. (1980). "Taxonomic proposals for the classification of marine yeasts and other yeast-like fungi including the smuts". J. Bot. Mar., V. 23 (6), pp. 361-373.

Morillo, E., Maqueda, C., Bejarano, M., Madrid, L., Undabeytia, T. (1994). “Cu(II)-glyphosate system: A study by anodic stripping voltammetry and the influence on Cu adsorption by montmorillonite”. Chemisphere, V. 28 (12), pp. 2185-2196.

Morillo, E., Perez-Rodriguez, J.L., Maqueda, C. (1991). “Mechanisms of interaction between montmorillonite and 3-aminotriazole”. Clay minerals, V. 26, pp. 269-279.

Morillo, E., Undabeytia, T., Maqueda, C. (1997). “Adsorption of glyphosate on the clay mineral montmorillonite: effect of Cu(II) in solution and adsorbed on the mineral”. Env. Sci. Tech., V. 31, pp. 3588–3592.

Morillo, E.; Undabeytia, T.; Maqueda, C.; Ramos A. (2000). “Glyphosate adsorption on soils of different characteristics. Influence of copper addition”. Chemosphere, V. 40, pp. 103-107.

Motekaitis, R.J., Martell, A.E. (1985). “Metal chelate formation by N-phosphonomethylglycine and related ligands”. J. Coord. Chem., V. 14 (2), pp. 139-149.

Mozgawa, W., Krol, M., Barczyk, K. (2011). “FTIR studies of zeolites from different structural groups”. CHEMIK, V. 65 (7), pp. 667-674.

Muhamad, H., Zainol, M., Sahid, I., Abu Seman, I. (2012). “Determination of hexaconazole in field samples of an oil palm plantation”. Drug Test. Anal., V. 4 (1), pp. 112-117.

Mui, J., Ngo, J., Kim, B. (2016). “Aggregation and colloidal stability of commercially available Al_2O_3 nanoparticles in aqueous environments”. Nanomat., V. 6 (5), pp. 90-115.

Munira, S., Farenhorst, A. (2017). “Sorption and desorption of glyphosate, MCPA and tetracycline and their mixtures in soil as influenced by phosphate”. J. Env. Sci. Health B., V. 52 (12), pp. 887-895.

Muszynski, P., Brodowska, M.S. (2014) "Effects of potassium, ammonium and calcium chlorides on the sorption of metamitron in soil". Pol. J. Environ. Stud. V. 23 (6), pp. 2125-2135.

Nandanwar, R., Singh, P., Haque, F.Z. (2013) "Synthesis and Properties of Silica Nanoparticles by Sol-gel Method for the Application in Green Chemistry". Mater. Sci. Res. India, pp. 85-92.

Nauen, R., Ebbinghaus-Kintscher, U., Elbert, S., Jeschke, P., Tietjen, K. (2001). „Acetylcholine receptors as sites for developing neonicotinoid insecticides". Biochem. Sites Insect., Action Resist., 1st ed., Springer-Verlag, Berlin, Heidelberg, New York: pp. 77–106.

Ng, N.-T., Kamaruddin, A.F., Ibrahim, W.A.W., Sanagi, M.M., Keyon, A.S.A. (2017). "Advances in organic-inorganic hybrid sorbents for the extraction of organic and inorganic pollutants in different types of food and environmental samples". J. Separ. Sci., V. 41 (1), pp. 195-208.

Nguyen, T.H., Goss, K.U., Ball, W.P. (2005). "Polyparameter linear free energy relationship for estimating the equilibrium partition of organic compound between water and the natural organic matter in soils and sediments". Environ. Sci. Technol., V. 39 (4), pp. 913-924.

Nibori, Y., Kunita, M., Tochiyama, O., Chida, T. (2000). "Dissolution rates of amorphous silica in highly alkaline solution". J. Nucl. Sci. Technol., V. 37 (4), pp. 349-357.

Nomura, N.S., and Hilton, H.W. (1977). "The adsorption and degradation of glyphosate in five Hawaiian sugarcane soils". Weed Res., V. 17, pp. 113-121.

Northcott, K.A., Miyakawa, K., Oshima, S., Komatsu, Y., Perera, J.M., Stevens., G.W. (2010). "The adsorption of divalent metal cations on mesoporous silicate MCM-41". Chem. Engin. J., V. 157, pp. 25-28.
Nowack, B., Bucheli, T.D. (2007). "Occurrence, behavior and effects of nanoparticles in the environment". Environ. Pollut., V. 150, pp. 5-22.

Nowell, L.H., Capel, P.D., Dileanis, P.D. (1999). "Pesticides in stream sediment and aquatic biota: distribution, trends, and governing factors". Lewis Publishers, Florida, United States.

Obana, H., Okihashi, M., Akutsu, P., Kitagawa, Y., Hori, S. (2002). "Determination of acetamiprid, imidacloprid, and nitenpyram residues in vegetables and fruits by High-Performance Liquid Chromatography with Diode-Array Detection". J. Agric. Food Chem., V. 50 (16), pp. 4464-4467.

Oberdörster, G., Oberdörster, E., Oberdörster, J. (2005). „Nanotoxicology: an emerging discipline evolving from studies of ultrafine particles". Environ. Health Perspect., V. 113 (7), pp. 823-839.

Oberholster, P., Musee, N., Botha, A.-M., Chelule, P., Focke, W., Ashton, P. (2011). "Assessment of the effect of nanomaterials on sediment-dwelling invertebrate Chironomus tentans larvae". Ecotox. Environ. Safety, V. 74, pp. 416-423.

Obojska, A., Lejczak, B., (2003). "Utilisation of structurally diverse organophosphonates by Streptomycetes". Appl. Microbiol. Biotech., V. 62, pp. 557-563.

Ololade, I.A., Oladoja, N.A., Oloye, F.F., Alomaja, F., Akerele, D.D., Iwaye, J., Aikpokpodion, P. (2013). "Sorption of glyphosate on soil components: the roles of metal oxides and organic materials". J. Soil Sed. Contam.: An intern. J., V. 23 (5), pp. 571-585.

Oravec, J., Petrilakova, A., Zelenak, V., Balintova, M., Estokova, A. (2014). "Mesoporous silica for sorption of copper and sulphates from the environment". Pollack Periodica, V. 9 (3), pp. 43-49.

Orcelli, T., di Mauro, E., Urbano, A., Valezi, D.F., da Costa, A.C.S., Zaia, C.T.B.V., Zaia, D.A.M. (2018). "Study of interaction between glyphosate and goethite using several methodologies: an environmental perspective". Water, Air, Soil Pollut., V. 229, pp. 1-18.

Otero, R., Esquivel, D., Ulibarri, M.A., Jimenez-Sanchidrian, C., Romero-Salguero, F.J., Fernandez Rodriguez, J.M. (2013). "Adsorption of the herbicide S-Metolachlor on periodic mesoporous organosilicas". Chem. Eng. J., V. 228, pp. 205-213.

Paktunc, D., Dutrizac, J.E., Gertsmann, V. (2008). "Synthetic and phase transformations involving seorodite, ferric arsenate and arsenical ferrihydrite: implications for arsenic mobilita". Geochim. Cosmochim. Acta, V. 72, pp. 249-272.

Palma, G., Demanet, R., Jorquera, M., Mora, M.L., Briceno, G., Violante, A. (2015). "Effect of pH on sorption kinetic process of acidic herbicides in a volcanic soil". J. Soil Sci. and Plant Nutr., V. 15 (3), pp. 549-560.

Pariente, J.P., Sanchez-Sanchez, M. (2018). "Structure and reactivity of metals in zeolite materials". Springer Nature Switzerland, Cham, eBook.

Pauling, L. and Hendricks, S. (1925). "The structure of hematite and corundum". J. Am. Chem. Soc., V. 47, pp. 781 – 790.

Peña, A., Rodriguez-Liebana, J.A., Mingorance, M.D. (2011). "Persistence of two neonicotinoid insecticides in wastewater, and in aqueous solutions of surfactants and dissolved organic matter". Chemosphere, V. 84 (4), pp. 464-470.

Perez, G.L., Vera, M.S., Miranda, L.A. (2011). „Effects of herbicide glyphosate and glyphosate-based formulations on aquatic ecosystems". InTech open, Argentina, C. 16, pp. 343-368.

Pessagno, R.C., dos Santos Afonso, M., Sanchez, T.R.M (2005). „N-(phosphonomethyl)glycine interactions with soils". J. Arg. Chem. Soc., V. 93 (4/6), pp. 97-108.

Pessagno, R.C., Torres, S.R.M., dos Santos Afonso, M. (2008). "Glyphosate behaviour at soil and mineral-water interfaces". Env. Pollution, V. 153 (1), pp. 53-59.

Pesticide Properties Database n.d., (2013). University of Hertfordshire, accessed 2 November 2018, <https://sitem.herts.ac.uk/aeru/ppdb/en/>

Petersen, J.R., Mohammad, A.A. (2001). "Clinical and forensic applications of capillary electrophoresis". Humana Press Inc., Totowa, NJ.

Pham., A.L.-T., Sedlak, D.L., Doyle, F.M. (2012). "Dissolution of mesoporous silica supports in aquous solutions: implications for mesoporous silica-based water treatment processes". Appl. Catal. B., V. 126, pp. 258-264.

Piccolo, A., Celano, G. (1993). "Modification of infrared spectra of the herbicide glyphosate induced by pH variation". J. Environ. Sci. Health, V. B28 (4), pp. 447-457.

Ping, L., Zhang, C., Zhu, Y., Wu, M., Dai, F., Hu, X., Zhao, H., Li, Z. (2010) "Imidacloprid adsorption by soils treated with humic substances under different pH and temperature conditions". Afr. J. of Biotech., V. 9 (13), pp. 1935-1940.

Pisa, L., Amaral-Rogers, V., Belzunces, L.P., Bonmatin, J.-M., Downs, C., Goulson, D., Kreutzweiser, D.P., Krupke, C., Liess, M., McField, M., Noome, D.A., Settele, J., Simon-Delso, N., Stark, J.D., Van der Sluijs,

J.P., Van Dyck, H., Wiemers, M. (2014). “Effects of neonicotinoids and fipronil on non-target invertebrates”. Env. Sci. Pollut. Res., V. 22 (1), pp. 68-102.

Podust, L.M., Poulos, T.L. and Waterman, M.R. (2001). “Crystal structure of cytochrome P450 14alpha -sterol demethylase (CYP51) from Mycobacterium tuberculosis in complex with azole inhibitors”. Proc. Nat. Acad. Sci. US, V. A98, pp. 3068-3073.

Popat, A., Liu, J., Hu, Q., Kennedy, M., Peters, B., Lu, G. Q. M., Zhang, S. (2012). “Adsorption and release of biocides with mesoporous silica nanoparticles”. Nanoscale, V. 4 (3), pp. 970-975.

Pose-Juan, E., Paradelo-Parez, M., Rial-Otero, R., Simal-Gandara, J., Läpez-Periago, J.E. (2009). “Detachment of sprayed colloidal copper oxychloride-metalaxyl fungicides by a shallow water flow”. Pest. Manag. Sci., V. 65 (6), pp. 615.623.

Pozniak, B.P., Cole, R.B. (2007). "Current Measurements within the Electrospray Emitter". JASMS. V. 18 (4), pp. 737–748.

PPDB, n.d (2015). “Aminomethylphosphonic Acid”, accessed 2 November 2018, <https://sitem.herts.ac.uk/aeru/iupac/Reports/842.htm>

PPDB, n.d., pesticides database, accessed 27 May 2014 <http://sitem.herts.ac.uk/aeru/iupac/Reports/397.htm;http://sitem.herts.ac.uk/aeru/iupac/Reports/382.htm;http://sitem.herts.ac.uk/aeru/iupac/Reports/551.htm;http://sitem.herts.ac.uk/aeru/iupac/Reports/630.htmhttp://sitem.herts.ac.uk/aeru/iupac/Reports/373.htm>

Prakasam, H.E, Varghese, O.K., Paulose, M., Mor, G.K., Grimes; G.A. (2006). “Synthesis and photoelectrochemical properties of nanoporous iron(III) oxide by potentiostatic anodization”. Nanotech., V. 17 (17), pp. 4285-4285.

Pusino, A., Petretto, S., Gessa, C. (2003). “Sorption of primisulfuron on soil, and inorganic and organic soil solloids”. Europ. J. Soil. Sci., V. 55 (1), pp. 175-182.

Quintas, G., Armenta, S., Garrigues, S., de la Guardia, M. (2004). “Fourier transform infrared determination of imidacloprid in pesticide formulations”. J. Braz. Chem. Soc., V. 15 (2), pp. 307-312.

Rahman, M.A., Abu Hasan, Md., Rahim, A., Alam, A.M.S. (2010). “Characterization of humic acid from river bottom sediments of Burigonga: complexation studies of metals with humic acid”. Pakistan. J. Anal. Environ. Chem., V. 11 (1), pp. 42-52.

Rampazzo, N., Todorovic, G.R., Mentler, A. (2013). “Adsorption of glyphosate and AMPA in agricultural soils”. Int. J. Env. Quality, V. 10, pp. 1-10.

Rashid, M.A. (1985). “Geochemistry of Marine Humic Compounds “. Springer, New York.

Rausell-Colom, J.A., Serratosa, J.M. (1987). “Reactions of clays with organic substances”. Chemistry of Clays and Clay Minerals. (A.C.D. Newman, editor). Miner. Soc. Monograph #6, pp. 371-422.

Repasi, J. (1993). “Selective complexometric determination of glyphosate and related compounds”. Pest. Science, V. 39 (4), pp. 287-292.

Ribeiro, F.R., Rodrigues, A.E., Rollmann, L.D., Naccache, C. (1984). „Zeolites: science and technology”. Martinus Nijhoff Publishers, The Hague.

Rongchapo, W. (2015). “Removal of paraquat and other pollutants by adsorption and photocatalysis”. Doctoral thesis, Suranaree University of Technology.

Rosch, A., Anliker, S., Hollender, J. (2016). “How biotransformation influences toxicokinetics of azole fungicides in the aquatic invertebrate Gammarus pulex”. Environ. Sci. Technol., V. 50 (13), pp. 7175-7188.

Rueppel, M.L., Brightwell, B.B., Schaefer, J., Marvel, J.T. (1977). “Metabolism and degradation of glyphosate in soil and water”. J. Agric. Food Chem., V. 25 (3), pp. 517-528.

Russel, J.D., Cruz, M.I., White, J.L. (1968). “Adsorption of 3-aminotriazole by montmorillonite”. J.Agric. Food Chem., V. 16 (1), pp. 21-24.

Rzymski, P., Klimaszyk, P., Kubacky, T., Poniedzialek, B. (2013). „The effect of glyphosate-based herbicide on aquatic organisms – a case study”. Limnolog. Rev., V. 13 (4), pp. 215-220.

Salazar, L.C. and Appleby, A.P. (1982). “Herbicidal activity of glyphosate in soil”. Weed Sci., V. 30, pp. 463-466.

Samnani, P., Vishwakarma, K. & Pandey, S.Y. (2011). “Simple and sensitive method for determination of imidacloprid residue in soil and water by HPLC”. Bull. Env. Contam. Toxicol., V. 86 (5), pp. 554-558.

Sánchez-Bayo, F., Goka, K. (2006). “Ecological effects of the insecticide imidacloprid and a pollutant from antidandruff shampoo in experimental rice fields”. Environ. Toxicol. Chem., V. 25, pp. 1677–1687.

Santoro, A., Scopa, A., Bufo, S.A., Mansour, M.M., Mountacer, H. (2000). “Photodegradation of the triazole fungicide hexaconazole”. Bullet. Environ. Contam. Toxicol., V. 64 (4), pp. 475-480.

Scholz, K., and M. Spiteller. (1992). “Influence of groundcover on the degradation of 14C-imidacloprid in soil”. Brighton Crop Prot. Conf., Pests and Diseases., V. 23-26, pp. 883-888.

Schuette, J. (1998) “Environmental fate of glyphosate”. Env. Monit. &Pest Manag. Dpt. of Pest. Regul., Sacramento, CA95824-5624, 13 pages.

Schultz, C., Powell, K., Crossley, A., Jurkschat, K., Kille, P., Morgan, A.J., Read, D., Tyne, W., Lahive, E., Svendsen, C., Spurgeon, D. (2015). “Analytical approaches to support current understanding of exposure, uptake and distributions of engineered nanoparticles by aquatic and terrestrial organisms”. Ecotox., V. 24, pp. 239-261.

Schwarz, J.A., Driscoll, C.T., Bhanot, A.K. (1984). “The zero point of charge of silica-alumina oxide suspensions”. J. Coll. Interf. Sci., V. 97 (1), pp. 55-61.

Schwarzenbach, R.P., Gschwend, P.M., Imboden, D.M. (1993). “Environmental Organic Chemistry”. John Wiley & Sons, New York, Chapter 11.7.

Schwarzenbach, R.P., Gschwend, P.M., Imboden, D.M. (2005) „Environmental organic chemistry, Chapter 9. Sorption I: General Introduction and Sorption Processes Involving Organic Matter”, John Wiley&Sons, New Jersey.

Schwarzenbach, R.P., Westfall, J. (1981). “Transport of nonpolar organic compounds from surface water to groundwater: Laboratory sorption studies”. Environ. Sci. Technol., V. 15 (11), pp. 1360-1367.

Shankar, A., Kongot, M., Saini, V.K., Kumar, A. (2018). “Removal of pentachlorophenol pesticide from aqueous solutions using modified chitosan”. Arab. J. Chem., in press, corrected proof.

Sheals, J., Granström, M., Sjöberg, S., Persson, P. (2003). “Coadsorption of Cu(II) and glyphosate at the water-goethite (alpha-FeOOH) interface: molecular structures from FTIR and EXAFS measurements”. J. Colloid. Interface Sci., V. 262 (1), pp. 38-47.

Sheals, J., Persson, P., Hedman, B. (2001). “IR and EXAFS spectroscopic studies of glyphosate protonation and copper (II) complexes of glyphosate in aqueous solution”. Inorg. Chem., V. 40 (17), pp. 4302-4309.

Sheals, J., Sjoberg, S., & Persson, P. (2002). “Adsorption of glyphosate on goethite: molecular characterization of surface complexes”. Environ. Sci. Technol., V. 36 (14), pp. 3090-3095.

Shi, X., Ji, L., Zhu, D. (2010). "Investigating roles of organic and inorganic soil components in sorption of polar and nonpolar aromatic compounds". Environ. Pollut., V. 158 (1), pp. 319-324.

Sidoli, P., Baran, N., Angulo-Jaramillo, R. (2016). “Glyphosate and AMPA adsorption in soils: laboratory experiments and pedotransfer rules”. Environ. Sci. Pollut. Res. Int., V 23 (6) pp. 5733-5742.

Simon-Delso, N., Amaral-Rogers, V., Belzunces, L.P., Bonmatin, J.M., Chagnon, M., Downs, C., Furlan, L., Gibbons, D.W., Giorio, C., Girolami, V., Goulson, D., Kretzweiser, D.P., Krupkpe, C.H., Liess, M., Long, E., McField, M., Mineau, P., Mitchell, E.A.D., Morrissey, C.A., Noome, D.A., Pisa, L., Settele, J., Stark, J.D., Tapparo, A., Van Dyck, H., Van Praagh, J., Van der Sluijs, J.P., Whitehorn, P.R. and Wiemers, M. (2015). “Systemic insecticides (neonicotinoids and fipronil): trends, uses, mode of action and metabolites”. Environ. Sci. Pollut. Res. Int., V. 22, pp. 5-34.

Simonsen, L., Fomsgaard, I.S., Svensmark, B., Spliid, N.H. (2008). “Fate and availability of glyphosate and AMPA in agricultural soil”. J. Environ. Sci. Health, V. B43, pp. 365-375.

Sims, G.K., Radosevich, M., He, X.T., Traina, S.J. (1991). “The effects of sorption on the bioavailability of pesticides”. In: Betts, W.B. (eds) Biodegradation. Springer Series in Applied Biology. Springer, London.
Slowing, I.I., Vivero-Escoto, J.L., Wu, C.-W., Lin, V.S.-Y.(2008). “Mesoporous silica nanoparticles as controlled release drug delivery and gene transfection carriers”. Adv. Drug Del. Rev., V. 60 (11), pp. 1278-1288.

Smit, E., Posthuma-Doodeman, C.J.A.M., Vlaardingen, P. v., de Jong, F.M.W. (2015). “Ecotoxicity of imidacloprid to aquatic organisms: derivation of water quality standards for peak and long-term exposure”. Human Ecol. Risc. Asses., V. 21 (6), pp. 1608-1630.

Smith, D.W. (1977) “Ionic Hydration Enthalpies”. J. Chem. Educ., V. 54 (9), p. 540.

Soloway, S.B., Henry, A.C., Kollmeyer, W.D., Padgett, W.M., Powell, J.E., Roman, S.A., Tieman, C.H., Corey, F.A., Horne, C.A. (1978). “Nitromethylene heterocycles as insecticides”. In: Shankland, D.L., Hollingworth, R.M., Smyth, Jr. T. (Eds.). Pest. Venom Neurotox. Plenum, New York, pp. 153–158.

Sparling, D.W. (2016). “Current use of pesticides”. In: Ecotoxicology Essentials, Environ. Contam. Biol. Eff. Anim. Plants, Academic Press, pp. 109-152.

Sposito, G. (1995). “The environmental chemistry of aluminium”. 2nd ed., CRC Press, Berkeley.

Sposito, G. (2008). “The chemistry of soils”. Inc, New York, Oxford University Press, 2-nd. Edition.
Steinrücken, H.C., Amrhein, N. (1980). "The herbicide glyphosate is a potent inhibitor of 5-enolpyruvyl-shikimic acid-3-phosphate synthase". Biochem. Biophys. Res. Commun., V. 94 (4), pp. 1207–1212.

Subramaniam, V., Hoggard, P.E. (1988). “Metal complexes of glyphosate”. J. Agric. Food Chem., V. 36**,** pp**.** 1327-1328.

Sudhakar, Y., Dikshit, A.K. (2010). “Competitive sorption of pesticides onto treated wood charcoal and the effect of organic and inorganic parameters on adsorption capacity”. J. Environ. Engin., V. 136 (10), pp. 1096-1104.

Sumon, K.A., Ritika, A.K., Peeters, E.T.H.M., Rashid, H., Bosma, R.H., Rahman, M.S., Fatema, A.K., Brink, P.J. (2018). “Effects of imidacloprid on the ecology of sub-tropical freshwater microcosms”. Environ. Pollut., V. 236, pp. 432-441.

Technical Information Bulletin for Propiconazole Fungicide, n.d., accessed 4 November 2018, <http://pmep.cce.cornell.edu/profiles/extoxnet/metiram-propoxur/propiconazole-ext.html>

Tiselius, A. (1948). “Electrophoresis and adsorption analysis as aids in investigations of large molecular weight substances and their breakdown products (English translation of a presentation in Swedish). In Les Prix Nobel en 1948, Imprimerie Royale, P.A. Norstedt&Söner, Stockholm, pp. 102-121.

Tomizawa, M., Casida, J.E. (2003). “Selective toxicity of neonicotinoids attributable to specificity of insect and mammalian nicotinic receptors”. Annu. Rev. Entomol., V. 48., pp. 339–364.

Tomlin, C.D.S. (1997). “The pesticide manual - World Compendium”. 11. ed., British Crop Protection Council, Surrey, England, p. 644

Traina, S.I., Onken, B.M. (1991). "Co-sorption of aromatic N-heterocycles and pyrene by smectite in aqueous solutions". J. Cont. Hydrol., V. 7, pp. 237-259.

Trivedi, P., Dyer, J.A., Sparks, D.L. (2003). "Lead sorption onto ferrihydrite. A macroscopic and spectroscopic assessment “. Environ. Sci. Technol., V. 37, pp. 908–914.

Trösken, E.-R. (2005). “Toxicological Evaluation of Azole Fungicides in Agriculture and Food Chemistry”. Ludwig-Maximilians University Würzburg, Doctoral thesis, Würzburg.
U.S. Environmental Protection Agency n.d. (1993). “Pesticide Tolerances for 1-[[2- (2,4-Dichlorophenyl)-4-Propyl-1,3-Dioxolan-2-yl]Methyl]-1H-1,2,4-Triazole and its Metabolites Determined as 2,4-Dichlorobenzoic Acid and Expressed as Parent Compound”. Federal Register Document 93-12130.

U.S. Environmental Protection Agency, n.d. (2010). “Imidacloprid”, accessed 4 November 2018, <https://www3.epa.gov/pesticides/chem_search/hhbp/R181434.pdf>

US Environmental Protection Agency, n.d. (2007). “What is a pesticide?” accessed 2 November 2018, <https://www.epa.gov/ingredients-used-pesticide-products/basic-information-about-pesticide-ingredients>

Van der Sluijs, J.P., Simon-Delso, N., Goulson, D., Maxim, L., Bonmatin, J.-M., Belzunces, L.P. (2013). “Neonicotinoids, bee disorders and the sustainability of pollinator services”. Curr. Opin. Environ. Sustain, V. 5, pp. 293–305.

Venkateswarlu, K., Kelly, D.E. and Kelly, S.L. (1997). “Characterization of Saccharomyces cerevisiae CYP51 and a CYP51 fusion protein with NADPH cytochrome P-450 oxidoreductase expressed in Escherichia coli”. Antimicrob. Agents. Chemoter., V. 41 (4), pp. 776-780.

Verordnung (EU) 2015/408. “Durchführungsverordnung des Europäischen Parlaments und des Rates über das Inverkehrbringen von Pflanzenschutzmitteln und zur Erstellung einer Liste mit Substitutionskandidaten vom 11. März 2015“.

Vialaton, D., Pilichowski, J.F., Baglio, D., Paya-Perez, A., Larsen, B., Richard, C. (2001). “Phototransformation of propiconazole in aqueous media”. J. Agric. Food Chem.**,** V. 49 (11), pp. 5377-5382.

Villegas, M.F., Garcia-Uriostegui, L., Rodriguez, O., Izquierdo-Barba, I., Salinas, A.J., Toriz, G., Vallet-Regi, M., Delgado, E. (2017). “Lysine-grafted MCM-41 silica as an antibacterial biomaterial”. Bioengin., V. 4 (4), pp. 80-93.

Vindevogel, S. (1992). “Micellar electrokinetic chromatography”, Hüthig Buch Verlag, Heidelberg.
Virta, R.L. (2001). “Zeolites”. U.S. Geological survey minerals yearbook.

Wadlinger, R. L., Kerr, G. T., Rosinski, E. J. (1967). US Patent 3 308 069.

Wang, Q.-Y., Sun, J.-Y., Xu, X.-J., Yu, H.-W. (2018). „Integration of chemical and toxicological tools to assess the bioavailability of copper derived from different copper-based fungicides in soil”. Ecotox. Environ. Saf., V. 161, pp. 662-668.

Wang, S., Seiwert, B., Kästner, M., Mittner, A., Schäffer, A., Reemtsma, T., Yang, Q., Nowak, K.M. (2016). „Biodegradation of glyphosate in water-sediment microcosms – A stable isotope co-labelling approach”. Water Res., V. 99, pp. 91-100.

Wang, W., Lofgreen, J., Ozin, G.A. (2010). "Why PMO? Towards functionality and utility of periodic mesoporous organosilicas". V. 6 (23), pp. 2634–2642.

Wang, Y.J., Zhou, D.M., Sun, R.J. (2005). “Effects of phosphate on the adsorption of glyphosate on three different types of Chinese soils”. J. Environ Sci. (China), V. 17 (5), pp. 711-715.

Wicht, A.-J. (2018). "Development and application of new analytical methods based on chromatographic and electrophoretic separations to assess the environmental behavior of anthropogenic pollutants and their uptake in fungi and chironomids", Doctoral thesis, University of Tübingen.

Wimmer, B. (2017). "Glyphosatanalytik: CE-MS Methodenoptimierung und Anwendung an Realproben“. Master thesis, University of Tübingen.

Woo, C., Daniels, B., Stirling, R., Morris, P. (2010). “Tebuconazole and propiconazole tolerance and possible degradation by basidomycetes: A wood-based bioassay”. Intern. Biodeter.&Biodegr., V. 64, pp. 403-408.

Wu, H., Chen, L., Gao, G., Zhang, Y, Wang, T., Guo, S. (2010). “Image processing for the CCD based lateral flow strip detector”. Nano Biomed. Eng., V. 2 (4), pp. 231-235.

Wu, Q.L., Riise, G., Kretzschmar, R. (2003). “Size distribution of organic matter and associated propiconazole in agricultural runoff material”. J. Environ. Q., V. 32, pp. 2200–2206.

Xiao, F., Pignatello, J.J. (2015). “Interactions of triazine herbicides with biochar; steric and electronic effects”. Water. Res., V. 80, pp. 179-188.

Xu, J., Gu, X., Guo, Y., Tong, F., Chen, L. (2016). “Adsorption behavior and mechanism of glufosinate onto goethite”. Sci. Tot. Environ., V. 560-561, pp. 123-130.

Xue, Z. (2018). “Redox reactions and sorption of quinones and natural organic matter at iron mineral/Fe(II) interfaces”. Doctoral thesis, University of Tübingen.

Yamaguchi, T., Echizen, M., Fujita, T., Taruta, S., Kitajima, K. (2002). “Pore properties of activated alumina prepared from polyhydroxoaluminum - tetraalkylammonium ion composite gels”, J. Ceram. Soc. Jap., V. 110 (10), pp. 954-958.

Yan, W., Jing, C. (2018). “Molecular insights into glyphosate adsorption to goethite gained from ATR-FTIR, two-dimensional correlation spectroscopy, and DFT study”. Environ. Sci. Technol., V. 52 (4), pp. 1946-1953.

Yoshida, Y. (1988). “Cytochrome P450 of fungi: primary target for azole antifungal agents”. Curr. Top. Med. Mycol., V. 2, pp. 388-418.

Zahoor, M. (2011). "Effect of agitation speed on adsorption of imidacloprid on activated carbon". J. Chem. Soc. Pakistan, V. 33 (3), pp. 305-312.

Zapolskiy, A.K. (1981). „Sernokislotnaya pererabotka visokokremnistogo aluminievogo sirja“. Kiev. [Запол ьский А.К., Сернокислотная переработка высококремнистого алюминиевого сырья. Киев, 1981.].

Zarn, J.A., Bruschweiler, B.J. and Schlatter, J.R. (2003). „Azole fungicides affect Mammalian steroidogenesis by inhibiting sterol 14 alpha-demethylase and aromatase”. Environ. Health Perspect., V. 111, pp. 255-262.

Zhang, K., Tang, M., Zhang, J., Li, Y., Han, X., Pan, S., Kong, X., Li, Meichuan, Chen, H., Zhang, W., Zhu, H., Zeng, S., Hu, D. (2015). „Fate of hexaconazole and isoprothiolane in rice, soil and water under field conditions”. Int. J. Environ. Anal. Chem., V. 96 (1), pp. 38-49.

Zheng, T-T., Sun, Z-X., Yang, X-F., Holmgren, A. (2012). “Sorption of phosphate onto mesoporous γ-alumina studied with in-situ ATR-FTIR spectroscopy”. Chem. Cent. J., V. 6 (26), pp. 1-10.

Zhu, X., Chang, Y., Chen, Y. (2010). “Toxicity and bioaccumulation of TiO_2 nanoparticle aggregates in Daphnia magna”. Chemosphere, V. 78, pp. 209-215.

Zhu, X., Zhu, L., Chen, Y., Tian, S. (2009). “Acute toxicities of six manufactured nanomaterials suspensions to Daphnia magna”. J. Nanopart. Res., V. 11, pp. 67-75.